

UPPER ATMOSPHERIC STUDIES USING RADIO METEORS

A thesis presented for the degree of
Doctor of Philosophy in Physics
in the University of Canterbury,
Christchurch, New Zealand.

by

P.J. Wilkinson

1973

ABSTRACT

The atmospheric motions in the 80-110 km height region, and methods of measuring them are discussed. Wind measurements using radio meteor trails are then considered in greater detail and an account is given of the equipment at the field station of the Physics Department of Canterbury at Rolleston near Christchurch, as well as details of the data reduction methods used. An analysis of the errors associated with the collection of data indicates that approximately half the variance in an average of wind velocities observed in a thirty minute period is due to atmospheric variability. Results from the first year's observations suggest that the solar diurnal and semidiurnal tides are of roughly the same magnitude, this magnitude being in agreement with the latitudinal variations observed at other stations.

To Lorraine

ACKNOWLEDGEMENTS

It is not possible to acknowledge, by name, all the people who have given encouragement and assistance during the course of my work. Some, however, deserve special mention; Professor A.G. McLellan, for financial aid in the form of a teaching fellowship;

Dr W.J. Baggaley, my supervisor, for all his assistance and advice, given generously at all times;

Dr R.G.T. Bennett for his considerable aid in the construction of the equipment;

Mr P.A.G. Howell for developing all the film;

The film readers Stephen Freeth, Bill Pannel, Tan Khee Siang, Brian Williams and my sister, Christine;

Mrs M. Sewell for the typing of this thesis;

and Mr C.H. Cummack and Dr G.J. Fraser for many interesting discussions.

Of the postgraduate students, all added to the friendly environment in which this thesis was written, but special mention must be made of Errol Wood, with whom I shared a room for four very pleasant years, and Murray Poulter, who is now carrying on from where I left off.

I would also like to thank my parents and my sisters for their intangible, but nevertheless very real contribution to this thesis.

Finally, but most important, I would like to thank my wife Lorraine for putting up with all the many disturbances associated with experimental degrees of this type. Her presence has made the work much easier.

CONTENTS

	<u>Page</u>
<u>CHAPTER ONE:</u> The Introduction	1
<u>CHAPTER TWO:</u> Atmospheric Movements in the Meteor Region	4
A. Prevailing Wind	
2.2 General circulation	5
2.3 Long period variations	9
B. Tidal Components	
2.4 History	10
2.5 Derivation of governing equations	12
2.6 Laplace's equation	13
2.7 Notation	15
2.8 Radial equation	16
2.9 Forcing term	17
2.10 The semidiurnal tide	18
2.11 The diurnal tide	19
2.12 Other tidal modes	21
C. Irregular Component	
2.13 Gravity waves	22
2.14 Turbulence	24
2.15 Summary	26
<u>CHAPTER THREE:</u> Experimental Work on Atmospheric Winds in the 80-110 km Region	28
A. Artificial Tracers	
3.2 Falling sphere	29
3.3 Chaff	30
3.4 Chemical trails	30
3.5 Gun probes	32
3.6 Grenades	32
3.7 Summary of artificial tracers	33
B. Naturally Introduced Tracers	
3.8 Optical methods	34
3.9 Ionospheric drifts	34
3.10 Baroms	37
3.11 Radio meteor observations	37
3.12 Discussion	45

<u>CHAPTER FOUR:</u>	The Apparatus	
4.1	Choice of equipment parameters	47
4.2	The transmitter	51
4.3	The receiver	57
4.4	The phase sensitive detector	59
4.5	The blanking channel	63
4.6	The discriminator	63
4.7	Camera control	66
4.8	The recording system	58
4.9	Additional equipment	71
4.10	Transmission lines	71
4.11	The aerial	73
4.12	Film reading equipment	81
<u>CHAPTER FIVE:</u>	Parameters Measured from Each Radio Meteor	82
A.	Height	
5.1	Heights using a deduced ambipolar diffusion coefficient	82
5.2	Measurement of decay rate from photographic records	88
B.	Velocity	
5.3	The observed phase variations in the returned signal	90
5.4	Measurement of the radial velocity from records	93
5.5	Type of Doppler	96
5.6	Wind shear measurements	96
5.7	Durations	97
5.8	Direction of trail drift	97
C.	Other Parameters Read from Film	
5.9	Range	97
5.10	Type of record	98
5.11	Amplitude of record	98
5.12	Summary	100
<u>CHAPTER SIX:</u>	Errors in Deduced Values of Wind Velocities	104
A.	The Individual Meteor Echo	
6.1	Durations	104
6.2	Heights	106
6.3	Wind Velocity	112
6.4	Type of record	118

	<u>Page</u>
B. Averaging Over Half an Hour's Records	
6.5 Contribution to variance from film reading	120
6.6 Effects of a finite aerial beamwidth	123
6.7 Vertical velocities	125
6.8 The error in a half-hour average	128
6.9 Summary	137
<u>CHAPTER SEVEN:</u> The Observed Meteor Wind Characteristics	140
A. The Analysis Method	
7.1 History	141
7.2 The time series	142
7.3 The power spectrum	143
7.4 Harmonic analysis	145
7.5 Method of analysis used	147
7.6 External errors in the analysis	149
B. Results	
7.7 The Data	154
7.8 The mean wind	156
7.9 Tidal components	165
7.10 Summary of the results	177
<u>CHAPTER EIGHT:</u> The Conclusion	179
8.1 Radio interference	179
8.2 Zero velocities	180
8.3 Decay heights	182
8.4 Data analysis	182
8.5 Significance of the mean velocity for half an hour	184
8.6 Harmonic analysis	185
8.7 The observed atmospheric winds	186
8.8 Comparisons	186
<u>APPENDIX:</u> The Computer Programs	187
A.1 The main program	188
A.2 Card Formats	189
A.3 The subprograms	191
A.4 The range calibration	192
A.5 Harmonic analysis	192
<u>BIBLIOGRAPHY</u>	194

C H A P T E R 1

THE INTRODUCTION

The atmosphere, which surrounds the earth, is in a state of continual motion. These motions are ultimately driven by solar radiation absorbed by the atmosphere. The variation in absorbed radiation over the globe is one of the major contributing factors in determining the circulation in the lower 12 kilometres of the atmosphere. However, as only about 1/20th of the solar radiation is absorbed above this level, it is probable that upward leakage of energy may also be an important factor in the circulation at higher levels.

While sufficient observations on the lower circulation have been obtained, making it possible to test theories explaining these motions, observations for altitudes above about 60 km are very limited. It is of considerable importance, if a picture of the circulation at all levels in the atmosphere is to be obtained, to increase the number of stations capable of observing high altitude winds. Several methods have been used to measure these winds, and one such method, called the radio meteor method, is the subject of this thesis.

On entry into the earth's atmosphere, meteoric material ablates forming an ionized trail, the large majority of which are observed at altitudes of 80 to 110 km. The trail, after formation, moves with the local atmosphere and may thus be used as a tracer of atmospheric motions. The wind velocity of the specular reflection point on the meteor trail may be measured by measuring the change in range between the observer and the trail. (This is accomplished best by observing the

change in frequency between the transmitted radio wave and the received echo.) After formation, the trail expands, the expansion rate depending on the local atmospheric density. It is possible to obtain the height of the trail by observing the rate at which the echo amplitude decays.

Provided the system sensitivity is sufficiently high, several hundred such trails will be observed in a day. This rate will exhibit seasonal and diurnal variations due to the earth's motion about the sun and rotation on its axis. To determine the wind field in the region of interest, the wind velocities obtained from several trails are averaged. The significance of these averages will depend on how many individual points are averaged, which in turn depends on the meteor rate.

Atmospheric winds observed using radio meteors were first reported by Manning, Villard and Peterson (1950). Several stations have since reported results, and from these a general picture of the winds in the 80-110 km region can be obtained. The mean flow is consistent with a positive temperature gradient from the summer to the winter pole, the opposite to that which would be expected from purely radiative energy sources. Atmospheric gravity waves, which conserve their kinetic energy with altitude, are observed to have amplitudes of similar (or greater) magnitude to the mean flow. Of particular importance are thermal atmospheric tides, being low frequency gravity waves. Both twelve and twenty-four hour periodicities are observed in the meteor wind data.

The major part of the work for this thesis was involved in assisting with the construction and early operation of the meteor wind station at the University of Canterbury field

station at Rolleston. As a result of this work, some results for the first year's operation are presented. The layout of the thesis is as follows.

Chapter 2. The atmospheric motions in the 80-110 km region are discussed, the motions being subdivided into three classes: the mean wind, atmospheric tides and an irregular component in which gravity waves and turbulence are considered.

Chapter 3. Various direct and indirect methods for measuring winds in this region are considered, particular attention being paid to the radio meteor method.

Chapter 4. A short discussion of the choice of equipment parameters for a meteor wind station is followed by a description of the equipment used in the present experiment that was constructed or modified by the author.

Chapter 5. All parameters measured from the photographic film are examined here with special emphasis being placed on the measurement of heights, using the echo amplitude decay, and the measurement of the radial drift velocity of the trail.

Chapter 6. First the errors introduced in measurements made on a single meteor are examined, and then the errors in the mean velocity for half an hour, possible sources of the observed variance in the results and the significance of the mean are considered.

Chapter 7. Preliminary results for the first year's operation are presented, preceded by a discussion of ^{the} harmonic analysis method and its relation to power spectral techniques.

Chapter 8. The major results of the thesis are summarized along with some general suggestions for improvements in the equipment and analysis procedures.

Appendix. The computer programs used are listed.

C H A P T E R 2

ATMOSPHERIC MOVEMENTS IN THE METEOR REGION

2.1 Introduction

Atmospheric motions in the meteor region extend over large time scales. Three main subdivisions, in this chapter, defined by equipment limitations are made. It is, however, convenient to make similar subdivisions from a theoretical point of view, but at no time is it intended that atmospheric motions can be simply decomposed into these sections.

1. Prevailing Wind. Because only a finite record of wind velocity is obtained, unresolved components in the form of a trend will be present in the results. The prevailing wind will thus be composed of a mean wind plus unresolved long period variations.

2. Tidal Components. Atmospheric winds in the meteor region are often dominated by tidal components, being of equal or greater magnitude than the mean wind. Because of their magnitude, it is difficult to obtain estimates of the mean flow unless at least twenty-four hours of data is obtained.

3. Irregular Component. Because of low space and time resolution, periodicities of only two or three hours will not be readily resolvable with the present equipment. Instead such features as gravity waves and turbulence will become mixed and contribute only to the scatter in observed results.

A. PREVAILING WIND

This is conveniently treated under three further subdivisions.

2.2 General Circulation

1. Thermal wind equation. Below 90 km use of the thermal wind equation indicates that wind and temperature gradients are closely related for seasonal averages (Murgatroyd, 1957).

The geostrophic wind equation may be deduced from the equations for fluid motion by assuming the fluid is incompressible and there are no accelerating or dissipating forces acting on the atmosphere apart from gravity, so that pressure gradient forces and rotational effects are in equilibrium. This gives

$$U = - \frac{1}{f\rho_a} \frac{\partial P}{\partial y} \quad (2-1)$$

$$V = \frac{1}{f\rho_a} \frac{\partial P}{\partial x}$$

the geostrophic wind equations, and

$$\frac{\partial P}{\partial z} = - \rho_a g \quad (2-2)$$

the hydrostatic equilibrium equation

where

U, V = zonal and meridional wind components

x, y, z = zonal, meridional and vertical coordinates.

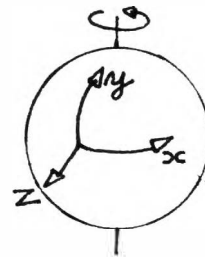
In the above the zonal coordinates are positive for a motion to the east (eastward) and the meridional coordinates are positive to the north (northward).

ρ_a = atmospheric density,

$f = 2 \times$ (the earth's rotational velocity)

\times (the sine of the latitude)

(for Christchurch, which is 43°S , $f = -10^{-4}/\text{sec.}$).



By using the ideal gas law, the thermal wind equations are obtained from (2-1) by replacing the pressure gradient term, giving

$$\frac{\partial V}{\partial z} = \frac{g}{fT} \frac{\partial T}{\partial x} + \left(\frac{V}{T} \frac{\partial T}{\partial z} \right) \quad (2-3)$$

$$\frac{\partial U}{\partial z} = - \frac{g}{fT} \frac{\partial T}{\partial y} + \left(\frac{U}{T} \frac{\partial T}{\partial z} \right)$$

where T = temperature.

In low latitudes both (2-1) and (2-3) fail as $f \rightarrow 0$ and the earlier derivation becomes inapplicable, and in polar regions where large-scale planetary waves become important atmospheric features they also become less useful. However, for mid-latitudes, where the relationship is applicable, it can be shown that the term in brackets in (2-3) is far less important and hence may be neglected, thus indicating that the vertical wind shear is closely related to the horizontal temperature gradient. For the troposphere, the equator to pole pressure and temperature gradients would, from (2-1) and (2-3), give rise to an eastward wind, that increases with altitude, as is observed.

However, it is apparent that no nett meridional transport is predicted by (2-3) and the equator would be expected to become hotter and hotter. Thus, the geostrophic approximation cannot be regarded as more than a first approximation, and before using it, the assumptions leading to its derivation should be considered. In applying the geostrophic approximations to the upper atmosphere, the most important addition will probably be dissipative forces, both kinematic viscosity and magnetic field effects on ionization present becoming increasingly important with height. These considerations suggest that (2-1) and (2-3) could be misleading at meteor heights.

2. Observations. From data obtained several authors have constructed models for zonal winds (Batten, 1961; Newell, 1968; Morris and Miers, 1969; Groves, 1969; CIRA, 1965; Murgatroyd, 1957, 1965). While there is some variability, above 85 km, between the different models, agreement on the major features of the wind is good. Using these models, the seasonal winds at 43°S were estimated. In ^{the southern hemisphere} summer there is a wind gradient of 2 m/s/km with wind velocities of the order of 10 m/s westwards at 80 km and 30 m/s eastwards at 100 km. The winter zonal wind gradient was -2 m/s/km, with velocities of the order of 50 m/s eastwards at 80 km and 10 m/s eastwards at 100 km. From (2-3), the wind gradients indicate a positive temperature gradient from the summer pole to the winter pole, a point which will be considered in the next section. These wind gradients agree well with wind gradients for Adelaide (35°S), but are a factor of two larger than those observed at Jodrell Bank, (53°N). However, the sense of the gradient is preserved at both localities.

Meridional winds being more variable, and generally giving much smaller average values, have only recently been incorporated in an atmospheric model (Groves, 1969). The general results of this model agree with observations, the meridional flow being directed towards the pole in winter and away from the pole in summer, consistent with a warm winter pole suggested by the zonal wind gradients.

3. Driving Forces. Because the temperatures deduced from winds by (2-3) are consistent with observation, it is evident that the driving force for the meteor region cannot be purely radiative - a dynamic source is probable. Several possibilities have been suggested.

- a. Chemical heating: Subsidence in the winter polar regions would transport atomic oxygen down from higher altitudes, where recombination to form molecular oxygen is exothermic, making heating of the atmosphere possible. The associated vertical velocities involved are only of the order of a few millimetres a second (Kellogg, 1961).
- b. Gravity Waves: Hines (1963,1965), showed that dissipation of gravity waves (to be discussed in a later section) could be a possible heating source, their dissipation being of the right order of magnitude, while seasonal changes in transmission could produce the observed seasonal variations. Dissipation may either be molecular or turbulent, and as turbulence shows some seasonal variation (Roper, 1966), being greater in winter than summer, the two points may be coupled to suggest turbulent dissipation of gravity waves as an important energy source in the meteor region.
- c. Molecular dissipation: From (2-3), Lindzen (1968) indicates that if no dissipation is present in the atmosphere, then when the latitudinal temperature gradient is zero, the wind velocity will be constant with height. Dissipation will result in $\frac{\partial U}{\partial z}$ becoming negative away from the driving region, and hence $\frac{\partial T}{\partial y}$ will become negative, implying a temperature gradient opposite to the radiative heating gradient.
- d. The refrigerator model: From observations of the lower stratosphere, it appears likely that the circulation is driven against the local temperature gradient due to vertical propagation of large-scale eddies from the troposphere (Starr, 1968). This is the action of a refrigerator.

In the upper stratosphere, ozone absorption of solar energy will result in a second region of direct circulation -

or, a heat engine. By analogy with the lower stratosphere, it is possible that the upper stratosphere drives the lower mesosphere resulting in refrigerator action again. This would produce a cold summer pole, as observed.

(Refs Newell, 1966; Murgatroyd, 1970)

4. Summary. The most likely driving sources for the observed lower mesospheric circulation are a result of upward energy propagation from the lower atmosphere. It is evident, in this respect, that c. and d. above are equivalent, the effects of motion in the lower region being damped out in the upper region. As indicated, chemical energy may also be important.

2.3 Long Period Variations

1. Planetary Waves. These are very low frequency atmospheric waves, having periods in excess of 24 hours, wavelengths that span the globe, and for which the earth's rotation is the major restoring force. From observations of wind velocities at meteor heights (Pokrovski, 1970; Müller, 1972), it is evident that periodicities of several days are present. However, the definite identification of these periodicities with planetary waves must wait until better spatial definition is obtained. Both authors tentatively identify these observations with similar lower altitude atmospheric periodicities.

Charney and Drazin (1961) showed that vertical propagation of planetary waves is inhibited by lower atmospheric winds in summer and winter, though some upward propagation is possible in the equinoxes. Later work (Dickinson, 1968) supported these general conclusions.

2. Semi-Annual Variation. In the thermosphere and exosphere six month periodicities in atmospheric density are observed covering a height range of 200 to 1000 km. Similar periodicities are observed in wind velocities and wind shears for the meteor region (Greenhow and Neufeld, 1961). Atmospheric density variations of this period have also been reported from falling sphere measurements, (Cook, 1969). However, analysis of atmospheric tides from several meteor stations shows only a twelve month period to be significant, though the authors place equal emphasis on higher harmonics of 12 months (Teptin and Starostin, 1971). Power spectra of zonal wind velocities do show a six month peak (Pokrovskiy, 1970) but meridional velocities do not.

The above indicates the apparent variability of this effect - a result that may possibly be due to insufficient data. The exact cause of the variation is not known. (Refs Cook, 1969; Kochanski, 1972).

B. TIDAL COMPONENTS

Definition: (Lindzen 1969). Tides are those oscillations resulting from the earth's rotation through gravitational and radiational fields. These oscillations have periods that are some integral fraction of a lunar or solar day.

Recent surveys by Siebert, 1961; and Lindzen and Chapman, 1969, are the major sources for additional references in this segment.

2.4 History

From early equatorial barometric records, it was evident that the atmosphere exhibited 12 hour tidal oscillations. However, the observed oscillation is periodic with respect to

the sun - if purely gravitational tides were involved, a lunar tide would be expected to predominate. Laplace observed that the 12 hour oscillation (S_2) must be of thermal origin, but because of theoretical problems in treating the forcing term, he concentrated on the smaller lunar tides. To explain the S_2 predominance, if thermal tides were involved, Lord Kelvin suggested an harmonic analysis of the thermal heating source would probably show this component more nearly matched a free oscillation period of the earth's atmosphere. (That is, a frequency that the earth's atmosphere would oscillate at if excited by an impulsive force. The eruption of Krakatoa in 1883 produced such an oscillation, and analysis revealed resonance was possible for the S_2 tide. (See Siebert, 1961, for more details).) Lamb, and other workers, showed that if strong resonance were possible, then the gravitational tide alone could account for the observations. Finally, Weekes and Wilkes (1947), and Wilkes (1949), showed that with the then acceptable temperature profiles for the upper atmosphere resonance of the S_2 tide was very probable, though to predominate over the lunar gravitational tide required it to be within six minutes of the earth's free period of oscillation. However, the calculations were particularly sensitive to the value of the temperature maximum at 50 km, and when rocket measurements showed this to be about 50°K too large in their profiles, it brought the whole resonance theory into question.

It is now apparent that the major atmospheric tides arise from thermal forcing by ozone and water vapour absorption (Siebert, 1961; Butler and Small, 1963). The predominance of the 12 hour over the 24 hour tide results from most of the 24 hour tidal energy being in evanescent modes (Kato, 1966;

Lindzen, 1966).

(Refs Siebert, 1961; Lindzen and Chapman, 1969 - hereafter referred to as L/C).

2.5 Derivation of the Governing Equations

(In this and successive sections only wind velocities will be considered. Pressure, density and temperature variations also occur, but these will not be considered in the later results of this thesis.)

The equations for fluid motion, the continuity equation, the first law of thermodynamics and an equation of state are solved in spherical coordinates, for a frame of reference rotating with the earth using various simplifying assumptions, (Siebert, 1961).

- 1) The earth is a smooth sphere.
- 2) No dissipative processes are considered.
- 3) All basic flow parameters are steady in time and independent of latitude and longitude and no background winds^{are} considered.
- 4) All temperature structure is introduced in the atmospheric scale height, (H).
- 5) All tidal parameters are periodic functions of latitude and longitude.

The resultant equations may be separated into radial and angular parts given by Laplace's Equation

$$F(\theta_n) + \frac{4a^2\omega^2}{gh_n} \theta_n = 0 \quad (2-4)$$

Radial Equation

$$\frac{d^2 y_n}{dx^2} - \frac{1}{4} \left[1 - \frac{4}{h_n} (\kappa H(x) + \frac{dH(x)}{dx}) \right] y_n = \frac{\kappa J_n}{\gamma g h_n} e^{-x/2} \quad (2-5)$$

where

θ_n = Hough function

F = a complicated operator that is a function of θ , ω
and the tidal period (see Siebert, 1961)

g = acceleration due to gravity

a = earth's radius

ω = earth's angular rotation rate

$\kappa = (\gamma-1)/\gamma = 2/7$, for an ideal gas

γ = ratio of specific heats

h_n = separation constant. This will correspond to a
particular Hough function, θ_n , and by analogy with
ocean tidal theory is called the equivalent depth

x = a height coordinate in terms of atmospheric pressure

y_n = this gives the radial variations of the term

$-\frac{1}{\gamma P_0} \frac{DP}{Dt}$, chosen because of convenience in
calculations (L/C).

J_n = heating source.

2.6 Laplace's Equation

By expanding the Hough functions in sets of associated Legendre polynomials, and using the boundary condition that the θ_n must be bounded at the poles, (2-4) has been investigated (Longuet-Higgins, 1969).

By putting

$$\epsilon = \frac{4a^2 \omega^2}{gh_n} \quad (2-6)$$

and considering variations in ϵ , several asymptotic solutions were found by Longuet-Higgins (1969). These reveal two classes of interest here - gravity waves which propagate freely in the vertical, and planetary waves, which are evanescent in

the vertical direction. The general results of interest here are -

1. $\varepsilon \rightarrow$ positive zero, waves of both types are allowed, and appear over the entire globe

2. $\varepsilon \rightarrow$ positive infinity, waves of both types are allowed, being found mainly within an order of $\varepsilon^{-\frac{1}{4}}$ degrees (latitude), of the equator.

For $\varepsilon < 0$, solutions exist but all modes are evanescent in the vertical. Longuet-Higgins points out that these solutions are probably only physically significant in a forced system of oscillations.

3. $\varepsilon \rightarrow$ negative zero. The planetary waves are continuous with the planetary waves of 1. above.

4. $\varepsilon \rightarrow$ negative infinity. Planetary wave energy is concentrated within an order of $|\varepsilon|^{-\frac{1}{4}}$ degrees of the poles.

For the earth (2-6) becomes,

$$\varepsilon = \frac{14.4 \times 10^4}{h_n} \quad , \quad (2-6A)$$

and using this in the above results, estimates of the areas where waves of both types may be found can be made.

TABLE 2.1

α	5	10	20	30	40
$ h_n $	0.01	0.26	2.4	10	38

where α = distance from pole or equator in degrees

$|h_n|$ = magnitude of h_n in kilometres.

While Table 2.1 cannot be applied too literally, it is evident that small values of h_n will result in considerable latitudinal asymmetry, these waves being found near the poles ($h_n < 0$), or equator ($h_n > 0$).

2.7 Notation

1. Forcing function. Because of the predominance of thermal tides over gravitational tides, no differentiation between the two will be made here. Thus the forcing terms are

Solar tide - S

Lunar tide - L.

Because radio meteor observations are made over only a few days, it has been recommended that tidal periodicities in these records would best be identified as 'daily variations' or 'x-hour variations', with 'tide' being reserved for more specific identifications (Hines, 1970). For convenience, the word 'tide' is retained, but a specific mode will be written, for instance, \bar{S}_2 , to denote an experimental result.

2. Tidal period. Various tidal components are observed in the lower atmosphere, (i.e. Siebert, 1961). The different periods may be denoted S_σ where

$\sigma = 1$ 24 hour tide

$\sigma = 2$ 12 hour tide

$\sigma = 3$ 8 hour tide

$\sigma = 4$ 6 hour tide.

3. Spatial Distribution. In the solution of Laplace's equation Hough functions were used, each of which may be associated with a characteristic three dimensional distribution over a sphere. If a particular solution is given by S_σ^S , then where $S = -\sigma, -(\sigma-1), -(\sigma-2), \dots, -1, 0, +1, \dots, (\sigma-1), \sigma$.

an idea of its spatial distribution may be obtained from the following rules,

a) the number of longitudinal nodes is 2σ ,

b) the number of latitudinal nodes is $(\sigma-S)$,

These rules are not applicable for the diurnal tide, however, and a renaming of the modes would be required before their use - thus, the S_1^1 tidal mode would become the S_1^3 tidal mode. More complete distributions may be found in Lindzen, 1967 and L/C.

2.8 The Radial Equation

1. Solution. Two boundary conditions are required to solve for the particular solution of (2-5), the specification of J_n being required for solutions of the complementary function. That the vertical velocity should be zero at ground level is the lower boundary condition. Specifying the upper boundary has led to some disagreement but Wilkes' (1949) condition, that there be an outward flow of energy, and Siebert's (1961), that the kinetic energy in a column of air remains constant, are both acceptable, (L/C). However, both have limitations also, Wilkes' being unsatisfactory if dissipation occurs too rapidly with height as tidal energy may be reflected down (Yanowitch, 1967; Lindzen, 1968) and Siebert's being sensitive to the type of atmospheric top assumed in the calculations.

2. Vertical Transmission. Wilkes and Weekes (1947) treated

$$\beta = \frac{1}{h_n} \left(\kappa H(x) + \frac{dH(x)}{dx} \right) - \frac{1}{4} \quad (2-7)$$

as being analogous to a refractive index, reflections resulting for $\beta < 0$. In terms of this it is evident that:

a) all negative h_n will be evanescent, or non-propagating modes.

b) $H(x)$ and $\frac{dH(x)}{dx}$ must be large and positive, if h_n is large for $\beta > 0$.

It follows from b) that for a given temperature structure, modes with smaller h_n are more likely to be transmitted.

3. Vertical Wavelength. By transforming the height coordinates to kilometres, an approximate wavelength may be associated with each h_n (i.e. Taffe, 1969)

$$k_z^2 = \frac{1}{H(z)h_n} \left[\frac{dH(z)}{dz} + \kappa \right] - \frac{1}{4H(z)^2} \quad (2-8)$$

where k_z is the vertical wave number

$$= \frac{2\pi}{\lambda_z}$$

Two properties follow from this:

a) Large values of h_n correspond to large vertical wavelengths.

b) The wavelength is dependent on the temperature structure.

Both (2-7) and (2-8) supply the same information in slightly different contexts.

2.9 Forcing Term

Two major sources of thermal tides have been considered, (a) absorption by H_2O vapour in the troposphere (Siebert, 1961), and (b) ozone absorption in the stratosphere (Butler and Small, 1963), the more important source being (b). (Butler and Small, 1963; Lindzen, 1968a). Only those modes that are directly related to solar absorption are found to be important, these being ones for which $\sigma = S$, representing modes migrating with the earth's rotation rate.

As the tidal component follows the sun, wind vectors associated with the tide will rotate in a counter-clockwise direction^{in the southern hemisphere}. However, if the dominant component at a particular altitude is not due to direct heating, the above rotation may not be observed. Hines (1972), points out that the wind vectors need not exhibit this phenomenon, and clockwise (northern hemisphere) or counter-clockwise (southern hemisphere) rotation of wind vectors cannot be used to identify a tidal component.

In light of (2-8) above, it is reasonable to expect that for large λ_z the forcing function will be in phase over a large portion of a wavelength and thus will more efficiently excite the associated mode of oscillation. Conversely, for small h_n , corresponding to small λ_z , oscillations will be less efficiently excited. It also follows that a mode will be more efficiently excited if it fits the horizontal distribution of heating.

2.10 The Semi-Diurnal Tide

The most important component of the S_2 tide in the troposphere is the $S_{2,2}^2$ component. It has $h_n \approx 7.9$ km, implying a large vertical wavelength which will match the forcing function well, and its latitudinal variation fits the latitudinal heating function quite closely. Furthermore, because of a large vertical wavelength it will be insensitive to atmospheric variations. In this respect, Butler and Small (1963) relate seasonal variations of S_2 to seasonal variations of ozone. However, the $S_{2,2}^2$ mode is evanescent in the mesopause region, and what energy leaks through to meteor regions may be small in comparison with

higher order components, having shorter vertical wavelengths, (see table 2.2).

Rocket and meteor observations of \bar{S}_2 suggest that it is quite variable, and Hines (1963) showed that unacceptably large variations in the atmospheric scale height would be needed to produce the observed phase variations at Jodrell Bank.

TABLE 2.2

(h_n values from L/C)

Mode	$s_{2,2}^2$	$s_{2,4}^2$	$s_{2,6}^2$	$s_{2,8}^2$
h_n (km)	7.9	2.1	1.0	0.5

From Table 2.1 it is apparent that the higher modes, if present at meteor heights, will become more important at lower latitudes.

2.11 Diurnal Tide

Lindzen (1966), and Kato (1966) independently suggested that the inclusion of Hough functions with negative eigenvalues was necessary to completely describe the S_1 response to solar heating. From a model based on internal atmospheric gravity waves on a rotating flat earth it is possible to show that vertical propagation is inhibited if the wave frequency is less than twice the local vertical component of rotation, (L/C). From Sec. 2.6, this was expected, though the role of rotation was not emphasized. Applied to the S_1 tide, propagating modes would not be expected poleward of 30° latitude.

TABLE 2.3

(from L/R)

Mode	$S_{1,1}^1$	$S_{1,3}^1$	$S_{1,5}^1$	$S_{1,-1}^1$	$S_{1,-4}^1$	$S_{1,-6}^1$
h_n (km)	0.7	0.1	0.05	-12.0	-1.8	-0.6

From Table 2.3 for $h_n > 0$, it is evident that these modes will be found close to the equator, from Table 2.1. However, the $S_{1,-1}^1$ mode has a very large h_n , and its latitudinal and longitudinal distribution very closely matches that of the heating source. It would be expected that the $S_{1,-1}^1$ mode is the dominant S_1 mode, but being evanescent, it will not propagate away from the forcing region. These results explain the observed predominance of the \bar{S}_1 tide in Adelaide's meteor winds (latitude 35°S), while data from Jodrell Bank (latitude 53°N) shows a much smaller \bar{S}_1 tide.

The height structure of the diurnal tide can be expected to be very complex (Lindzen, 1967) because of the superposition of evanescent modes (that will have little effect outside the forcing region) and propagating modes both of which have differing latitudinal distributions. Added to this is the possibility that the diurnal tide will probably be unstable in the meteor region, at least at low latitudes. In relation to this, a possible explanation for the formation of the turbo-pause (the height above which turbulent activity plays a minor role to molecular diffusion) is that above this height, because of kinematic viscosity and heat conduction, the S_1 tide ceases to be unstable (Lindzen and Blake, 1971).

2.12 Other Tidal Modes

1. Lunar Tide. Because the forcing function in this case depends only on gravity, the lunar tide is of particular theoretical importance. However, it is not expected from theory (L/C) that this tide will give rise to wind velocities greater than 5 m/s as has been confirmed by observations (Greenhow and Neufeld, 1961).

2. Terdiurnal Tide. Butler and Small (1963) suggest that the \bar{S}_3 tide is mainly due to solar absorption by H_2O vapour, and ground level seasonal variations may be related to annual variations in the heating source. At meteor heights, \bar{S}_3 shows considerable variability, Greenhow and Neufeld (1961) suggesting it is significant only in yearly averages.

3. Six Hour Oscillations. Both eight and six hour oscillations are observed in equatorial pressure records, (Siebert, 1961), and Müller (1966) obtains an \bar{S}_4 component from meteor results, but notes that its significance is uncertain.

C. IRREGULAR COMPONENT

This component is considered in two sections -

- i) Gravity waves, ii) Turbulence.

Because of the low resolution of our system, these components will not be uniquely specified by our data, though they will collectively add to the observed scatter in results obtained. From Greenhow and Neufeld (1959), it is apparent that velocities of order 30 m/s can be associated with these components collectively.

2.13 Gravity Waves

Hines (1960) suggested that vertical and horizontal spatial scales, and time scales for irregular motions in the meteor region as observed by Greenhow and Neufeld (1959) could be explained in terms of internal atmospheric gravity waves. The high frequency limit for gravity waves is the Väisälä-Brunt frequency. This is the frequency of oscillation of a parcel of air displaced vertically in an atmosphere with a stable lapse rate - i.e. greater than the dry adiabatic lapse rate. If such a parcel is moved vertically upwards, in a density stratified fluid, then it will find itself in a region less dense than itself. A buoyant force thus acts downwards on the parcel, causing it to sink. With no damping forces present, the air parcel will exhibit simple harmonic motion about its equilibrium position with the Väisälä-Brunt frequency. All motion, in this case, is in the vertical direction. If the frequency of oscillation is less than the Väisälä-Brunt frequency, then buoyant forces will constrain the parcel's motion more and more to the horizontal, and the resulting motion will tend to be transverse to the direction of propagation. The low frequency cutoff for these waves occurs when rotational restoring forces exceed buoyant restoring forces, and was mentioned in connection with the S_1 tide - atmospheric tides being low frequency gravity-waves. The waves of interest here have periods of only a few hours. Considerable horizontal structure would be expected, i.e. from Hines (1960),

$$\frac{\text{Horizontal Wavelength}}{\text{Vertical Wavelength}} = \frac{\text{horizontal perturbation velocity}}{\text{vertical perturbation velocity}} = \frac{\text{Period of oscillation}}{\text{Väisälä-Brunt period}} . \quad (2-9)$$

where the Väisälä-Brunt ^{Period} is about 5 minutes, thus vertical variations = $\frac{1}{20}$ x horizontal variation.

The most important feature of gravity waves, and tides, is that the energy density remains constant with height, in the absence of dissipation, resulting in an increase in the wave parameters (i.e. the horizontal velocity component) according to $\rho^{-\frac{1}{2}}$. Thus, as the atmospheric density, ρ , decreases, the effects of the wave increase, making it an important feature of the upper atmosphere.

Another property of interest is that the group velocity, and hence the energy flow, is in the opposite direction to the phase velocity. Thus, the downward propagating phase observed for atmospheric tides in the meteor region may be associated with an upward energy flow.

Gravity wave interactions with the atmosphere are of two broad types.

1. Dissipation. For the region of interest, molecular dissipation processes will prove most important, though as ionization becomes greater at greater heights, more complicated effects can occur. The effects of kinematic viscosity and thermal conduction have been treated by several authors (i.e. Pittway and Hines, 1963), thermal conduction being found slightly more important.

Hines (1960) indicates that the basic effect of dissipation is to damp out the short wavelength waves, thus with increasing height, dissipation becomes more important and the waves left propagating will have longer and longer wavelengths.

2. Temperature and Wind Structure. Variations in atmospheric temperature structure can give rise to reflection and ducting of atmospheric waves (Pittway and Hines, 1965).

These are possibly important as the effects of a partially reflected wave have been reported (Revah, 1970), and the author suggests this is due to temperature effects in the lower ionosphere.

Wind structure may also reflect waves, but the processes are more complicated. From Hines and Reddy (1967)

$$\Omega = \omega - \underline{K} \cdot \underline{u} \quad (2-10)$$

where $\Omega \equiv$ the modified wave frequency in a coordinate system moving with the wind,

$\omega \equiv$ wave frequency in the absence of a wind

$\underline{K} \equiv$ horizontal wave number

$\underline{u} \equiv$ horizontal background wind.

The height at which $\Omega = 0$ is called a critical level though if \underline{K} and \underline{u} are in opposite directions this can never occur. The behaviour of gravity waves at a critical level (Booker and Bretherton, 1967) indicates that while a reflected and a transmitted wave may occur, there will also be a loss of momentum to the mean flow. In this way gravity waves may affect the mean atmospheric motion. This is taken further by Jones and Houghton (1972), who suggest that by interaction with the mean flow, a gravity wave could generate its own critical level - the resultant wind profiles being every bit as complicated as observed from rocket trails.

2.14 Turbulence

Turbulence may be defined as motions in the atmosphere which are non-propagating, dissipative, non-linear and, perhaps of most importance, are described most conveniently in terms of their statistical properties. While it is evident, from this definition, that the basic difference between waves

and turbulence is the ability a wave has to propagate an effect, in practice it is difficult to separate the two effects uniquely.

The major dynamic role of turbulence is the dissipation of energy and momentum in the atmosphere. The presence of turbulence in the meteor region was initially thought responsible for the considerable irregular motions observed. While gravity waves now appear likely to account for a substantial section of this, the expansion of rocket released trails, and meteor trails suggests it is still an important component to be considered.

Though turbulent parameters deduced from vapour trails are generally accepted in the literature (Blamont and Barat, 1967), there is some criticism of the methods used (Layzer and Bedinger, 1969). In obtaining turbulence measurements from velocity components at different points on a meteor trail (Roper, 1966) contamination of the results due to gravity waves would be expected. This experiment revealed that the irregular component had a seasonal variation comparable to the diurnal tide, which could relate these measurements to results obtained above on the S_1 tide at meteor heights.

The nature of turbulence in the meteor region is thus an open question, the most likely source being windshear, with gravity waves being a probable source of these. While it might be expected that molecular diffusion, which becomes increasingly important with increasing height, would damp out turbulent motions, the observed abrupt division between turbulent and non-turbulent flow is not easily explained (Low et al., 1969).

As neither turbulence nor gravity-waves will be resolvable, as such, with our equipment these problems will not be considered further.

2.15 Summary

It is convenient to treat the wind motions in the meteor region as a superpositioning of several different time scales, the spatial extent being limited at the same time. These may be summarized as follows:

1. The mean flow will show a seasonal variation consistent with a positive temperature gradient from the summer to the winter pole. The driving forces maintaining this general circulation pattern against the radiative energy influx are not well known, though the influx of dynamic energy from the lower atmosphere is a likely source.
2. The possibility of wind variations with periodicities of a few days (planetary waves) and over a six month period (semi-annual oscillation) is apparent in other wind measurements and could be expected in the present observations, though their role in the overall dynamics of the region are not obvious.
3. Of equal importance with the general circulation, are atmospheric tides. At 43°S the effects of the earth's rotation may be expected to inhibit the propagation of the S_1 tide from the forcing region, most likely in the stratosphere, but the S_2 tide would not be affected in this way and might be expected to be observed. As thermal heating due to the sun causes these observed tides, wind vectors, following the course of the sun, would be expected to show a counter-clockwise rotation with time.

4. Atmospheric gravity waves, which exhibit large horizontal variations because of the dominant effects of gravity, are expected to be of importance. By allowing for molecular dissipation and reflections due to temperature variations in the stratosphere, Hines (1960) showed that periods of an hour or two might be expected in the meteor region. However, until the source of these waves is better understood, their complete contribution cannot be estimated.
5. Atmospheric turbulence is also expected from the expansion of vapour trails, but its source is not clearly understood. The diurnal tide, wind-shears due to gravity waves either propagating freely or in the vicinity of a critical layer have all been cited as possible sources. The observation that turbulence ceases to be important at a well defined height does, however, place a considerable restraint on theories accounting for its presence below this level.

Because the general circulation, atmospheric tides and gravity waves are all expected to contribute to the wind spectrum with similar velocities, the observational problems involved in separating them will be considerable if only short lengths of data are procurable. Whether such a subdivision is valid is not obvious, and until a better idea of the possible interactions between the various components is available it must remain open.

C H A P T E R 3

EXPERIMENTAL WORK ON ATMOSPHERIC WINDS IN THE 80-110 KM REGION

3.1 Introduction

Information on atmospheric motions may be obtained by observing some tracer of the motion for sufficient time to allow the tracer's motion to be unambiguously defined. Provided the tracer follows the atmospheric motions, wind fields may be deduced from these observations. If this process is repeated at different points in time and space, a four dimensional picture of the winds will emerge, but because of the recognized non-stationary properties of atmospheric statistics, this picture can never be complete. However, the accumulation of sufficient data will allow the estimation of repetitive patterns in the motions, if present - for instance, seasonal variations or tides. In this context, "sufficient" will depend on the scale of motion being considered and its dominance over other scales of motion present.

Tracers may be subdivided into various categories. For the region of interest (80-110 km) several tracers, to be considered in later sections, are classified in Table 3.1.

Table 3.1 Classification of Wind Tracers

	Artificially introduced	Naturally Occurring
Direct	Rocket trails (i.e. Na, T.M.A.) Ejected sensors (i.e. falling sphere, chaff)	Noctilucent clouds Airglow Meteor trails (both radio and visual)
Indirect	Sound (Grenades)	Baroms Drifts of ionization irregularities (partial and total)

The term 'direct' suggests a close relationship between the tracer's motion and the neutral atmosphere's motion in contrast to 'indirect' where winds are inferred from physical arguments based on what an observed property would look like in the absence of any motions. Ionization drifts are included in this section because of doubts held on what motions they measure. These will be discussed later.

In the following sections, the tracers in Table 3.1 will be discussed, radio meteor methods being left to the last section. In all cases, it must be remembered that, in the region of interest, the tracer must be very light, otherwise gravity will dominate over the aerodynamic drag forces, thus distorting deduced wind motions.

A. ARTIFICIAL TRACERS

3.2 Falling Sphere

A rocket is used to release an inflatable (or rigid) sphere which, after inflation, is tracked until deformation in the lower atmosphere, due to increased pressure, occurs. Two basic types are used.

i) Passive Sphere. All information is gained from ground based observations of the sphere's trajectory.

ii) Active Sphere. Additional information may be obtained by including an accelerometer inside the sphere, which will be more sensitive to small changes in acceleration, than ground based observations.

From a knowledge of the sphere's drag coefficients, the various aerodynamic flow regimes it passes through and its flight trajectory, atmospheric densities (from about 100-140 km) and atmospheric winds (from below 80 km) may be estimated. Only horizontal winds are measured, any vertical winds being

interpreted as changes in atmospheric density by the analysis used. Errors arise in radar tracking, and in assigning the correct drag coefficients. Atmospheric winds are quoted as being typically in error by ± 3 m/s. For the 80-110 km region, this method is at the limits of its useful range, when applied to wind measurements, gravity dominating drag forces on the sphere. This system is mainly applied to atmospheric density measurements.

(Refs. Smith^{U.S.} 1969, Jones^{U.M.} 1967, Bollerman 1970).

3.3 Chaff

Rockets are used to release a quantity of plastic or metal whiskers with a typical length of 0.005 inches, which are tracked by ground based radar systems. A major problem with chaff is that after release it disperses over quite large regions of space making it unusable as a radar target, and because of a reduced descent rate in the more dense lower atmosphere, it will also present an interference problem for radars. Use over 85 km is limited by low drag coefficients, though results for atmospheric winds up to 95 km have been obtained. However, Bollerman suggests that though decreased chaff size is possible, the accompanying dispersion and slowed descent will probably be enhanced. (Refs. Bollerman 1970)

3.4 Chemical Trails

Trails are formed by emitting a thin trail of the tracer (Sodium (Na) or tri-methyl-aluminium (T.M.A.) usually) from a rocket on the upward, and on occasions the downward, legs of flight. The trail, initially at a high thermal temperature with respect to its environment, rapidly attains ambient characteristics. Trail life-time depends on the type of chemical, rate of release and altitude - for high altitudes,

the mean free path becomes large enough to prevent thermal equilibrium from being reached before the trail is too faint to observe.

Sodium trails are observed due to resonant scattering of sunlight and are observable only at dusk and dawn. T.M.A. trail emission apparently arises from chemical reactions with atomic oxygen, the exact process being little understood at present. The trail is chemi-luminescent, and may thus be observed at night, though it is not bright enough for daytime observations (Smith 1971). Because of the nature of their formation, these trails appear only above 90 km as chemi-luminescent trails, though T.M.A. has been used for smoke trails (Marshall, 1969). Data reduction involves reconstructing the trail in three dimensions by triangulation methods using photographs supplied from suitably placed camera sites. Time variations in the trail are then deduced for different heights, wind velocities and directions being obtained. Because it is trail shape that is traced, it is not possible to unambiguously define the actual wind field causing the deformation, and some assumptions must be made, the major one being the presence of horizontal velocities. ~~There~~ *is* Initial methods of reduction involved stereoscopic projections of the trail and identification of specific features. More advanced methods now involve fitting spline functions to the trails thus removing the more subjective decisions in identification, but still assuming no vertical velocities exist (Quesada, 1971). Accuracies of ± 3 m/s in wind velocity and ± 0.1 km in height have been quoted, but this may be a little optimistic in view of the data reduction problems (Smith 1971).

While the gross features of rocket trails are indicative of atmospheric motions, some controversy exists over the question of trail diffusion rates when interpreted as molecular or turbulent diffusion. Trail structure shows a distinct change in characteristics around 105 km, going from a disturbed region below 105 km in which the trail has been described as 'puffy' and 'stringy' to a region above this in which it is fairly smooth. This has been interpreted as a cessation of atmospheric turbulence at the turbopause, (Blamont 1961, 1967) though others (Layzer and Bedinger 1969) claim the effect is induced by the rocket and suggest that there is no turbulence in this region of the atmosphere. While not affecting the results for the observed winds, until the arguments are resolved, it will cast some doubts on deduced turbulent parameters.

3.5 Gun Probes

Chemical trails may also be laid by gun launched probes. The ability to place a target accurately in a given region and the lack of effect of local weather conditions on launching are the two chief advantages. However, the advantage of having a reusable launching mechanism is apparently offset by gun maintenance costs and the restrictions placed on payloads because of higher accelerations (Bollerman 1970).

3.6 Grenades

An explosive charge is ejected from a rocket as it travels upwards and the sound wave generated is recorded at ground based receiving stations. From directions of arrival, and arrival times, along with precise knowledge of the times and positions of several such explosions, temperature and wind

profiles may be obtained. For heights up to 85-95 km this technique is useful, but to extend it further will require the use of larger explosive charges and observation of lower frequencies in the 1 Hz range. The larger payloads, in comparison with chaff and falling sphere experiments, as well as the considerable ground based data collection and collation facilities make this a relatively expensive experiment. Errors increase considerably above 90 km, due to reduced signal returns, accuracies of ± 5 m/s being considered reasonable. (Refs Bollerman, 1970; Groves, 1968).

3.7 Summary of artificial tracers

All the methods above may be employed in the region 80-110 km with varying amounts of success. It is apparent that for other than atomic tracers, the aerodynamic drag forces are too small to reveal useful results. The only useful method, then, is the chemical trail.

It is possible to deduce wind-fields from observed temperature fields (Murgatroyd 1957) but this route is not explored here, as this will only be reasonably accurate for long term averages and probably of less value for the short-term measurements implied by the above methods.

It is also apparent that because of the expense and organization required routine measurements by any of these methods are unlikely. Add to this the present time restrictions placed on chemical trail methods, being possible only from dusk to dawn, and it is apparent that alternative methods may be required.

B. NATURALLY INTRODUCED TRACERS

3.8 Optical Methods

1. Noctilucent Clouds. Because of limited height and latitudinal coverage as well as limited occurrence, these are of limited value for wind measurements. However, they do reveal striking wave motions in the atmosphere often showing waves moving in the opposite direction to the bulk motion of the clouds (Witt 1962).

2. Optical Meteor Trails. Again, a rare feature in the atmosphere, it is possible, if such a trail is photographed from two or more separate camera sites, to interpret the distortions that occur in the observed trail as being due to atmospheric motions. Reversals in wind direction over small vertical distances have been deduced from such observations (Liller and Whipple 1954).

3. Airglow. Although the oxygen 5577⁰Å line, coming mainly from 100 km, is observable over the entire globe, and thus a potentially useful tracer, the exact interpretation of observations of isophote motions is in doubt, and thus it is not possible to deduce unambiguous horizontal velocities (Kent 1970).

None of these three methods is thus used for systematic wind measurements.

3.9 Ionospheric Drifts

1. Introduction.

Radio waves reflected, either totally or partially, from ionization irregularities in the upper atmosphere produce a moving diffraction pattern on the ground from which wind motions may be deduced. Here it is the irregularities that are used as a tracer of atmospheric motions.

The diffraction pattern is usually observed by three or more spaced aërials, but because of its fading properties, the data reduction is not simple. In effect, the illuminated ionosphere is a moving, four dimensional, random diffraction screen which gives rise to an angular spectrum of superimposed waves that in turn form the fading pattern at the ground. By sampling only a portion of the pattern in time, or by using total reflections, a small height segment of the results of this screen may be sampled at the ground. The fading pattern at each of the aërials is thus a combination of wavefronts with differing phases. However, because the diffraction pattern may also vary in time, the wavefronts will only be similar - not the same.

2. Analysis

There are varying degrees of complexity in the analysis of these records. The two most generally used are:

a) Similar Fades: The time delay between similar features in the wave amplitude fading patterns for the aërials may be estimated and a velocity for the moving pattern deduced. If it is assumed that the pattern only varies slowly with time, then this velocity may be associated with the velocity of the irregularities giving rise to the pattern, and in turn, with the neutral atmosphere in which the irregularities are imbedded.

b) Correlation Analysis: Properties of the diffraction screen are discussed in Ratcliffe, 1956, in which it is shown that the autocorrelation function of the complex amplitudes of the ground pattern will be the same as the autocorrelation function of the complex amplitude distribution over the diffraction screen in the ionosphere. Using cross-correlations

between receivers it is possible to compute velocities from the time delays between the functions which are no longer so dependent on variations in the pattern (Refs Kent 1971).

3. Problems

Two problems have been suggested in interpreting the observed velocities.

a) The point source effect: In diffraction theory, if the moving screen is illuminated by a point source (i.e. by spherical wavefronts) the observed velocity at the ground will be twice that of the screen in the ionosphere. On experimental grounds, Wright (1968) suggested this factor may be incorrect. However, the retention of the factor of 2 is required by theory, and later experiments (Felgate 1970) show it is also required experimentally. Further experimentation (Golley and Rossiter, 1970) showed that if the aerial separation was smaller than the irregularities of the diffracting screen, then the deduced velocities would be lower than the true velocities, constituting a possible explanation for Wright's observations.

b) Irregularity Formation: If the irregularities forming the diffraction screen are formed by atmospheric waves then the deduced motion will be that due to the wave rather than the neutral atmosphere (Hines, 1960). Furthermore, because some filtering ^{of the waves} by lower atmospheric winds is expected, the wave spectrum forming the irregularities may have a preferred direction and averaging of results might be expected to reveal this direction rather than the neutral wind direction.

However, comparisons of drift methods with other systems show quite good agreement. (See Kent and Wright 1968 for discussion.) It has been suggested (Hines 1968), that rather

than atmospheric waves forming the irregularities, they could be a result of dissipation of gravity waves as they reach their critical levels in the local wind fields.

The mechanism for the formation of the irregularities, and hence the diffraction screen, is still uncertain, and so the drifts method for wind measurements should be regarded as an indirect method.

(Refs Kent and Wright, 1968).

3.10 Baroms

Recent ground observations of naturally occurring infrasonic sound waves, called microbaroms, in the frequency range 0.1 to 1 Hz, have shown these could be possible tracers of the upper atmosphere. It is suggested that, although the height resolution is poor, because variations in intensity of these waves can be explained in terms of high altitude wind reversals, they could prove a cheap probe. (Ref. Donn and Rind, 1972)

3.11 Radio Meteor Observations

The range variation of an ionized trail, left by a meteor, may be tracked by radar, the most accurate results being obtained if a phase coherent system is used. The change in range of the trail will be due to atmospheric winds, the trail moving with the local atmosphere, thus direct measurements of the atmospheric winds can be carried out by detecting radio meteors. Some features of the trail formation, detection and origin are of relevance to these results, and are considered briefly.

1. Trail formation. A meteoroid is a solid object moving in interplanetary space. When such an object enters the Earth's atmosphere it is heated, by collisions with

atmospheric molecules, and if sufficient heating occurs, the meteoric atoms will ablate. The ablated atoms, with velocities of the order of 40 km/s, will have a much greater kinetic temperature than the local environment and ^{the trail} will expand rapidly for the first millisecond, ^{the atoms} undergoing collisions with atmospheric molecules which result in the formation of an ionized trail behind the meteoroid. When thermal equilibrium is established, the subsequent ambi-polar diffusion is much slower and depends on the meteoroid height. The trail radius, when thermal equilibrium is considered to be established, is referred to as the initial radius, and this becomes larger as the atmospheric mean free path increases with increasing altitude.

Maximum ionization of the trail formed will occur at an atmospheric density, ρ_a , given by the classical theory (Kaiser, 1953) as

$$\rho_a = Z \cdot \frac{m^{1/3} \cos \chi}{v^2} \quad (3-3)$$

where m = meteoroid mass before ablation starts

χ = zenith angle of meteoroid trajectory

v = meteoroid velocity before ablation (km/s)

Z = constant of proportionality.

Z depends on: (a) the meteoroid shape, density and heat transfer properties; (b) ionization probability for collisions of ablated atoms with atmospheric molecules, and (c) the atmospheric scale height. This indicates the effects of m , χ and v , being the more variable parameters in the trail location.

2. Height distribution of trails. The mass distribution of material incident on the Earth's atmosphere follows a power law of the form

$$N \, dm \propto m^{-s} \, dm \quad (3-4)$$

where N = number of meteoroids in the mass interval m to $m + dm$

s = mass power law exponent.

For sporadic meteors $s \approx 2.0$, (Kaiser, 1962), is the accepted value. If (3-3) is considered in the light of (3-4), it is apparent that the peak in the height distribution for observed meteors will be strongly weighted towards the height at which the smallest detected meteors occur. It is thus possible to get a reasonable estimate of this peak's height by only considering the height for the smallest detected return. The height for maximum ionization, h , is given by McKinley (1961) as

$$h = 82 + 49 \log_{10} v - 4.4 \log_{10} q \quad (\text{km.}) \quad (3-5)$$

where q = electron line density, (electrons/m)

the electron line density being directly proportional to the meteor mass (Kaiser, 1953).

3. Meteor radiants. Two points of importance above are λ and v - the meteor zenith angle and velocity, both of which are modified by the Earth's rotation and orbital motion. Observed meteor velocities show a spread of 20 to 70 km/s with a broad peak around 40 km/s.

The radiant for a meteoroid is defined as the point at which a backward projection of the meteor trajectory meets the celestial sphere, and is measured with respect to the

local vertical

by λ . A meteor shower is a group of meteoroids with a common orbit, and hence a common radiant. However, for wind measurements, sporadic meteors will more normally be used, these not being associated with a common radiant.

The radiants of sporadic meteors may be considered randomly distributed over the celestial sphere if the earth is stationary in space. Because of the earth's motion around the sun there will be a concentration of radiants and an increase in meteoroid velocity in the direction of the apex of the earth's way. Added to this is the earth's rotation on its axis, which produces a diurnal variation of the apex with respect to a fixed point on the earth. These two effects modify the observed meteor rate and observed velocity distribution so that:

a) a maximum rate is observed at about 0600 L.M.T., the minimum being at about 1800 L.M.T.

b) meteoroid velocities will be higher near 0600 L.M.T. than 1800 L.M.T.

In (3-5), it is evident that a diurnal variation in the ^{distribution} velocity_A will produce a diurnal variation in the height distribution of observed meteors.

4. Trail detection. The ionization of the meteor trail will reflect radio signals, the reflected power being dependent on the ionization in the trail. For the present purposes, two major classifications are important.

(a) Underdense: If the electron density of the trail is low enough for the Born approximation to be used - that the incident and scattered electric fields on an electron in the trail are independent of the electrons position in the trail - then from McKinley (1961)

$$P_R = 2.5 \times 10^{-32} P_T G^2 \left(\frac{\lambda}{R}\right)^3 q^2 \cdot \frac{1}{2} [C^2 + S^2] \text{ watts} \quad (3-6)$$

where G = aerial gain
 λ = operating wavelength (m)
 P_R = received backscatter power (watts),
 P_T = transmitted power (watts),
 R = range to the trail (m).

C and S are Fresnel integrals and equal unity if the trail is assumed infinite in length. For a trail to be observed, it must be specular to the transmitted signal. Trails with all the above characteristics are called under-dense, or decay type echoes. As the trail expands the transverse trail dimensions, assumed negligible in the above derivation, become important. From McKinley, the observed reduction in P_R is

$$P_R(t)/P_R(0) = \exp[-32\pi^2 D_a t/\lambda^2] \cdot \exp[-8\pi r_0^2/\lambda^2], \quad (3-7)$$

where D_a = ambipolar diffusion coefficient (m^2/s),
 r_0 = initial radius of the trail (m),
 t = time (sec.).

From (3-7) it is evident that for a large r_0 , the initial amplitude will be considerably reduced. A further loss of initial amplitude will result if the meteor fails to cross the first Fresnel zone before diffusion effects cause the trail to expand by $\lambda/2\pi$ meters, this being the finite velocity effect. From McKinley, (1961) these three effects, diffusion, initial radius and finite meteoroid velocity produce a total loss,

$$\text{loss in dB} = 970 \frac{R^{\frac{1}{2}} D_a}{\lambda^{3/2} v} + 343 \left(\frac{r_0}{\lambda}\right)^2. \quad (3-8)$$

For a particular wavelength, this gives an echo ceiling above which there will be a considerable reduction in the number of observed meteors.

(b) Overdense: If the ionization is great enough for secondary scattering by electrons in the trail to become important, (3-6) is replaced by (3-9) (McKinley, 1961)

$$P_R = 1.6 \times 10^{-11} P_T G^2 (\lambda/R)^3 q^{\frac{1}{2}}. \quad (\text{watts}) \quad (3-9)$$

Such trails are termed overdense or persistent. Normally these trails are of less use for wind measurements as atmospheric winds can deform the trail, resulting in several interfering specular reflections, before the electron density in the trail reduces sufficiently, making it underdense, thus allowing the height to be estimated from (3-7). It is possible, however, that an overdense trail will expand rapidly enough to become underdense before wind deformation becomes important.

5. Types of radar systems used. Two broad modes of operation are possible - a) continuous wave method, in which a few hundred watts power is radiated continuously and a narrow bandwidth receiver, at a separate site, records the return echoes; and b) coherent pulsed method, in which larger amounts of power (of the order of a kilowatt or more) are radiated in short bursts, a receiver at the same site being used to record any returns. Although the two systems are equivalent with regard to the information obtainable, problems associated with operating two sites and the high number of spurious echoes received from aeroplanes has led many experimenters to use coherent pulse modulated radars in preference to continuous wave methods (i.e. Nowak, 1967). It was pointed out by McKinley (1961) that both frequency and phase modulated systems would accomplish the same results, the choice of pulse modulation possibly being a product of popularity rather than necessity.

a) Continuous Wave Systems: Various continuous wave systems have been, and are being used.

Stanford: The first published meteor wind results were obtained at Stanford (Manning, Villard and Peterson, 1951). A half-wave dipole a quarter of a wavelength above ground was used as the transmit aerial. Only echo azimuth and wind velocity were recorded and from the results it was shown that a consistent wind which was predominantly horizontal was present at meteor heights.

Adelaide, Australia: Initially this consisted of a 26.77 MHz, 250 W transmitter and three receiving aerials (horizontally polarized dipoles), which gave the echo height and line of sight drift velocity. By periodically retarding the ground-wave phase by 90° the sense of the frequency change in the returned echo could be detected. Ranging was accomplished by periodically increasing the transmitter power to 4 kW for 10 μ S. Later additions of a series of out-stations for atmospheric turbulence studies is reported by Roper (1960).

All data was recorded on photographic film and reduced by film readers.

Ref. Huxley (1956), Elford (1968).

Garchy, France: Here the transmitter is situated at Garchy and the receiver at Sens-Beaujeu, 30 km away, a region approximately 150 km east-west and 80 km north-south being observed in the meteor region. Accuracies are given as, direction of arrival 0.2° , distance 0.3 km and velocity 1 m/s. All observed parameters are deduced from phase comparisons and recorded on photographic film.

(Ref. Revah, 1969).

College, Alaska: All parameters are deduced from phase comparisons and are recorded on magnetic tape for automatic data analysis (Hooke, 1970).

b) Pulse Modulated Systems:

Jodrell Bank, England: Using a common transmit/receive aerial system pointed alternately in two orthogonal directions, average wind components could be deduced. The radial velocity of the meteor trail was obtained from a phase comparison, heights from the amplitude decay of the echo and range from the time delay of the returned echo pulse. All information was recorded on photographic film.

This particular station design has been duplicated at many other sites, and is the basic design for the equipment discussed in this thesis. Russian stations are apparently all of this design.

(Refs Greenhow, 1954; Lysenko, 1969; Zadorina, 1967.)

Sheffield, England: Also of the Jodrell Bank design, this now has the added capabilities of measuring heights and echo azimuth.

(Refs Müller, 1970; Müller, 1972).

Stanford, U.S.A.: The Mark II system developed at Stanford was recommended as an international prototype standard at the 1971 ^{I.U.G.G.} meeting in Moscow (Barnes, 1972). The major advantage here is the automatic recording of all information. Heights are measured by echo decays, though on site calibration by a separate system could be used. Ranging is accomplished using a phase modulated pulse, giving 1 km accuracy. Phase information, for radial velocities, was obtained from one phase output offset by 40 Hz - thus allowing both direction and velocity to be measured at once.

(Refs Nowak, 1967; Nowak et al., 1970)

This summarizes the types of system in use for measurements of meteor winds. Because of the large quantities of data that must be recorded to obtain useful wind determinations, it would seem that an automatic recording system would be a considerable advantage, though the associated problems of echo identification ^{would} need some thought.

3.12 Discussion

Of the systems summarized, it is evident that for the atmosphere above about 90 km tracers of atmospheric motion will need to be of atomic, or molecular, size to allow accurate interpretation of results. Furthermore, the tracer must be usable at any locality and at any time, if independent observations are to be made. While vapour trails, ionospheric drifts and radio meteor trails all satisfy the requirements to some extent, it is difficult to obtain drift measurements at night-time, or use vapour trails in the day-time. Meteors are available at all times of the day, though the diurnal variation in meteor rate, having a minimum in the evening, can place limitations on this method if the system sensitivity is not good enough - this will depend on the power output for a given system.

In view of the scales of motion discussed in chapter two, it is evident that observations over half a day will probably be considerably contaminated by tidal components, thus complicating the determination of a mean flow. Single rocket shots might also be expected to be contaminated by gravity wave components of motion, further complicating analysis. Furthermore, the presence of wind velocity periodicities of

several days will contaminate longer data records that might otherwise be used to separate the effects of the previously discussed components.

For a satisfactory knowledge of upper atmospheric motions routine measurements must be made. While such measurements may be made using radio meteors, the small height region over which meteors may be observed considerably reduces their effectiveness, and associated data analysis problems will remain, until fully automatic recordings are made.

Of the other systems discussed, ionospheric drifts, and in particular partial drifts (Fraser 1968) appear very useful, at least for monthly averages. Vapour trails, while giving considerable detail about fine structure in the atmosphere, are expensive and unlikely to be used on a regular basis.

The rest of this thesis will be devoted to the radio meteor method of measuring atmospheric winds.

C H A P T E R 4

THE APPARATUS

Introduction

A coherent pulsed radar operating at a frequency of 27.12 MHz was connected to a rotatable aerial consisting of two six element yagis mounted 0.6 wavelengths above electrical ground. Connected to the same aerial via a transmit-receive switch is a receiver consisting of a pre-amplifier, mixer and intermediate frequency amplifier tuned to 1.62 MHz, a videostage and a phase sensitive detector. The phase and amplitude information from the phase sensitive detector and I.F. amplifier are displayed on a four beam "Tektronix" oscilloscope, the display being photographed using a camera. Activation of the oscilloscope time-base sweep, and triggering of the camera were accomplished using a discriminator that allowed only signals of a required pulse length, amplitude and pulse period to be recorded. Further radio frequency noise spikes were suppressed using a blanking channel tuned to 1.9 MHz in parallel with the I.F. channel.

4.1 Choice of Equipment Parameters

1. Wavelength. As indicated by Nowak (1967), the choice of an operating wavelength for meteor winds observations using underdense returns depends on:

i) the phase variations due to the drifting trail and the expected trail duration for a given wavelength.

$$\text{i.e.} \quad \frac{T}{S} = \frac{v_r}{8\pi^2 D_a} \lambda \quad (4-1)$$

where T = echo duration (secs)

v_r = radial component of the wind velocity (m/s)

λ = operating wavelength (m)

S = time for the trail to drift a distance of $\frac{\lambda}{2}$ metres (secs).

ii) the length of the first Fresnel zone - wind variations over this length should be as small as possible. Greenhow and Neufeld (1959) indicate that wind velocities with vertical separations of 2.5 km have a correlation coefficient of 0.5. Thus, length of first Fresnel zone = $\sqrt{2\lambda R} < 2.5 \times 10^3$ (4-2) where $R \equiv$ range to specular point (m), is required as an order of magnitude approximation.

iii) the received power from a train and background radio frequency cosmic noise. Assuming a $\lambda^{2.3}$ dependence of cosmic noise, this gives a signal to noise dependence of $\lambda^{0.7} q^2$ where q is the electron line density. For a given signal to noise ratio

$$\text{Meteor rate proportional to } \lambda^{0.35} \quad (4-3)$$

iv) the meteor traversing the first Fresnel zone before diffusion effects become too great thus

$$\lambda^{1.5} > 223 D_q^{\frac{1}{2}} v_m^{-1}$$

where $v_m \equiv$ meteor velocity. (4-4)

If the following representative values are used, $v_r = 20$ m/s, $R = 2 \times 10^5$ m, $v_m = 3 \times 10^4$ m/s, $D_q = 5.08$ m²/s for a height of 95 km, the above expressions become -

$$(4-1) \quad \frac{\text{Duration}}{\text{Drift period}} = \frac{1}{20} \lambda$$

$$(4-2) \quad \lambda < 16 \text{ m; frequency} \approx 18 \text{ MHz}$$

$$(4-4) \quad \lambda > 7 \text{ m; frequency} \approx 43 \text{ MHz.}$$

Further restrictions will be placed on the selection of an operating wavelength by D-region absorption, local r.f. interference and the wavelengths available for use. The wavelength used was 11.05 m (27.12 MHz), lying roughly in the middle of the desired wavelength range above.

2. Pulse period, T. The major considerations in choosing the pulse period will be:

i) an unambiguous range determination for the train observed,

$$\text{i.e. period, } T > \frac{2R}{c} \quad (4-5)$$

where c = the speed of light in free space = 3×10^8 m/s

ii) that the shortest phase variation due to atmospheric winds will be resolved,

$$\text{i.e.} \quad T < \frac{\lambda}{8v_r} \quad (4-6)$$

if one pulse is allowed for a 90° change in phase.

If the following representative maximum values are used, $R = 6 \times 10^5$ m, $v_r = 200$ m/s, then the above expressions become

$$(4-5) \quad T > 4 \text{ millisecs}$$

$$(4-6) \quad T < 6.9 \text{ millisecs.}$$

Note: The effects of height have been considered in the choice of an operating wavelength, and it is of secondary importance in choosing the pulse period, the resolution of the phase information being the important parameter here. If the train duration is too short to allow the phase information to be measured, the height of the train will be of no consequence.

A pulse period of 6.6 milliseconds was chosen being in the required range and compatible with available equipment.

3. Pulse duration. Two considerations of importance here are:

- i) the required range accuracy of echoes;
- ii) the power output characteristics of the valves in the final amplifier of the transmitter.

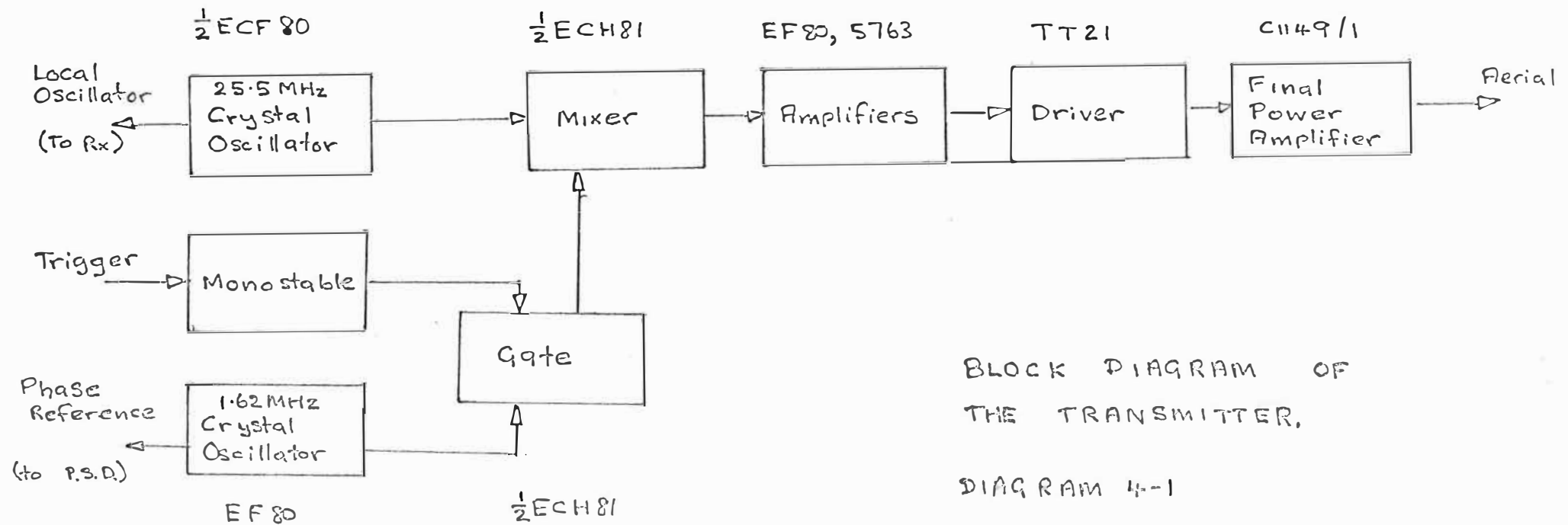
While as small a pulse width as possible will be desirable, the peak anode current allowable in the output valves will place a limit on this. A choice of 66 μ S was found convenient, giving a range uncertainty of ± 10 km and a duty cycle of 0.01 for the transmitter.

4.2 The Transmitter

This was constructed in the electronic workshop, and the author was concerned mainly with its use.

The low power stages consisted of a 1.62 MHz crystal oscillator, the output of which was pulse modulated by an externally triggered monostable and mixed with the output of a 25.5 MHz oscillator. The resultant higher frequency component (27.12 MHz) was amplified through several stages and transmitted (see diagram 4-1). In addition, the receiver local oscillator (25.5 MHz), and the phase sensitive detector phase reference (1.62 MHz) were also obtained from the crystal oscillators.

The power output limitations of the transmitter are defined by the characteristics of the final amplifier valves. As water cooled valves were not wanted, and the peak pulse powers used were to be 10-50 kW, Mullard type C1149/1 valves were found to be a convenient choice for the final power amplifier stage. The final P A. consists of four class C, push-pull amplifiers in parallel, thus for the valves and duty cycle chosen, the maximum average output power will be 480

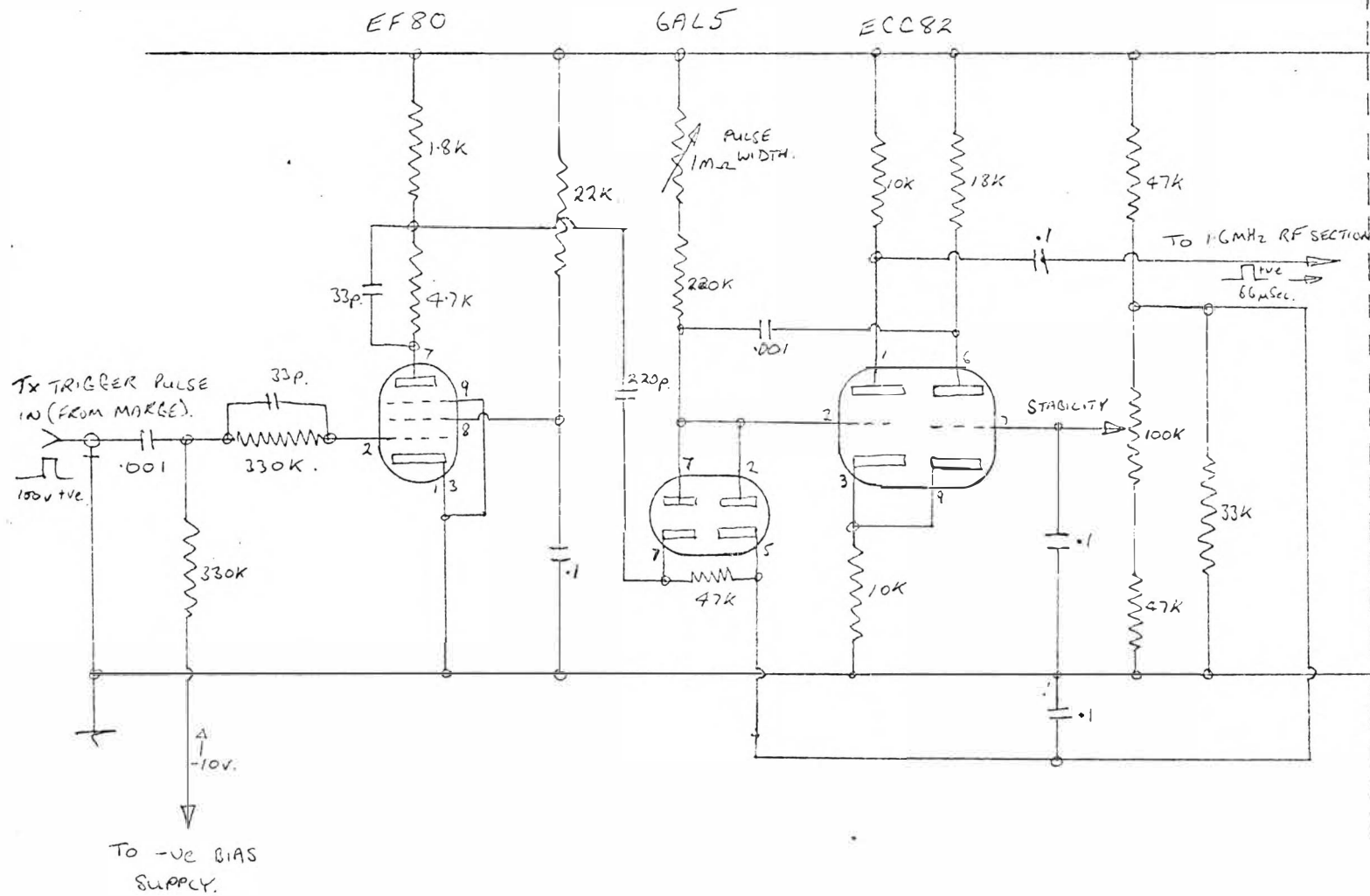


BLOCK DIAGRAM OF
THE TRANSMITTER.

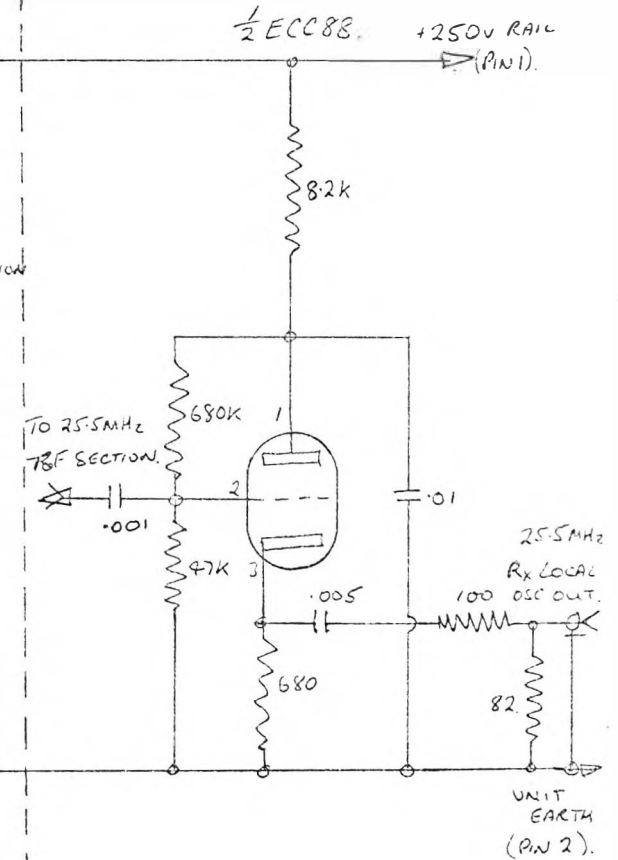
DIAGRAM 4-1

27.12MHz Tx - PULSE CIRCUITS

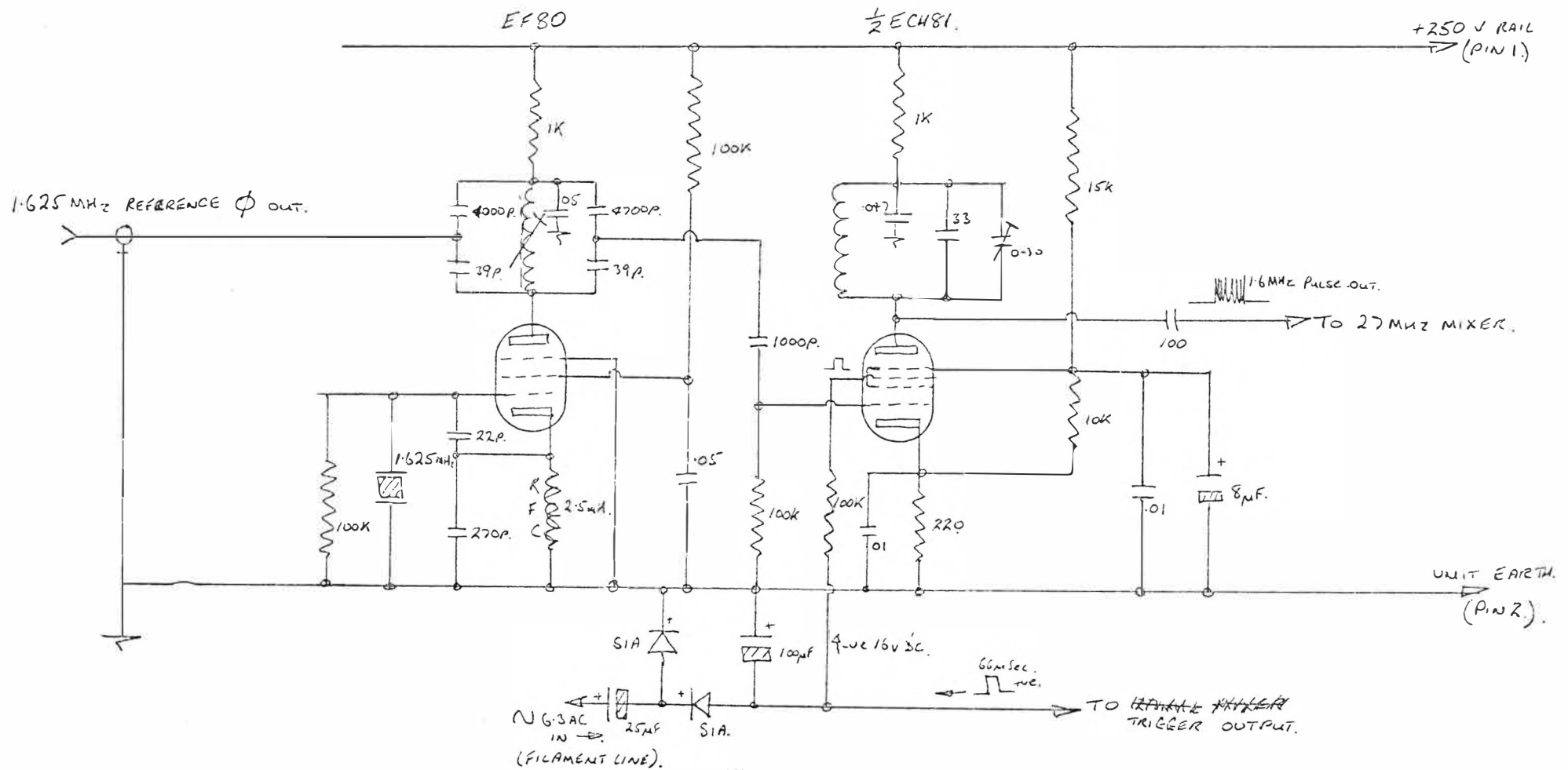
TRIGGER CCT.



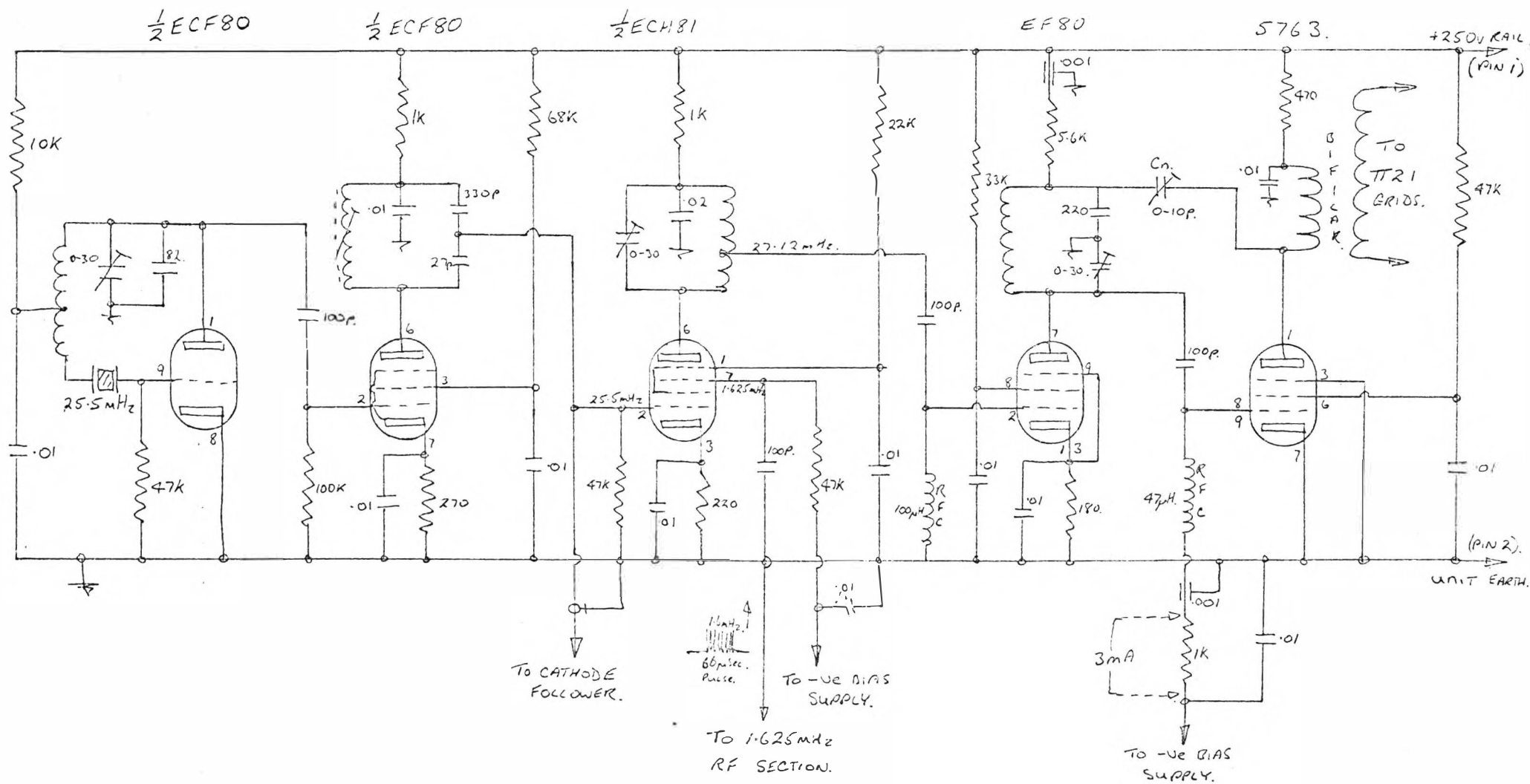
CATHODE FOLLOWER



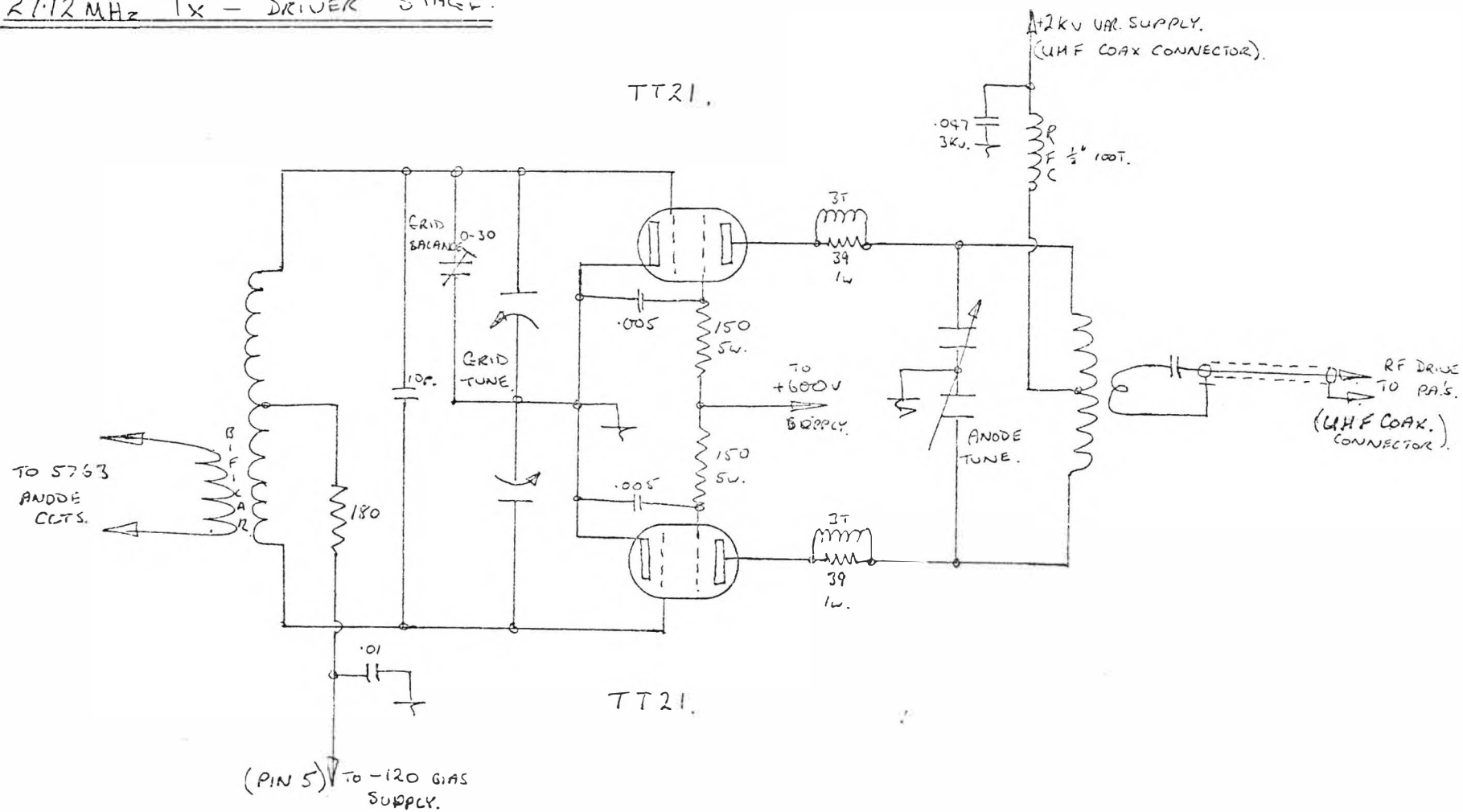
27.12 MHz TX - 1.625 MHz RF SECTION



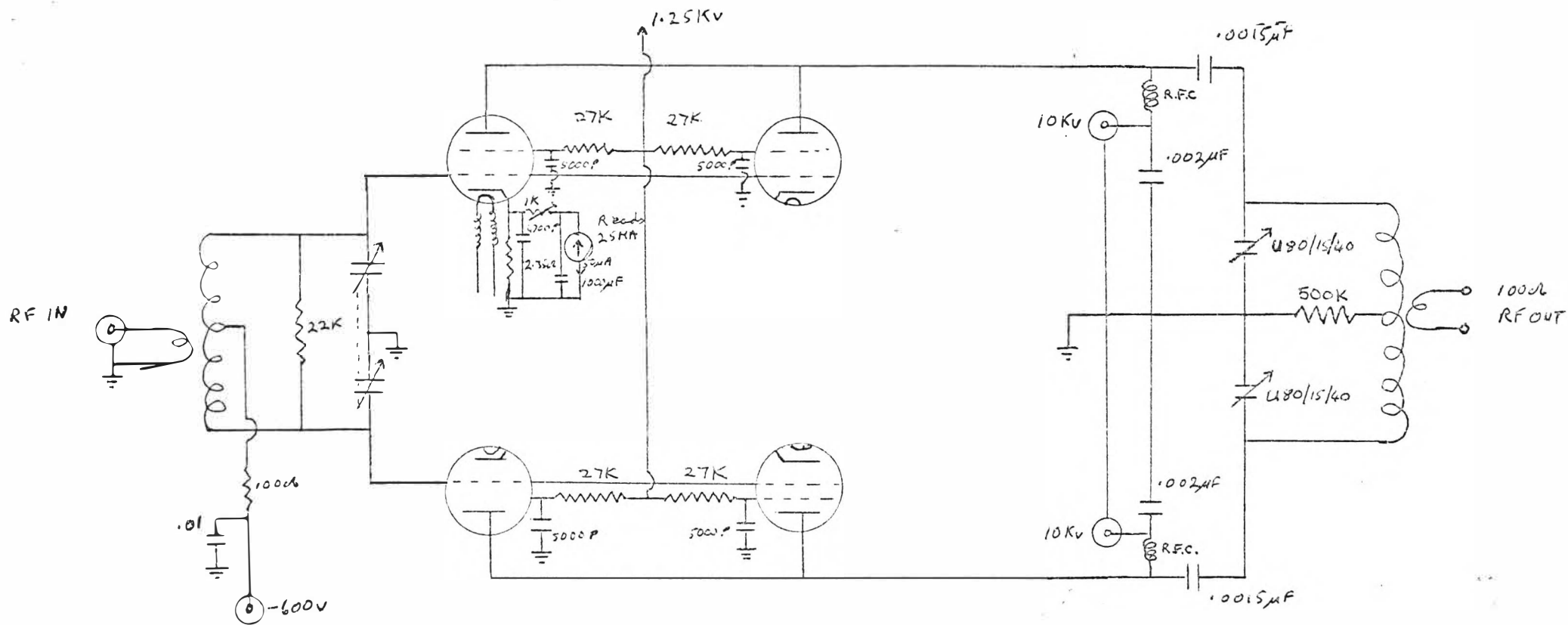
27.12 MHz TX - RF SECTION - 25.5 MHz to 27.12 MHz



27.12 MHz Tx - DRIVER STAGE.

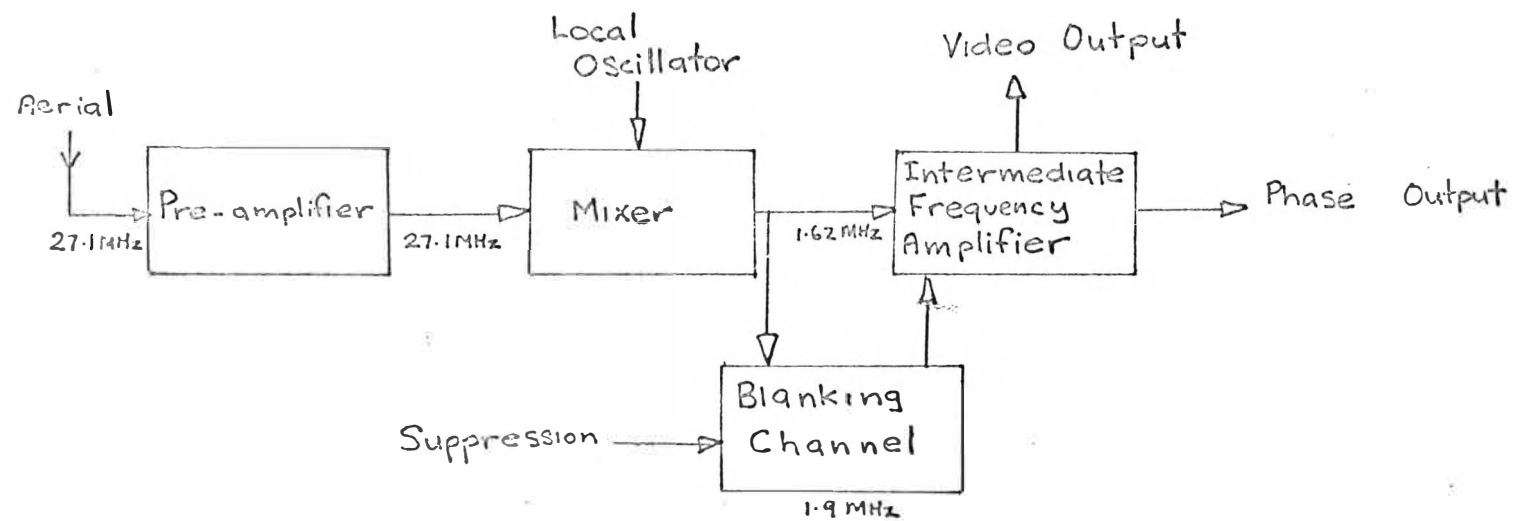


P.A. Stage



C1149/1

F.K	F.
O	O
(
O	O
G:	G2



BLOCK DIAGRAM OF THE RECEIVER.

DIAGRAM 4-2

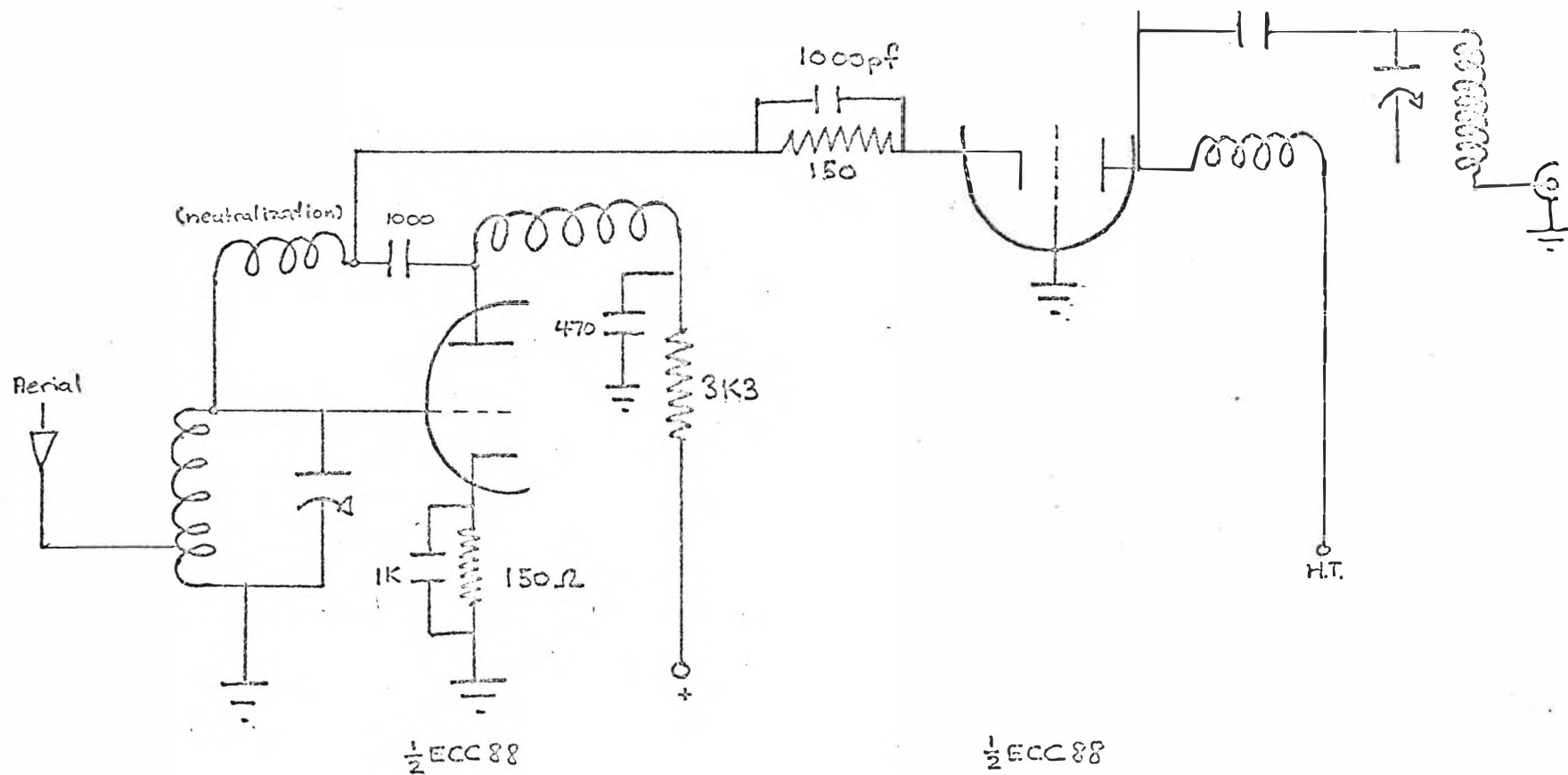


DIAGRAM 4-3

27 MHz PRE-AMPLIFIER.

DIAGRAM 4-4

27 MHz RECEIVER MIXER.

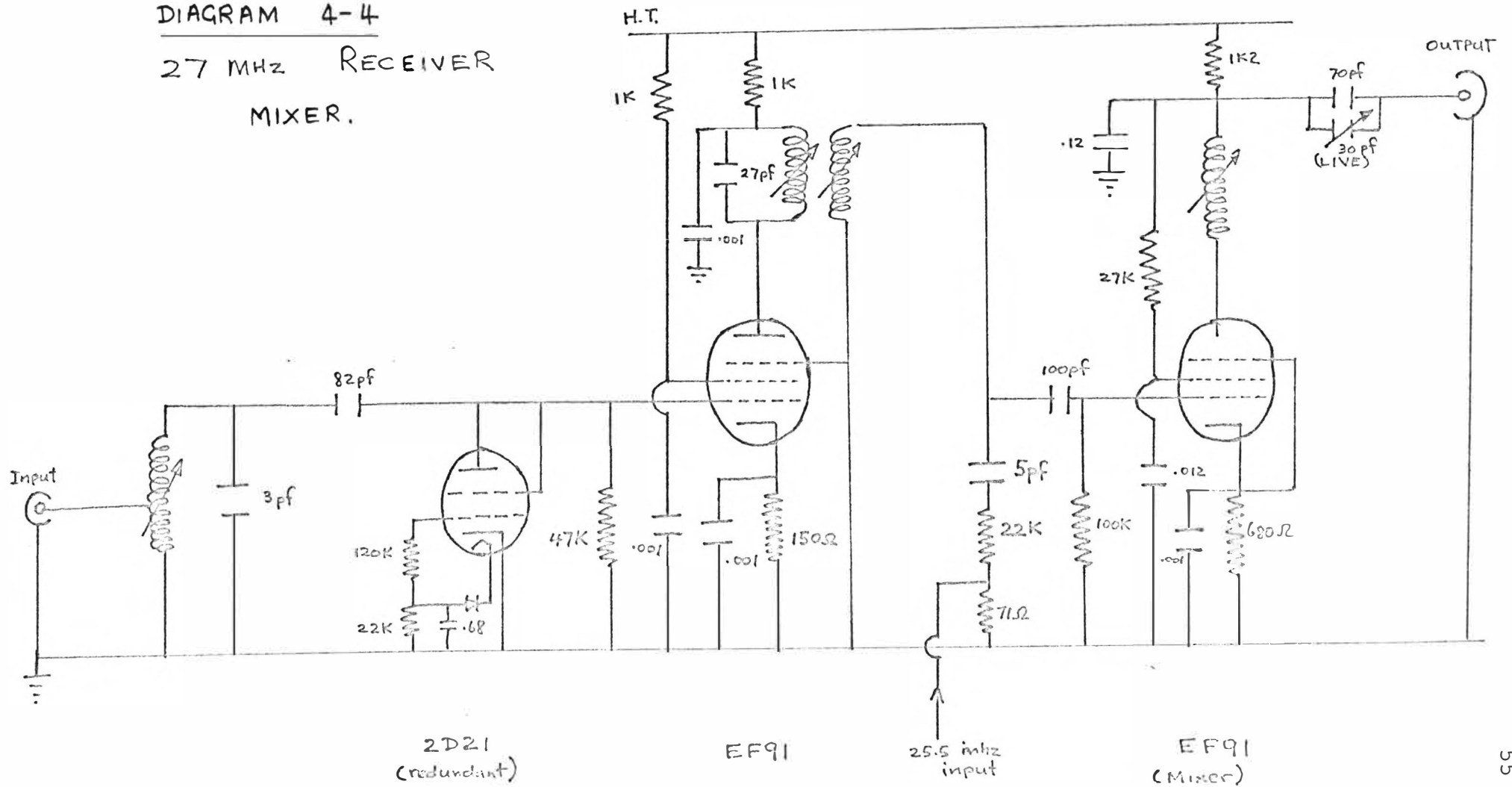
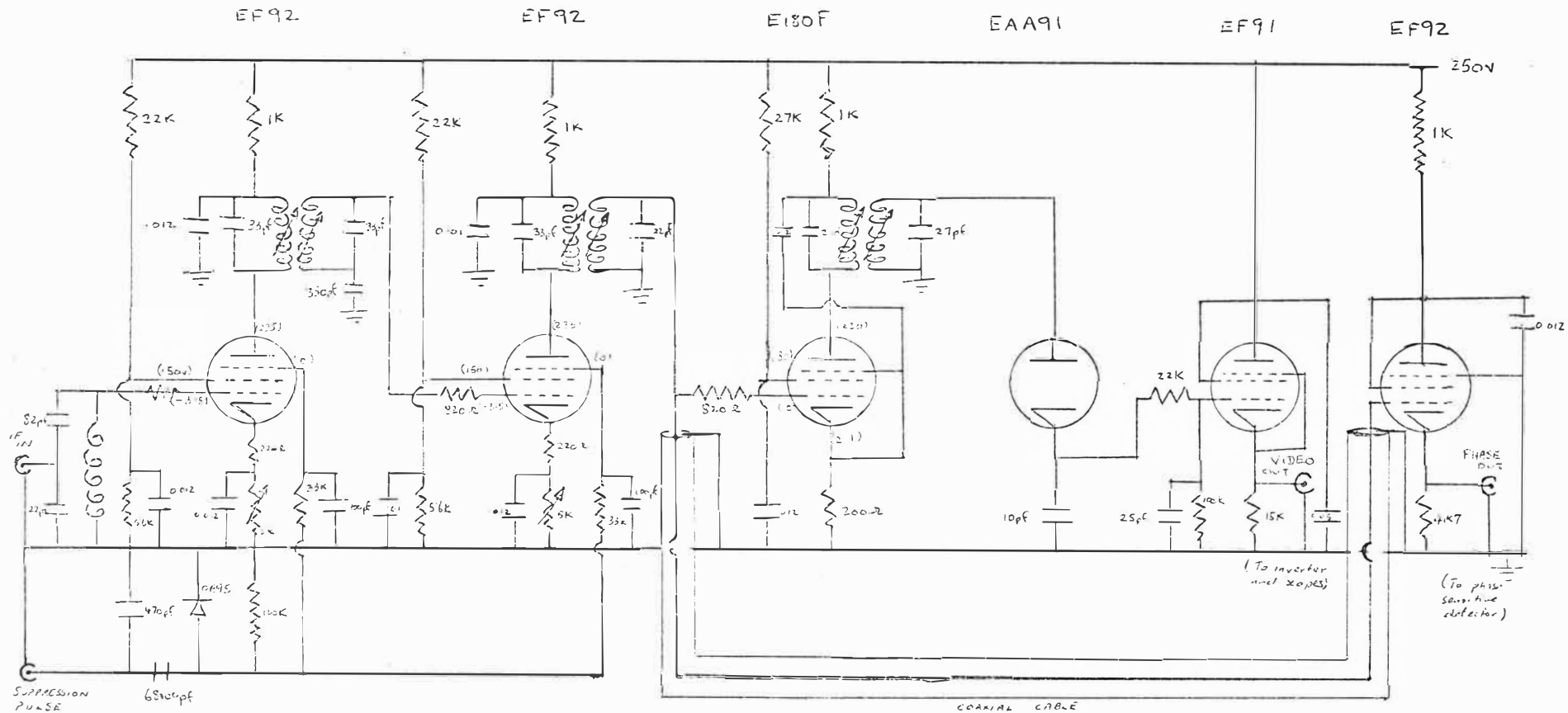


DIAGRAM 4-5

IF SIGNAL CHANNEL 162MHz



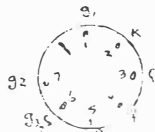
SUPPRESSION
PULSE

(from
H.A.G.C.)

8202 - reduces gain.

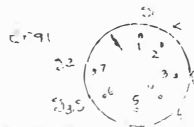
the voltages measured from ground are given in brackets.

EF 3.2

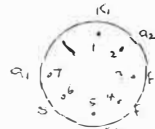


ERB EISOF

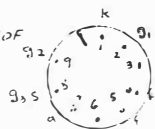
Pin ① connected to pin ⑤
Pin ① and ⑤ are interconnected.
Pin ⑥ connected to ground.



CAA91



E 180



is a internal connection

watts, being limited by the anode dissipation. This lies within the limits set by the peak anode current allowed when the chosen power supply voltage of 10 kv is considered, so that for a duty cycle of 0.01 the peak allowable power output for the transmitter is 48 kW.

4.3 The Receiver

The receiver, as used, required three chassis, one each for the pre-amplifier, the mixer stage and the intermediate frequency amplifier. This was a matter of convenience, rather than basic circuit design - the three chassis were available already, though some modifications were required before use. The local oscillator signal was obtained from the transmitter 25.5 MHz oscillator. A block diagram of the receiver is given in diagram 4-2, and circuit diagrams for the three separate chassis are given in diagrams 4-3 to 4-5.

Without the pre-amplifier, the noise figure for the receiver was found to be 7 dB, with most of the receiver noise being due to the mixer stage. When the low-noise cascode pre-amplifier was included the noise figure was reduced to 2 dB, though the overall gain of the receiver was found to be too great and it was necessary to reduce the gain of the I.F. channel.

The optimum bandwidth for the receiver, given by

$$\text{Bandwidth} \times \text{Pulse period} = 1.2 \quad (\text{Lawson and Uhlenbeck, } 1950)$$

was 18 kHz for a pulsewidth of 66 μ S, and a bandwidth of 20 kHz was obtained for the present receiver. Receiver gain over the period of operation was 125 dB and the video output of the I.F. stage was linear to 30 dB above sky noise. (As few echoes were observed to exceed this amplitude it was

considered satisfactory.) The measured time delay for the receiver was 13 μ S, corresponding to a range error of 4 km.

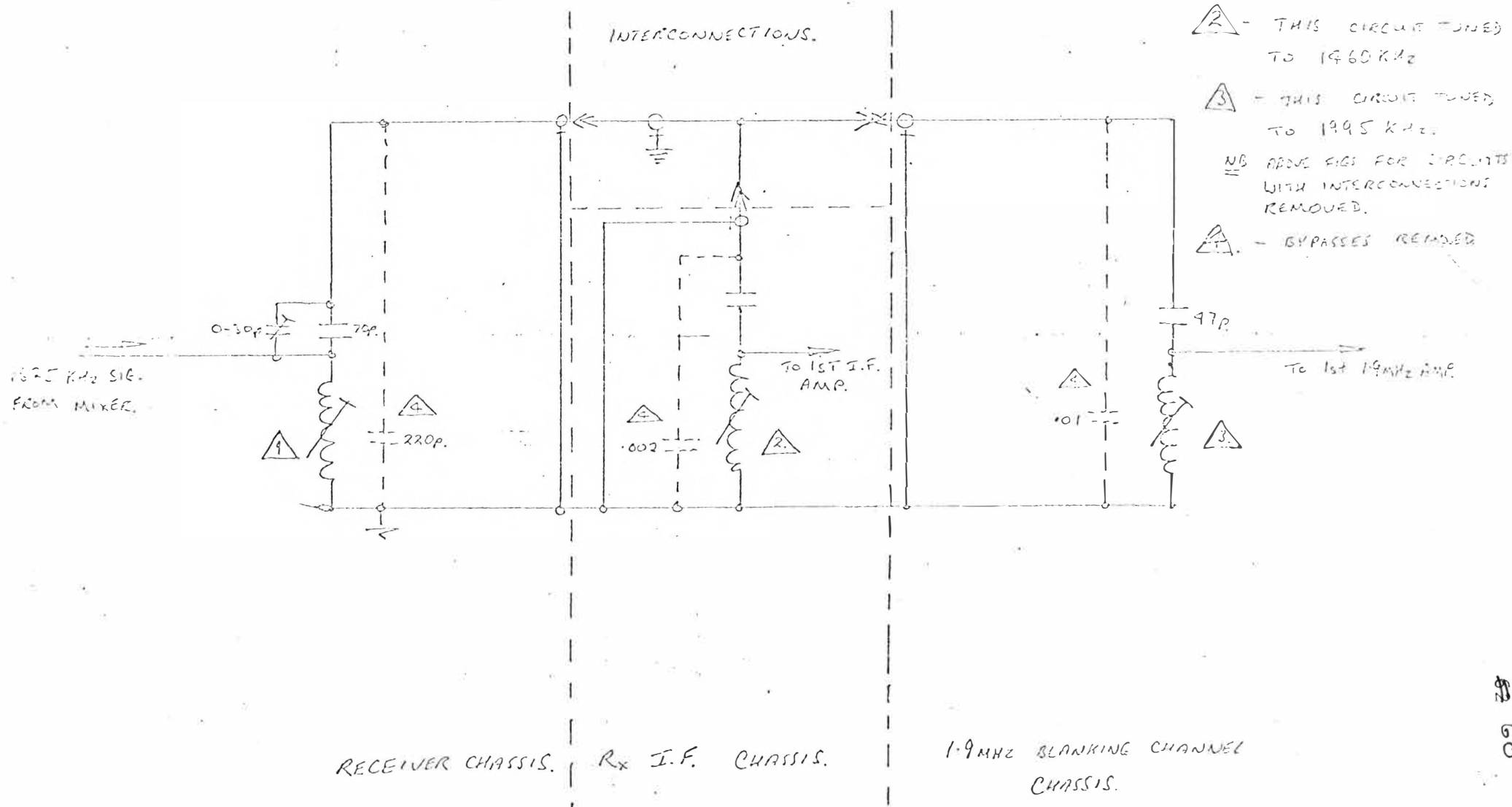
Suppression during the transmitter on period was necessary to prevent over-driving of the I.F. channel and was accomplished by placing a negative bias on the suppressor grids of the first two amplifiers. Suppression pulses during transmission and in the presence of noise spikes were obtained from the blanking channel.


4.4 The Phase Sensitive Detector

The frequency change between the transmitted and received signals due to the meteor trail motion will not be more than 40 Hz and thus phase variations over a single pulse will be small. The phase sensitive detector will therefore measure the phase difference between the pulsed, returned signal and the continuous wave reference signal from the transmitter - the speed of the observed train being indicated by the change in phase between two pulses. Indication of the direction of the train's drift is obtained from a second phase-sensitive detector coupled to the phase reference by a transformer, resulting in a 90° phase shift between the two detectors. Comparison of the two outputs will show whether the frequency change is positive (for a train drifting towards the aerial) or negative (for a train drifting away from the aerial).

The circuit diagram for the phase sensitive detector is given in diagram 4-6. A transformer is tuned to resonate at 1.62 MHz and additional resonances due to tapping are damped out with the 1.2K resistor. A parallel resonance wave-trap, tuned to 1.62 MHz, is placed between the phase input, from the I.F. channel, and electrical ground to filter out some of the

INPUT CONNECTIONS FOR BLANKING CHANNEL




NOTES  - THIS CIRCUIT TUNED TO 1742 KHz

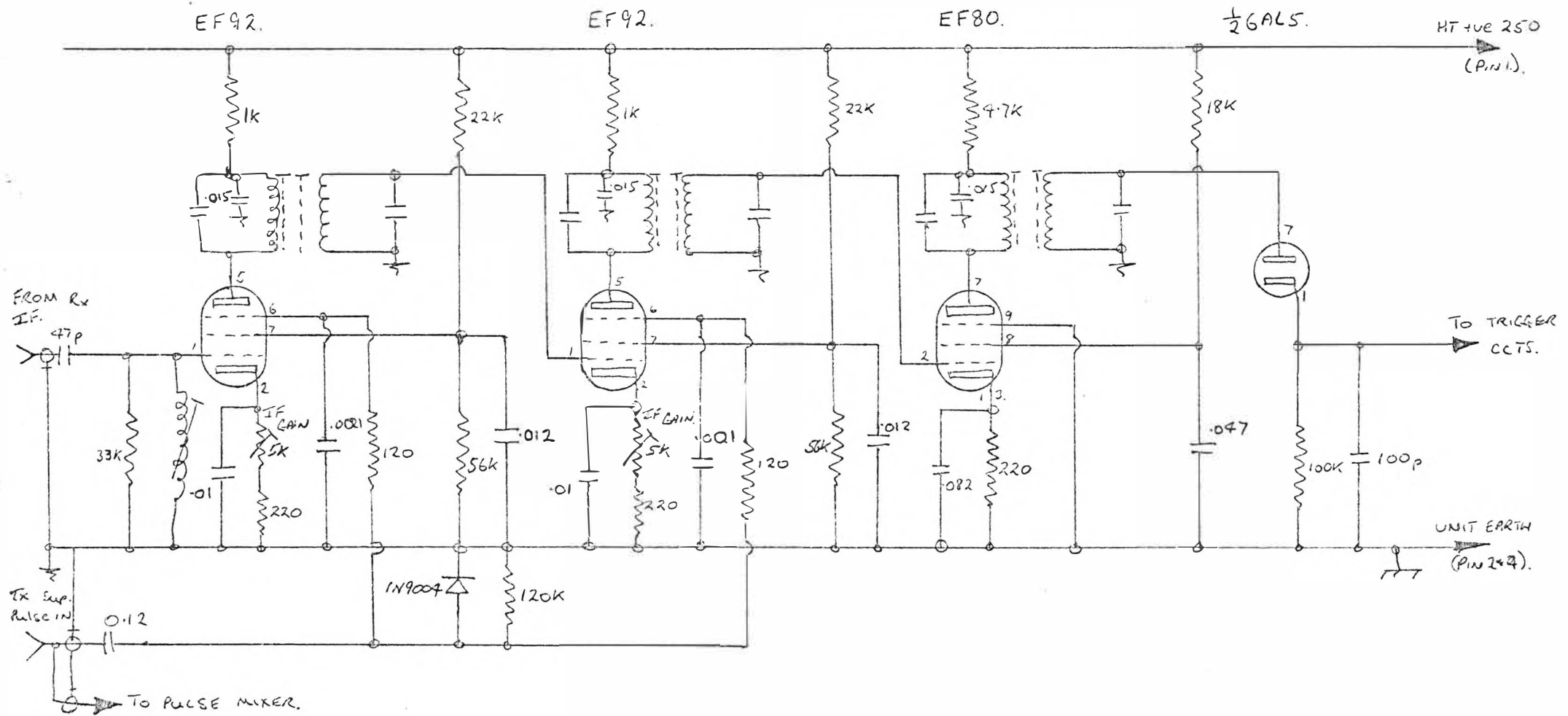
△2 - THIS CIRCUIT TUNED
TO 1960 KHz

3 - THIS CIRCUIT TUNED
TO 1995 kHz.

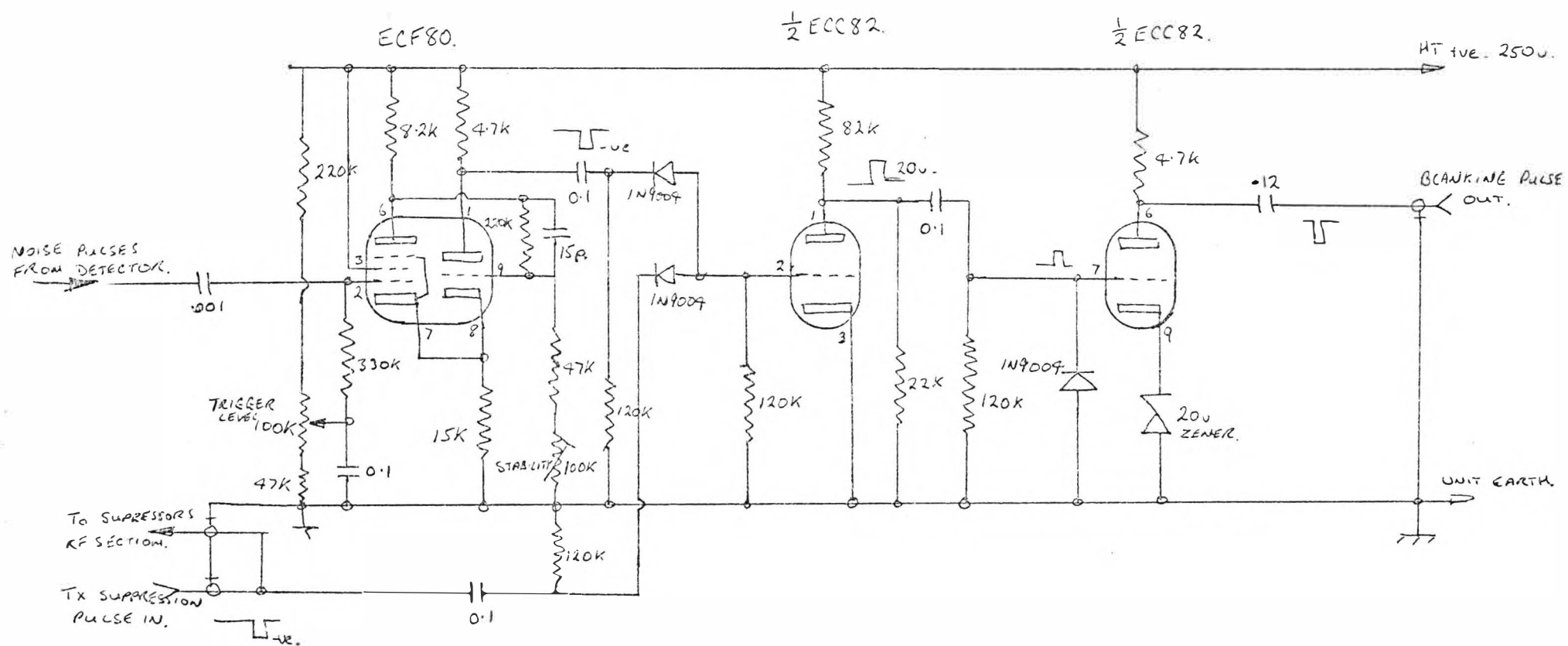
NB ABOVE FIGS FOR CIRCUITS
WITH INTERCONNECTIONS
REMOVED.

 - BYPASSES REMOVED

I.F. BLANKING CHANNEL (1.9 MHz) RF SECTION.



PULSE TRIGGER & MIXING CIRCUITS. (1.9 MHz BLANKING CHANNEL).



noise in the signal and a series resonance tuned to 1.62 MHz is placed between ground and the output labelled 2 in the circuit diagram to remove any 1.62 MHz signal. Because of display area limitations, the phase reference signal was limited, using a potential divider on the phase reference output in the transmitter; the phase output was unaffected by signal amplitude variations greater than 12 dB above sky noise.

4.5 The Blanking Channel

This was constructed in the electronic workshop and was not initially used in the experiment.

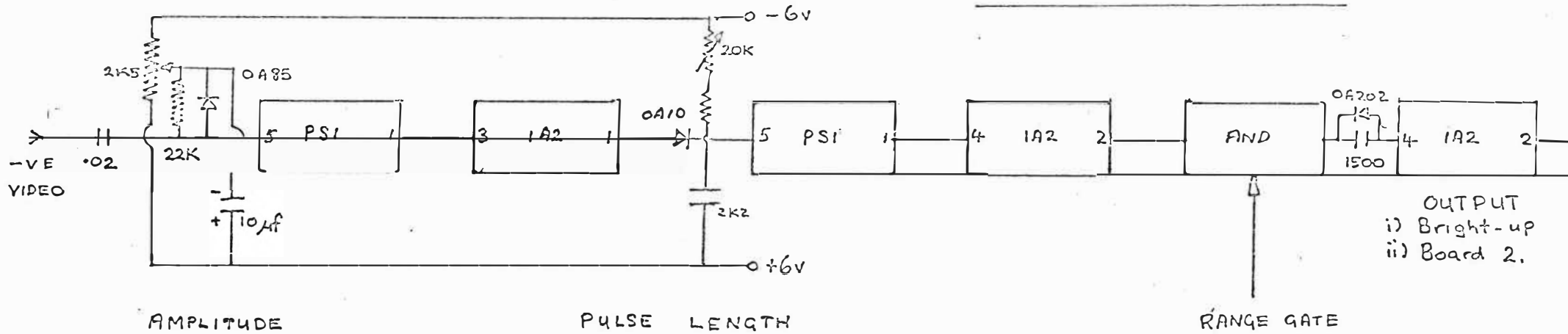
The blanking channel is tuned to 1.9 MHz, and is thus sensitive to a frequency of 27.4 MHz. As its bandwidth, 100 kHz, is greater than the I.F. channel, the signal delay is less. A noise spike, having a wide frequency response, will be observed at both 27.12 MHz and 27.4 MHz, thus the output of the blanking channel may be used to generate a suppression pulse for the I.F. channel. In addition to noise spikes, any broad-band interference is also suppressed which is particularly useful if intermittent interference is present.

4.6 The Discriminator

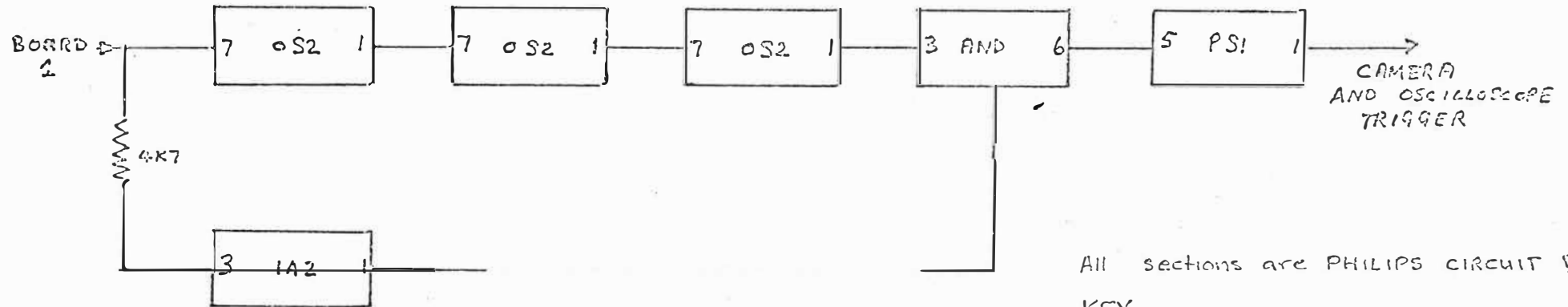
To conserve film some form of signal discrimination is used. With minor modifications, a discriminator already in existence was made compatible with the present equipment. This required the video output of the I.F. channel to be inverted and attenuated as the discriminator requires, less than -6V input. It was convenient to control the minimum detectable signal amplitude at this stage.

DIAGRAM 4-7.

THE DISCRIMINATOR



BOARD 1



BOARD 2

PULSE REPETITION RATE

All sections are PHILIPS CIRCUIT BLOCKS

KEY

PSI = pulse shaper

IA2 = inverter amplifier

OS2 = one shot multivibrator

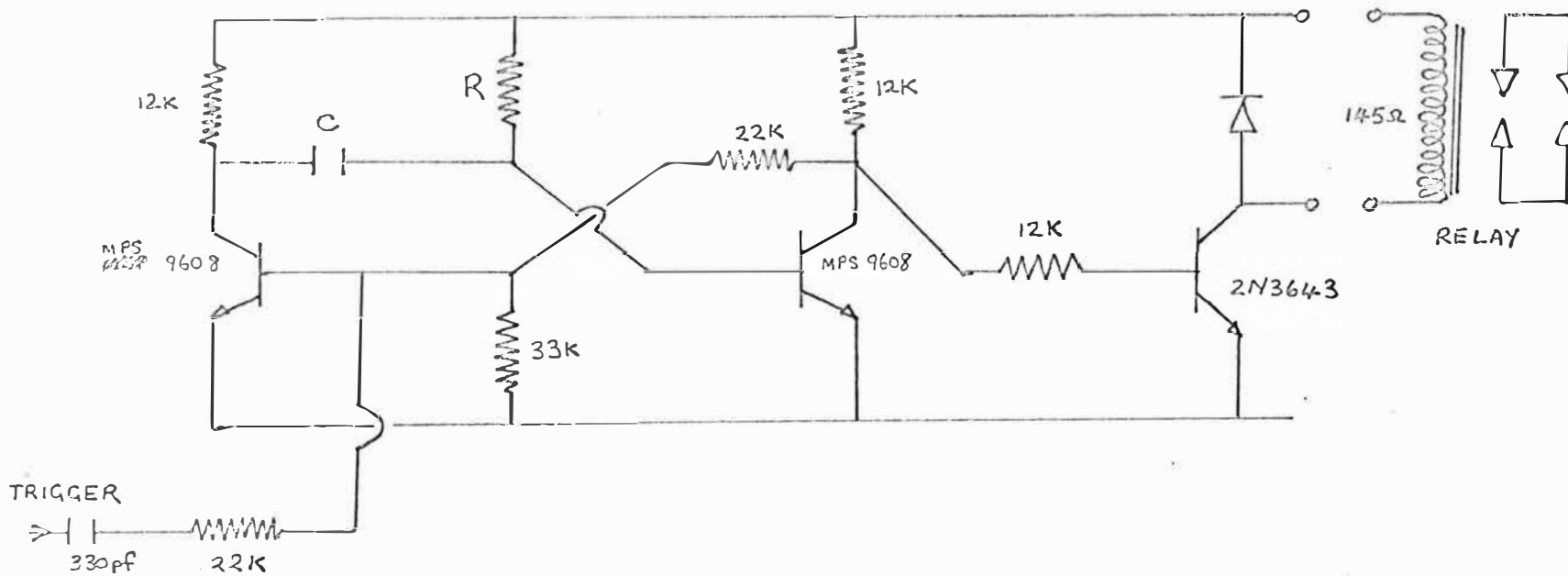


DIAGRAM 4-8. CAMERA TRIGGER CONTROL.

(The time constant, RC , was varied as described in the text)

Board 1 of the discriminator, see diagram 4-7, is activated by a pulse of sufficient amplitude with a pulse-width in excess of 50 μ S (though because of the receiver bandwidth the latter criterion is of limited use) and with a range less than 600 km. The range gate was obtained from a monostable multivibrator triggered by the transmitter trigger pulse and was ON for 4 msec after transmission. The output from the base of the passive transistor, in the monostable, was used for the range display. By calibrating this output for each time the equipment was used any changes in the monostable period, and the non-linearity of the ramp could be accounted for. The main reason for using a range gate was to eliminate triggering due to groundscatter observed in the 600-1000 km region.

The output from board 1 activates the bright-up control of the oscilloscope and also triggers a chain of three monostables that produce a gate 110 μ sec long, 6.6 msec later on board 2. If the next signal to pass through board 1 lies within this gate then a trigger pulse activates the time-base trigger on the oscilloscope, and the camera monostable.

4.7 Camera Control

The basic camera control unit was a monostable multivibrator (see diagram 4-8) that, when triggered by the discriminator output, produced a pulse that activated a relay used to close a switch in the camera. Because the mode of camera operation was varied during the experimental period, various pulse lengths were used.

Initially, the camera was triggered with a pulse length of 0.5 msec, exposure time and film rewind being automatically controlled by the camera. While the shutters took 20 msec to

open, this did not result in a loss of information as the initial sections of the display involved were found to be visible on the film, because of the phosphor persistence of the oscilloscope screen. However, because of either faulty construction, or overwork, the shutter mechanism started to wear rather badly and though the use of shutters was perservered with using alternative trigger pulse lengths, it ultimately was necessary to dispense with the shutters completely. By replacing the single contact relay with a twin contact relay, placing a switch in the graticule illumination circuit of the oscilloscope which was closed by one of the relay contacts, and by extending the pulse period to 1 sec. the camera control without shutters was accomplished. The graticule was found particularly useful in reading film and was retained for this reason. No fogging was apparent when the shutters were removed and, in retrospect, it would have been preferable if the final mode of operation had been employed throughout, as the advantages in using shutters are outweighed considerably by the subsequent disadvantages.

In its present state, the camera control is particularly sensitive to contact-bounce upon activation of the relays and some film and data loss, due to premature winding occurs. This could be removed by more direct switching, possibly using silicon-controlled rectifiers, but has not been attempted at present.

4.8 The Recording System

1. The Camera. A C4 camera, manufactured by Grass Instruments, U.S.A., was used, being triggered as indicated above. Some features of its operation are as follows.

i) Focal Ratio. For a spot speed of 10 mm/sec^{on the film}, the makers recommended a focal ratio of 2.0. As a spot speed of 25 mm/sec. was used, the f value of 2.0 was appropriate. Experimentation with different f values supported this choice.

ii) Film capacity. Though the film magazines could hold 200 ft lengths of film, it was found convenient to use only 100 ft lengths.

2. Timing on films. Available with the camera is a data card holder which is attached at the side of the camera, the data card image being projected onto the film via an internal mirror. Timing was inserted at the beginning of every half-hour while operating, details of the date, bearing of the aerial and time being recorded on film. At the end of the experimental period, finer timing was required, and so an automatic switch was constructed for the data card control. A monostable, activated by a switch closed every three minutes by a Sangamo motor, closed a double pole relay which in turn switched the data card light on for 0.1 sec. and then wound the film on one frame. This addition was found particularly useful and has become a permanent feature of the equipment.

3. Film. Two types of film were used during the experiment - Ilford 5G91 and Kodak Linograph, the choice being dictated by local availability. Both films showed slight background fogging, but this was of no consequence in use. The Kodak film appeared marginally superior, but as all tests were of a subjective nature, and as neither film is now available

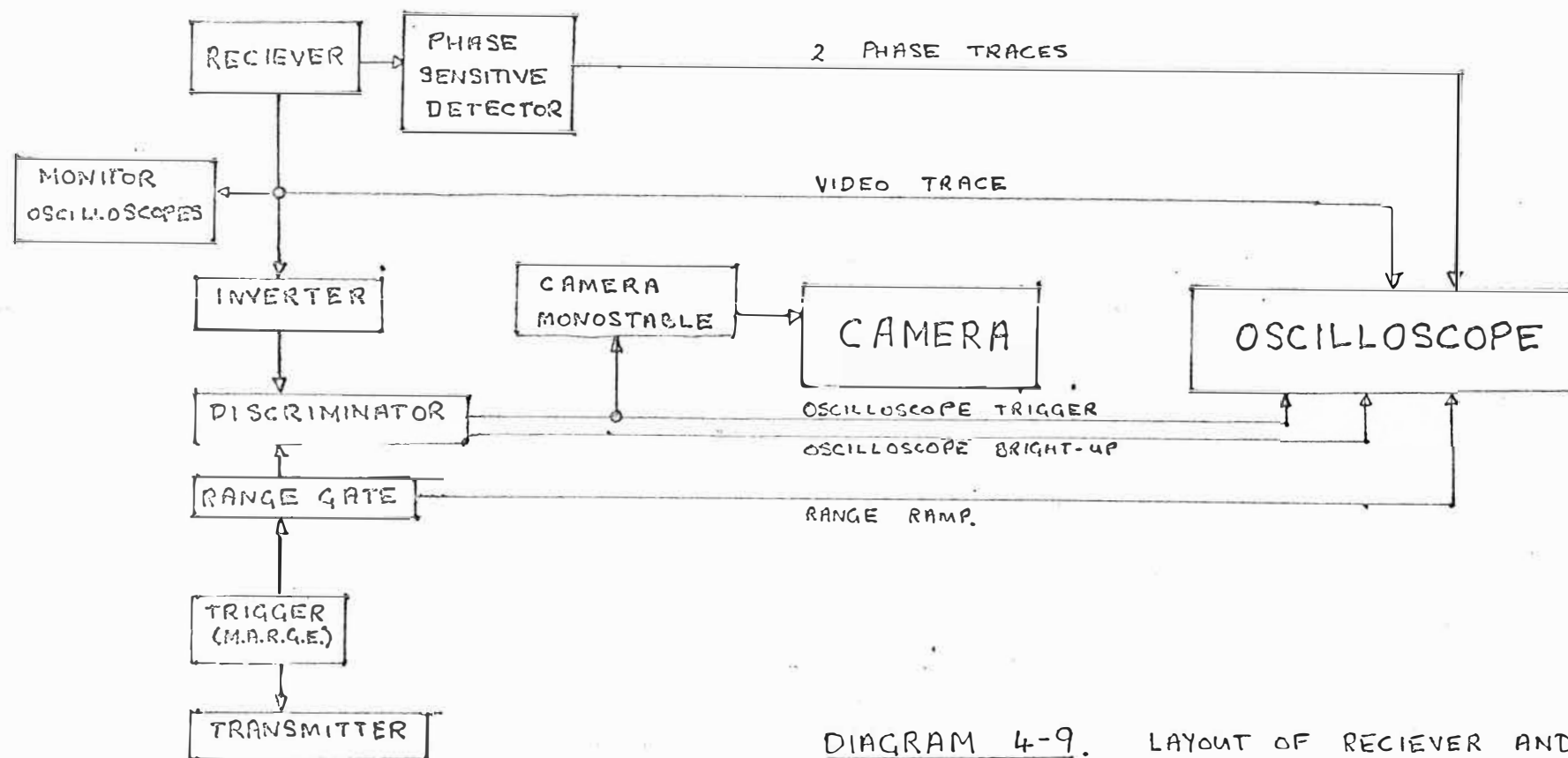
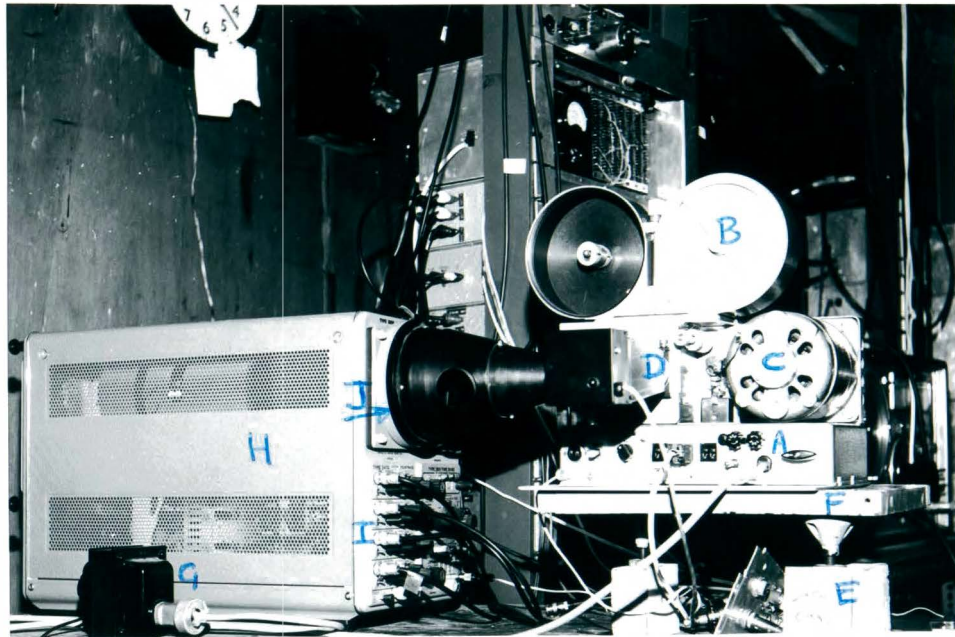


DIAGRAM 4-9. LAYOUT OF RECIEVER AND RECORDING EQUIPMENT.

CAMERA AND OSCILLOSCOPE SET
FOR OPERATION.



KEY

- A. CAMERA CONTROLS.
- B. FILM MAGAZINE.
- C. CAMERA MOTOR.
- D. DATA CARD HOLDER IN POSITION.
- E. SAMPLE DATA CARD.
- F. TEMPORARY STAND FOR CAMERA.
- G. TRANSFORMER FOR CAMERA. (CAMERA RUNS ON 110V)
- H. OSCILLOSCOPE.
- I. OSCILLOSCOPE CONTROLS.
- J. HOOD FOR CAMERA.

commercially, it does not seem relevant to pursue this. A significant feature, however, is that while both are fine grain films designed for oscilloscope recordings, equally satisfactory results were obtained using Ilford FP4 film. Because the recording film now available locally is double the cost of FP4 film, the latter is probably a more suitable choice, in future.

4. The Oscilloscope. An oscilloscope manufactured by Tektronix, USA, and using a plug-in type 3B3 time base and a type 3A74 four-trace amplifier plug-in unit with a chopping cycle of approximately 125 kHz was used to display the data that was recorded on film. The oscilloscope is operated on external trigger, and the intensity is reduced so that only when a bright-up pulse is applied does any signal appear on the screen. In normal use a sweep speed of 10 cm/sec was used and the signal amplitudes on the four beams were adjusted for most convenient display size.

5. Layout of Traces. The layout of the four beams is indicated in Plate ^{5-3, Plot} and the appropriate inputs in diagram 4-9. When a meteor activates the system, the bright-up pulse illuminates both Doppler traces, the video output trace and a spot on the range ramp which indicates the time delay, after transmission, of the meteor echo.

The video trace was adjusted so that sky noise filled approximately 2 to 4 mm on the screen, thus most usable echoes occupied less than three-quarters of the display area.

The two Doppler traces were each allowed to fill a quarter of the bottom of the screen, with some allowance for overlapping, so that both traces could be recorded. As indicated, section 4-4, the phase reference amplitude is limited to make this possible.

4.9 Additional Equipment

1. Pulse Supply. All trigger pulses for the transmitter and discriminator, and suppression for the receiver were obtained from M.A.R.G.E. (Keay, 1956), a piece of equipment constructed for earlier experiments. The basic operation uses a 50 Hz crystal oscillator, locked to the 50 Hz mains frequency, as the frequency base for 50 Hz pulse oscillator. The pulse output is then used to obtain other pulse frequencies, of which 150 Hz is one.

2. Manual Switches. Because of considerable r.f. noise, manual switches were incorporated in the equipment to allow the operator to turn the camera on and off at will. This is also useful if a particularly long duration overdense echo is observed, since this leads to multiple frames of the same meteor.

4.10 Transmission Lines

Parallel twin copper wire lines with a characteristic impedance of 450Ω were used as the transmission line. The transmission line and impedance matching transformations are shown in diag. 4.10. The impedance matching transformations being,

1. Receiver. A balun was used between the transmission line and the 50Ω unbalanced coaxial cable of the receiver line, this segment being 1λ long.

2. Aerial. As a rotatable aerial was used, it was necessary to have a more flexible line feeding it - 50Ω high voltage coaxial cable was used. The impedance transformation between the 450Ω transmission line and the two balanced 50Ω coaxial cable feeders consisted of a quarter wavelength of "dural" tubing.

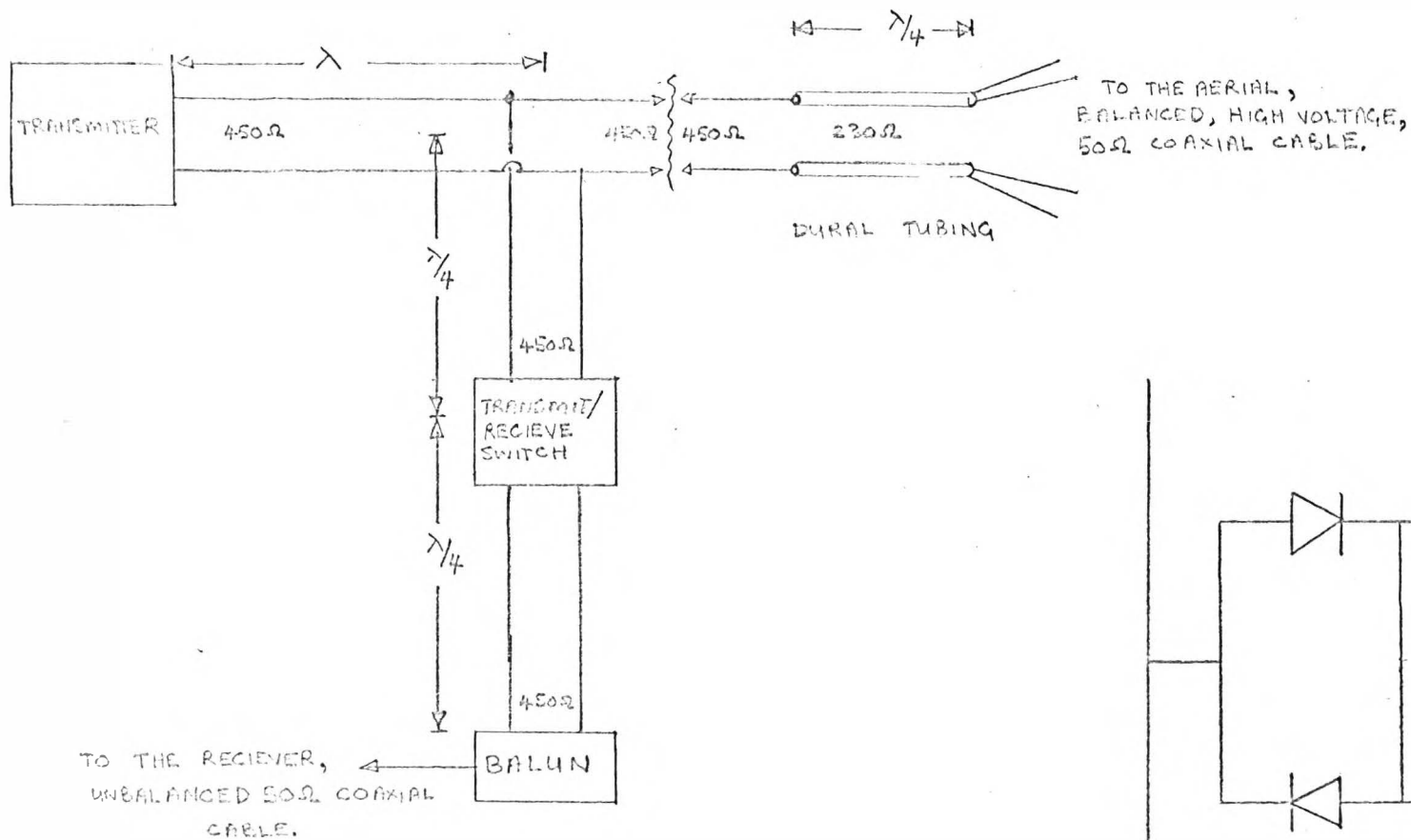


DIAGRAM 4-10 THE TRANSMISSION LINE.
(Impedances and impedance matching are indicated)

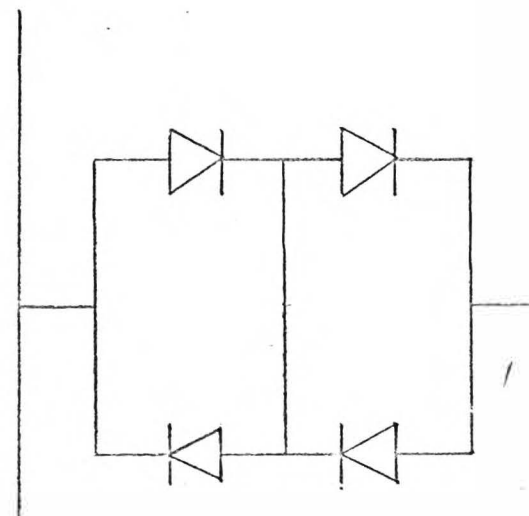
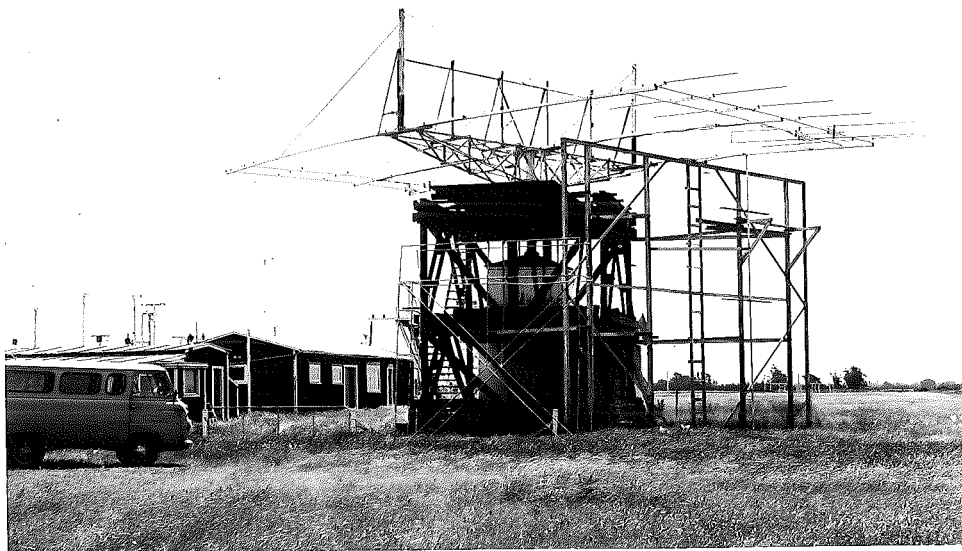


DIAGRAM 4-11 THE TRANSMIT-RECEIVE SWITCH.
(all diodes are SX 635)



THE AERIAL.

As both the receiver and transmitter were operated on a common aerial a transmit-receive switch consisting of four Sx635 diodes, as indicated in diagram 4-11, was placed a quarter wavelength from the junction of the receiver and transmitter lines. By shorting the transmission line $\lambda/4$ on either side of the junction for the receiver and transmitter and coupling a signal generator to this junction, a loss of 6 dB on reception, due to the T/R switch was measured. However, as a passive switch was felt to be easier to maintain, and because no diodes with lower forward resistance were found capable of operating in this fashion, this particular switch was persevered with. As both cosmic noise and signal were attenuated to the same degree, it does not present a significant loss of information. The T/R switch was heat-sinked by attaching the contact leads to thick copper plates and sealed in plastic for weather proofing. On a radio frequency admittance bridge, these additions had no obvious detrimental effects on the switch operation, and the complete unit was considerably more robust physically.

4.11 The Aerial

The aerial was a collinear array of two six-element, horizontally polarized Yagi aerials with centres 1.3λ apart and mounted on a rotating tower 0.65λ above electrical ground. The resulting array had a beamwidth of 22° between half-power points and 40° between first nulls, side-lobe levels were 8 dB and 10 dB down on the main lobe and the back-lobe was 12 dB down, and the beam maximum elevation was 23° above horizontal. The vertical and horizontal polar diagrams were estimated using simple aerial theory and these results were confirmed experimentally.

1. Calculated Polar Diagram

a) Horizontal. The radiation pattern of an array depends on the relative positions of the individual radiators with respect to each other, and the radiation patterns of the individual radiators. Assuming the phases and magnitudes of the current in the individual radiators are equal, and using a simple array approach, the individual elements may be considered as a correction to the pattern deduced by assuming isotropic point sources at the positions of these radiators (Blake, 1966).

$$E_A = E_R \left| \cos \left(\frac{\pi d}{\lambda} \sin \phi \right) \right| \quad (4-7)$$

where E_A = magnitude of array electric vector

E_R = magnitude of radiator electric vector

d = distance between radiators

λ = operating wavelength

ϕ = angle, as shown in diagram 4-12.

The array factor for $d = 1.3\lambda$ will therefore have a beamwidth of 48° between first nulls.

The polar diagram for a single yagi is the sum of the polar diagrams of the drive element, a folded dipole in this case and five parasitic elements. The driven

element induces currents in the parasitic elements which depend on their length, cross-sectional area and distance from the driven element. It is possible to show (Fishenden and Wiblin, 1949) that if the length of the parasitic element is less than 0.47λ , then there is an increase in signal amplitude in the direction of the parasite and there is a decrease if

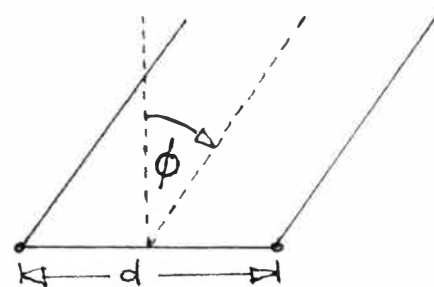


Diagram 4-12

the length is greater than this. The positioning of parasitic elements in close proximity to the fed element also modifies the input impedance considerably. Because the calculation of a polar diagram, allowing for these variables, is complicated (Walkinshaw, 1946), and because it is only necessary, in the present context, to be able to establish that the aerial is operating satisfactorily, the present aerial diagram was taken from Fig. 4 of Fishenden and Wiblin (1949). They give the polar diagram for a six-element Yagi and a parallel array of two such Yagis operating on 212 MHz is given. The required results are given in Table 4-1, being within $\pm 5^\circ$ of their results.

The array factor above will define the main lobe dimensions while the element factor will reduce side and back lobes.

TABLE 4-1

	Beamwidth		Front-to-Back Ratio
	$\frac{1}{2}$ power	first nulls	
Single Yagi	45°	100°	10 dB
Array	20°	45°	

b) Vertical. The ground factor for the vertical polar diagram, for an aerial a height 0.65λ above ground, gives a maximum at 23° to the horizontal, a minimum at 48° and a smaller maximum at 90° .

The vertical pattern for a single Yagi is slightly broader than the corresponding horizontal pattern, a half power beamwidth of 47° being quoted by Greenblum, 1956. This will be the same for the array of two such Yagis in parallel, the

vertical pattern of the array being independent of the horizontal pattern. Note: this is not the case for the two patterns of a single yagi.

As a result of the ground factor, the main lobe will have an elevation of 23° and a first null at 48° . In view of the horizontal pattern discussed above, side and back lobes will be expected to be present.

2. Measured Polar Diagram

a) Horizontal. A dipole aerial driven by a signal generator situated on the ground 140 metres from the array was used as a signal source to measure the polar diagram. For such measurements to be representative of the far-field pattern, the following expression must be satisfied,

$$R_d > \frac{(A+a)^2}{\lambda} \quad (4-8)$$

where a = dimension of test aerial (5 m)

A = largest dimension of array (16 m)

R_d = distance between aerials.

(Blake, 1966).

Thus, provided R_d exceeded 40 m, the measurements would be representative. If the aerial separation is not large enough, the main effect will be to fill in the minima and slightly spread the maxima of the polar diagram. Because of this, any error in determining the far-field pattern due to insufficient separation will favour a conservative estimate of the aerial's capabilities, and cannot therefore be considered detrimental.

Because the signal generator was not a stable signal source, it was necessary to replace the receiver local oscillator by another signal generator and peak up the signal

amplitude before a reading was made. However, as the drift was not greater than the receiver bandwidth, the observed amplitude variations will be closely related to the aerial orientation.

TABLE 4-2: Results for horizontal polar diagram of the aerial

Set	Front-to-Back Ratio (dB)	Beamwidth: 3 dB Degrees	First Mulls	Side-lobes dB
1	12	20	44	8,10
2	13	18	42	6,10

In Table 4-2 the results for two sets of measurements are recorded. Those in set 1 are the same as results obtained in an earlier survey of the main lobe and two side lobes by W.J. Baggaley. The earlier measurements were carried out by receiving a signal transmitted from the aerial for different aerial positions, the separation of aerial and receiver being approximately 10 km. A feature of these polar diagrams, and measurements made on the separate Yagis, were a set of bumps that were displaced from one side of the aerial to the other. (The two surveys were approximately 180° apart with respect to the aerial.) As a wire mesh reflector for an earlier aerial was assymmetrically placed, with respect to the aerial, this was thought to be responsible for the effects observed, and was therefore taken down. The results in set 2 indicate that only slight changes in the polar diagram occurred, though the bumps were no longer present. It is probable that by adjusting the lengths of the directors in the individual Yagis, the side-lobes and back-lobe could be reduced in size, but this has not yet been attempted. The final horizontal

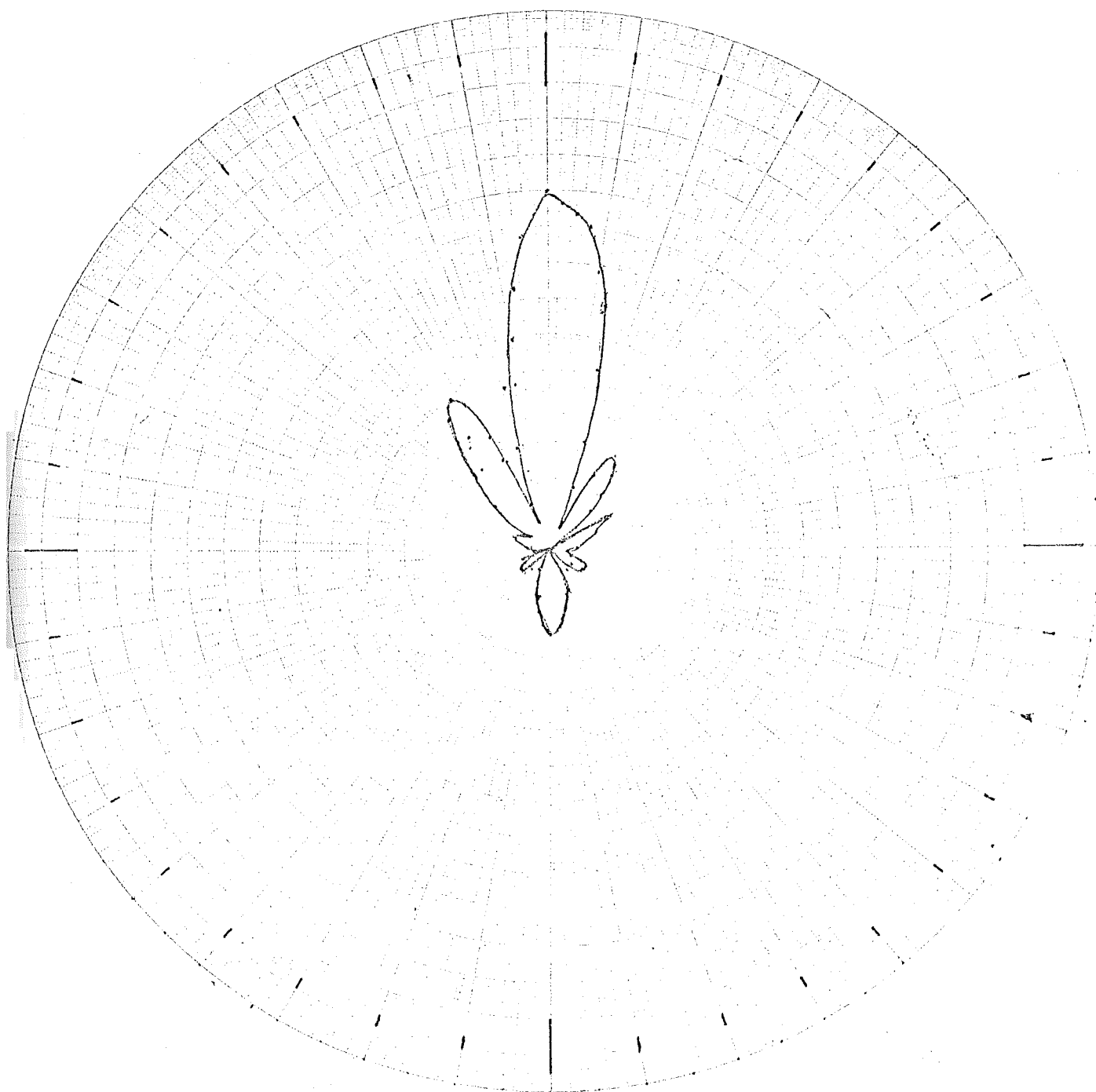


DIAGRAM 4-14
HORIZONTAL POLAR DIAGRAM OF AERIAL
(with chicken wire removed)

polar diagram is shown in diagram 4-14.

b) Vertical. The aerial elevation polar diagram may be calculated from the range distribution of observed meteors. This follows from Kaiser, 1954, 1961, 1962. As the meteors used to construct the distribution were collected over a six month period and for a large sky area, the meteor radiant distribution will be smoothed over the observed region, and the distribution of meteor radiants over the celestial sphere may be assumed isotropic. A simple approach may now be adopted to estimate the relative frequency of meteors in a range interval. The number of meteors, N , with line densities in excess of q is given by

$$N \propto q^{-1} \quad (4-9)$$

for a mass exponent, $s = 2.0$. From eq. 3-6

$$q \propto R^{3/2} G^{-1} \quad (\text{underdense}) \quad (4-10)$$

Thus, the relative number of meteors, N_u , in a range interval $R \rightarrow R+dR$, with line densities in excess of the minimum line density is given by

$$N_u = G \cos \phi R^{-2/3} \quad (4-11)$$

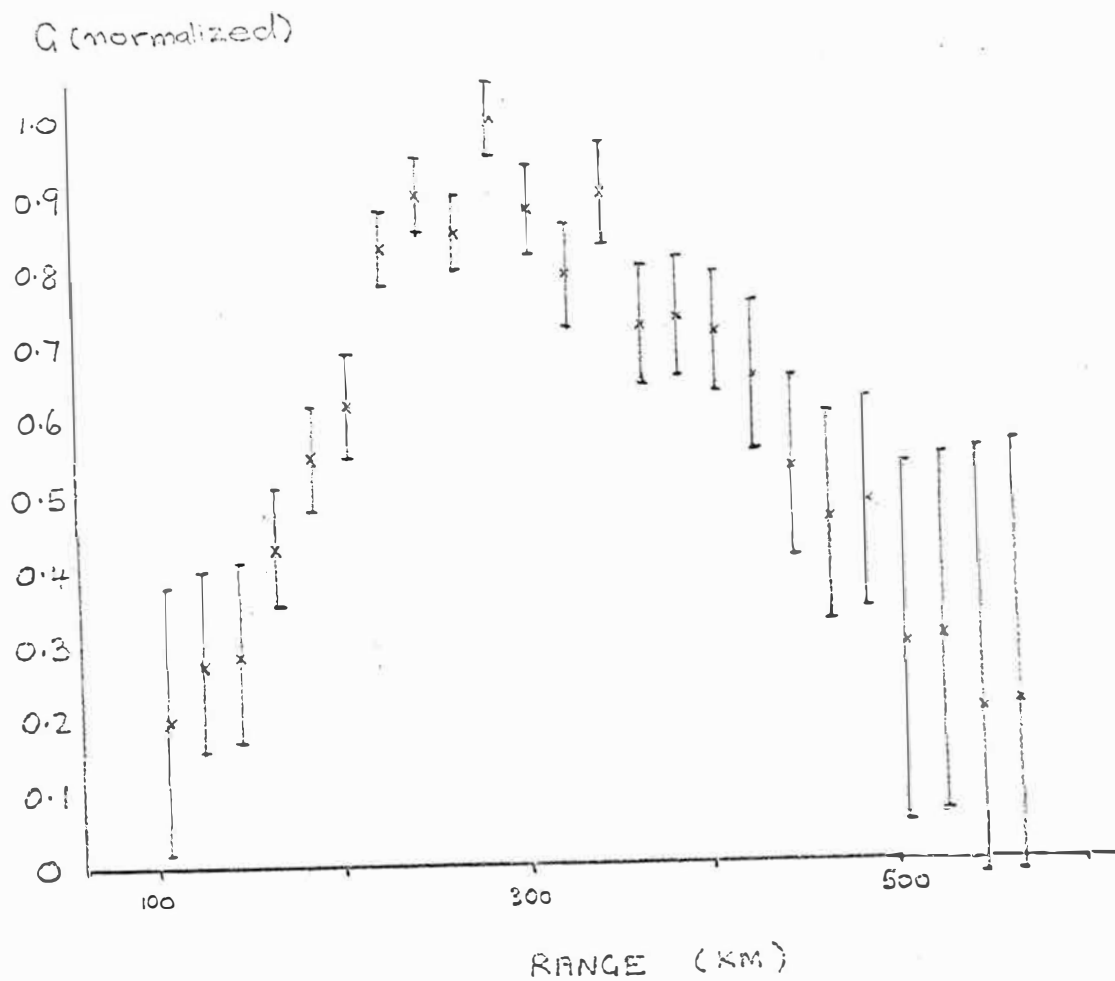
where ϕ is the elevation angle to the reflection point on the observed meteor trail.

The range, R , for a curved earth is given by

$$R = R_E \left[\left(\sin^2 \phi + \frac{2h}{R_E} \right)^{1/2} - \sin \phi \right] \quad (4-12)$$

and h = height, R = slant range.

DIAGRAM 4-13 VARIATION OF Q WITH RANGE
(see text for details)



Using (4-11) and (4-12) and assuming a constant reflection height of 97 km for all meteors, the variation in G is plotted against range in diagram 4-13. From this, the maximum aerial sensitivity in the vertical plane is $20^{\circ} \pm 5^{\circ}$, which is in reasonable agreement with the estimated 23° . From the present measurements, it is not possible to estimate the effects of the side-lobes and back-lobes in the vertical.

4.12 Film Reading Equipment

All films were read in the department, eight different people being employed in this during the experimental period.

Several methods of projecting the film for reading were tried, the two most successful methods being

- i) the use of a micro-film reader,
- ii) a vertically mounted film projector.

The less intense light in micro-film reader is the major drawback with this method, while the cost of replacing projector bulbs would be the major disadvantage in the use of a film projector. In both cases, the image was projected onto the table in front of the person reading film. Projection of the film image onto a ground glass screen was considered, but it was suggested (C.L. Miles, Private communication) that this method can cause considerable eyestrain if used for any great length of time.

C H A P T E R 5

PARAMETERS MEASURED FROM EACH RADIO METEOR

Introduction

All information was read off photographic film and recorded on computer data cards for analysis using an IBM 360/44 computer. Details of the relevant computer programs and data card formats are to be found in ^{the} Appendix. In this chapter, the parameters measured from film records of radio meteors are discussed, the more important ones being height, velocity, range and type of record.

A. HEIGHT

5.1 Heights using a Deduced Ambipolar Diffusion Coefficient

Heights of the observed echoes may be measured directly (i.e. Nowak, 1966), or indirectly inferred from the rate of decay of the returned signal if the echo is underdense. From equation (3-7) it is apparent that after the initial rapid expansion of the meteor trail, the subsequent expansion will be controlled by the ambipolar diffusion coefficient, which is inversely proportional to the local atmospheric density and thus exponentially increases with increasing altitude. Records measured may thus be divided into height intervals by subdividing the observed decay rates. It is important to realize that these subdivisions are constant density intervals, density being the variable parameter, and are identified by heights obtained from a standard atmosphere or from a direct calibration of decay heights against real heights.

1. The Ambipolar Diffusion Coefficient, D_a

As pointed out, Section 3-11(4), the decay in echo amplitude is governed by the change in electron density resulting from the trail expansion. The rate of expansion of the electrons is reduced by the formation of space charge fields due to the separation of electrons and ions in the trail, and the observed expansion rate is governed by a modified ion diffusion rate. This modified diffusion coefficient is called ambipolar. In Kaiser, 1953, D_a is shown to be approximately twice the ion diffusion coefficient, an ion diffusion coefficient being obtained from kinetic theory. This gives

$$D_a = 3.35 \times 10^{-6} T^{\frac{1}{2}} / \rho_a \text{ cm}^2/\text{sec.} \quad (5-1)$$

where T = local atmospheric temperature ($^{\circ}\text{K}$)

ρ_a = local atmospheric density (gm/cc).

Alternative expressions are to be found in the literature for D_a (Dalgarno, 1961; Weiss, 1955; Greenhow and Neufeld, 1955), all of which give the same ρ_a dependence, though they differ in the temperature dependence and constant of proportionality. However, as pointed out by Dalgarno, 1961, agreement between the various expressions is quite satisfactory, at least in the region 80-110 km.

Assuming the atmospheric density is the only important variable in the expression for D_a , and that this varies exponentially with height, it is possible to obtain

$$\frac{d(\log_e D_a)}{dh} = \frac{1}{H_D} \quad (5-2)$$

where h = height (km)

H_D = diffusion scale height (km).

This will be referred to in the next section.

2. Experimental Calibration of Echo Decay

By measuring the heights of echoes directly, the observed echo decay may be calibrated against height. Some of the comparisons in the literature are compared in Table 5-1, using equation 5-2 to give a diffusion scale height.

TABLE 5-1

Experimenter(s)	Scale Height (± 1 km)
Greenhow and Neufeld (1955)	6.5
Murray (1959)	26.0
Greenhow and Hall (1961)	8.0
Southworth (1970)	6.0
Verniani (1968)	5.0

Greenhow and Hall, 1961, have criticized Murray's results and suggest that selection effects and incorrect analysis invalidate the very large diffusion scale height obtained. Two important features appear in the above analyses,

a) there is a considerable scatter in the diffusion coefficients observed for a particular height, and

b) the diffusion scale height may be slightly larger than the atmospheric scale height.

3. Possible Sources of Scatter in Decay Heights

Several potential sources of scatter have been discussed in the literature.

a) Ionization irregularities. These fall into two groups.

i) The ionization distribution along the meteor trail will have a maximum (Herlofson, 1948) and as the trail expands there

will be a weighting of the returned signal to the regions of higher ionization. This is not expected to be important, (Rice and Forsyth, 1963).

ii) Irregularities in the ionization with scales less than a Fresnel zone may occur and this will possibly be important, so it is discussed further.

Rice and Forsyth, (1964), showed that diffusion coefficients calculated for the same meteor trail at different wavelengths were often different. They identified these variations with ionization irregularities. Jones, J. (1969) however, suggests that irregularities are not important. The source for the irregularities will most likely lie in the ablation processes. Southworth (1970) suggests that fragmentation in meteoroids may be more important than previously supposed, though Poole and Kaiser (1967) consider it to be of lesser importance than inhomogeneities in the meteoroid heating as a source of modified trail ionization. This is consistent with the treatment of meteoroid ablation by Jones and Kaiser (1966).

b) Wind Effects. Analogous to a) (i) above, is the change in D_a due to trail rotation, in a wind shear, shifting the specular reflection point. McIntosh (1969) found this to be a possible contribution to the scatter. Jones (1972) considered the effects of small scale wind shears of vertical extent less than 6 km and concluded that this too would be contributory to the scatter.

c) Geomagnetic Effects. Meteor trains parallel to the geomagnetic field are expected to exhibit modified diffusion coefficients, (Kaiser et al., 1969) and this could be responsible for some of the observed scatter. Later experimental work, (Watkins et al., 1971) suggests that this

will be further enhanced as the meteor train apparently produces field aligned irregularities irrespective of the train orientation. However, these effects are only expected to be important above 95 km, and as the observed scatter is not height dependent, it is unlikely that this is a significant source of scatter.

d) Variation of Atmospheric Parameters. Murray (1959)

considered the possibility that the scatter may be due to local temperature and pressure variations, but discounted it on the subjective observation that the scatter for echoes with similar heights appeared independent of time, implying an unrealistic variability in atmospheric parameters. However, in view of the observed density, pressure and temperature variations from rocket observations, such effects could prove important if data were collected over a long period of time.

By deriving values of diffusion coefficients using rocket data supplied by Smith, W.S. et al. (1967) hourly and daily variations in decay heights were estimated. Seasonal variations calculated using the 1962 U.S. standard atmosphere were also considered, as were diurnal variations in atmospheric density observed from meteor data (Greenhow and Neufeld, 1960). Using this information it was found that height variations for the associated time scales were approximately 3 ± 1 km.

e) Instrument Errors. At least some of the observed scatter will result from measurement errors, but in analyses mentioned above, the authors indicate that a residual scatter is left after allowing for this effect. However, the effects of the signal amplitude to background cosmic noise is shown (Jones and Read, 1972) to be a contributing source to the scatter in the results that has not previously been considered.

From the above, it is apparent that no single dominant source of scatter exists. Height resolution using the echo decay is limited by the expected variability in the diffusion coefficients with height and in the present experiment a height error of ± 2.5 km was used, being larger, by 0.5 km, than the values suggested in Jones, J. (1970).

4. The Observed Scale Height

There is some evidence to suggest that the diffusion scale height may be larger than the atmospheric scale height, though Jones, J. (1970) suggests that in view of the uncertainties the difference is not significant. Southworth (1970) suggested that the effects of recombination are sufficiently great to produce the observed larger scale height of Greenhow and Hall (1961) by enhancing the observed decay rates of lower altitude meteors. However, more recent work on meteoric ion processes suggests that the important reaction rates are too slow to have significant effects in less than 0.5 secs (Baggaley, 1972), the probable echo duration for the above data.

In view of the uncertainties, the atmospheric scale height will be taken as the same as the diffusion scale height.

5. Summary

i) From kinetic theory, it is possible to derive an expression for the ambipolar diffusion coefficient. As pointed out, several expressions exist in the literature, there being no significant differences between them in the altitude region of interest. The expression,

$$D_a = 4.4 \times 10^{-6} \frac{T^{-\frac{1}{2}}}{\rho_a} \quad (\text{cm}^2/\text{s}) \quad (5-3)$$

given by Greenhow and Neufeld (1955) was chosen to calibrate

the echo decay amplitudes. The choice was not guided by any particular criteria other than the suggestion (Barnes, 1968) that the empirical relationship

$$\text{Log}_{10} D_a = 0.067h - 5.6 \quad (5-4)$$

where the units are, $D_a - \text{m}^2/\text{s}$, and $h - \text{km}$, deduced by McKinley (1961) from Greenhow and Neufeld's results, was generally acceptable and that (5-3) was apparently in good agreement with (5-4). In retrospect, it would probably have been preferable to have used (5-1) as the derivation of (5-3) in Greenhow and Neufeld (1955) is apparently amended in Greenhow and Hall (1961), though here (5-1) is quoted as an ion diffusion coefficient.

ii) The considerable variation observed in calibrations for D_a place a limit on the accuracy with which heights can be determined. Furthermore, variations in T , P and ρ_a will be expected to produce variations in D_a . In view of these points, an error in determined heights of $\pm 2.5 \text{ km}$ was adopted.

5.2 Measurement of Decay Rate from Photographic Records

The video output voltage of the receiver was displayed on the oscilloscope and recorded on film. As amplification was linear over the echo amplitude, the decay constant from equation (3-7) becomes

$$T_D = \lambda^2 / 16\pi^2 D_a, \quad (5-5)$$

where T_D = the time for the echo amplitude to reduce to $1/e^{\text{th}}$ of its initial value. From section 5-1, D_a is known as a function of height, so T_D is a height measure also. Various methods for deducing heights are possible.

- a) A direct measurement of T_D can be made by recording the time for the echo to reduce to $1/e$ of its initial amplitude. This was not attempted.
- b) By measuring the time, t_1 , for the echo to decay from an amplitude A_0 to a lower amplitude A_1 , T_D may be calculated using,

$$T_D = \frac{t_1}{\text{Log}_e (A_0/A_1)} \quad (5-6)$$

This was attempted but the necessity for three measurements was considered too time consuming in view of the quantity of data that had to be analysed. Furthermore the errors in T_D could be quite large for each individual measurement though these can be minimized either by taking several measurements from each echo or by fitting a curve by eye to the observed decay and then apply equation (5-6).

- c) To obtain maximum use from the echo decay recorded, and to minimize the number of measurements required, values obtained from equation (5-3) for D_a , using the 1962 U.S. Standard atmosphere values of ρ_a and T , were used to draw sets of decay curves. These curves were then fitted to the observed decay by eye. Curves drawn for one amplitude may be used for smaller amplitudes by keeping the bottom of the echo and the zero line for the curves coincident and then the two are moved with respect to one another until a curve matches the observed decay.

This method was adopted throughout most of the data analysis. The major problem arising from using this method was the grouping of decay heights about the particular heights used to draw the curves.

B. VELOCITY

5.3 The Observed Phase Variations in the Returned Signal

There are several sources of phase variations in the observed signal.

1. Finite Meteoroid Velocity

Rapid variations in the recorded amplitude and phase of an echo during the first 0.05 secs may be due to the time it takes for the trail to be formed due to the finite meteoroid velocity. However, for the pulse period used these effects will not be expected to be recorded. From observation of the collected data, a very small number, probably less than 1 to 2%, show considerable phase variations in the initial stages of the record, that could be associated with finite velocity effects.

2. Plasma Resonance

If the radio wave electric vector incident on the meteor trail is transverse to the trail, enhanced scattering, resulting in doubling of the echo amplitude and a phase shift in the returned echo phase of 180° is possible (Kaiser and Closs, 1952). These effects have been observed, (Greenhow and Neufeld, 1956) to fit the reflection theory. From these observations, the resonance effect is expected to be over within 25 msec. The effect is most noticeable if wind velocities, discussed in section 5.3(3), are small.

From the data collected, resonance effects have been observed readily, only where the drift velocity of the trail is small, consistent with the observations above. Because the effect is not large and does not last very long, it is unlikely to cause any significant errors in determining velocities or heights for meteors with durations in excess of 0.15 secs.

For durations less than 0.1 secs, resonance effects may not be detected in the course of normal analysis, but again, because it is not seen in many records (Greenhow and Neufeld, 1956) its effects will not be expected to be significant.

3. Wind Velocity

This is the major source of phase changes in the observed signal. The effects on the returned signal due to the motion of the meteor trail in the local atmosphere may be considered from one of two points of view.

a) (Nowak, 1967) The transmitted radio wave frequency is Doppler shifted by the trail motion resulting in a slightly different frequency being received back. Thus

$$f_R = f_T \cdot \left[\frac{1 + v_r/c}{1 - v_r/c} \right] \quad (5-7)$$

where f_R = received frequency
 f_T = transmitted frequency
 v_r = radial drift of trail
 c = velocity of light.

As $v_r \ll c$ and $f_R \approx f_T$ so (5-7) becomes

$$f_T - f_R = \Delta f = v_r (2f_T/c) \quad (5-8)$$

where Δf will be detected as a small change in the phase of f_T .

b) (Müller, 1970) Alternatively, the change in phase of the received signal will be 2π radians if the trail drifts a distance $\lambda/2$. Thus,

$$\frac{\text{change in phase}}{\text{change in time}} = \frac{\Delta\phi}{\Delta t} = \frac{4\pi v_r}{\lambda} \quad (5-9)$$

The expressions (5-8) and (5-9) are equivalent, though for measurement purposes, (5-9) proves more useful in envisaging the methods used.

Because the phase variation is here due to v_R , the radial drift of the meteor trail, it will be present for the entire meteor duration. This is the phase variation measured to obtain the wind velocities.

4. Wind Shear Effects

Two effects due to wind-shears occur.

- a) For meteor durations less than about 0.4 secs (Manning, 1959) wind shears will result in a change of the radial velocity with time due to rotation of the trail in the wind field. Müller (1968) used this to derive information on the windshears in the meteor region. Provided only a linear wind-shear is present, the observed radial acceleration will always be positive, and Müller interprets negative accelerations as being due to non-linear wind shears.
- b) For durations in excess of about 0.4 secs wind shears may be sufficiently severe to produce more than one specular point, or glint, on the trail. These points will produce different phases for reflection and interference will result between the glints (Manning, 1959), resulting in considerable amplitude fading and associated variations in the observed phases. For the special case of only two glints, Müller 1968, indicates that additional windshear information may be obtained.

In general, overdense echoes, with durations of several seconds, will exhibit this type of fading behaviour, making the phase information unusable. However, providing there is no amplitude fading, the Doppler information of an overdense echo can be used to determine the wind velocity.

From the above, it is evident that the major contribution to observed signal phase variations will be due to atmospheric

winds. Finite meteoroid velocity and resonance effects are not expected to affect more than the first 50 msec of the echo lifetime and windshears, unless severe, are not expected to affect the subsequent phase information until after 0.4 secs. For meteor durations in excess of 0.4 secs, especially long duration overdense returns, amplitude fading may occur. For less severe wind-shear effects, in which only the observed phase changes, the errors in the determined Doppler will usually be less than the measurement errors. If the wind shear was sufficiently large to be clearly evident to the film reader as a change in the wavelength of the observed Doppler beat then the phase error will probably exceed measurement errors. For this reason, readers were requested to note down such shears if present.

5.4 Measurement of the Radial Velocity, v_r , from Records

Two limiting methods for measuring v_r are suggested in equation (5-9), either

- a) variations in $\Delta\phi$ for constant time intervals, Δt , can be measured, or
- b) the time, Δt , for a constant phase variation, i.e. $\Delta\phi = 360^\circ$, may be measured.

Provided the observed phase variation is in excess of 180° (b) can be used. However, for variations less than 180° it is difficult to determine $\Delta\phi$, and it is suggested (Greenhow, 1954) that (a) be adopted, in this case phase differences for individual pulses are considered.

In general, the two phase traces from the phase sensitive detector may be expressed as

$$y_1 = A_1 \sin (\phi + \psi)$$

$$y_2 = A_2 \cos \phi$$
(5-10)

where A_1 , A_2 are the amplitudes of the two traces. If the two traces have amplitudes a_1 and b_1 at time t and amplitudes a_2 and b_2 at time $t + \Delta t$, then

$$\frac{\Delta \phi}{\Delta t} = \frac{1}{\Delta t} \cdot \tan^{-1} \left[\frac{\sec \psi \cdot (A \frac{a_1}{b_1} - B \frac{a_2}{b_2})}{1 + \sec^2 \psi \cdot (A \frac{a_1}{b_1} - \sin \psi) (B \frac{a_2}{b_2} - \sin \psi)} \right]$$
(5-11)

where $A = A_2/A_1$ at time t , and $B = A_2/A_1$ at time $t + \Delta t$.

When $A = B = 1$ and the phase shift between the traces is 90° , then (5-11) reduces to

$$\frac{\Delta \phi}{\Delta t} = \frac{1}{\Delta t} \cdot \tan^{-1} \left[\frac{a_1 b_2 - a_2 b_1}{a_1 a_2 + b_1 b_2} \right]$$
(5-12)

Thus, if the two phase detectors are not identical, or $\psi \neq 0$, errors will be introduced in a rather complicated fashion. A further random error in both (5-11) and (5-12) exists if the zero base-line from which pulse amplitudes are measured is not known exactly.

In the present equipment, the phase reference is amplitude limited (section 4.4), and this produced variations in A_1/A_2 of up to 20%, depending on the signal amplitude applied. As the variation depends on signal amplitude, $A \neq B$ in general. Partly because of this, and partly because measurements could be made ^{more} quickly, method (b) was adopted for phase measurements. The time for a phase change of 360° was estimated from the observed phase variations.

The errors in velocities may thus be split into three groups -

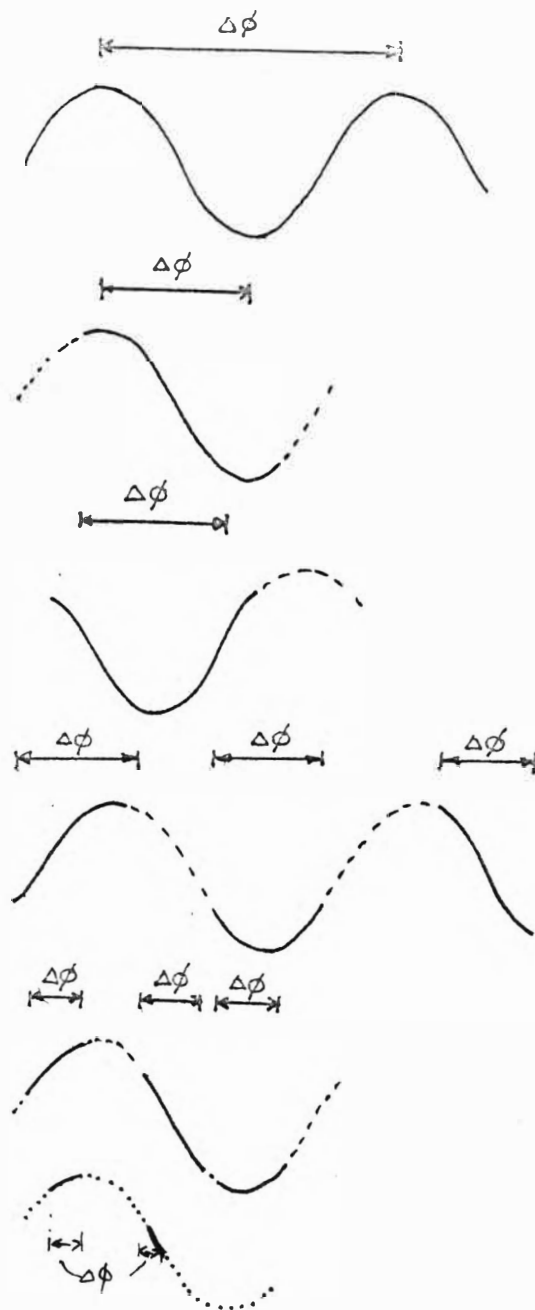


DIAGRAM 5-1 TYPE OF DOPPLER

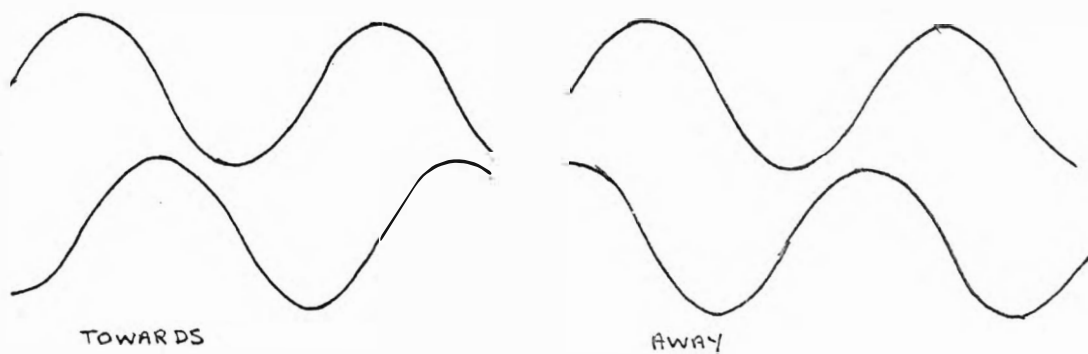


DIAGRAM 5-2

DIRECTIONS.

- i) for $\Delta\phi > 180^\circ$ over the entire record, it is possible to estimate the time for 360° phase change objectively, all errors being those due to measurements.
- ii) for $180^\circ > \Delta\phi > 90^\circ$ it may be possible to obtain an objective measurement for 360° phase change by observing the positions of maxima, or zero points, on the two traces. This must, however, be considered a little subjective, as these points are not generally obvious.
- iii) for $\Delta\phi < 90^\circ$ any estimate for 360° variation will really be no better than a lower limit. Errors here will be subjective.

5.5 Type of Doppler

In an effort to keep some control over the different errors possible, the type of Doppler from which measurements were made was classified according to how much of a phase change was observed during the complete echo duration. The various types are indicated in diagram 5-1.

5.6 Wind Shear Measurements

In an effort to explore some of the results obtained by Müller, (1968), an attempt was made to measure wind-shears from the records obtained. Although phase variations for a constant time interval were recorded, because of the reasons cited in sec. 5-4, it was decided to use only one trace, and estimate the phase variations from

$$\frac{\Delta\phi}{\Delta t} = \frac{1}{\Delta t} \cdot \left[\sin^{-1}\left(\frac{a_1}{A}\right) - \sin\left(\frac{a_2}{A}\right) \right],$$

as this gave greater control on the possible errors present.

A statistical analysis of the results obtained were in good agreement with those obtained by Müller (1968), (Poulter, 1971).

5.7 Durations

From equation (5-9) it is evident that for a given $\Delta\phi$, the minimum observable radial velocity will be limited by the meteor duration. To assess the effects this had on the observed velocities, the durations of underdense meteors were recorded. This duration is the time for which the record was observable and is only indirectly related to T_D in equation (5-5).

5.8 Direction of Trail Drift

From equation (5-10), if $\psi = 0$, the sign of y_1 and y_2 will indicate whether ϕ is positive or negative, corresponding to a velocity away from or towards the aerial. The two orientations are shown in diagram 5-2. As with the determination of velocities, the direction will become more subjective for smaller observed $\Delta\phi$. By careful observation of the positions of the maxima, minima and zeros of the two Doppler traces it is usually possible to estimate the direction of the trail drift for $\Delta\phi > 90^\circ$, but this becomes considerably more subjective for $\Delta\phi < 90^\circ$.

C. OTHER PARAMETERS READ OFF FILM

5.9 Range

As indicated, (section 4.8(5)) the range was recorded by brightening up a section of a ramp corresponding to the time delay of the echo after transmission of the output pulse. The position of the range mark is recorded by measuring the number of centimetres it is from the top of the graticule. The range is calculated in the computer program by making a first order interpolation using the measurement above and a calibration tabulating the range in equal steps. The error in

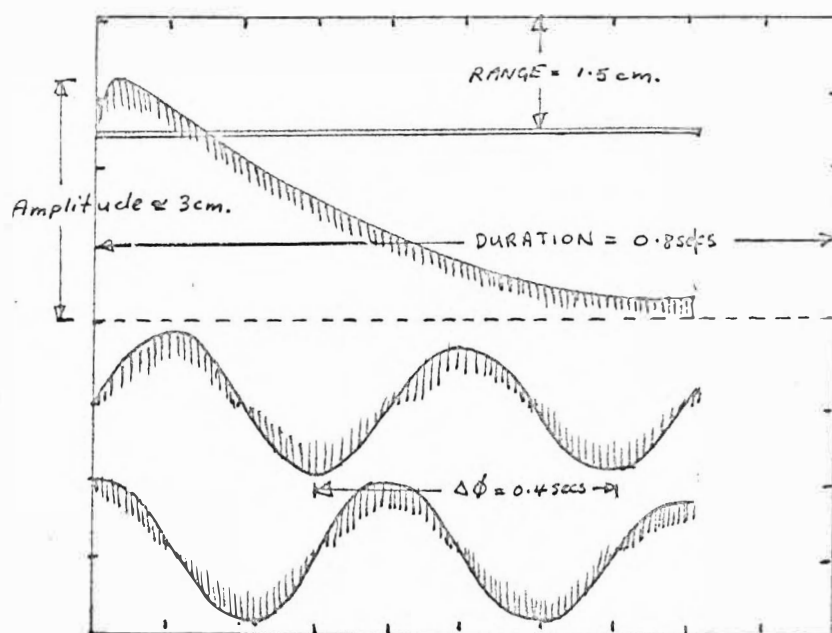
the range will be ± 10 km.

5.10 Type of Record

Both underdense and overdense meteor trains were recorded on film. However, it was generally not possible to determine satisfactory wind velocity and height information from the overdense records due to amplitude fading and rather confused phase traces. It is not obvious what relationship this phase information bears to the trail drift velocity so wind velocities were calculated using underdense records. Film readers judged whether a record was underdense or overdense. It is important to realise that though fading is not expected to affect the initial trail returns, it is possible for a trail that is not initially specular to be so disturbed by atmospheric winds that specular reflection subsequently occurs. Such trails will thus exhibit fading when initially observed.

5.11 Amplitude of Record

It seemed useful to have some measure of the echo amplitude as observed on the oscilloscope, so this was recorded to the nearest centimetre thus dividing the observed amplitudes into four groups. Those records whose amplitudes were greater than the display size available were lumped together as 5 cm. Because of variations in the operating conditions throughout the experiment due to improvements in the apparatus, no attempt was made to relate the observed echo amplitudes to the signal power at the aerial. Amplitudes measured will thus only be comparable within a given set of data. Little use has been made of this information as yet.



Height ≈ 92 km.

Range = 1.5 cm.

Amplitude = 3 cm.

Duration = 0.8 sec.

V_R (doppler) = 0.4 sec

Error (in V_R) = 0.05 sec

Type of doppler = 1

Direction = A (away)

Type of record = d (decay)

DIAGRAM 5-3. An indication of the parameters measured.

5.12 Summary

The parameters measured are best summarized by reference to diag. 5-3. The photograph, ^{plate 5.3,} is of an underdense meteor and would be used to give the following:

1. Height
2. Radial Velocity. Time for a 360° phase change is 0.21 ± 0.01 sec., which gives a radial velocity of 13 ± 0.7 m/s. There are three points to note here:
 - a) The maxima of the phase traces are noticeably smaller towards the end of the echo,
 - b) The zeros of the phase traces are not as clear as the maxima and minima, for purposes of measurements,
 - c) There is evidence of an increase in the phase variation with time, but it is not significant in light of the errors present.
3. Type of Doppler. It is possible to measure a 360° change in phase. This is a type 1 Doppler.
4. Duration. The meteor is present for 0.46 seconds.
5. Direction.
6. Range. This is 0.7 cm, measured down from the top of the frame.
7. Type of Record. This is a decay, or underdense record.
8. Amplitude. The amplitude exceeds the display size; it therefore has an amplitude of 5 cm.

The photograph was taken with the oscilloscope time base sweeping 0.1 sec/cm, and is representative of a good record. The sketch below the photograph represents the same meteor as observed with a faster sweep time on the oscilloscope and indicates,

- i) the layout of the four traces

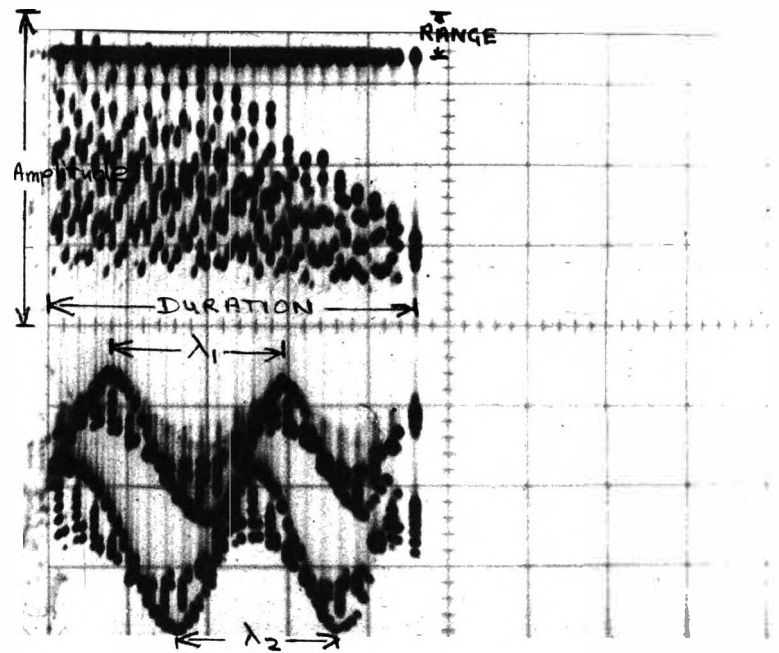
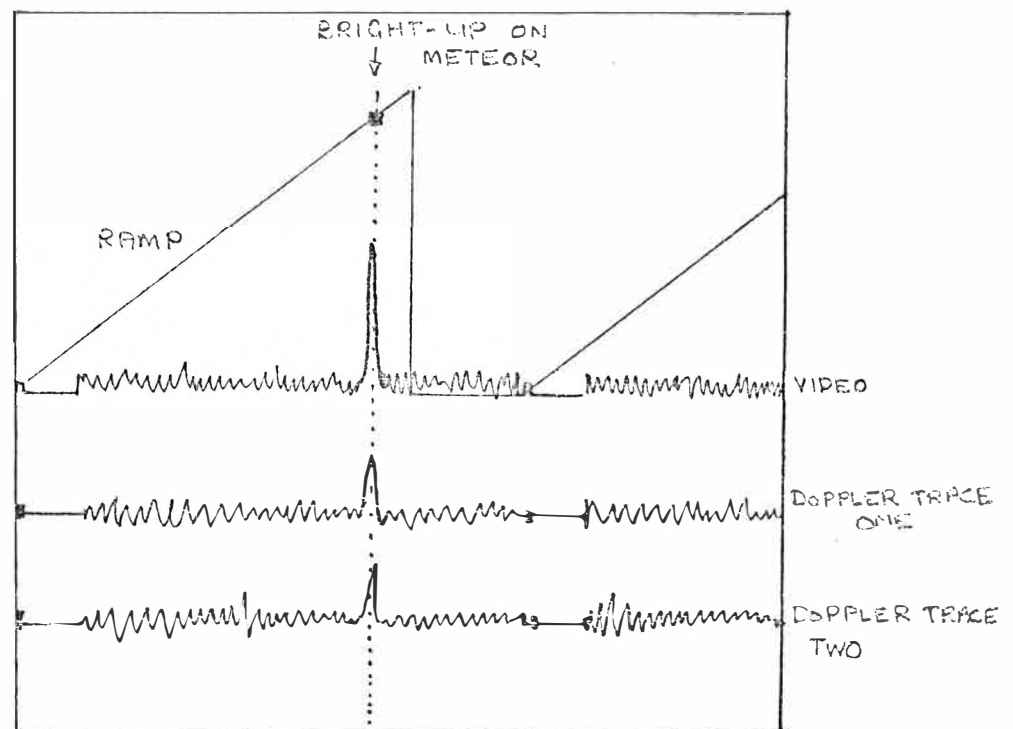


PLATE 5-3. LAYOUT OF TRACES
(SWEEP SPEED 0.1 sec/cm)



THE SAME ON 6.6 msec/cm SHOWING
MORE CLEARLY THE POSITION OF THE
RAMP FOR RANGE INFORMATION.

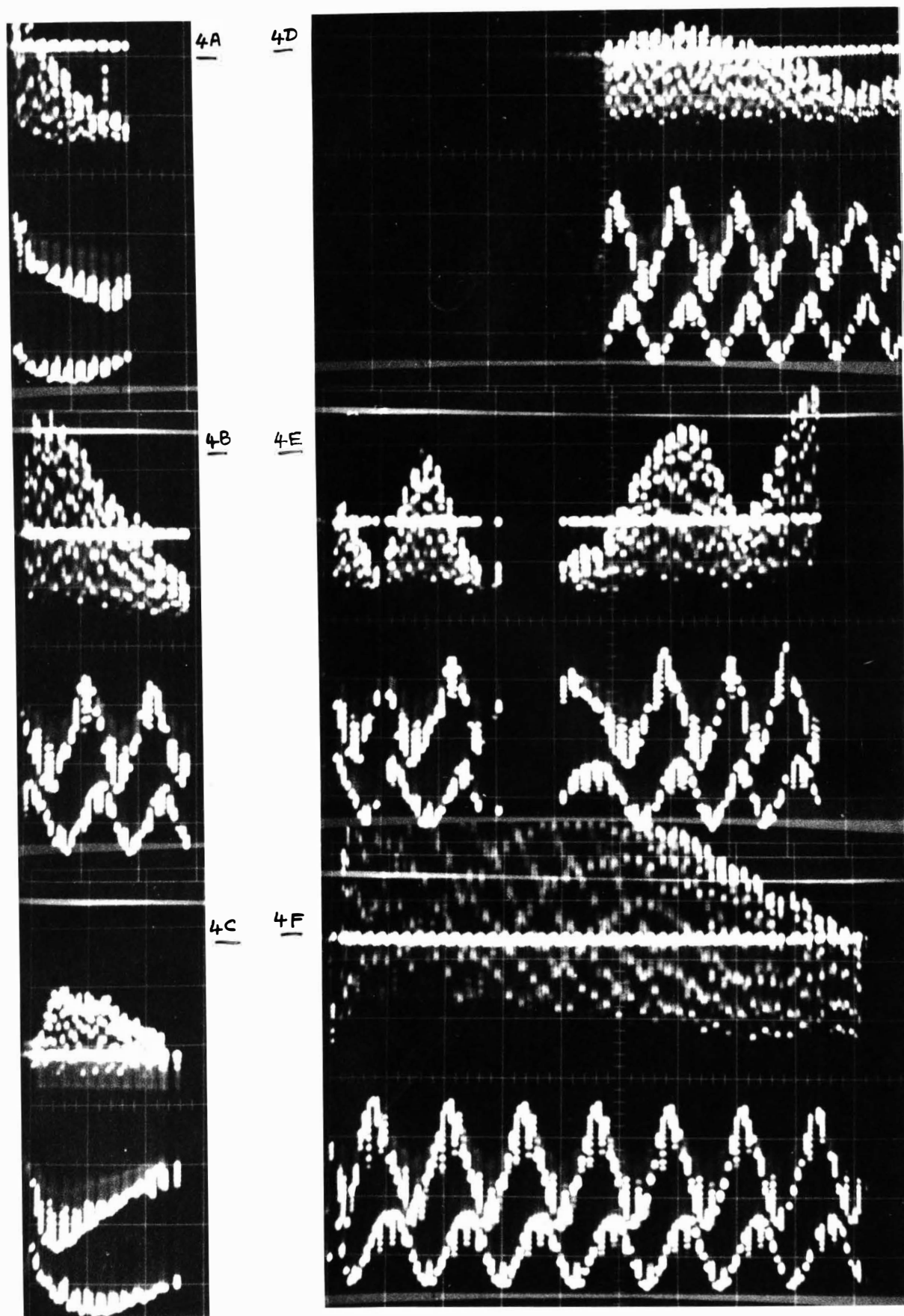


DIAGRAM 5-4. EXAMPLES OF OBSERVED METEORS.

(all frames from 0500-0510 on day 124, year 1971)

ii) the action of the bright-up pulse.

Some further examples of observed meteors are given in diagram 5-4.

4A An underdense meteor, good decay and an average duration. The direction is easily read, but the phase change is less than 180° . It is thus a type 4 Doppler.

4B An underdense record, with a faster phase change than 4A, and in the opposite direction.

4C This has a slow rise time, and a possible variation in the initial phase. It is the type of record that would give film readers trouble in classifying it.

4D, 4E These are two frames of the same overdense meteor - note the range is the same in both cases. There is considerable amplitude fading in 4E, but in both frames the phase varies almost as regularly as in 4B.

4F Another underdense meteor with a long duration, 0.9 secs.

C H A P T E R 6

ERRORS IN DEDUCED VALUES OF WIND VELOCITIES

Introduction

To obtain the average wind velocity for 30 minutes, all wind velocities obtained from underdense meteors are used, the mean being found for all values together, and also when subdivided into height intervals. It is important to assess the significance of these averages, and in this chapter, the errors due to the present system of recording and analysing meteors are considered. In the first section, systematic and random errors in the parameters obtained from a single meteor echo are considered. The second section deals with the complete average over half an hour.

Particular attention was paid to the uncertainties introduced by film reading in both these sections by comparing the data obtained from three people reading the same section of film, hereafter referred to as the test film. Every frame on the film was numbered, so that the results for individual meteors could be compared.

A. THE INDIVIDUAL METEOR ECHO

6.1 Durations

Although the value of the meteor echo duration is not used in the present experiment, its effects are important in considering the observed height and velocity distributions. From histograms of the observed durations, diagram 6-1, the major points of interest are -

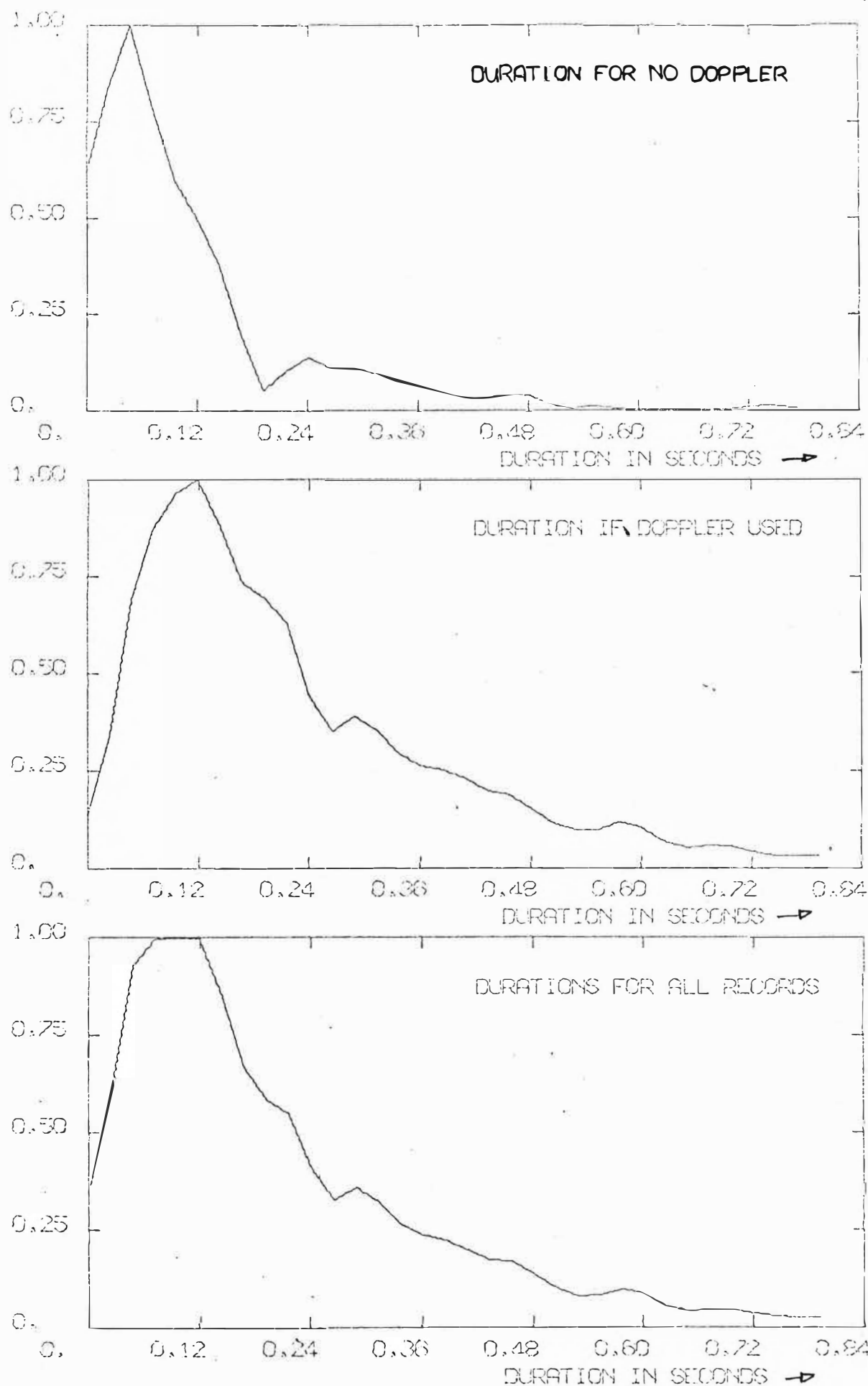


DIAGRAM 6-1 HISTOGRAMS OF OBSERVED METEOR DURATIONS.

(these are all normalized by the maximum value)

- a) The most likely duration for all meteors for which wind velocities are calculated is 0.12 secs.
- b) The mean duration, for 8300 meteors, was 0.2 secs.
- c) There is a loss of short duration meteors which is due to film reader selection, see diag. 6-1. If a meteor has too short a duration, it becomes difficult to obtain a satisfactory determination of the wind velocity. (Longer durations may be mistakenly classed as overdense if the phase information shows any irregularities.)
- d) The peak of the duration distribution moves to shorter durations as the altitude increases. This is expected, as there is an increase in the decay constant with altitude. The change in the peak position for 2700 meteors was 0.01 ± 0.005 secs/km.

6.2 Heights

1. Random Errors

From a comparison of heights obtained from the test film, differences in heights between different readers for the same meteor had the following distribution properties:

Mode = 2 ± 1 km

Mean = 2.3 ± 1 km.

From this, the worst height error due to film reading would be ± 2 km. As the earlier height error, due to diffusion properties (Sec. 5.1) will be independent of this error, the height error due to both sources will be

$$(2.5^2 + 2^2)^{\frac{1}{2}} = 3.2 \text{ km.}$$

In view of this, an error in the height of ± 3 km was considered reasonable, though for convenience a height

interval of 5 km was used when wind profiles were constructed.

2. Systematic Errors

i) Film Reader Selection of Heights: In diag. 6-2, a height histogram for 1 km intervals is shown. The peaks that occur in this distribution show the effects of fitting curves to the observed amplitude decay to obtain the meteor height - each peak corresponds to a height curve used in measuring the heights from film. The height for a particular meteor will thus be misleading as it is more probably the decay height on the curve fitting card nearest to the observed height.

To obtain smoothed curves, with the peaks removed, it was found convenient to use a running average over a 5 km interval. This means that all the heights had equal weight in the interval. The smoothed curve is shown on the same plot, and will be considered further in the next section.

ii) The Height Distribution of Observed Meteors: In order to check if any systematic errors occur in estimating the echo heights, the observed distribution peak of the echo heights is compared with the expected peak in the distribution.

For the present equipment, cosmic noise normally produced a 3 μ V pulse signal at the receiver input. If the only external noise source is cosmic noise, it would be possible to detect all meteors that produce 6 μ V or more at the receiver input. However, additional noise due to local radio frequency sources often required a higher level for discrimination. A reasonable choice for the minimum observed signal would be 10 μ V. From (3-6) the minimum line density detected will thus be

$$q = \frac{V_R}{(2.5 \times 10^{-32} ZGP_T)^{1/2}} \cdot \left(\frac{R}{\lambda} \right)^{3/2} \text{ electrons/m.} \quad (6-1)$$

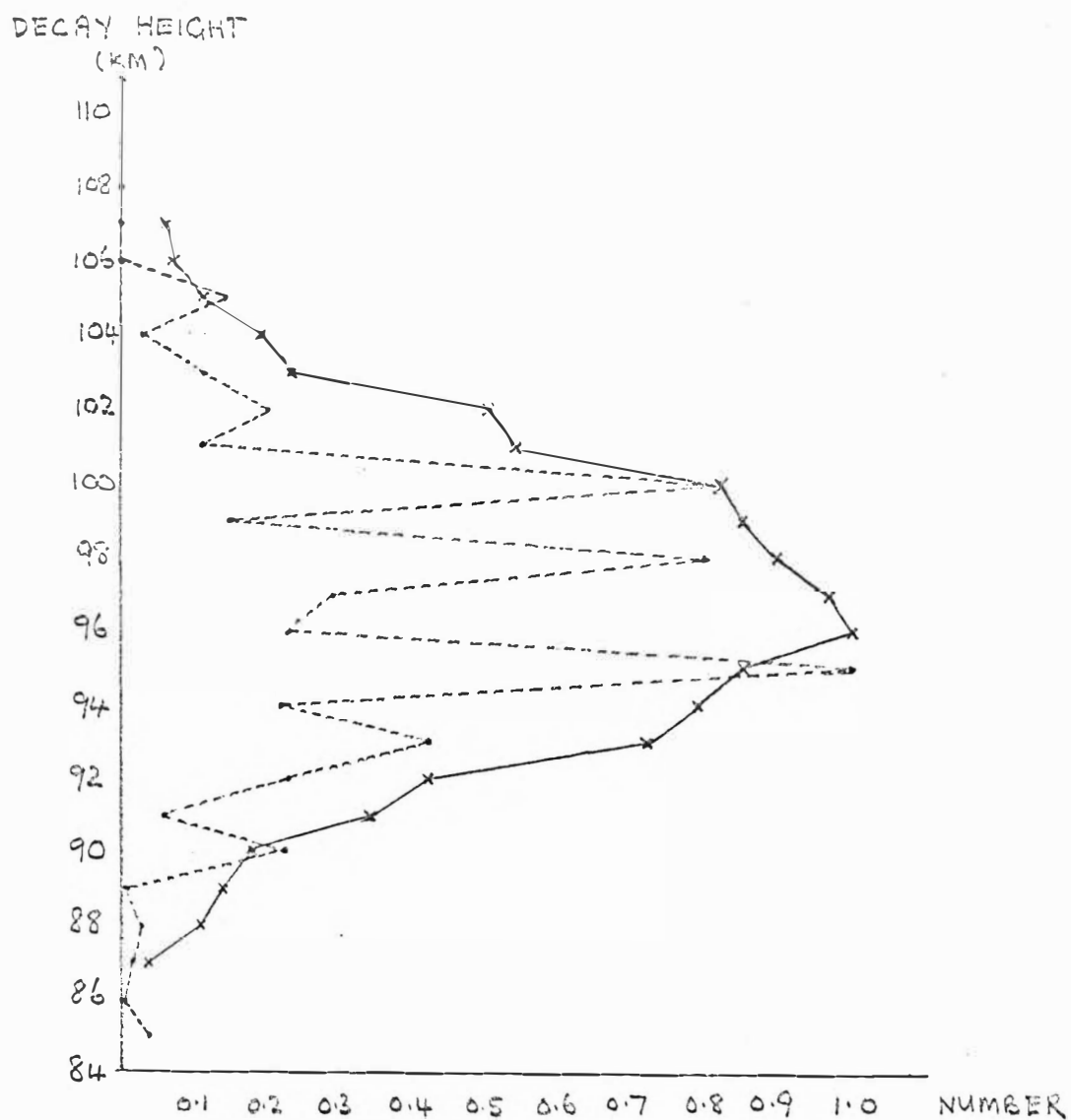


DIAGRAM 6-2 NORMALIZED HISTOGRAM OF
OBSERVED DECAY HEIGHTS.

----- HEIGHTS OBSERVED (IN 1KM INTERVALS)
——— HEIGHTS, SMOOTHED BY RUNNING AVERAGE
OVER FIVE 1KM INTERVALS.

where V_R = voltage at the receiver input

Z = receiver input impedance (ohms)

The received power was replaced by

$$P_R = G \cdot V_R^2 / Z \quad (6-2)$$

which is valid in the present context provided the losses between the aerial and receiver input do not affect the signal to noise ratio of the complete system. As the major loss in this segment occurred in the T/R switch, and this was found to be constant over the receiver bandwidth, equation (6-2) is acceptable. Using $V_R = 10 \mu V$, $Z = 50 \Omega$, $P_T = 40$ kwatts, $R_0 = 3 \times 10^5$ m, $\lambda = 11$ m, and $G = 10$ (Fishenden and Wiblin, 1949),

$$q_{\min} = 2 \times 10^{13} \text{ electrons/m.}$$

Before continuing, it is of interest to obtain the limiting magnitude of the system using, (Kaiser, 1953),

$$M = -2.5 \log_{10} q + 40.$$

Thus, the present system should record all meteors down to magnitude +7. When this was repeated using a more sensitive display system, a $1 \mu V$ pulse signal was detected, giving a magnitude of +9 as the limiting magnitude. Since short duration meteors are lost because of film reader selection, this will be the lower limit to the minimum detectable meteor.

Using $q_{\min} = 2 \times 10^{13}$, then, the peak of the height distribution may now be found from eqn (3-5), as meteors with the minimum detectable line density will produce most of the observable meteors. Thus, the maximum for the height

distribution, taking an average meteor velocity of 40 km/s, will be at 102 km.

However, allowance for the echo ceiling due to finite meteor velocity and the initial radius effect will shift this peak down. By allowing for these effects, using (3-8) and an initial radius of 1.1 m (Baggaley, 1970) at 100 km the power loss is found to be 8 dB. This results in a lowering of the height distribution peak to 100 km.

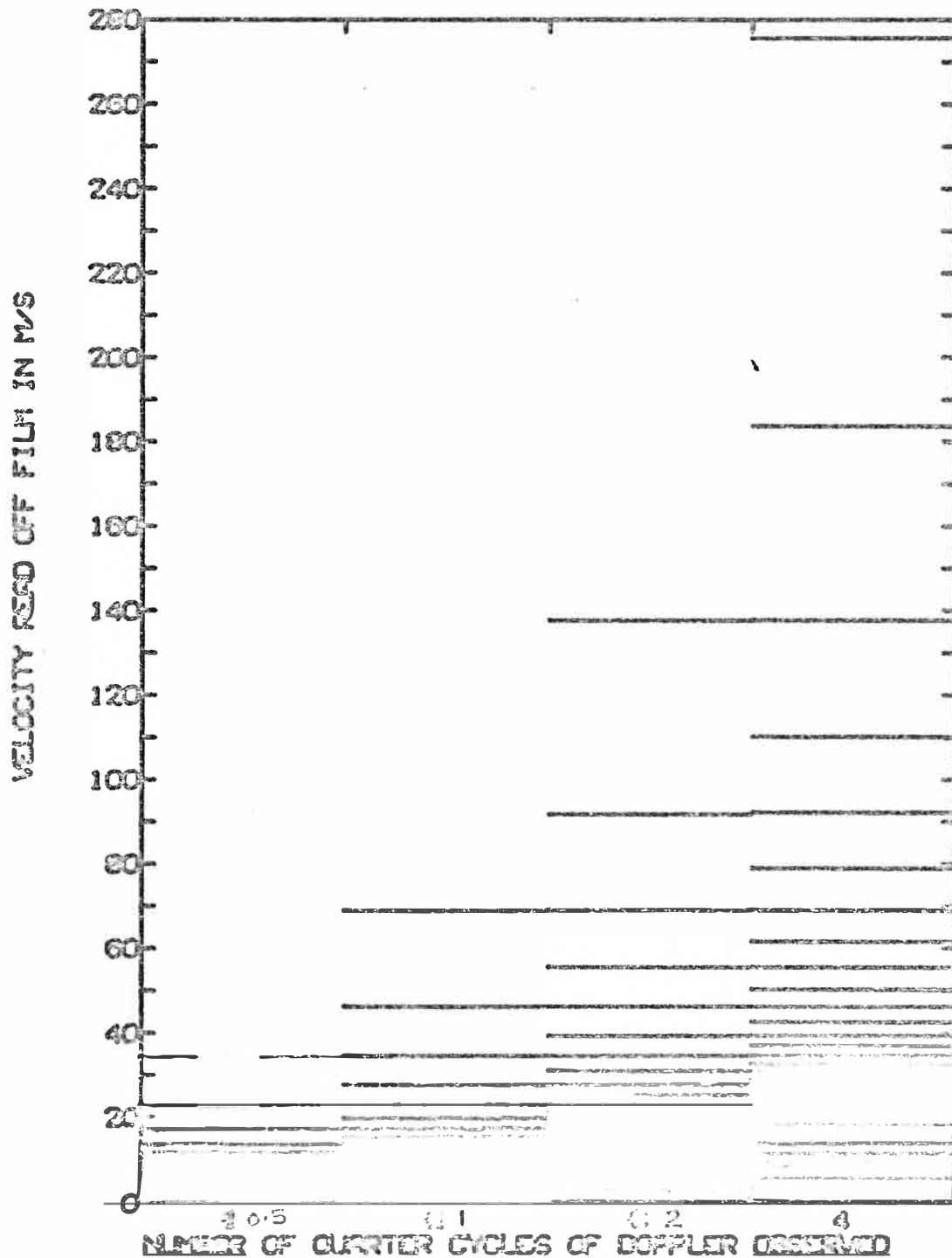
As was indicated in Sec. 6-2, there is discrimination against short duration echoes by film readers because insufficient phase information is available to determine the wind velocity. This effect will be more significant at greater altitudes, because durations are lower. From diag. 6-1, there is a peak for such meteors at a duration of 0.04 secs. A meteor must have sufficient amplitude to have a duration greater than 0.04 secs before it may reasonably be expected to be detected. Using,

$$\frac{P_R(0)}{P_R(t)} = \exp \left(\frac{32\pi^2 D_0 t}{\lambda^2} \right) \quad (6-3)$$

and putting in $t = 0.04$ secs, it can be shown that a meteor must initially be at least 7 dB above noise before it will be detected at 100 km. The distribution peak would thus be expected to occur at 97 km, because of this further loss.

The observed height distribution given by the running average in diag. 6-2 is peaked at 96 km, in good agreement with the expected result.

On the basis of this evidence, the observed peak in heights is not considered systematically different from that expected from theoretical calculations. The assumed height dependence of the ambipolar diffusion coefficient is thus in



VELOCITIES FROM FILM READING
DIAGRAM 6-3

good agreement with the experimental results.

Height histograms were also calculated for results obtained by the different film readers and no systematic differences were observed either in the peak position or the curve shape.

6.3 Wind Velocity

The wind speed was obtained by measuring the time taken for a meteor trail to produce a phase change of 360° between the transmitted and received signals. As a result of the recording method used systematic and random errors will be introduced.

1. Random Errors

a) Apart from errors in measurements, there was also an error in the windspeed due to the incorrect assessment of the fraction of 360° phase change present. Using the test film, the average error for a single record, including subjective errors, is 8 m/s. If the errors assessed by film readers are used, then this reduces to 4 m/s, suggesting that subjective errors involving the type of Doppler will involve half the error in the determination.

b) The average percentage error in 8500 meteors was found to be 18%, which agrees well with the above calculation where the average velocity was 26 m/s, giving a 15% error.

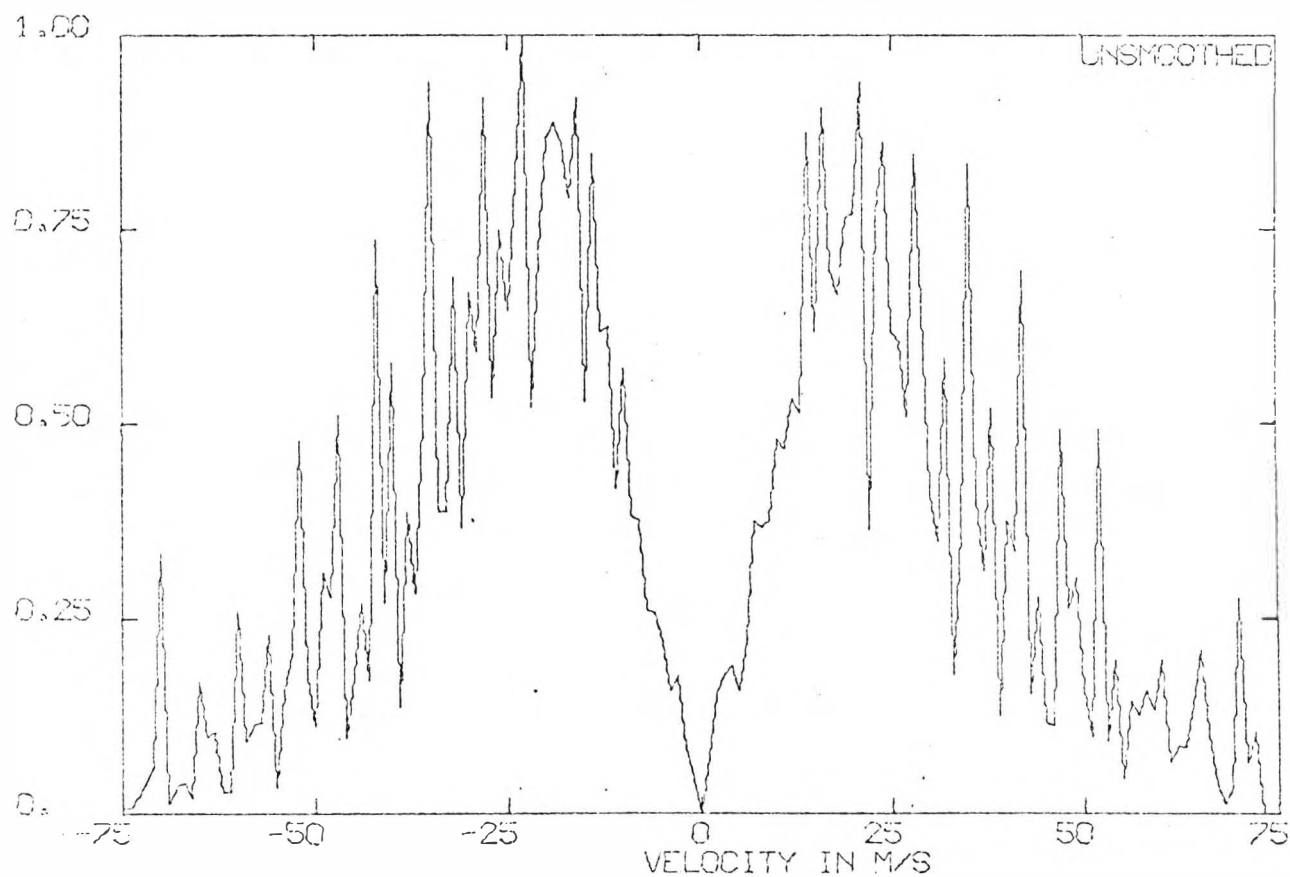
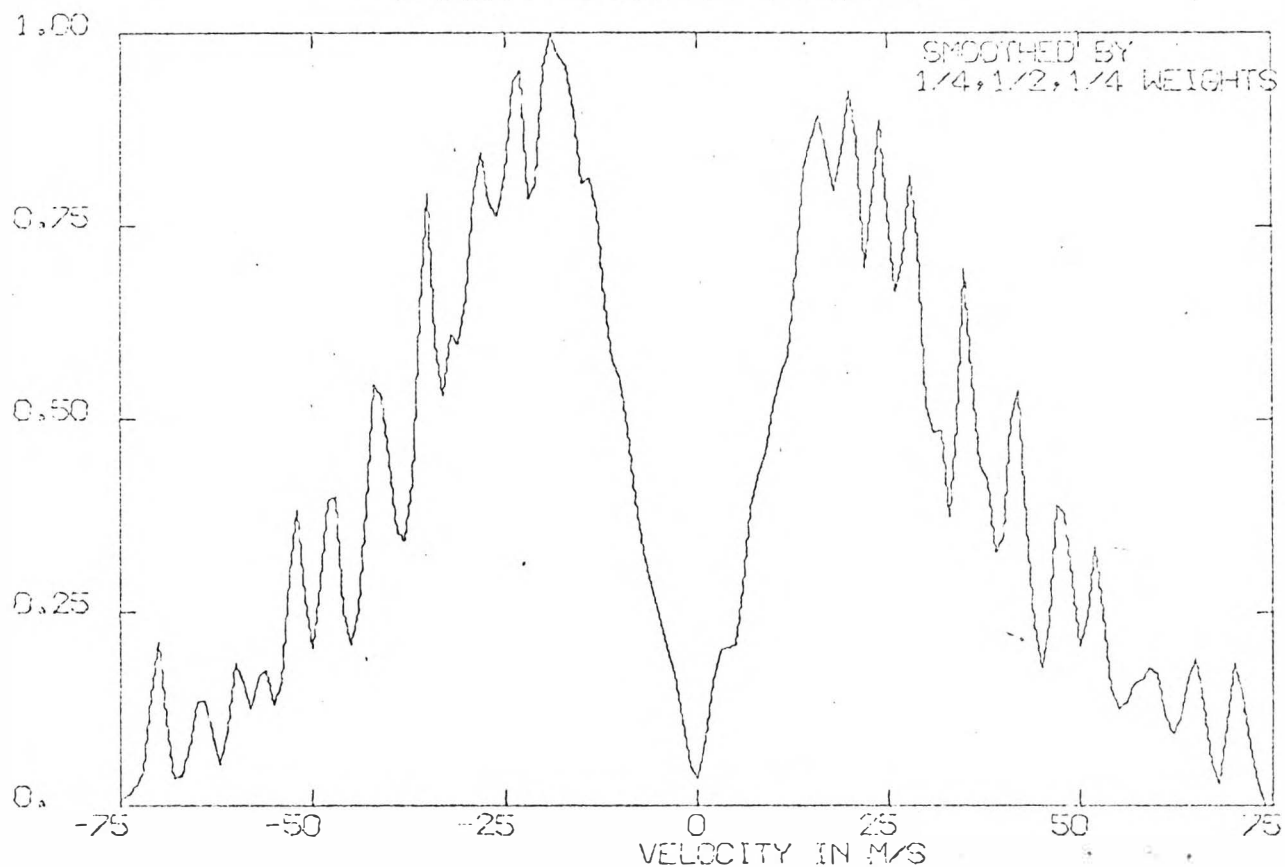
c) The percentage errors assigned by film readers was found to be the same for all film readers.

2. Systematic Errors

a) Of minor importance will be the effects of the coarse grid used for measurements, see diag. 6-3. The smallest increment used for time measurements was 0.01 secs. Peaks in the wind speed distributions may be readily related to this

DIAGRAM 6-4NORMALIZED HISTOGRAM OF
OBSERVED VELOCITIES

(VELOCITY INCREMENT IS 1M/S)



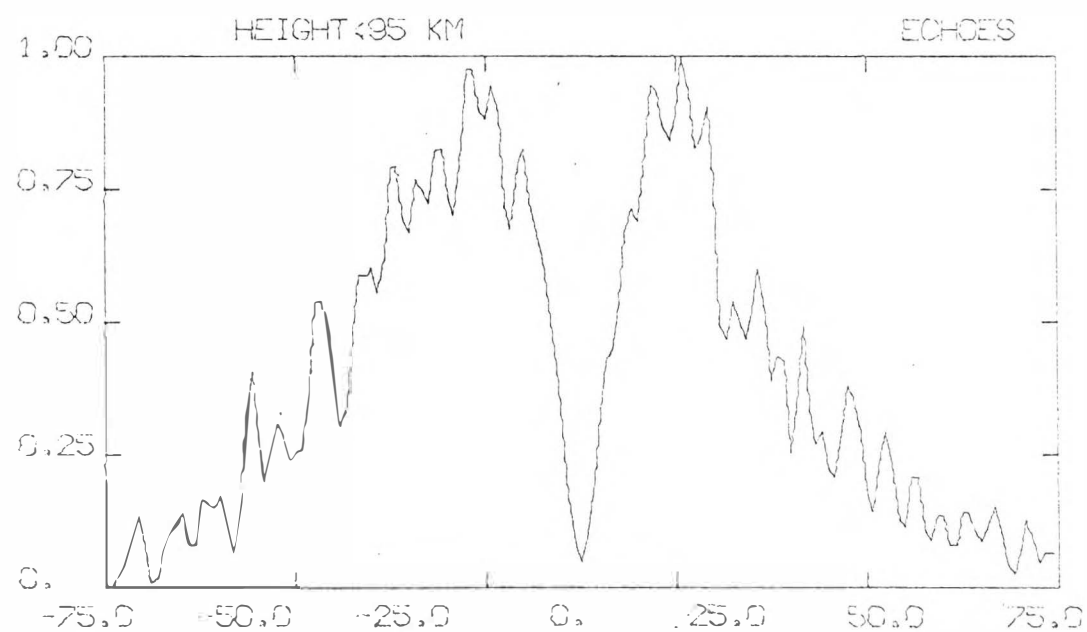
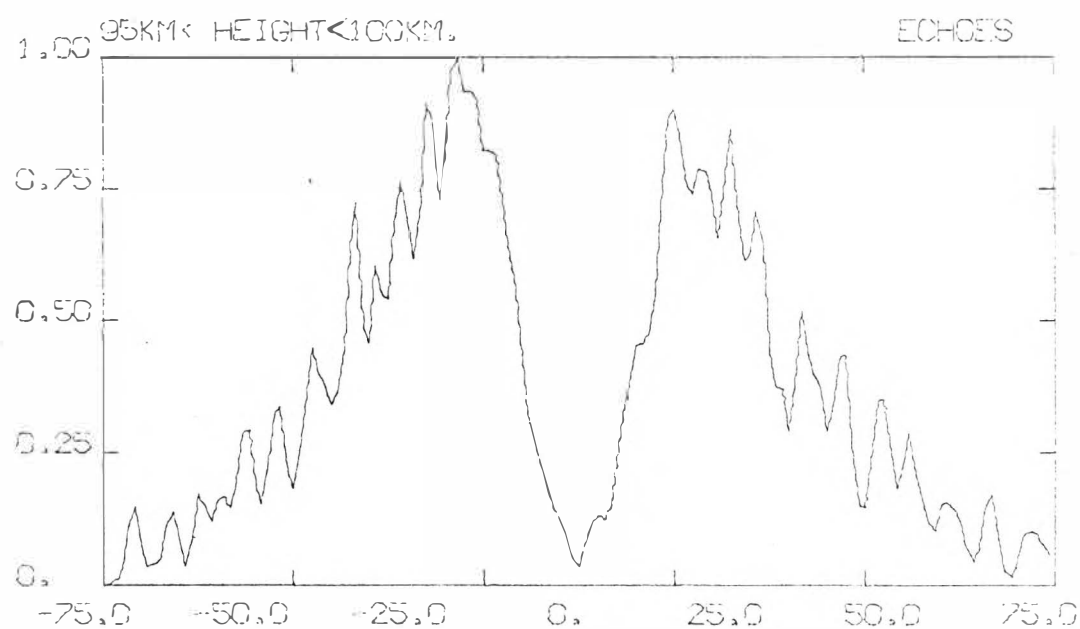
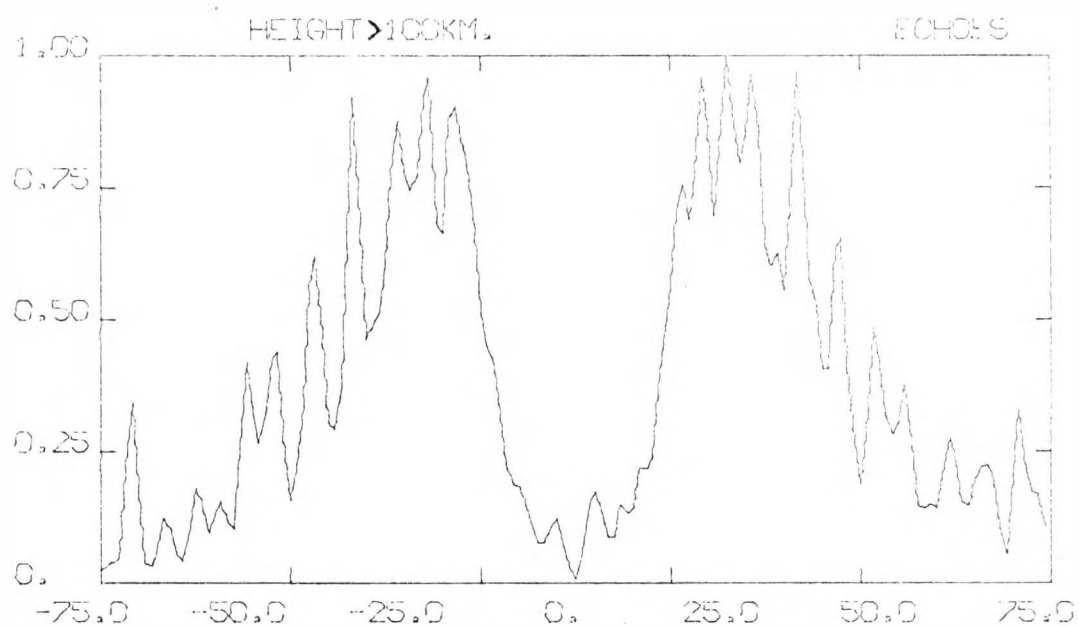


DIAGRAM 6-5. VELOCITY HISTOGRAMS FOR
DIFFERENT HEIGHT INTERVALS.

feature of the measurements, and because of this, it is not reasonable to attach too much significance to any one velocity. (Peaks observed in diagram 6-4 may be related to diagram 6-3.)

b) Of much greater importance are the effects of the finite meteor duration. For very low wind speeds, the meteor duration must be longer if the velocity is to be satisfactorily measured. As demonstrated (Sec. 6-2) the duration distribution has a mean of 0.2 secs. If a phase change of π radians is required to obtain objective measurements of wind speeds, then the durations indicate a bias against speeds less than approximately 20 m/s. From diagram 6-4, it is evident that such a loss of low speeds does occur, the most probable speed being approximately 20 m/s.

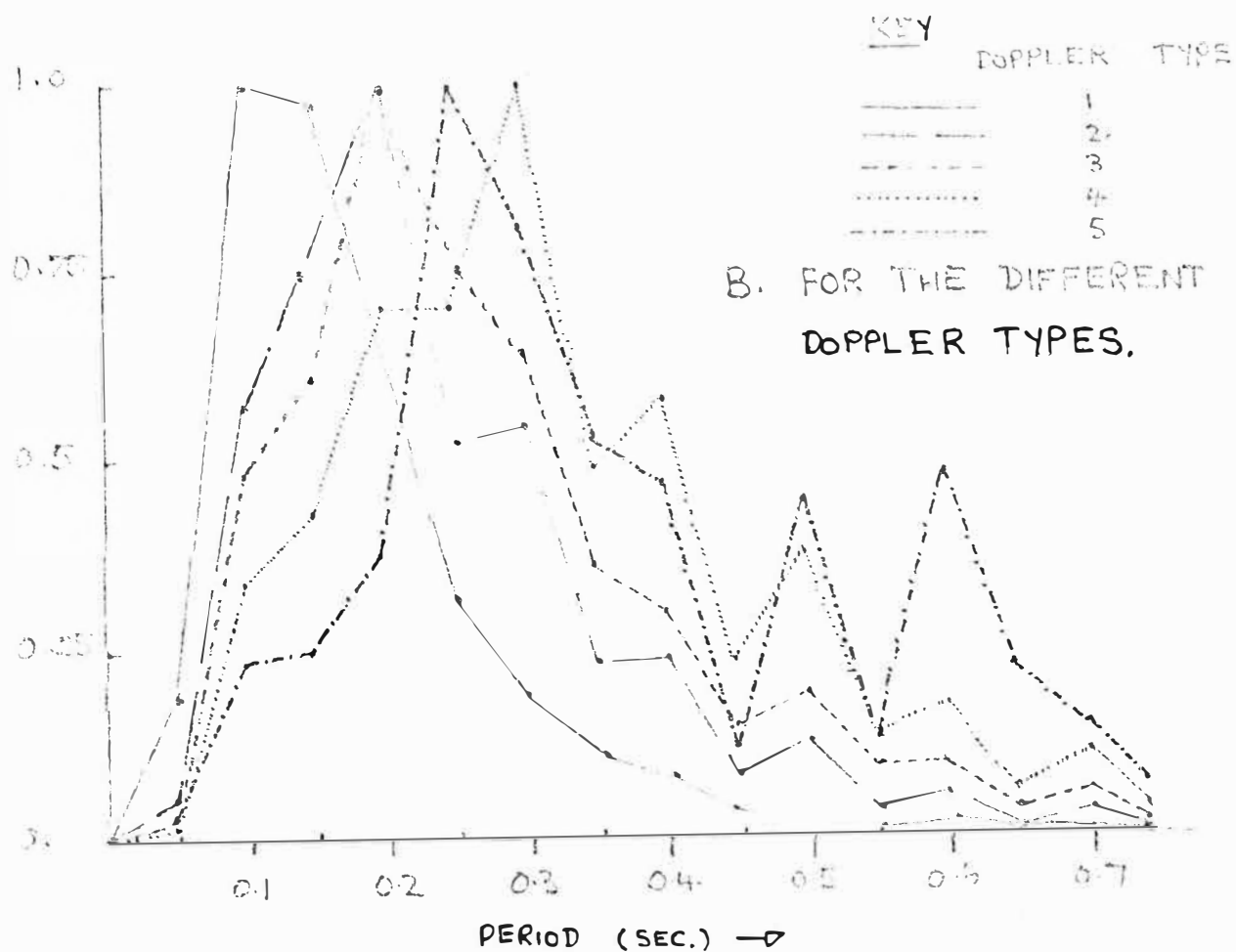
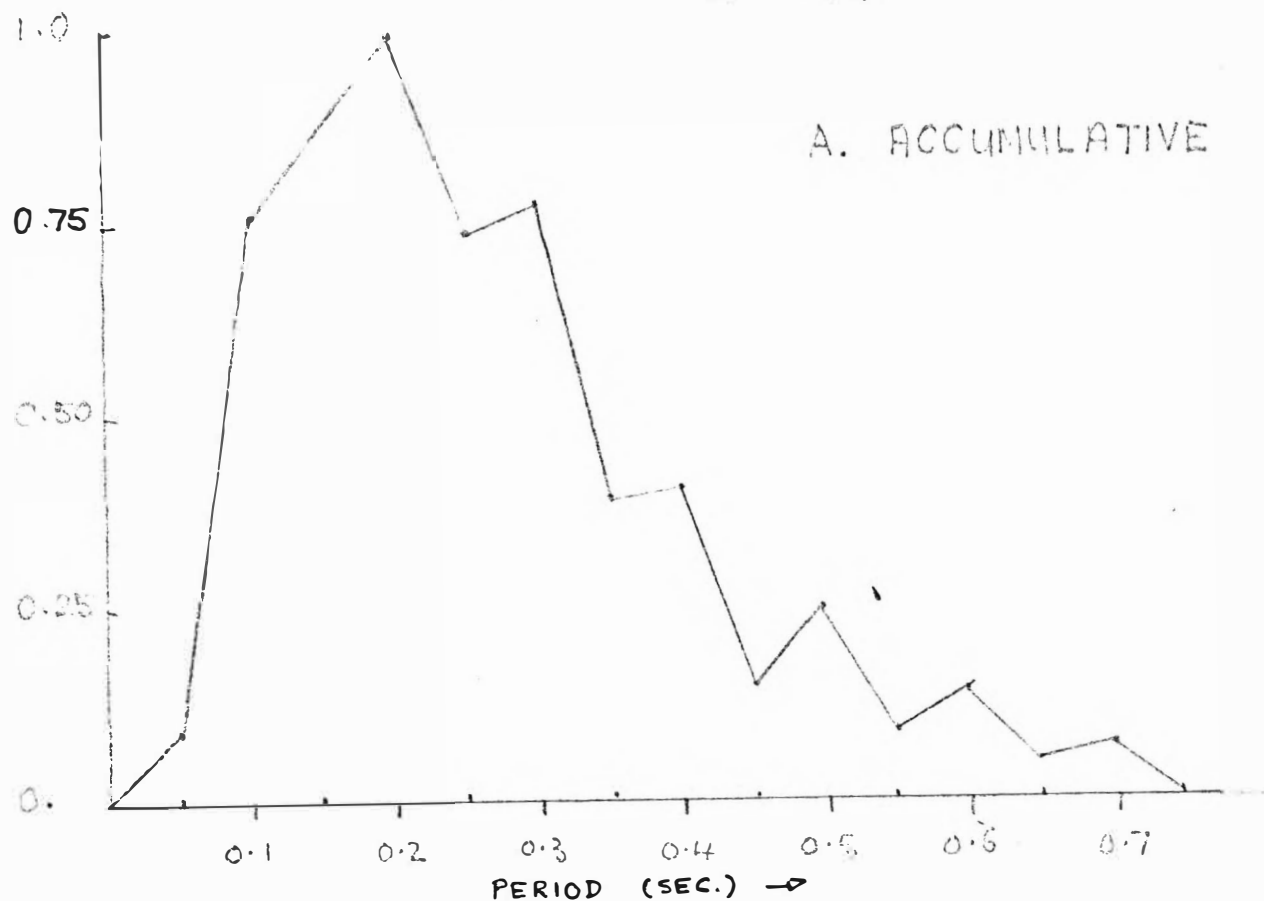
c) As the mean duration decreases with increasing altitude, the loss of low speeds would be expected to be more evident at greater altitudes. Diagram 6-5 supports this, showing a considerably greater loss at greater altitudes.

In both diagrams 6-4 and 6-5, positive and negative velocities are included to emphasise that the loss is not dependent on direction. The peaks in the positive and negative velocities for all heights correspond to approximately the same values, as indicated in (a) above.

To overcome the loss of low velocities Nowak (1964) suggested offsetting the phase reference frequency by a sufficient amount to allow all velocities to produce phase changes in excess of 360° within the duration of the meteor. However, the use of a single offset frequency will only shift the zero velocity loss in the direction of the frequency offset producing an asymmetric loss of velocities. To remove this possibility, a second phase-sensitive detector with the

DIAGRAM 6-6 HISTOGRAM OF OBSERVED
DOPPLER PERIODS.

116



phase reference frequency offset in the opposite sense would be necessary. These points were not pursued in the present experiment.

3. Type of Doppler (see section 5-5, and diagram 5-1 for definition)

a) The selection of only those records with phase changes in excess of 180° will modify both the observed meteor durations and the observed wind speeds. (This system was used by AFCRL, (Barnes 1968), and it will artificially lower the observed meteor height distribution in the same way that film reader discrimination against short duration meteors does.) Diagram 6-6B shows histograms of the observed Doppler periods for different Doppler types. Phase changes less than 180° are associated with longer periods. This is more evident from the mean period, given in Table 6-1.

TABLE 6-1

Type of Doppler	1	2	3	4	5
Total No. of Meteors	1712	1878	874	2652	657
Mean Doppler period (secs)	0.18	0.24	0.27	0.32	0.47
Associated Radial velocity (m/s)	15	11.5	10	8.6	5.9
Mean duration (secs)	0.29	0.22	0.20	0.14	0.1

From Table 6-1 the mean duration is seen to drop. This is significant as the duration decreases with altitude producing a loss at high altitudes as suggested.

b) A possible systematic error was suspected in wind speed determined from type 3 Dopplers as the zeroes in the Doppler traces are difficult to observe. As the histograms of type 2 and type 3 Dopplers are similar (diag. 6-6B), and differences

in the mean Doppler period and mean duration are not greater than the differences from other Doppler types, any systematic error present is considered insignificant.

4. Direction

The errors in direction were assessed using the test film. It was found that for 88% of the meteors the direction was correctly assigned. In 7% of the cases one film reader differed from the other two, but expressed doubt in the result obtained and in 5% of the cases one film reader definitely disagreed with the other film readers.

5. Summary of Velocity Errors

- a) Subjective errors in recognizing how much of a phase change is present account for much of the random errors in individual velocities.
- b) Because of the finite meteor duration there is a loss of zero wind velocities.
- c) This loss may be enhanced by selecting records showing at least 180° phase change.
- d) The error in an individual velocity is approximately 18% and the direction has a 90% chance of being correct.

6.4 Type of Record

Because of the uncertainty in velocities obtained from overdense trails, the two types of trail were distinguished. However, because underdense echoes are characterized by an exponential decay, it was usual for any records that were not obviously exponential to be classified as overdense. In most cases, if there was any doubt about identification of a meteor, it would be classified as overdense, thus the overdense classification will be contaminated by underdense records.

TABLE 6-2

	Number of readers in agreement	3	2	1
1	Positive Identification	82%	10%	8%
2	All readers give same classification in 1	69%	87%	(100%)
3	All readers classify record as overdense in 1	40%	62%	99%

Table 6-2 shows that as there is less agreement between film readers about the type of record, so the percentage of persistent observed increases consistent with increasing doubt in the classification of a record. However, of all the records judged usable, only 56% were classified the same by all film readers. In view of this, the classification of the meteors observed cannot be considered satisfactory, though the increasing number of overdense classifications as fewer film readers identified a record as usable suggest that the underdense records are less likely to be contaminated by overdense records than vice versa.

B. AVERAGING OVER HALF AN HOUR'S RECORDS

It is apparent, from the previous section, that the wind velocities determined from a single record will be in error due to the method of analysis; the aerial used has a finite beamwidth and this will introduce additional errors. It is also assumed that the observed velocities are largely horizontal motions. Both these points will be considered later. However, from previous studies, (Greenhow and Neufeld, 1959), it is also known that the wind velocities recorded over

half an hour show considerable variability. By using a sufficiently large number of wind velocities, the average velocity will indicate the mean flow for the time over which the averaging was carried out.

However, as discussed in chapter 2, atmospheric tides will also be present in the data and if these are to be determined, averaging must not be carried out over too large a time interval. Furthermore, it will be necessary to observe the wind in two orthogonal directions if the complete wind vector is to be found. Thus, it is necessary to balance the meteor rate in time against the time resolution necessary to determine the atmospheric tides. For most of the experimental period, the initial teething problems associated with new equipment made it difficult to anticipate how many usable underdense records were recorded during a particular time period until the film was read. Because of this, and the desire to keep a uniform time interval throughout all the data collected, the recommendation (Barnes, 1968) that time increments of half an hour were satisfactory, was adopted. Having chosen a constant time interval, the significance of any one result will depend on the number of meteors recorded in that interval.

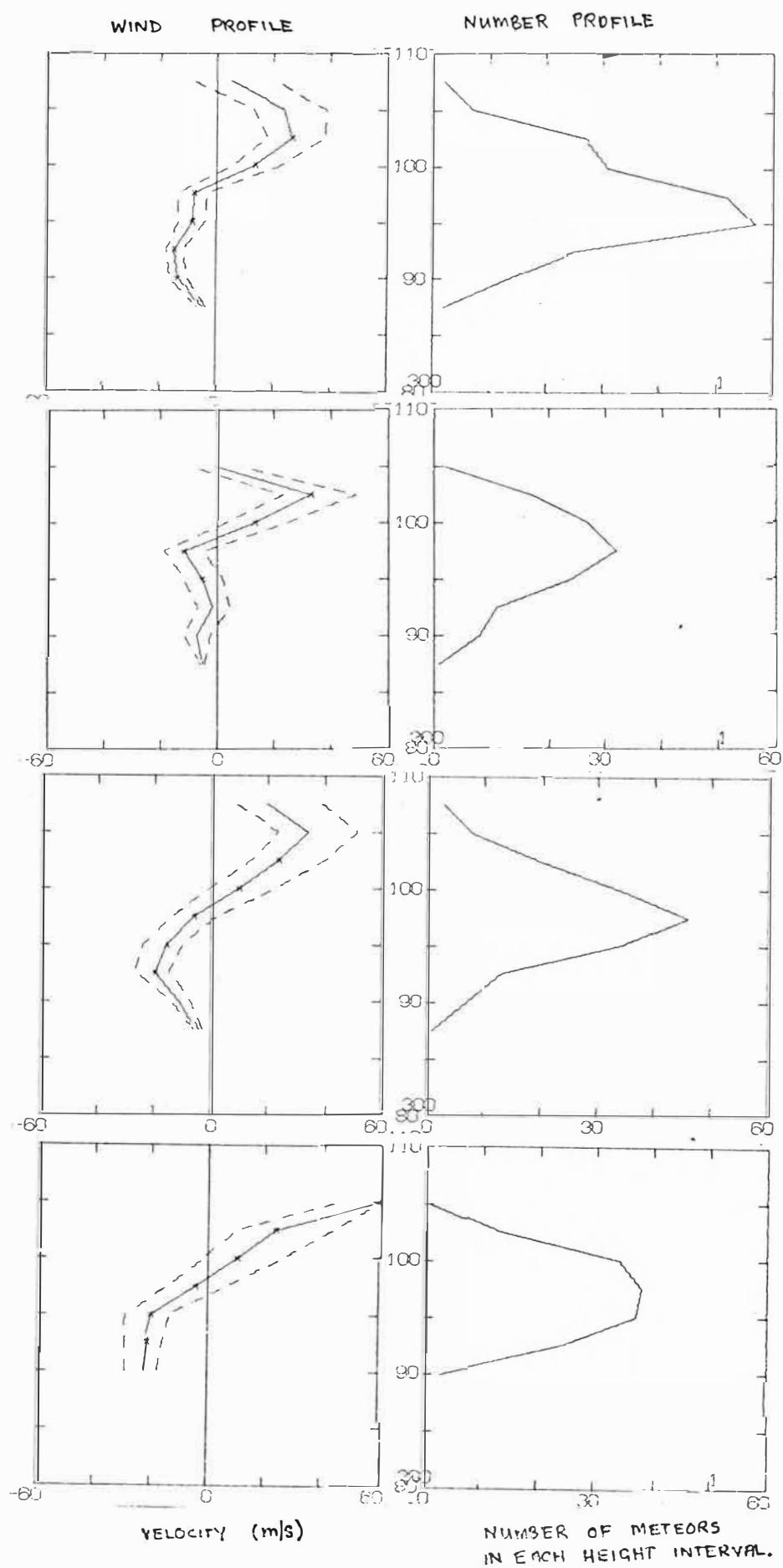
Before considering this point further, contributions to the errors in a half-hour's record will be considered.

6.5 Contribution to Variance from Film Reading

By calculating the sum of the squares of the differences in averages obtained for four film readers reading the same film segments, an estimate of the variance introduced by the various errors discussed in the first sections is obtained. Two important points emerge.

DIAGRAM 6-7

WIND PROFILES OBTAINED FOR
FOUR FILM READERS READING
THE SAME SEGMENT OF FILM.



- a) The variance introduced by film reading is of the order of $60 \text{ m}^2/\text{s}^2$, giving a standard deviation of the order of 10 m/s.
- b) If only those velocities for which film readers agree on the direction, type of Doppler and type of record are used the variance is of the order of $3.5 \text{ m}^2/\text{s}^2$ and the standard deviation is 2.5 m/s.

This indicates that subjective errors account for approximately 90% of the variance due to film reading errors. Furthermore, analysis of each of the subjective classifications taken on its own gives the same result as above, indicating that the separate subjective errors are not independent. Because the above results are based on a limited comparison using four film readers and three half hour segments, these results can only be considered indicative of the general trend.

Diagram 6-7 shows the variation of wind velocity with altitude obtained from the four film readers' results for the same half hour, 0300, on day 166. The crosses on the unbroken line for the wind profile indicate points for which ten or more records were used to give the average velocity. The broken lines indicate the average of the errors in each record as assessed by the film readers. Included also are the numbers of records averaged for each point. The profiles are calculated by making a running average over 5 km, for steps of 2.5 km, all heights having equal weight in the averages. Agreement is good, within the limits of film reader accuracy, the zero being within 2.5 km in each profile.

A final point in association with film reading is the effects of short durations with increasing altitude. As the meteor duration reduces, so the subjective errors become worse.

While not quantitatively analysed, it is possible that the increase in variability observed in the present records for altitudes in excess of 100 km, as compared with altitudes less than 90 km, may be a result of analysis rather than atmospheric effects - the lower meteor rate, in association with a higher average velocity because of enhanced zero-velocity losses giving rise to a greater apparent variability.

6.6 Effects of a Finite Aerial Beamwidth

It is assumed that all the meteor trails observed have radial drifts in the direction of the beam axis. However, as the aerial beam has a finite width, it is possible to record trails drifting in directions at angles to the beam axis. This will modify the statistics describing the wind field - of particular interest here are the average velocity and the variance. This problem was treated by Pupyshev and Teptin, 1971. Taking the observed velocity distribution to be a Gaussian dependent on the wind velocity, V , and the angle, θ , between the beam axis and the wind vector, they consider the effects of a variable meteor rate on the average wind velocities and found

- a) The diurnal meteor rate variation across the aerial beam will be small, with respect to other errors discussed.
- b) Seasonal variations will produce, at most, an 18% error.
- c) Meteor showers would add large perturbations to (a) and (b) but would be serious only if the shower rate was assymetric with respect to the beam axis.

The effects of the aerial used in the present experiment may be estimated to an order of magnitude by assuming:

- a) The meteor rate is constant at all angles to the beam axis

- b) The wind velocity, \bar{V} , is constant in the direction of the beam axis, having zero variance. The velocity distribution across the main lobe is thus $\bar{V} \cos \theta$.
- c) To a reasonable approximation, the present aerial main-lobe may be represented by $\cos^{16} \theta$, this being slightly broader than the measured aerial main-lobe. Pupyshev and Teptin suggest that side-lobes are of secondary importance for all results, so they are not considered here.

1. Velocity

The observed wind velocity, V_0 , will be

$$V_0 = \frac{\int_{-\infty}^{\infty} \int_{-\pi/2}^{\pi/2} \cos^{16} \theta \cdot \bar{V} \cos \theta \, V \, dV d\theta}{\int_{-\infty}^{\infty} \int_{-\pi/2}^{\pi/2} \cos^{16} \theta \cdot \bar{V} \cos \theta \, dV d\theta} \quad (6-5)$$

and using $V = \bar{V} \cos \theta$, the above gives

$$V_0 = 0.97 \bar{V}.$$

If the wind were directed at 90° to the beam axis, then the wind distribution across the main lobe would be $\bar{V} \sin \theta$, and

$$V_0 = 0.27 \bar{V}.$$

However, this accounts for only one side of the aerial, when both sides are considered $V_0 = 0$. Thus the aerial will have little effect on the magnitude of the observed average wind velocity.

2. Variance

Here, using the same assumptions,

$$\sigma^2 = \frac{\int_{-\infty}^{\infty} \int_{-\pi/2}^{\pi/2} \cos^{16} \theta \cdot \bar{V} \cos \theta (V - \bar{V})^2 dV d\theta}{\int_{-\infty}^{\infty} \int_{-\pi/2}^{\pi/2} \cos^{16} \theta \cdot \bar{V} \cos \theta dV d\theta} \quad (6-6)$$

where σ^2 = observed variance.

Giving an observed variance of,

$$\sigma^2 = 0.003 (\bar{V})^2$$

which gives a standard deviation of

$$\sigma = 0.055 \bar{V}$$

For the transverse case, where $V = \bar{V} \sin \theta$,

$$\sigma^2 = 0.52 \bar{V}^2$$

and

$$\sigma = 0.72 \bar{V}$$

The variance shows an enhancement due to the aerial beamwidth in the transverse case.

These results are in general accord with the calculations by Pupyshev and Teptin, 1971, though the transverse variance is double the value they obtained.

6-7 Vertical Velocities

As was indicated in chapter 3 in discussing other methods of measuring winds in the meteor region, it is usually necessary to assume vertical wind velocities are negligible. It is also necessary to make this assumption in measuring meteor winds. From chapter 3, it is apparent that even the small scale phenomena are found to be mainly horizontal. Furthermore, errors due to vertical motions are minimized by

the low elevation angle of the aerial beam used.

In diagram 6-8 V_R is the observed radial drift, V_W is the wind causing V_R and is at an angle ξ to the horizontal. V_H is the deduced horizontal velocity, assuming all winds are horizontal. Thus,

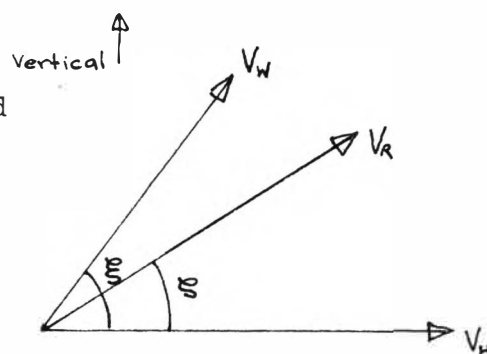


Diagram 6-8.

$$R = \frac{V_H}{V_{W_H}} = (\cos \xi + \sin \xi \cdot \tan \zeta) \cos \xi \quad (6-7)$$

where V_{W_H} = horizontal component of V_W .

TABLE 6-3

($\xi = 23^\circ$, the aerial beam elevation)

ζ°	5	10	15	20	30	45
R	1.03	1.04	1.04	1.02	0.93	0.71

From table 6-2 the observed and true horizontal components of the wind velocity are going to be correct within a 5% error for vertical velocities up to half the horizontal velocity.

When the results are collected over half an hour, errors in the horizontal wind will be reduced further if there are variations in ξ . For gravity waves values of 3° to 5° for ξ are predicted and longer period motions will have smaller ξ , thus expected errors from this source may be considered negligible. It is thus unlikely that vertical wind velocities will contribute greatly to the errors in the average horizontal velocity.

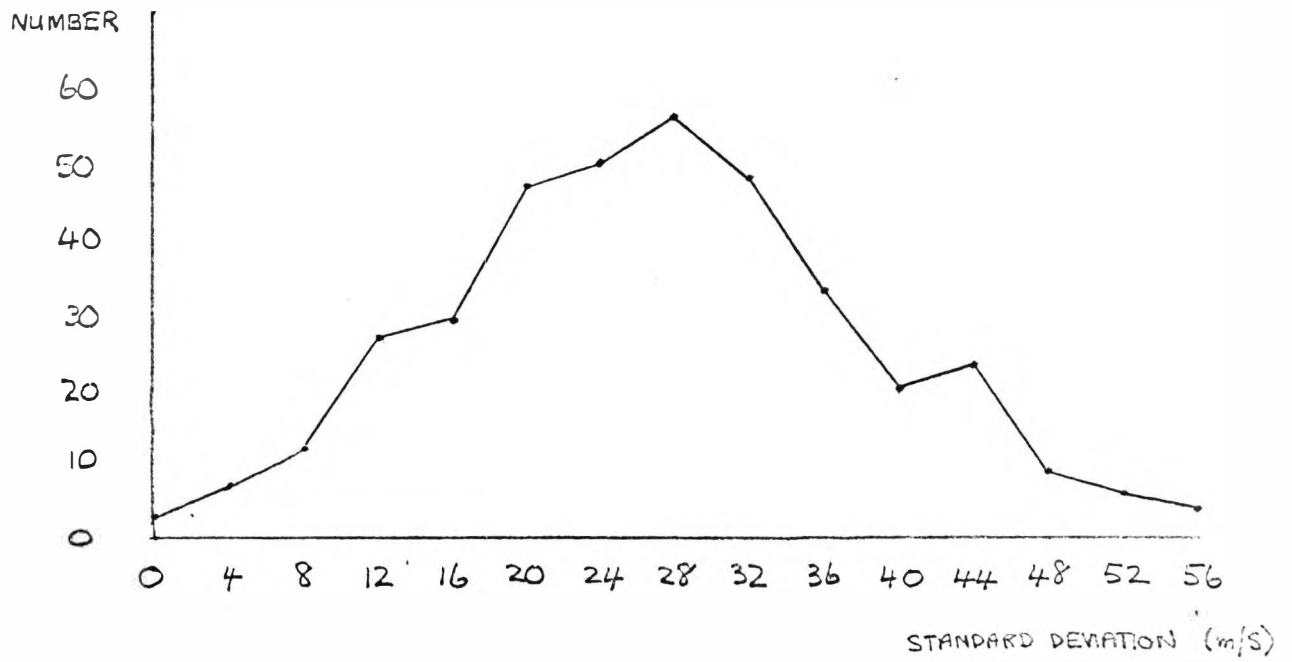


DIAGRAM 6-7. HISTOGRAM OF OBSERVED
STANDARD DEVIATION FOR ALL
HALF-HOUR SEGMENTS OF
UNDER-DENSE METEORS.

6.8 The Error in a Half-hour Average

1. Contributions to the variance

From the foregoing discussions, errors in the individual meteors will result in a spread in the observed velocities for any one height interval. Contributions to the variance from film reading and finite aerial beamwidth give

$$\sigma^2 = 60 + 0.5 \bar{V}^2 \quad (\text{m/s}) \quad (6-8)$$

where the worst aerial error is used. As the average wind velocity observed for a half hour was 21 ± 4 m/s, (6-8) gives a variance of $280 \pm 80 \text{ m}^2/\text{s}^2$. A histogram of the number of half hour intervals with a standard deviation, σ , in intervals of 4 m/s was plotted for 376 half-hours, see diag. 6-7, and this has a peak at 28 m/s. As the average number of meteors in a half-hour interval is 21, the average variance will be

represented by σ^2 , which gives $784 \text{ m}^2/\text{s}^2$. (The following estimation is necessary as the standard deviation and not the variance was found initially.) This result shows that over 50% of the variance will be due to sources other than the equipment and film readers. As a more careful calculation of the aerial effects (Pupyshev and Teptin, 1971) indicates that the variance for the transverse case is roughly half the value used here, it is apparent that the atmospheric contribution may well be more than 50%.

2. Contributions to the Atmospheric Variance

The observed variations in velocity may arise from variations in velocity with altitude. As mentioned (sec. 5.1) heights deduced from ambipolar diffusion have a spread about the true height due to various deviations from ideal conditions. This will contribute to the observed variance in the average

DIAGRAM 6-9

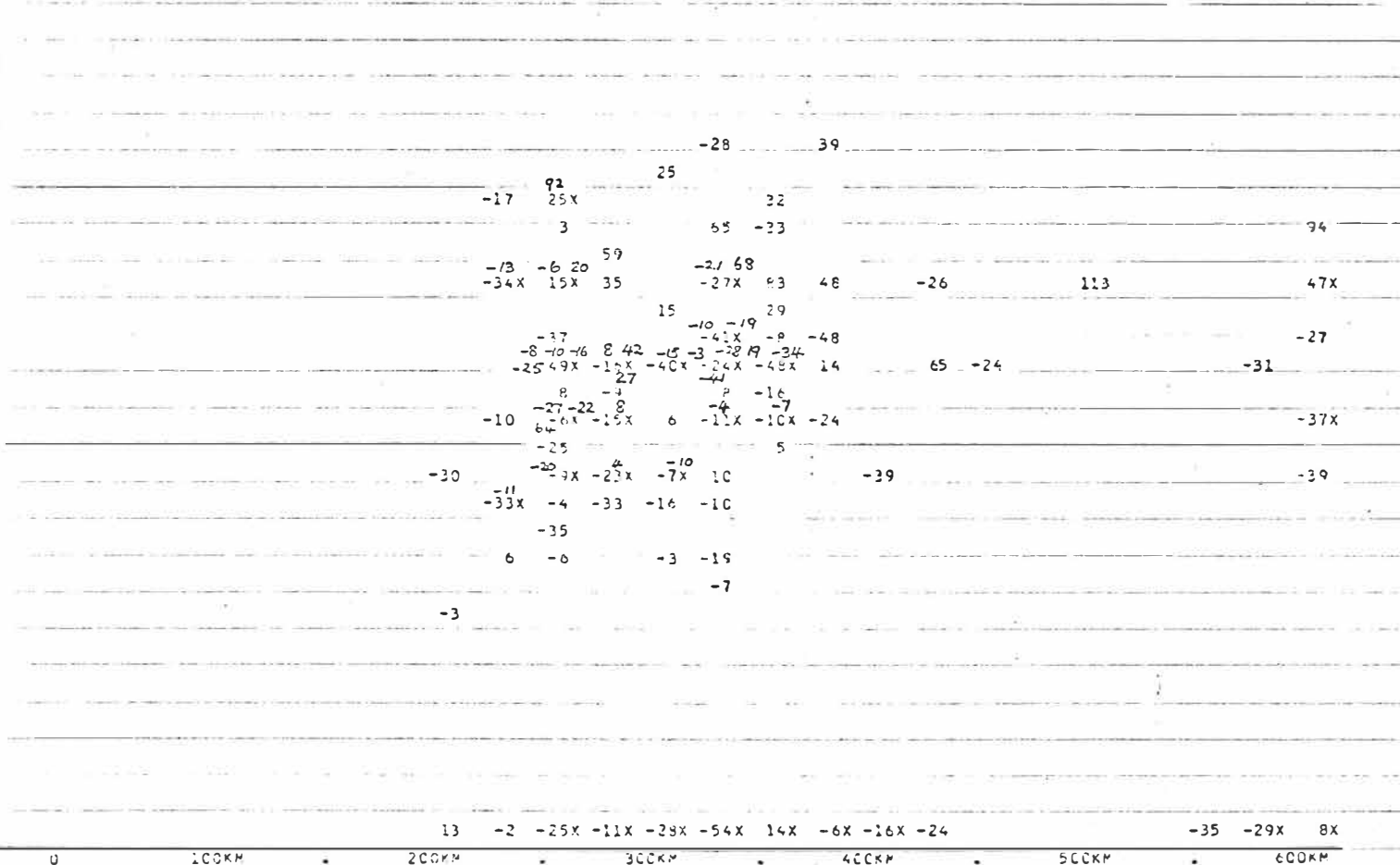
HORIZONTAL RANGE / HEIGHT PLOT.

YEAR 1971 DAY 166 TIME 0300 BEARING 90 DEGREES

DECAY
(KM)

HEIGHT
110.0
109.0
108.0
107.0
106.0
105.0
104.0
103.0
102.0
101.0
100.0
99.0
98.0
97.0
96.0
95.0
94.0
93.0
92.0
91.0
90.0

HEIGHT



(EACH NUMBER REPRESENTS A VELOCITY DETERMINED FROM A SINGLE METEOR.)

(FROM DIRECTLY ABOVE THE AERIAL)

wind velocity. The wind-shear could be produced by both the general circulation, and short term fluctuations, such as gravity waves.

Alternatively, there could be a real variation in the wind velocity over time periods less than a few minutes. Gravity waves might be expected to produce time variations in excess of 10 to 30 minutes and atmospheric turbulence could be important for shorter time periods.

The scatter in the observed velocities is more evident if plotted using the measured height and horizontal range as coordinates. This is shown in diagram 6-9. (The crosses indicate points at which more than one meteor occurred, the additional values being inserted manually.) This indicates rather more clearly the extent of the variation in wind velocity in space. From gravity wave theory (Hines, 1960) horizontal wavelengths of about 150 km, associated with vertical wavelengths of about 6 km might be expected to add to the spatial variability, along with the other effects discussed.

With the present equipment there is neither the time nor spatial resolution necessary to gain more information on these points. It is apparent that errors in the decay heights will produce a scatter in the observed velocities, but it is not obvious that variations in space and time during a half-hour will not also add to this scatter.

3. Some Justification for Averaging

a) Averages for regions bearing 180° apart: In order to investigate averaging of the individual velocities collected over half an hour, meteors were collected from regions of the sky that were 180° different in bearing. Diagram 6-10

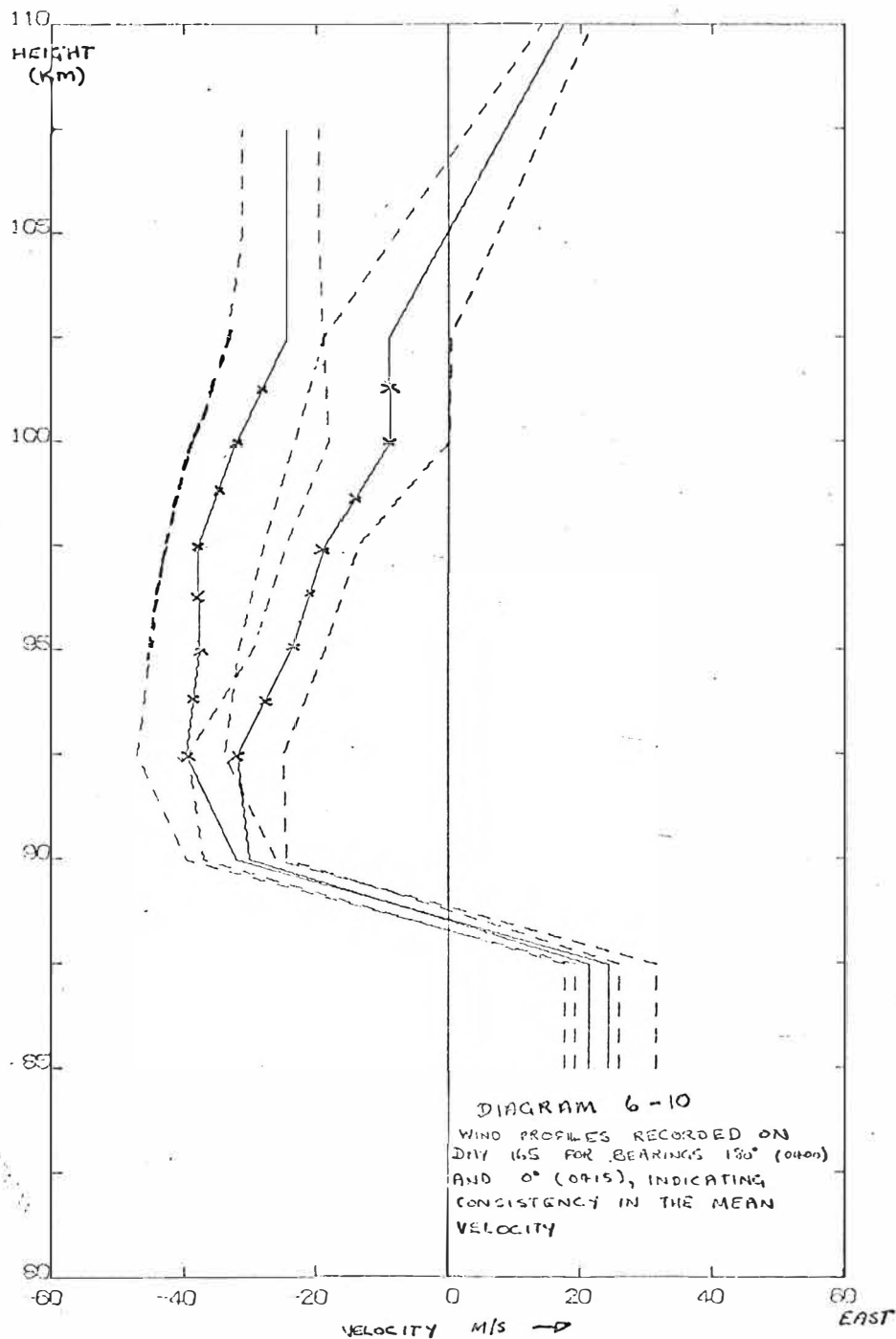
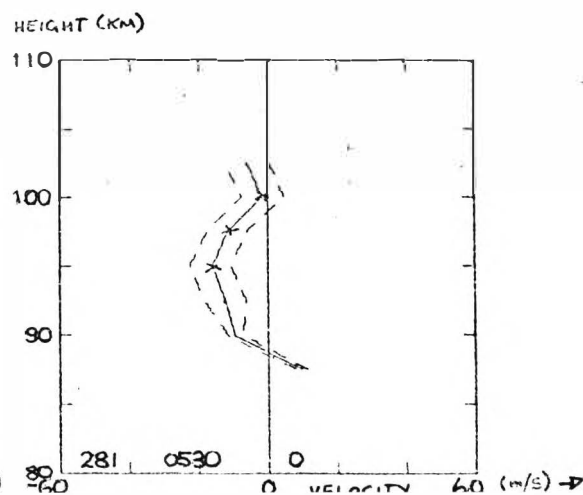
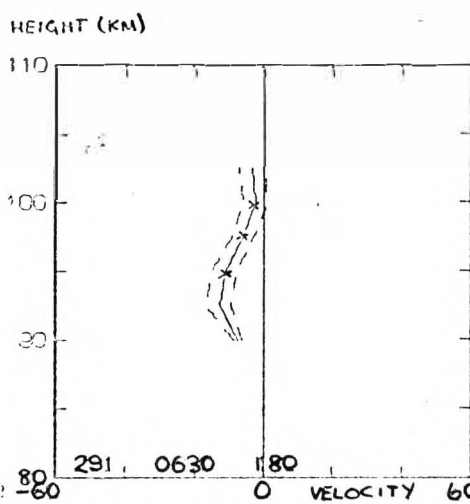


DIAGRAM 6-11. THE SAME AS ABOVE FOR TIME INTERVALS
SEPERATED BY 60 MINUTES.



indicates that within experimental errors, the two wind profiles are very similar when at least ten meteors are used to obtain the average velocity. The very close correspondence below 92.5 km is rather surprising as less than five meteors were used in each average.

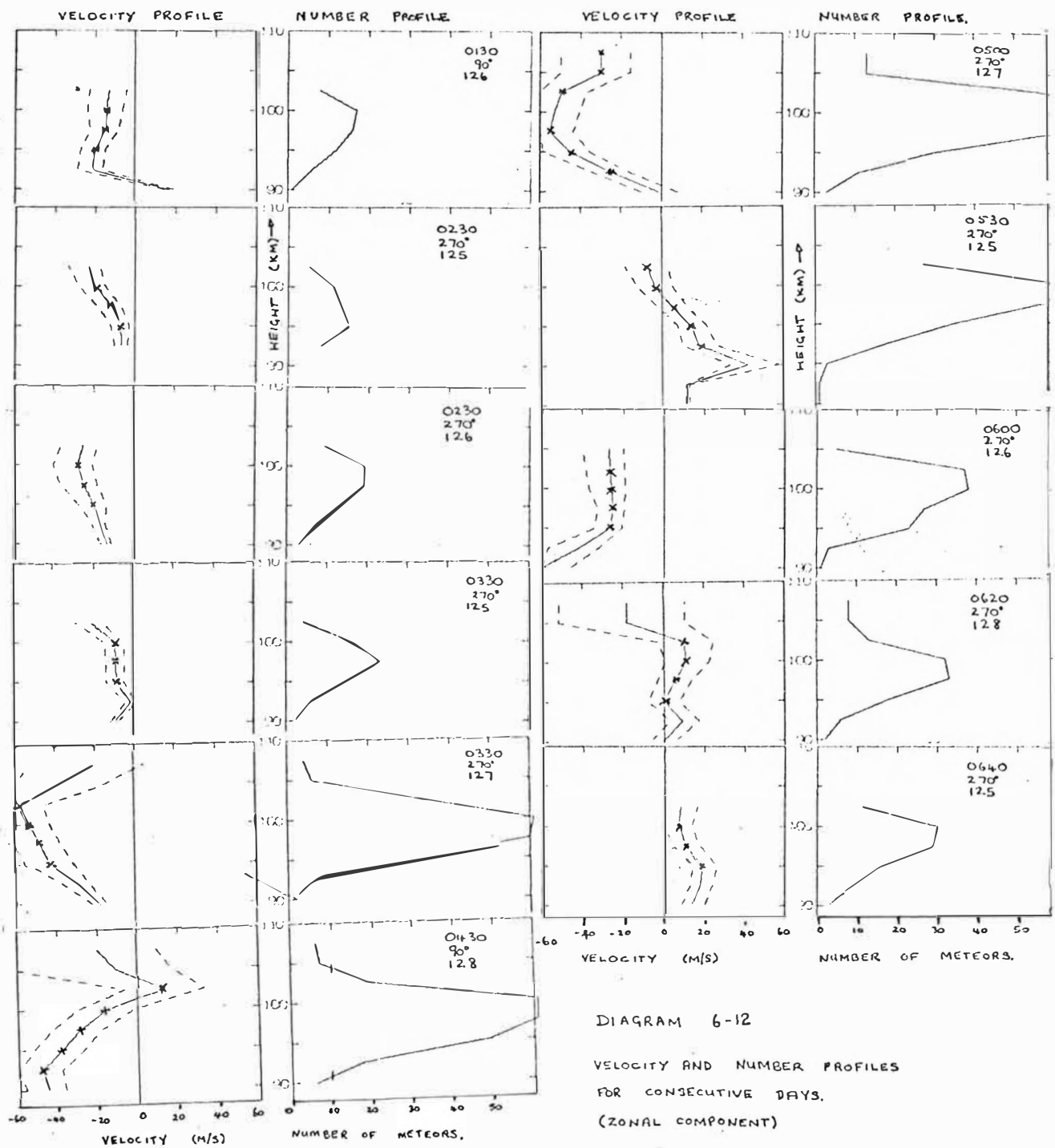
Diagram 6-11 shows the same thing, only here the regions are separated in time by one hour. The correspondence is still good.

b) Averages for regions separated in time: It is also possible to see strong similarities in wind profiles for the same time of the day and bearing, but for different days. Some examples are given in diag. 6-12, 6-13. The numbers in the upper right-hand corner of the number profiles gives the time, day and bearing for the half hour. Three features appear,

- i) the averages are similar for changing time on the same day. Because of this, it seems reasonable to consider that the slow variations in the profiles are a product of the atmosphere.
- ii) Large wind gradients do not recur in other profiles, (i.e. 0403, 0°, 128 in diag. 6-13), suggesting that these are probably analysis effects.
- iii) Similar profiles are observed for successive days.

4. The error in the mean

All the profiles in diag. 6-12/13 have crosses to indicate where in excess of ten meteors were used to obtain an average. The choice of ten meteors was suggested in Barnes, 1968. Müller, 1966, suggests that the major error in averages over half an hour will result from equipment limitations. The present results do not support this view. Rather than instruments, it is the atmosphere that places the limitations



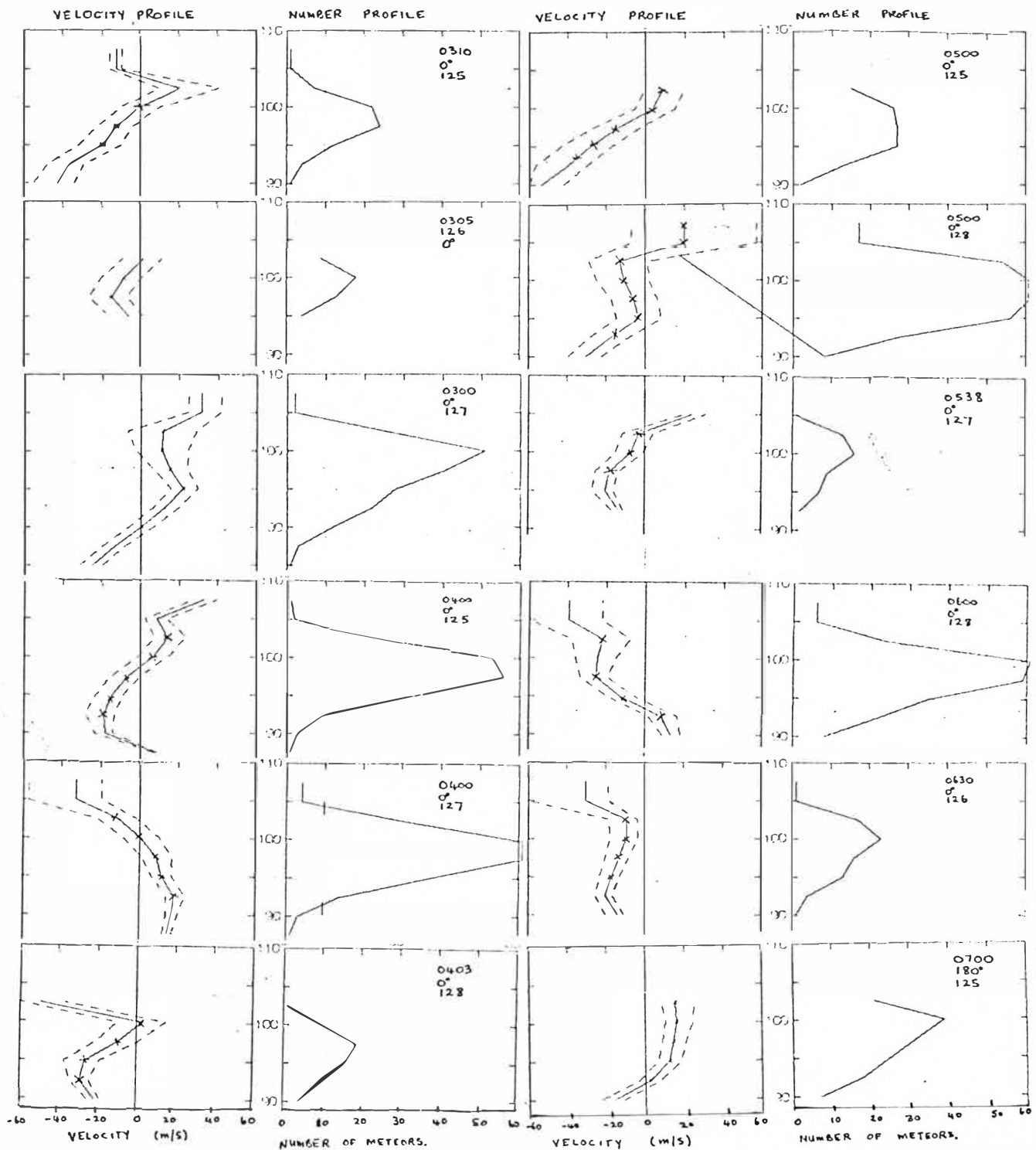


DIAGRAM 6-13 VELOCITY AND NUMBER PROFILES FOR CONSECUTIVE DAYS.
(MERIDIONAL COMPONENT.)

on the significance of the average velocity.

In view of this, it seems reasonable to quote accuracies of wind averages in terms of the sample. The most useful estimate of the significance of the mean is the standard error of the mean, or the standard deviation of the mean, given by (Topping, 1965),

$$\text{Standard error} = \frac{\sigma}{\sqrt{N}} \quad (6-9)$$

where N = the number of values averaged

σ = standard deviation of population.

The errors for each half-hour are thus related to the standard deviation in the results. A percentage error based on the number of meteors present seems misleading. The average standard deviation mentioned in part 1 gives an average percentage error of 30%. To obtain a 10% error would require 200 meteors per half-hour - a rate achieved only in the early morning with the present equipment. This is considerably different from the estimate by Müller, 1966, who suggested two meteors gave the average wind to 10% accuracy.

The standard error in the mean is the standard deviation that one would observe for the distribution of the means for a number of populations, each smaller in size than the total population from which they are drawn. It is a measure of the spread of the different means about the total population mean, and is thus the logical choice for the error in the mean.

When this is used with meteor winds results, the total population will be the complete specification of the wind-field in the meteor region in time and space, and the sample of this population will be the meteors recorded in a particular half-hour. The distribution of the means of several such samples

will approach a normal distribution curve with a variance of σ^2/N where N is the sample size and σ^2 is the population variance. This result is known as the central limit theorem (Hays and Winkler, 1970). Because only a sample of the total population is obtained, a correction must be applied to the sample variance, S^2 , is a biased estimator of the population variance as it depends on the sample mean. An unbiased estimator of the population variance is,

$$\sigma^2 = \left(\frac{N}{N-1}\right) S^2. \quad (6-10)$$

The population standard deviation, σ , indicates how the N elements of the sample are distributed about the mean value. While this is an important property, it does not give any direct information on the mean. Barnes, 1972, used σ as a measure of the significance of the mean; this is not correct. The correct estimator for the spread in sample means about the population mean is the standard deviation in the mean given by (6-9). If (6-9) and (6-10) are combined,

$$\text{Standard error} = S/(N-1)^{\frac{1}{2}} \quad (6-11)$$

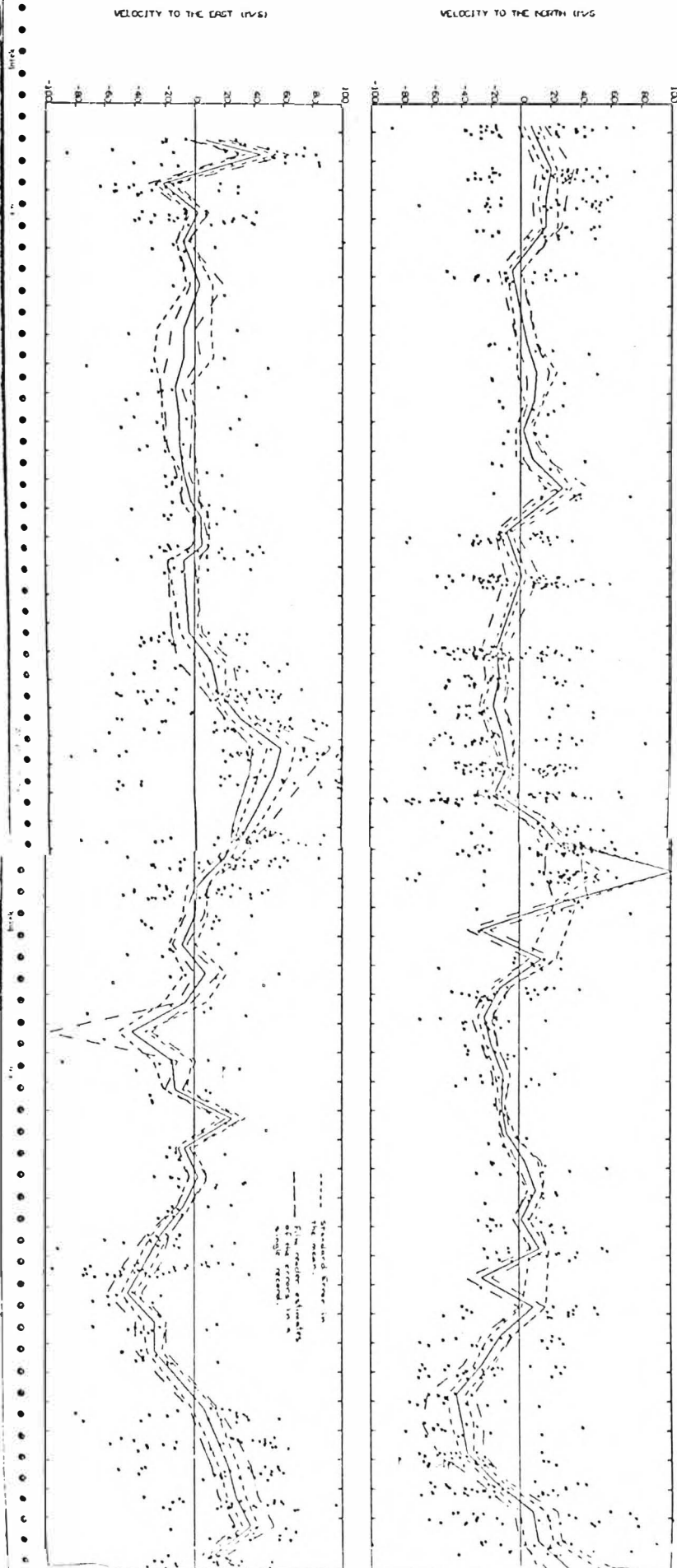
gives the error in the mean in terms of the sample standard deviation.

6.9 Summary

a) Diag. 6-14 shows the complete run for October 1971. The crosses are underdense meteors and the continuous line is the mean for each half-hour. The two error curves, for the film reader error estimates and the standard error are very similar in magnitude. (Points where large deviations occur are associated with a single meteor determining a half-hour average.)

OCTOBER THE 7TH TO 9TH 1971
 BEGIN 0900 END 1030

DIAGRAM 6-14. COMPLETE RUN FOR OCTOBER 7th - 9th 1971
 FOR ALL UNDER-DENSE METEORS.



As the film reader error curves are the worst possible error estimates of height, range and velocity, it is not surprising that they are similar to the curves using (6-9), though the small magnitudes observed for small numbers of meteors indicates that they are not wholly useful.

Other points evident in diagram 6-14 are,

- i) the variability of individual velocities
- ii) the loss of zero velocities
- iii) the diurnal meteor rate.

b) At least some of the scatter could be removed by preventing subjective errors on the part of the film readers to enter. It might be hoped that an automatic system, applying the same selection criteria to each observed meteor, would be superior. However, the system reported by Barnes, 1972, is an automatic system, yet the standard deviation is the same as ours. This further supports the view that the variability observed in the results is a real feature of the atmosphere. The major advantage of an automatic system is the ease of analysis, making operation over long time periods possible. The major drawback with film records is the time it takes to analyse the results of a run.

c) As indicated in section 6-8, the most useful estimate of the error in the mean for half an hour will be the standard error, given in (6-9) and (6-11). Percentage errors, while being useful for order of magnitude estimates, are of little value when applied to a particular average.

C H A P T E R 7THE OBSERVED METEOR WIND CHARACTERISTICSIntroduction

The results for the mean wind and tidal components presented in this thesis are quite unsatisfactory as much of the data was collected in adverse operating conditions associated with equipment failures. This was reflected in the data by low meteor rates making it difficult to obtain satisfactory averages for a half-hour. Unfortunately the full significance of this was not appreciated until a complete analysis of the results was made. Tidal data obtained from several of the runs were far from satisfactory. This has meant that the results for the mean flow are probably contaminated by tidal components. These points will be discussed further in successive sections. Those results that are presented must, at this stage, be considered preliminary. Seasonal averages, which might show greater stability, have not been calculated as yet. This was because a new computer is shortly to be installed at Canterbury University with magnetic tape facilities. At present all the data are stored on punched cards and will all be put on magnetic tape, thus considerably easing handling problems. With this in mind, it was decided to delay this step until the improved facilities are available.

In the following sections the method of analysis is discussed and the results are presented.

A. THE ANALYSIS METHOD

7.1 History

The normal presentation of meteor wind data has been to give the components of a harmonic analysis of the data. Results from Jodrell Bank (Greenhow, 1954) were the first to appear in this form. Here twenty-four hours of data was subjected to harmonic analysis and the mean wind, \bar{S}_1 and \bar{S}_2 tides were found. Estimates of the errors in these terms were also presented. Results obtained at Adelaide, (Elford, 1959) used an epoch analysis method because of the low data return. Here, individual velocities obtained over several days were summed together to give twenty-four hours of data and a harmonic analysis of this was made. This method assumes that the atmospheric winds are constant over the time the data is collected. Because the meteor rate has a diurnal variation, later workers have made allowances for this by weighting periods of high meteor rate (Müller, 1966; Zadorina, 1967). To deal with the low data rate at Adelaide a least squares method of analysis over the time and space domain was developed by Groves, 1959.

In this thesis the analysis method used in the early Adelaide results was adopted and will be discussed further in this chapter.

In addition to the harmonic analysis of the wind data, power spectrum techniques have also been used. Rather than treat the observed time series of velocity averages as a line spectrum, as is assumed in harmonic analysis, the time series is treated as the result of a frequency continuum; the lines of the harmonic spectrum are now thought of as peaks. These methods have been used to investigate periodicities longer

than 24 hours in the wind velocities, (Müller, 1972; Pokrovskiy and Teptin, 1970). Transitory effects, due possibly to gravity waves, have been isolated by this technique also (Revah, 1968).

Although little emphasis was placed on power spectrum methods in this thesis, it is useful to consider some features of this before considering harmonic analysis. Before this is done, some features about the data will be considered.

7.2 The Time Series

Some definitions are useful here.

Sample: the mean of the individual velocities obtained from meteors observed over a half hour period.

Interval: the half hour period over which the meteors are collected.

Time Series: the length of time for which samples are collected.

Run: this is the length of time that the equipment was operated for each month to collect data.

As each run was about two days long, the time series for the northward and eastward directions would normally have at least 48 points in them.

1. Nyquist Frequency

In sampling a periodic phenomenon, it is necessary that the sampling rate be sufficiently rapid to define all high frequency components present. As two samples, at least, are required to define a complete cycle, the minimum resolvable period, or equivalently maximum resolvable frequency, will be twice the sampling period. This is called the Nyquist frequency, f_N . Frequencies greater than f_N will be under sampled, and will appear as low frequencies in the time series. The appearance of high frequencies in the phenomenon being

observed as low frequencies in the time series of observations is called aliasing.

2. A trend

The longest period that can be completely specified by the time series is one that is just the same length as the time series. Periods longer than this will be unresolved by the time series, though they will be present as a trend.

7.3 The Power Spectrum

It is very often easier to study a phenomenon in the frequency domain than the time domain, being especially true of periodic phenomena. Power spectrum analysis as discussed here, involves taking information obtained in the time domain and transforming it into the frequency domain.

1. The transform

The power spectrum is found by taking the Fourier transform of the time series. This means that the time series is now represented by a series of orthogonal sine and cosine terms.

Two methods of obtaining this transform have been used.

- a) The Autocovariance method (Blackman and Tukey, 1959). For computational convenience the autocovariance function for the time series is calculated, and then the power spectrum is obtained by Fourier transforming this - a result which follows from the Wiener-Khintchine theorem (Rayner, 1971). This route takes considerably less computer time than a direct transform.
- b) Fast Fourier transform. The fast Fourier transform method, involving a more efficient method of obtaining the Fourier transform now makes it possible to Fourier transform the complete time series on a digital computer in considerably less time than method (a).

Because the time series is finite in length, it is necessary to consider what effects this has on the spectrum.

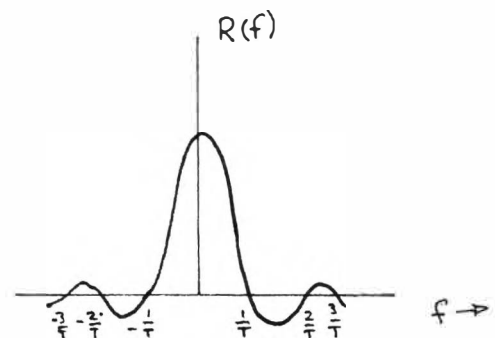
2. The Data Window

The effects of finite time series length are best treated by introducing the concept of a data window. The finite time series may thus be thought of as an infinite time series observed through a window which obscures most of the observable series. The infinite time series and the data window are thus multiplied in the time domain, or equivalently, the power spectrum is convolved with the frequency response of the window in the frequency domain. The effects of this may be seen if the simplest window is considered. This is the box-car window, having a frequency response

$$R(f) = 2T \cdot \frac{\sin 2\pi fT}{2\pi fT} \quad (7-1)$$

where T = length of window in the time domain. It is apparent that the convolution of (7-1) with a single line in the spectrum will result in several spurious responses appearing in the power spectrum.

This shifting of energy at one frequency, in the time domain, to another, when transformed into the frequency domain is called leakage.



Diag. 7-1

Alternative data windows having less leakage are available, the most common being the cosine bell. The effects of leakage may be minimized using pre-whitening, a reversible process carried out in the time domain to level the frequency spectrum and thus even out the window leakage over the complete spectrum.

3. Bandwidth, resolution and bias

These terms are all related to the choice of a spectral window. The bandwidth gives an estimate of the width a spectral line will have in the frequency domain. Blackman and Tukey, (1959) suggest $(1/T)$ is a convenient estimate. If two spectral lines are separated by less than $1/T$ in the frequency domain, they will be smeared together. The resolution is thus inversely proportional to the bandwidth.

When a data window is used, smoothing of the spectral estimates occurs making the spectrum more stable. However, this reduces the resolution, and even if an infinite number of time series were averaged, the actual spectrum would never be obtained. The smoothed spectrum is a biased estimator of the true spectrum. The more smoothing a window produces, the more stability, and also the more bias, it produces.

4. Significance

The statistical significance of the results obtained from power spectrum analysis is made using a χ^2 -test. The number of degrees of freedom depends on the number of independent samples from the time domain that were used, and will be modified by the data window. For further discussions see Tukey (1961) and Jenkins (1961).

7.4 Harmonic Analysis

Harmonic analysis is a special form of power spectrum analysis in which some general knowledge about the spectrum is already known making certain simplifications possible in the analysis of the data. The time series is known to contain only spectral lines that are at known frequencies.

Harmonic analysis of such a time series will give the amplitude and phase of the frequency component of interest.

The phase information is normally lost, or lacks significance in power spectrum analysis. The harmonic analysis may be carried out by taking the Fourier transform of the time series, as before, though now it is not useful to use the auto-correlation method as normally the phase information is required.

The data window used will be the box-car window, only here as the frequency spectrum is known, it is possible to choose the length of the window so that $f = 1/mT$, where f is the frequency being observed and $m = 1, 2, \dots$. When this is convolved with the spectrum, a delta function at frequency, f , only one peak occurs, at frequency f . Thus there will be no problems of leakage to other frequencies.

If there are several lines present in the spectrum then these arguments may not be true and leakage will be present. However, the problems associated with the bandwidth and resolution will not be important unless two lines fall close together. It will be possible to resolve lines greater than $1/T$ apart in the frequency domain, though this will not affect the present analysis.

In general, the spectrum will consist of the expected line spectrum and an unwanted signal. The χ^2 -test of significance will not be relevant here, giving only two degrees of freedom for the observed peaks (Jenkins, 1961) as these are identified with lines. To obtain some estimate of the error present, some additional assumptions must be made about the results of the harmonic analysis to obtain some estimate of the errors present.

1. If some estimate of the accuracy of the individual samples in the time series can be made, then this may be

used to estimate the limits on the observed results.

Because of the considerable scatter in the results, this approach was not obviously useful, the error limits discussed in chapter 6 being unreliable when applied to samples resulting from averaging only two or three meteors.

2. If it is assumed that all the unwanted signal is a white noise spectrum, this then will contribute equally at all frequencies. If it is further assumed that the observed time series consists only of the line spectrum plus white noise, then an estimate of error may be made by comparing the amplitude of the line spectrum observed with the amplitude of the white noise. It was considered that the observed variations of the time series, due to low meteor rates, would be sufficiently random in nature to make the assumption of white noise a useful method to gauge the reliability of the results.

Neither of these methods is more than a measure of the internal error in the results, and are useful only in that they place some limits on these results.

7.5 Method of Analysis Used

To cope with the low meteor rate at Adelaide, the meteors collected on several consecutive days were grouped together as one day before a harmonic analysis was carried out. This is called epoch analysis. (The meteor rate referred to here is the rate of usable meteors and not the actual meteor rate.)

In the present experiment various factors have produced a low usable meteor rate.

1. The transmitter was initially operated at a lower power output, thus reducing the meteor rate to some extent.
2. Equipment failures resulted in some early runs being terminated prematurely.
3. Problems with the camera resulted in some film recorded being very difficult to read.
4. Ground-scatter, especially during Autumn 1971, and a daytime increase in radio frequency interference often made it difficult to operate the equipment. This has meant either no meteors were recorded (or very few) after about 1000 hrs L.M.T. Coupled with the minimum in meteor rate at about 1800 hrs, this meant very low meteor rates were often recorded from 1000 hrs through until 0100 hr the next day.

Because of the low rate of usable meteors for most runs, some attempt has been made at obtaining results by using the epoch analysis method. All meteors for the same hour of the day have been averaged together to give the sample point for that hour. An harmonic analysis of the resultant series was made assuming that it was due to a mean wind, the \bar{S}_1 , \bar{S}_2 , \bar{S}_3 , \bar{S}_4 tidal components and white noise. An estimate of the mean noise contributions to the other components was made by averaging all higher frequency components than \bar{S}_4 . The \bar{S}_4 component was retained in the analysis as a possible tidal contribution rather than white noise. However, if gravity waves contributed to the high frequency spectrum, their effects would enhance the error estimate. This was not considered important, though if it were, it would only produce a more conservative estimate of the reliability of the tidal components.

7.6 External Errors in the Analysis

In the data recorded, several potential error sources exist due to the nature of the atmospheric winds being observed and the method used to record them.

1. Trends in the Data

It is evident from observations by Müller (1972) that periodicities longer than a day are present in the wind velocities observed at meteor heights. Such long periods will not be orthogonal with the tidal components derived from the harmonic analysis and will thus enhance the deduced amplitudes. It is necessary in both power spectrum and harmonic analysis to remove any trends in the data if present.

Provided the periodicities are greater than four times the data length, the trend may be approximated by a straight line. It is suggested (Granger and Hatanaka, 1964), that on visual inspection of the time series, if no linear trend is obviously present, then if a trend is present, it will not be large enough to affect the results. While no trend was apparent in the data inspected, it was decided to obtain the regression of time on velocity for the time series data and treat this as a possible trend. The trend was removed by subtracting the regression line from the complete time series, and the result was used for epoch and harmonic analysis.

If trends are present with periods less than four times the data length, a linear approximation is not satisfactory. As the time series used in the present experiment were in excess of 36 hours long, the linear trend approximation may be inadequate but because the data was of fairly poor quality, as discussed, it was decided to only allow for a linear trend in the analysis.

2. Gaps in the Time Series

Even though two or three days results were used to obtain a 24 hour time series, some undefined points could still occur due to daytime radio interference losses.

For power spectrum analysis, it is possible to allow for these effects by obtaining the autocorrelation function for only those points present. Granger and Hatanaka⁽¹⁹⁶⁴⁾ suggest that provided gaps account for no more than 10% of the time series this will produce reliable power spectra.

For harmonic analysis it is not so easy to allow for these effects. Any gaps in the time series were left as zeroes in the present analysis. It would probably be preferable to interpolate between points adjacent to any gaps to find values to fill the gaps with. Analysis of a dummy series did not suggest this was likely to be a serious problem, and it was not pursued in the present work.

3. Diurnal Meteor Rate

No attempt was made to allow for the meteor rate in the results obtained. In view of the problems associated with the low rate observed, this allowance could be a valuable addition to the analysis method. Unfortunately those workers who have used this method have not indicated what order of correction results, (i.e. Müller, 1966). It would appear that if the sample points are to be weighted in the analysis, it would be preferable to relate the weighting to the standard error in the result. However, with rates of less than five to ten meteors per half hour, it is difficult to see how either method will be wholly successful.

4. Spatial Averaging

The results for winds depend on observing two regions of space in two orthogonal directions. The regions will normally be separated by about 400 km. For the \bar{S}_n tidal component, this amounts to an error in phase of $3n^\circ$. This is not significant in light of other errors discussed. A similar error results from averaging over a finite aerial. Here points up to 500 km apart are averaged, but the average separation results in smoothing over about 200 km. This too is an insignificant correction.

5. Time Averaging

By using averages over half an hour, the tidal amplitudes will be reduced. It has been shown, (Chapman and Bartels, 1940) that this is a small amplitude correction and not significant in the present work, amounting to 5% for the \bar{S}_4 tide, and being less for the longer period components.

6. Aerial Direction

More serious will be the errors resulting from an early technique used in recording the meteors. It was decided to optimize the meteor rate by pointing the aerial where the r.f. noise was least, thus improving marginally the number of meteors recorded. Adjacent half hours were recorded from orthogonal directions, but there was some variation in the actual direction from which meteors were collected, during the run. This method was dropped in favour of observing only south and west. As the runs involved produced low quality average velocities, it was decided, for convenience, to lump all velocities within 45° of a compass point together, rather than use pairs of adjacent orthogonal directions and to resolve components in the compass directions.

At the very most, this could produce an error of 45° in the observed phase of the tide. A check was made on runs where this technique was employed and it was found that the mean error was never greater than 10° and the spread in bearings used for each half hour about this value had standard deviations of a similar magnitude. A section of one record, where considerable variation in components was used, was converted using the orthogonal components to obtain the north and east components of the wind. When compared with the unresolved components the variations were found to be insignificant. It was decided that this did not add greatly to the errors in the experiment.

7. Aliasing

The possibility existed that components with frequencies unresolved by the present sampling could be present. Experiments by Greenhow and Neufeld (1959) indicated that this was not the case, the autocorrelation function for a time series was found to reach zero after about 90 minutes, indicating periods considerably larger than the sampling period were important.

A time series $8\frac{1}{2}$ hours long with a sampling period of 3 minutes was made and the auto-correlation function calculated on the basis of the averages for three minutes, and for all the individual velocities in the three minute interval. No attempt was made to remove a trend, other than the mean, from the time series. The results agreed well with Greenhow and Neufeld, indicating that aliasing will not produce significant errors in the analysis.

Further weight is added to this conclusion by the observation that the form of wind profiles deduced at times of high meteor rate are consistent within the estimated film reader errors from one hour to the next. If aliasing, or coherent high frequency contributions were dominant features of the winds observed, then this result would not be expected.

8. Loss of Zero Velocities

It was shown in chapter 6 that there will be a loss of zero velocities, and that this increases with altitude. Barnes (1972) suggested that this would have no effect on the phase of the tide observed, but would increase the amplitude. To test this, as well as to test the harmonic analysis program, a dummy series was constructed consisting of an S_2 tide of 10 m/s and a Gaussian distribution of velocities with a mean of 0 m/s and a standard deviation of 50 m/s. A variable meteor rate with a maximum of 120 and a minimum of 6 meteors was arbitrarily used. Velocities near zero were removed to simulate the histograms in diagram 6-5 for different heights. As low velocities are not removed, but are misinterpreted in practice, the simulated series will not be generated in the same way as the real series. This should not alter the general conclusions. Two points emerged from this.

- i) The loss of zero velocities had no effect on the calculated tidal amplitudes for the S_1, S_2, S_3 and S_4 components, though the S_3 and S_4 components were slightly larger than the estimated error parameter in all cases, including the case where no zero velocities were removed.
- ii) The calculated phase was found to vary, outside the error limits, from the expected phase. This variation was not related to any specific feature in the dummy series making

the evaluation of the phase of the tidal components doubtful if only one set of data is used.

To overcome this last problem, two methods were used.

- i) The dummy time series was started at different points in time, and the phase measured for each trial. The average of these measurements gave the correct phase.
- ii) Using what height information was available, the real data were analysed in 2.5 km height segments and the phase for each segment was compared with the phase observed when all the decay meteors were lumped together. For the \bar{S}_1 and \bar{S}_2 components somewhat more variable behaviour was observed. The phases observed for the \bar{S}_1 and \bar{S}_2 tides are most probably satisfactory, though the \bar{S}_3 and \bar{S}_4 phases may lie outside the error limits.

The above discrepancy is due to the large variability of the sample. When no velocity variability was included, the phase was always correct.

(Please see P192, section A.5, for further comments.)

B. THE RESULTS

7.7 The Data

Within the limits of the experimental observations, results for the year 1970-71 made at the Rolleston field station near Christchurch and having geographic coordinates $172^{\circ}24'E$, $43^{\circ}37'S$, will be presented and compared with other experimental results and expected theoretical results. In the case of the mean wind, some additional information is presented on the analysis to illuminate the results obtained. Throughout the analysis, the height information obtained could only be used to check that in averaging all meteors to the same height, no additional errors were introduced due to substantial height variations in the phase of the component. Such variations

TABLE 7-1 Dates and details of data recorded

Month	Date	Start and finish time N.Z.S.T.	Fraction time series present	Comments on run	Comments on data
November 1970	17-18	2200-1875	0.6	High r.f. interference during the day. First run.	Low usable rate for complete run. Of no use.
Nov/Dec. 1970	31-1	1900-2130	0.9	High r.f. interference and ground scatter.	Low rate after 0800. Averages possibly useful.
December 1970	20-22	1500-1000	0.96	Run terminated by Tx failure. High r.f. interference and ground-scatter until 1900 on 20 th and 21 st .	Low day-time rate introduced considerable variability into the averages. Averages and wind gradients useful.
February 1971	9-10	1330-1340	0.6	Time lost adjusting camera trigger and oscilloscope. Film wastage due to camera adjustment.	Low but usable rate for about half a day. Inadequate for results.
March 1971	16-18	1100-1211	0.96	Very low receiver sensitivity due to transmission line mismatch, after moving equipment. Over 6 hrs lost due to r.f. interference. Run terminated due to noise.	Very few meteors in daytime averages. No useful height information.
April 1971	22-24	1715-1345	0.7	5 hrs lost due to r.f. interference and ground scatter. Some film yet to be read.	Good rate, for film read.
May 1971	4-8	1630-0930	1.0	Some film wastage due to camera malfunction. Run terminated due to r.f. interference. Some film yet to be read.	Some low rates during the day but generally good time resolution. Height less useful apart from early morning results.
June 1971	14-16	2000-0900	0.9	R.F. interference and discriminator failure caused time loss. Some film yet to be read.	Good usable rate 2200 to 1000. Averages biased to morning results. Tidal components not perfect, but indicative of observations
July 1971	i) 19-21 ii) 23rd	1540-1630 0630-1530	0.9	Almost complete camera failure made film very difficult to read.	Very poor data rate, though meteors evenly spread over the run, so mean should be useful.
August 1971	25-26	0130-1130	-	Low power output. Run terminated by transmitter failure and September lost during maintenance. Some film to be read.	Poor data rate. Averages biased to early morning. Incomplete analysis.
October 1971	7-9	0900-1030	1.0	Some r.f. noise, transmission line failure.	Generally good meteor rate. Tides and means useful. Insufficient daytime meteors to make height resolution very useful.
November 1971	11 16-18	0730-1230 0900-1600	0.9	R.f. noise during afternoons. Most of film yet to be read.	Good meteor rate. Means useful.

might be expected from the theory of the diurnal tide (Lindzen, 1967), for instance.

A brief survey of the runs made is given in table 7-1. The 'fraction of time series present' indicates how much of 24 hours was obtained from the epoch analysis. In general, equipment problems and r.f. interference had considerable effects on the results obtained. It would appear, however, that most of these problems have now been overcome and October and November 1971 were quite successful runs. Results are quoted irrespective of the limitations on the data and then allowance for this is made in the discussion following.

7.8 The Mean Wind

1. The Analysis Technique

Because atmospheric tides produce winds of similar magnitude to the mean wind in the meteor region, it is necessary to be able to account for their effects before the mean wind can be obtained accurately. If the method used to measure the wind can only be used at a particular time of the day (i.e., sodium vapour trails may only be used at twilight and dusk) it is not usually possible to take full account of the tidal components. The resultant averages may be expected to reflect this fact. However, even if the results are obtained with the above restrictions, it may be possible, by observing for several successive days, to minimize the effects of the tidal components. This is satisfactory if the observed tides are sufficiently variable in phase and amplitude, (Fraser, 1968).

As it is possible to measure winds using radio meteors at all times of the day, it is theoretically possible to take account of the tidal components and obtain good estimates of the mean wind. This is normally done by carrying out an

harmonic analysis of the data as the mean velocity obtained by this analysis is orthogonal with the tidal components. Provided the time series completely specifies the tidal components, the mean term will specify the mean wind. This method has been used by previous authors, (i.e. Greenhow, 1954).

If long period components are present, they will modify the observed mean wind also. In the present analysis a regression line was used to fit any possible trend and minimize its effects on the tidal components observed. In doing this the mean flow for the run will also be removed and can be found from the constant, c , and gradient, m , of the regression line. Thus

$$\text{Mean flow} = c + \frac{1}{2}(mT) \quad (7-2)$$

where T = length of the run. Within the error limits of the harmonic analysis, the two methods give the same result.

As both the methods use the average velocity, it was decided to attempt a third method where this requirement was minimized because of the low data rates often encountered making the averages less useful. The alternative method involved finding the mean velocity for all the decay meteors in a 1 km interval. The mean wind was found from the mean for all velocities, and the wind gradient was obtained by fitting a regression line to the 1 km averages, allowing for the number of meteors present. This method suffers from the effects of the diurnal meteor rate, in that a large majority of the meteors recorded will be from the early morning and this will be expected to bias the results to this time of the day.

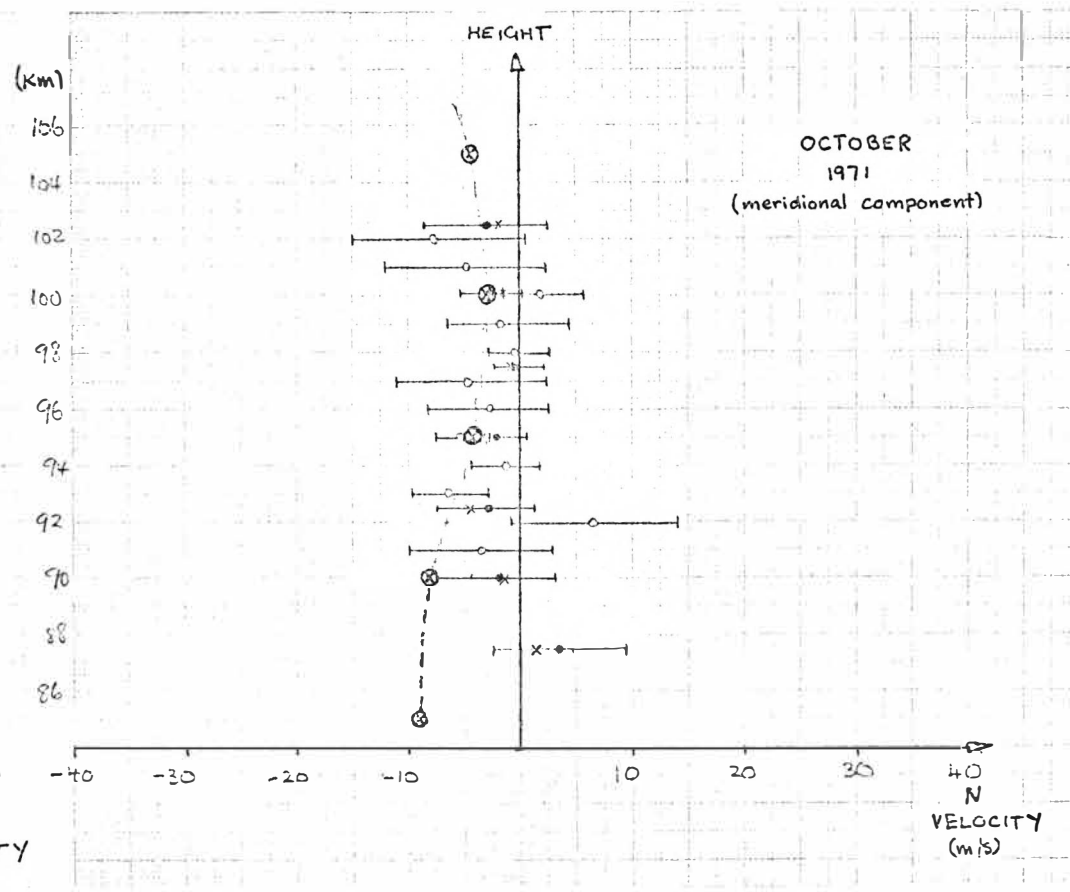
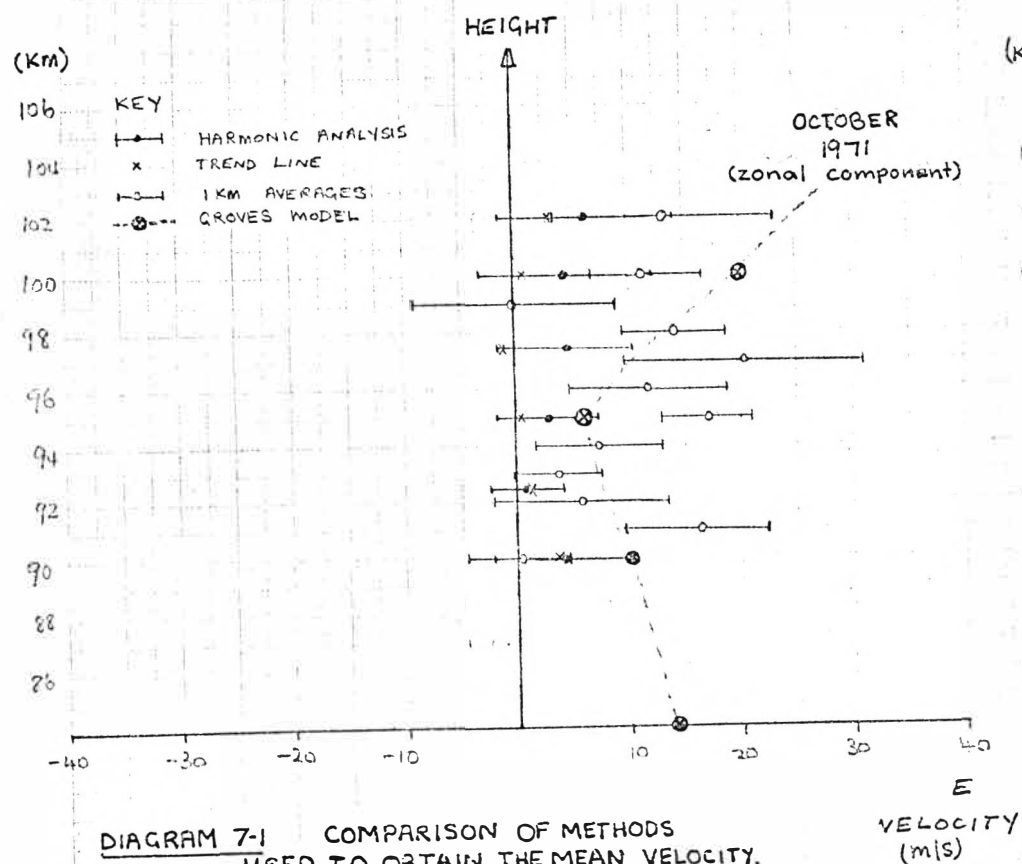
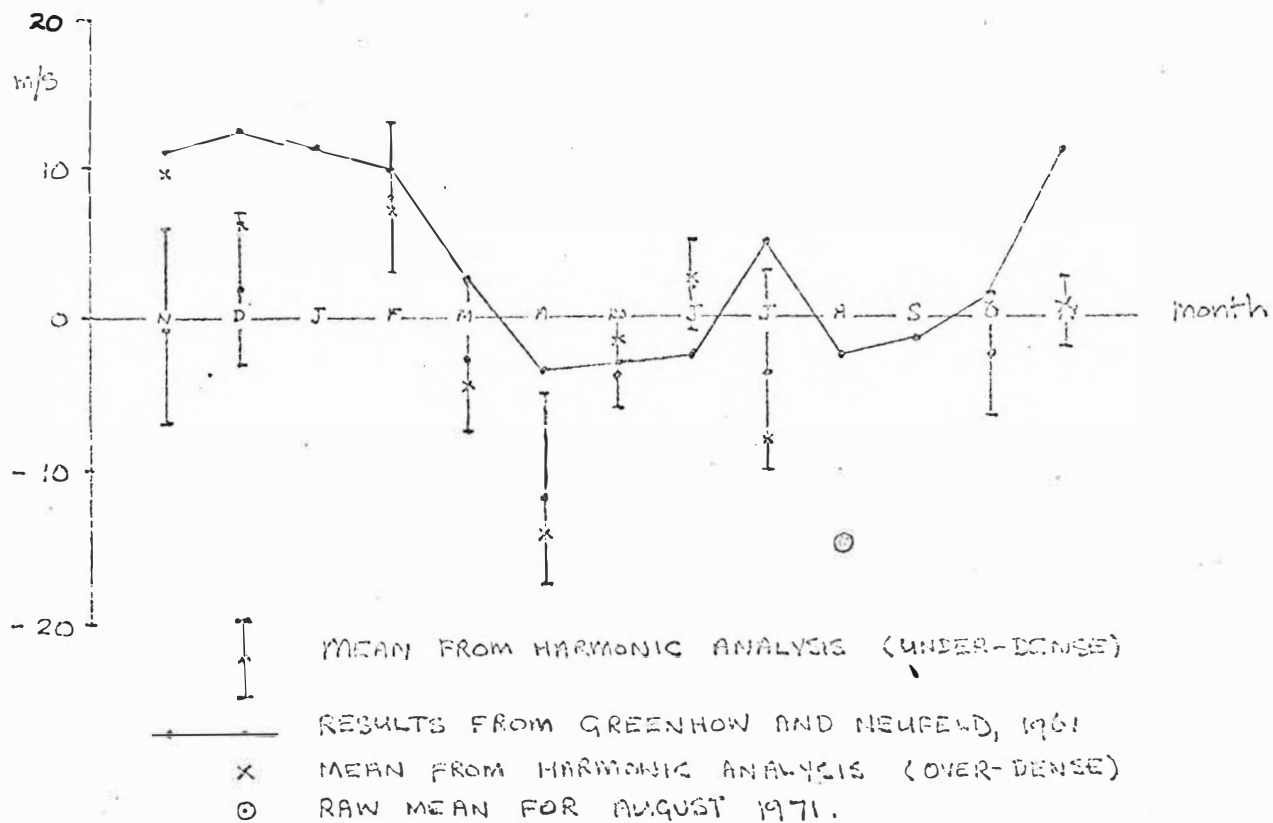


DIAGRAM 7-1 COMPARISON OF METHODS USED TO OBTAIN THE MEAN VELOCITY.

NORTH

DIAGRAM 7-2. THE MEAN WIND.



EAST

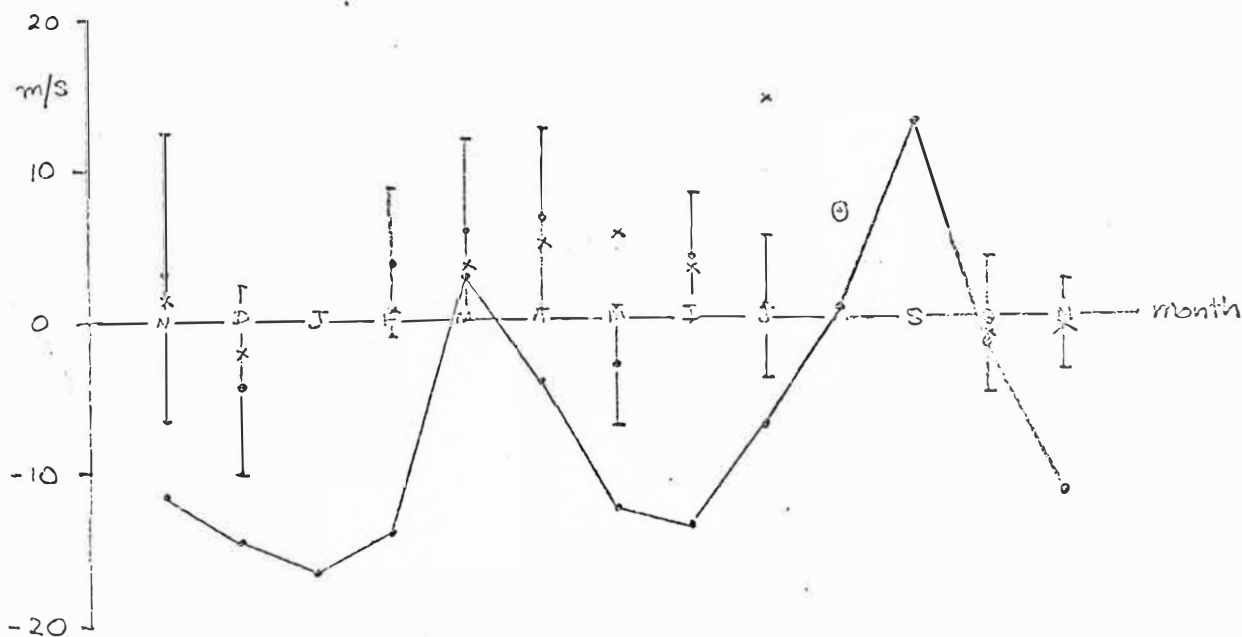


Diagram 7-1 shows the height variation of the mean component for the 7-9th of October, 1971. The results for a harmonic analysis without allowance for a linear trend, the mean flow obtained from a trend line, and 1 km averages for all the meteors taken together. The northward component shows no variations outside the error limits, and differences in the eastward component, though more evident for the 1 km averages, are still inside the error limits. Also sketched on the curves are neutral wind profiles taken from Groves, 1969. In all cases agreement is good, suggesting that while the three methods of analysis are different in basis, the results for a reasonably good run are the same.

2. Results

a) The Mean Wind Obtained: Diagram 7-2 gives the zonal and meridional components for the period of observations. The results for all decay meteors are given with error bars arising from harmonic analysis. For comparison, the continuous line is the monthly mean wind given by Greenhow and Neufeld, (1961) using five years data. The crosses are the monthly mean values for overdense meteors. Because of the poor data rates, it is inappropriate to consider differences between these values. However, some general points are worth noting.

i) The mean values obtained for decay and for overdense meteors are the same, within experimental errors, apart from three instances. Some agreement would be expected because of contamination of the overdense classification by underdense meteors. However, the generally good agreement between the two suggests that accidentally classifying an overdense meteor as a decay will not introduce a significant error in the velocities. The

only instances of serious disagreement ~~are~~ the zonal components for ^{July and} May 1971.

As height distributions for overdense meteors peak at a lower altitude than underdense meteors this difference could be real, as the wind gradient observed has the right sign.

- ii) The present results do not agree in magnitude with the Jodrell Bank results, but the general trend, showing a semiannual variation is apparently present. In view of the variability of the prevailing wind, as indicated in Greenhow and Neufeld (1961), this could be considered satisfactory.
- iii) In view of the large uncertainties in the means obtained from harmonic analysis it is not possible to obtain much information on the seasonal winds. As an indication, averages for winter and summer months are given in Table 7-2.

TABLE 7-2

	Winter	Summer
Meridional	-2 m/s (-2)	2 m/s (5)
Zonal	0.7 m/s (8)	0.9 m/s (.1)

The values in brackets are for overdense meteors. These suggest a mean meridional wind away from the south pole in summer and towards it in winter. The zonal component is about half the size of the meridional component and is directed

eastwards in both seasons.

These results are in general agreement with those previously obtained for Jodrell Bank and Adelaide, though the large meridional component may be spurious.

b) The wind gradient obtained: Because the height information obtained was generally incomplete for a twenty-four hour period, even when two or three days data are used together, wind gradient information is difficult to obtain.

i) From Table 7-2, the results for overdense meteors (if assumed representative of a lower altitude than the underdense averages) suggest a negative wind gradient in winter and a positive gradient in summer. Provided the calculations made in section 6.3(2) for the height distribution of underdense meteors are reasonable for overdense meteors, then if a minimum line density of 2×10^{14} electrons/meter is used, the height distribution of overdense meteors will be expected to peak about four or five kilometers below the underdense meteors. Taking a value of 4.5 km, the wind gradients are calculated from Table 7-2 and given in Table 7-3.

TABLE 7-3

	Winter	Summer
Meridional	0 m/s/km (1.2)	-0.7 m/s/km (-0.5)
Zonal	-1.6 m/s/km (+0.6)	+0.2 m/s/km (-0.4)
Zonal (Adelaide)	-3.3 m/s/km	+2.3 m/s/km
Zonal (Jodrell)	+0.8 m/s/km	+0.8 m/s/km

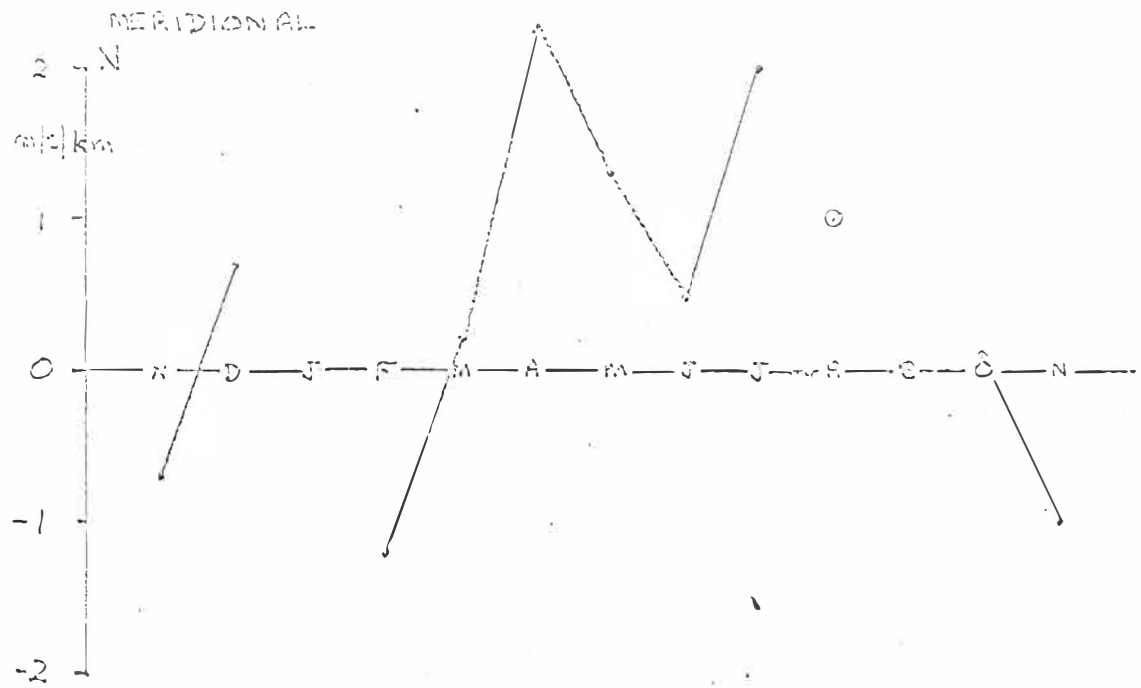
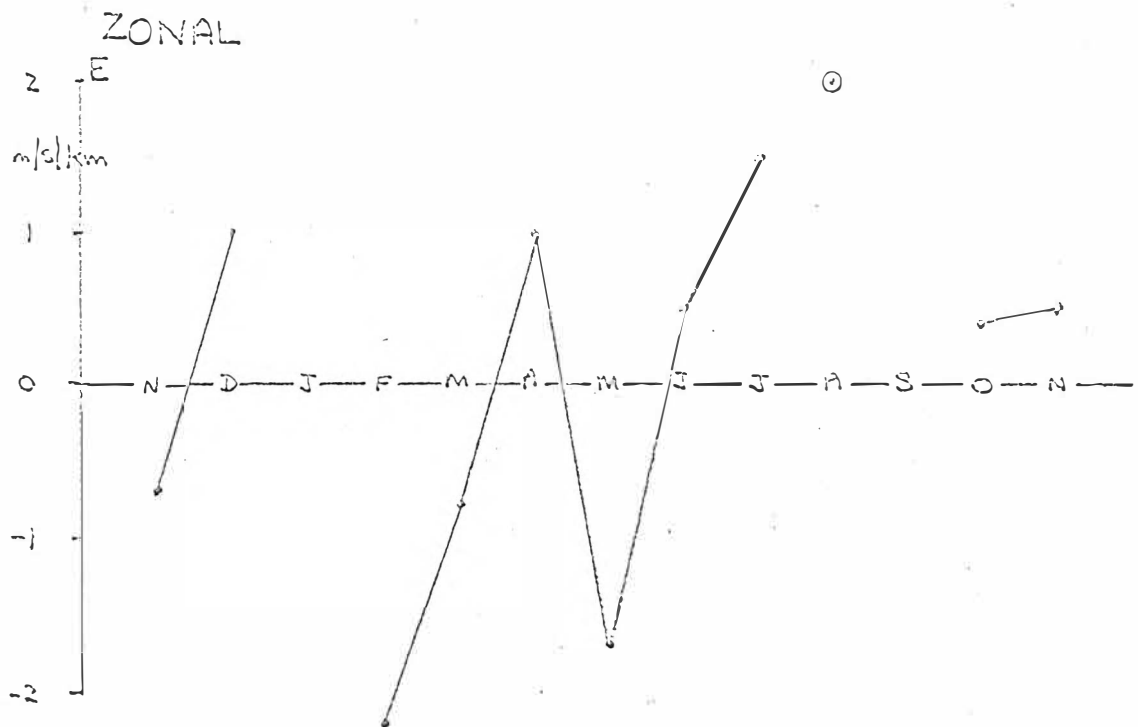


DIAGRAM 7-3. WIND GRADIENTS.
(a positive gradient increases to the east or north
with increasing altitude.)



Results for Jodrell Bank and Adelaide (Elford, 1959) are included for comparison. The present results lie between these two sets. Northward shears of 0.3 m/s/km were observed at Jodrell Bank, (Greenhow and Neufeld 1961), which agrees with the present result.

ii) If wind gradients are considered for the 1 km averages mentioned in section 7.8(1), then poor agreement with other station's results is found, although agreement with the harmonic analysis results is satisfactory. The results are given in diagram 7-3, no estimates of the significance of the values being made. The winter (May, June, July 1971) and summer (November 1970, 1971, December, February 1971) wind gradients are given in brackets in Table 7-3. The two sets show disagreement in both sign and magnitude. As the 1 km averages, and the harmonic analysis results give wind gradients opposite to those observed for winter and summer in Jodrell Bank, Adelaide and Birdlings Flat (Fraser, 1968) data, as well as disagreeing with standard atmospheres available for this region, it seems unlikely that much faith can be placed in the height resolution of the results.

c) Summary of Mean Wind

- i) There is little significant difference between the values of the zonal and meridional wind components, though there is some evidence to suggest that the meridional component is larger than the zonal component (Table 7-2). As this is at variance with other results and with theoretical expectations, it must be regarded as suspect.
- ii) The magnitudes of both wind components are small, being less than 15 m/s in all cases. This order of magnitude

is in keeping with results from Jodrell Bank, as shown in diagram 7-2, but is less than wind velocities observed for both Adelaide and Birdlings Flat. While the results are tentative, this is indicative of the observed winds.

iii) Because each month is specified by a single run, it is not reasonable to consider these results as monthly averages. It is possible that discrepancies observed in the present results, when compared with monthly averages, are, at least in part, due to this.

7.9 Tidal Components

In view of the poor results for the mean wind, tidal components would also be expected to show irregular behaviour. Furthermore, as only two of the runs used, May and October 1971, gave complete 24 hour time series from an epoch analysis, these results can only be considered tentative.

In all results that follow, the phase of the tidal component is given as the time, in degrees, from 0000 hrs L.M.T. to the first maximum of the component. To obtain the phase in hours, it is necessary to use equ. 7-3

$$x_p = t_p / 15n \quad (7-3)$$

where x_p = phase in hours

t_p = phase in degrees

and n is given by \bar{S}_n .

Only runs with more than 18 hours used in the epoch analysis will be recorded here. The amplitude of the maximum is given in metres per second.

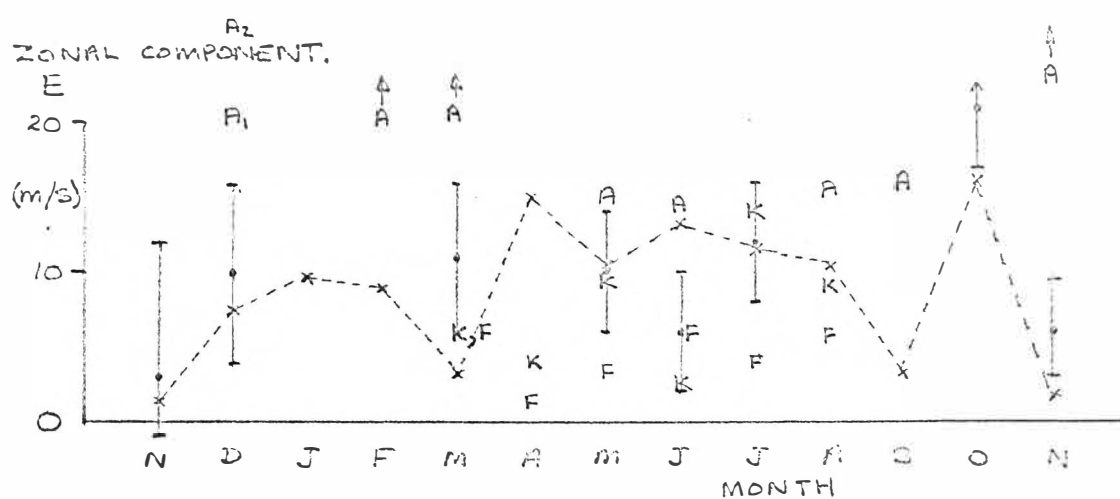
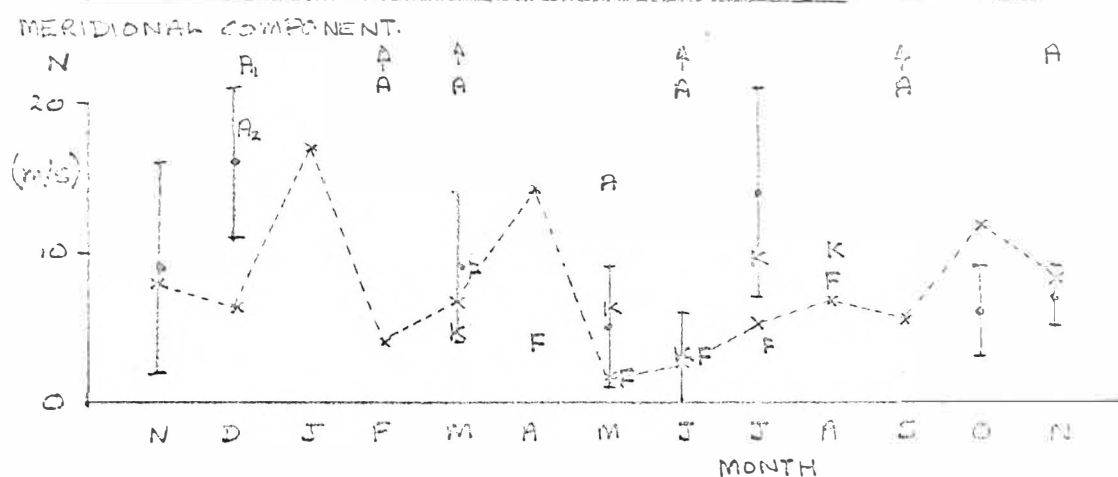
1. Solar Diurnal Tide, \bar{S}_1

a) Results

TABLE 7-4

Run	1	2	4	6	7	8	10	11
Month	NOV/DEC	DEC	MARCH	MAY	JUNE	JULY	OCTOBER	NOV.
Meridional, Amp.	9±7	16±5	9±5	5±4	3±3	14±7	6±3	7±2
Phase	15±40	10±30	331±50	159±50	232±50	247±40	190±30	302±20
Zonal, Amp.	3±9	10±6	11±5	10±4	6±4	12±4	21±4	6±3
Phase	9±40	304±50	186±40	179±40	231±40	68±30	110±15	126±40

DIAGRAM 7-4. THE DIURNAL TIDE, AMPLITUDE



\bar{S}_1 TIDE FROM HARMONIC ANALYSIS, 1970-71

-x---x RESULTS FOR SHEFFIELD, 54°N , 1964-65, (Müller, 1968)

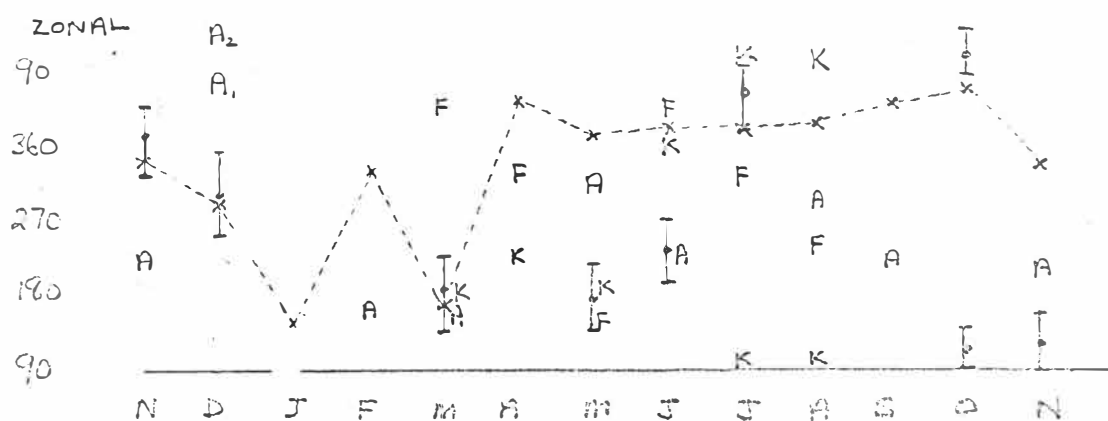
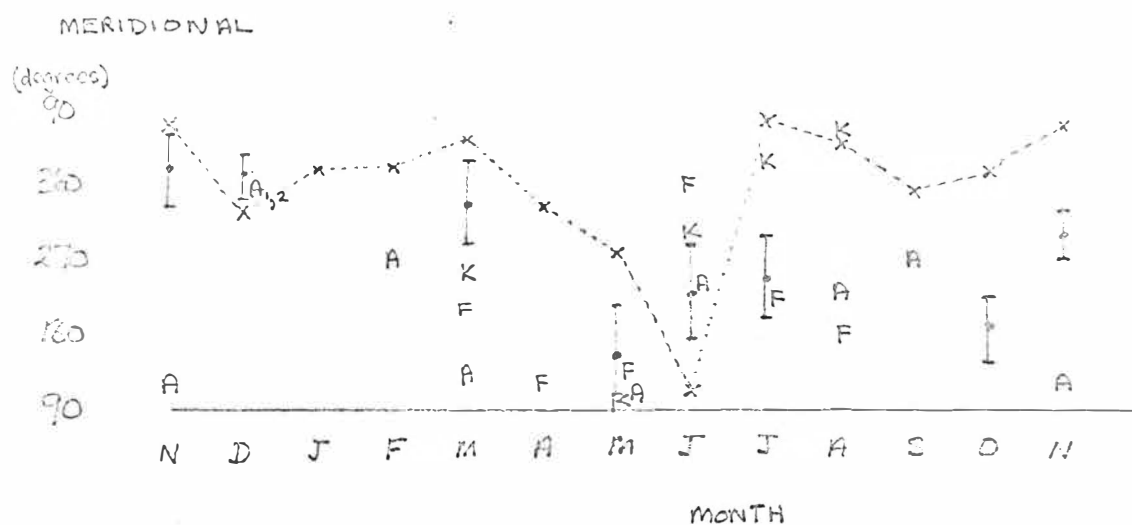
K RESULTS FOR KHAR'KOV, 49°N , 1965-66, (Lysenko, et al,

F RESULTS FOR FRUNZE, 43°N , 1965-66 1969)

A RESULTS FOR ADELAIDE, 35°S , 1953-55, (Eibrd, 1959)
(only the 95-104km results used)

NORTHERN HEMISPHERE RESULTS ARE ADJUSTED BY SIX MONTHS
FOR SEASONAL DIFFERENCES.

DIAGRAM 7-5 THE DIURNAL TIDE, PHASE



THE SAME ABBREVIATIONS AS DIAGRAM 7-4 ARE USED
HERE.

Table 7-4 gives the results of harmonic analysis for the runs noted. While little significance can be placed on height variations of the tidal components, an investigation of these variations for each month showed generally steady phases, within the error estimates. The amplitudes showed some tendency to increase in July but were constant for other months.

For purposes of comparison, the tidal amplitudes are given, in diagram 7-4, along with results for Adelaide, Frunze, Khar'kov and Sheffield. From this it is apparent that results obtained at Christchurch, 43°S , are of similar magnitude to the higher latitude results, and consistently smaller than the results for Adelaide. In several cases the agreement is remarkably good in view of the large time and space separations.

Diagram 7-5 shows the variation of phase for the runs made, and is compared with other results. Some agreement is observed, but it is much less evident than for the amplitudes.

Rough seasonal averages have been made from the previously cited papers and are given in Table 7-5. The number in brackets is the phase of the tide and all amplitudes are given in metres per second. The winter values are obtained from an average of the months May, June and July, or November, December and January in the Northern Hemisphere. The summer average uses the same months reversed for the different hemispheres. Theoretical predictions for latitudes 45° and 60° at the equinoxes, for an altitude of 95 km, are also included. These were obtained from diagrams in Lindzen, 1967. The results for Jodrell Bank and Adelaide are taken from seasonal averages given by Haurwitz, 1964.

TABLE 7-5

	Winter		Summer	
	Meridional	Zonal	Meridional	Zonal
Present Results	7 (210)	9 (160)	12 (350)	6 (146)
Sheffield	4 (250)	12 (260)	9 (210)	2 (90)
Jodrell Bank	3 (210)	4 (358)	9 (95)	4 (326)
Adelaide	12 (55)	4 (249)	20 (123)	24 (160)
Frunze	4 (148)	4 (249)		
Khar'kov	7 (123)	9 (197)		
Theory 45°	20 (135)	28 (45)		
Theory 60°	2 (45)	4 (0)		

b) Discussion

i) Magnitude of the tide: The results for 43°S agree in magnitude with those for higher latitudes in the northern hemisphere rather than results obtained for Adelaide. In the seasonal averages, this is more apparent in Summer than Winter. There is some evidence of increased amplitude of the diurnal component in Summer, but it is not strong. It is, however, in keeping with the other results. Considering the large variation in amplitude expected from theory, the tabulated results can be considered in good agreement with the theoretical predictions.

ii) Phase of the tide: Here good agreement is less evident, the meridional component in diagram 7-5 fitting the other experimental points better than the zonal components. However, the scatter of all points is great enough to make it difficult to draw any conclusions. Little can be inferred from the seasonal averages either, though considerable phase variations in the months averaged make these tentative anyway.

Müller (1966) observed that there was no clear tendency for the two components to be 90° out of phase in the Sheffield results. In view of the errors in the phase measurements, amounting to approximately 80° between the two components, it is not possible to make definite statements on this point.

iii) Summary: From theoretical considerations, the height variations of the diurnal tide are expected to be very irregular in both phase and amplitude (Lindzen, 1967). The present results show little variation in either amplitude or phase with changing altitude. There is, however, some tendency for increasing amplitudes with increased altitude.

From the results obtained, the \bar{S}_1 tide at 43°S is of similar magnitude to the higher latitude stations quoted. The phase for all stations in diagram 7-5 is sufficiently variable to make comparisons on this basis rather fruitless at present.

2. Solar Semi-diurnal Tide, \bar{S}_2

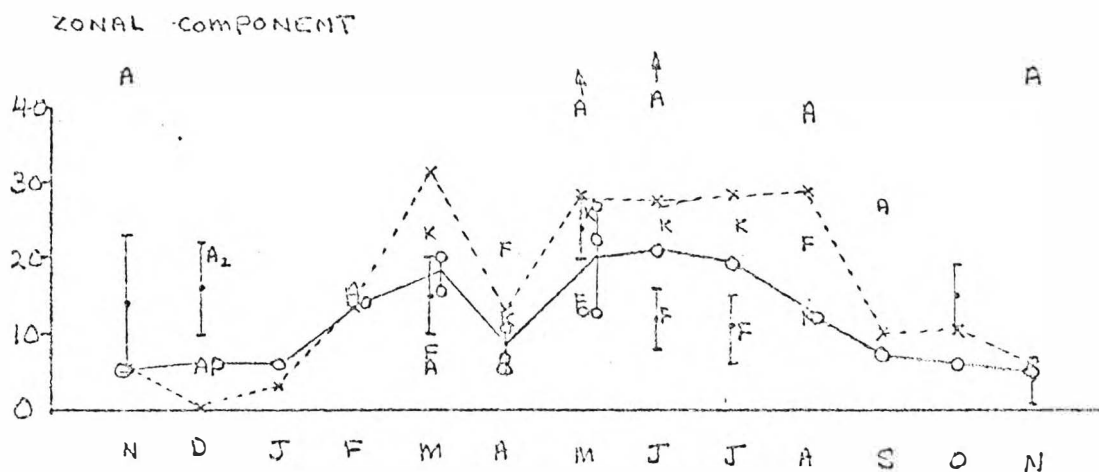
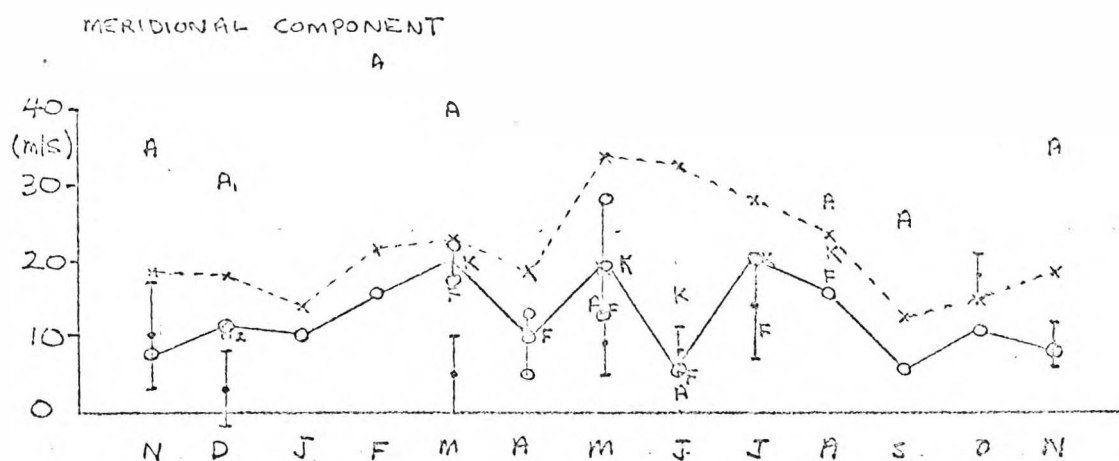
a) Results

Table 7-6 gives the observed semidiurnal tidal components for the present results. Comparisons made for the \bar{S}_1 component are made in the same way for the \bar{S}_2 component, diagram 7-6, giving the amplitude comparison. Table 7-7 gives the seasonal averages.

b) Discussion

i) Magnitude of the Tide: The results for Sheffield are consistently larger than for Jodrell Bank, though the two stations are at virtually the same geographical locality. However, the general trends in both sets of data are sufficiently similar for this discrepancy in amplitude to be due to time variations. Results for Adelaide are generally large, though this is not found in the seasonal averages

DIAGRAM 7-6 THE SEMI-DIURNAL TIDE, AMPLITUDE



(THE SAME ABBREVIATIONS AS DIAGRAM 7-4)

—○— RESULTS FOR JODRELL BANK, GREENHOW AND NEUFELD, 1961.

TABLE 7-6

Run	1	2	4	6	7	8	10	11
Month	NOV/DEC	DEC	MAR	MAY	JUNE	JULY	OCT.	NOV.
Meridional, Amp.	10±7	3±5	5±5	9±4	8±3	14±7	18±3	9±2
Phase	328±30	240±40	358±60	285±30	350±30	44±40	291±15	191±20
Zonal, Amp.	14±9	16±6	15±5	24±4	12±4	11±4	15±4	4±3
Phase	231±40	69±30	301±30	290±15	282±20	257±30	209±20	144±50

TABLE 7-7

	Winter		Summer	
	Meridional	Zonal	Meridional	Zonal
Present Results	10 (226)	16 (276)	7 (253)	8 (148)
Sheffield	31 (185)	28 (275)	15 (140)	11 (230)
Jodrell Bank	20 (200)	16 (280)	12 (135)	7 (200)
Adelaide	11 (300)	13 (316)	16 (200)	12 (216)
Frunze	13 (140)	15 (120)		
Khar'kov	10 (67)	21 (110)		

because of considerable variability of this component from day to day. Lysenko et al. (1969) report a considerable variation in \bar{S}_2 amplitude with latitude; their results showing a maximum in amplitude near latitude 50° . The good agreement between the present results and Frunze, and the generally larger results for Sheffield could thus support a latitudinal variation. However, this is not supported by the monthly averages of diagram 7-6 for Jodrell Bank.

ii) Phase of the tide: For Sheffield and Jodrell Bank data clear evidence of a 90° phase shift between the meridional and zonal components is found in Table 7-7. This is not so evident from the other localities, being clearly untrue for Adelaide data. The results for seasonal averages of the Christchurch data are not perfect, but as with the \bar{S}_1 tide, the 90° phase change is apparent within the experimental error.

iii) Summary: Again, some evidence for increasing amplitude with increasing altitude, is observed but it was only significant for May 1971, where a height gradient of $2 \pm 1 \text{ m/s/km}$ was observed for both components. No significant phase variations accompanied this.

The tidal amplitudes tabulated appear to fit the observed latitude variations for other stations, though the phase variations show only slight similarities. The good agreement between the Jodrell Bank and Sheffield data, and the observed agreement with theoretical predictions (Müller, 1966) indicates good consistency between these sources. There is also reasonable agreement, in Winter, between these results and the present results. In Summer, however, the zonal and meridional components appear reversed with respect to the other results. Little further comment can be made on these results at present.

3. The \bar{S}_3 Component

Greenhow and Neufeld, (1961) suggest that the S_3 component is only significant in yearly averages. Müller (1968) observes that there is reasonable evidence for a 90° phase shift between meridional and zonal components, though regular patterns do not appear evident. Table 7-8 gives the \bar{S}_3 tide observed for the present data.

As no significant seasonal variations are reported by other workers, only yearly averages are presented in Table 7-9.

From the two tables no consistent results emerge. It is apparent that for some runs the \bar{S}_3 component is quite large, however, because of the variability of the sample, it is not clear whether these results are representative of tidal action or random fluctuations in the data. Results using the simulation program described in sec. 7.6(8) revealed \bar{S}_3 and \bar{S}_4 components that exceeded the error term in some cases, implying that such components could be spurious.

4. The \bar{S}_4 Component

Müller (1966) finds some evidence for a \bar{S}_4 tidal component at meteor heights, but suggests that this will be lost, to some extent, in the short term atmospheric variations that are also present. A significant six hour oscillation does appear in the present results, but this was closely associated with fluctuations in the mean velocity when the meteor rate was low. In view of this, and the rather poor quality of the data available, further investigation of the \bar{S}_4 tide appears inappropriate at present.

TABLE 7-8

Run	1	2	4	6	7	8	10	11
Month	NOV/DEC	DEC	MARCH	MAY	JUNE	JULY	OCT.	NOV.
Meridional, Amp. Phase	5±6 198±40	9±5 359±40	6±5 300±50	2±4 116±50	4±3 163±50	6±7 132±50	9±3 77±20	2±2 130±35
Zonal, Amp. Phase	10±10 357±40	15±6 6±50	6±5 151±60	3±4 60±50	6±4 309±40	7±4 239±45	7±4 177±50	6±3 21±44

TABLE 7-9

	Christchurch	Sheffield	Jodrell Bank	Frunze	Khar'kov
Meridional	6 (184)	3 (275)	2.5 (250)	7 (272)	5 (160)
Zonal	7 (165)	3 (30)	3 (310)	5 (180)	3 (260)

5. Summary of Tidal Results

As with the mean wind and wind gradients, the rather poor quality of the present data makes it difficult to draw any substantial conclusions. There does appear to be some consistency in the results, however.

- i) The \bar{S}_1 and \bar{S}_2 tidal components are of similar magnitude, being roughly 10 ± 5 m/s for both zonal and meridional components.
- ii) The amplitude of the \bar{S}_1 tide agrees with results for similar latitudes in the northern hemisphere.
- iii) The amplitude of the \bar{S}_2 tide fits the latitudinal variations observed by Lysenko et al. (1969), which revealed a large increase in amplitude as latitude 50° is approached.

It does not seem reasonable to make comparisons of the phase of these components. As observed, errors in the phase measurements are large enough to make definite conclusions difficult to obtain. Furthermore, the quite considerable variability in the data obtained, due to low meteor rates, makes the \bar{S}_3 and \bar{S}_4 tides observed rather tentative at present. The presence of these components, especially the \bar{S}_4 component, in variable data implies some care must be taken in interpreting the observed results.

7.10 Summary of the Results

The results presented in this thesis are preliminary results for the apparatus for three reasons:

- i) Because these are the first results obtained with the apparatus, they are affected by radar equipment modifications made in the first year's operation, and by the low meteor rate that was initially obtained before

these adjustments to both the transmitter and transmission line.

- ii) As shown in Table 7-1, a certain amount of film is yet to be read. Though their inclusion in the analysis should not significantly affect the present results, which are derived from as complete a 24 hour time segment as could be obtained in each case, it does not seem reasonable to draw any final conclusions until all the film has been read.
- iii) These results are not monthly averages, but are the results of single runs made once a month. Because of this, there may well be real discrepancies between these results and subsequent monthly averages obtained at a later date.

Although the present results are not considered very satisfactory, the general agreement with results obtained by other workers is satisfying to some extent. If, as is suggested by these results, the \bar{S}_1 and \bar{S}_2 tides are generally three or four times larger than the mean wind, it is not surprising that agreement with tidal results appears better than for the mean wind.

It is not possible, on the basis of the present results, to measure any significant long period variations in the wind motions implying that if any are present they must be smaller than 10-15 m/s.

C H A P T E R 8

THE CONCLUSION

Several points warrant further comment in light of the results of the previous chapters. As the present thesis has primarily been concerned with the establishment of the meteor winds station at Christchurch, and the general problems associated with the analysis of meteor winds data as measured from photographic film, it seems appropriate that these points should be discussed in the concluding chapter.

8.1 Radio Interference

In normal operation the equipment is arranged so that only meteor echoes are recorded on film. Radio interference may also trigger the apparatus resulting in film wastage, or in extreme circumstances, no echoes may be observable. Spurious echoes from aircraft was cited as a reason for using a pulsed system (Nowak, 1967) and even when a pulsed system is used, operation near a large city can prove difficult. In addition to r.f. interference, in temperate latitudes ground-scatter from sporadic E layers can also be a problem during daytime operation.

In the present experiment, considerable interference due to ground-scatter was encountered during the early runs. However, the major source of r.f. interference was found to be associated with 50 Hz hum and transmissions on the citizens band. These sources of interference were basically a daytime phenomenon and were normally associated with ground-scatter. On one occasion, observations were made on 27.12 MHz at two localities, roughly 100 miles apart and the r.f. interference

made operation impossible at both localities. The drop in intensity of this noise occurred at roughly the same time suggesting that both localities were being affected by the same noise source. It is likely, then, that little relief from the interference will be acquired by shifting the locality of the station. There is, however, some possibility that the operating frequency, if shifted to 35 MHz or greater, would produce a substantial reduction in the interference level. At the end of the present runs the equipment had been considerably improved, resulting in higher meteor rates at all times of the day, suggesting that the interference problems were no longer as great as in the early runs. However, on some occasions the receiver was completely saturated by the interference. Such events could probably only be avoided by the choice of a higher frequency.

The choice of an operating wavelength discussed in sec. 4.2(1), while indicating the region in which operation is desirable, does not consider local r.f. interference. As it can be a particularly serious problem in recording meteor echoes the selection of an operating frequency should take into account the interference likely to be encountered at the chosen site. This will probably need to be measured experimentally, but is sufficiently important to warrant the extra time required.

8.2 Zero Velocities

Wind velocities obtained by comparing the received and transmitted (reference) signals will always show a loss of zero velocities because of the finite meteor duration. To overcome this, the reference signal may be off-set making it

possible to determine both the magnitude and the direction of the velocity from one measurement. However, there will now be a bias in the direction of the offset frequency. This may be overcome by using two offset frequencies, which if chosen carefully will allow wind velocities to be determined independently of the meteor duration. There will still be a theoretical bias against zero velocities with respect to other velocities, but this will now be insignificant. Thus, if the off-set frequencies are ± 20 Hz, then for $\lambda/2$ change in the phase an echo duration of at least .05 secs is required, all other velocities requiring smaller durations.

While not investigated very thoroughly, there was some evidence, sec. 7.7(8), that the loss of zero velocities observed in the present results would not have any significant effects on the results of the harmonic analysis. This should be investigated further. Though it implies the bias against low speeds is not significant, making the zero offset an unnecessary addition, there are two strong arguments in favour of the offset.

- i) It should make the reading of film records far simpler, all measurements being objective in determining the velocity.
- ii) While the loss of zero velocities may not be significant in tidal analyses, it is likely to be important if the variability in the wind-field is being considered, or if two systems are being compared. At present, the individual velocities have little significance on their own.

8.3 Decay Heights

The calibration of decay heights by more direct methods, and the resultant scatter in the results obtained has been discussed in sec. 5.1. Possible sources of the scatter discussed were, ionization irregularities, geomagnetic effects, wind-shears, variation of atmospheric parameters and instrument effects. As the next stage in the development of the present station will involve the direct measurement of azimuth and elevation of the echo reflection point, it will be possible to carry out the calibration of decay heights. It should be possible to investigate at least some of the effects giving rise to the observed scatter with these new facilities.

8.4 Data Analysis

The present system relies on manual reduction of the data recorded on film. As approximately 250 ft of film are recorded in 24 hours, and it takes a film reader about 30 hours to read 100 ft, (about 1.5-2 minutes per meteor), a considerable amount of time is spent on data reduction at this stage. In the present experiment, apart from film read by the author, all film was read by part-time film readers. This has meant a considerable delay in obtaining the complete results from a single run.

Even if it were possible to have one or two people reading film full time, there would still remain the problem of subjective errors discussed in chapter 6. To overcome this, it would be preferable to use an automatic recording system, as has been done at Stanford. This would greatly reduce the analysis problems and should be more objective. Furthermore,

it will be possible to increase the number of meteors recorded by having longer runs - the major drawback in long runs at present being the large volume of data that must be read.

However, a major problem arises in identifying which records to record and which ones to ignore. From observation of the present discriminator, provided there is only the normal sky noise present, it is possible to only trigger the system when a meteor occurs. In conditions of moderately heavy interference, similar results were observed when the blanking channel was incorporated. The identification of a meteor from a noise spike should be handled by the present system.

Having identified that a record is a meteor, it is necessary to determine whether it is overdense or underdense. The present results suggest that results obtained from only overdense meteors will closely match those obtained from underdense meteors. To include overdense records with the underdense ones will probably not produce significant errors. However, because an overdense record can last for several seconds, it is possible that the velocity associated with it could be counted several times. To avoid this, the range of the echo could be used to discriminate against repeated use of the same meteor. As the repeated use of the same meteor would seem to produce a greater error than the incorrect estimation of the type of record, the range of the meteor could be the more important parameter for selecting an echo in an automatic system.

8.5 Significance of the Mean Velocity for Half an Hour

- i) No simple estimation can be made of the error in the mean velocity derived from a given number of meteors without some knowledge of the standard deviation of the observed velocities about the mean. The correct term to estimate the significance of the mean is given by equations 6-9 or 6-11, and this is the standard deviation, or the standard error, in the mean.
- ii) With respect to the observed variability of the recorded wind velocities in half an hour, there was some indication that the variability increased with increasing altitude. This may be real, though it is more likely due to a greater bias against zero velocities associated with a low data rate. At present, insufficient data is available to assess this point.
- iii) It was shown in chapter 6 that about half of the variance in the observed wind velocities could not be accounted for on experimental grounds. This was considered to be due to two causes, the general variability of the atmosphere, and windshears associated with the expected errors in height determinations. As the height error is ± 3 km, and the mean wind gradient, though not reliably determined by the present data, was never more than 2 m/s/km, a variation of 12 m/s would be expected for any one height interval. Considerably larger variations are observed. If the shorter duration wind shears measured by Müller (1968) are considered, then a representative value of 16 m/s/km is expected, giving a change of 96 m/s across a 6 km interval. In this case, the observed variability can

be completely explained. This would appear to be a plausible explanation of the observed variance, though it is impossible to verify this with the present equipment.

8.6 Harmonic Analysis

- i) It is possible to allow for the diurnal variation in the meteor rate in carrying out an harmonic analysis. This should be investigated further as at present all points are given equal weights with regard to the meteor rate.
- ii) If the observed meteor rate can be improved, either by increasing the output power of the transmitter, or by shifting the operating frequency so that less r.f. interference is encountered, then it should be possible to avoid gaps in the data in future. It should also be possible to obtain sufficient meteors to allow atmospheric tides to be obtained for the individual days in a run. Results from Adelaide suggest that the tides vary from day to day. It would be of interest to investigate this.
- iii) The significance of the results of harmonic analysis are difficult to assess. In this thesis, the assumption was made that the observed time series was a result of the tidal components and white noise. The tidal components were then assumed to be in error by the magnitude of the white noise spectrum. This is not at all satisfactory, though it does give some measure of the importance of the individual components. It does not indicate the importance of the individual tidal components in the atmosphere. However, because it does give some indication of the value of each individual result with respect to the time series from which it was derived, it seems reasonable to use it as an error estimate, this being preferable to no error estimate at all.

8.7 The Observed Atmospheric Winds

Until all the film has been read and data processed for the first year's operations, the complete results cannot be presented. It was hoped that by reading at least 24 hours of each run, some indication of the monthly variation in winds at meteor heights could be obtained. However, this has not turned out to be the case, the effects of low data rates considerably affecting some of the runs. From the data that has been analysed it would appear that the \bar{S}_1 and \bar{S}_2 tides are of similar magnitude - the magnitudes observed fitting the expected latitudinal variations in these components quite well. In particular, there appears to be good correspondence between results obtained at Christchurch and those obtained at Frunze, in the U.S.S.R., for a similar period of the year.

8.8 Comparisons

Because the meteor wind measurements are confined to a narrow height region, its usefulness as a general method for measuring atmospheric winds is limited. However, because the meteor trail is a direct tracer of the neutral atmospheric motions other less direct methods may be compared with it. Because of this possibility, special attention was paid to the errors present in assessing atmospheric winds using radio meteors in this thesis. From this analysis, it seems unlikely that velocities derived from individual meteors will prove generally useful because of the considerable uncertainties associated with them. Provided a meteor rate in excess of 100 meteors per half hour is attained, quite reasonable wind profiles can be obtained which will probably prove quite useful for comparison purposes. If the systems to be compared are not operated at the same time, however, care will need to be taken to ensure that the results for each system are representative of monthly, or annual means.

APPENDIX

The Computer Programs

To handle the large amount of data obtained computer programs were written to handle the analysis after the information had been read off photographic film. The analysis of the data passes through four steps:

1. Meteors are recorded on film at the field station.
2. Films are developed and read in the physics department, all information being recorded on punched cards.
3. The wind velocities for each half-hour time interval are processed in the computer to produce, on punched cards, the mean velocity, root mean square velocity and the number of meteors used in averaging.
4. These averages are then used to obtain the tidal data and mean wind using a harmonic analysis technique.

Sections 1 and 2 have been dealt with in the main body of the thesis, and results obtained to date from section 4 have also been discussed. In this appendix the main analysis program and associated subprograms used in section 3 are discussed, and some comments are made on the harmonic analysis program.

All computer programs were written in Fortran IV programming language for an IBM 360/44 computer. With the replacement of the IBM 360/44 at Canterbury University by a Burroughs B6714, it may be necessary, or desirable, to modify some of the analysis programs used. In particular, the main program is expected to be considerably modified, and for this reason it is not as fully documented as the subprograms.

It is, however, included for completeness. Of particular importance to later users are subroutines REDIN and METEOR. Using REDIN, the raw data can be read off cards and then calling METEOR will result in the card information being printed out on the line-printer, giving the horizontal and radial ranges and velocities observed for each meteor. All information stored on cards is the raw data, as read off film.

A.1 The Main Program

The following results are obtained from the present main program.

- i) For a half hour set of wind velocities derived from meteors, the mean velocity, the root mean square velocity and the number of records is found for all overdense meteors and all underdense meteors when taken collectively and when divided into 5 km height intervals depending on the decay height of the individual meteor. All these averages are punched on cards and printed out on the line-printer.
- ii) A plot is made of the run using all the individual wind velocities (plotted as crosses). Also the mean velocity for each half-hour, the limits of film reader accuracy and the limits depending on the standard error in the mean are plotted. Diagram 6-14 is an example of such a plot.
- iii) The mean and r.m.s. velocities, and the total number of meteors for 1 km height intervals are found using all the underdense meteors in the run.
- iv) The mean standard deviation and number of half-hours used to define the bearings North, South, East and West are

calculated to indicate the possible errors arising from not directing the aerial in only one of these directions. The various sections are, for the most part, treated separately in the main program. While being poor programming technique, this allows the user to delete any section of the program with a minimum of program modifying. As there were no significant losses in operating time, and sufficient storage was available, this has seemed a reasonable approach.

A.2 Card Formats

1. A run

All data associated with a single run is defined by a header card at the front and a blank card at the back of the data. The format of the header card is:

- i) Cols 1-6, floating point number giving the length of the plot to be made in thousandths of an inch (each half hour is 25/1000").
- ii) Cols 7-40, and cols 41-80 may be used to print a two line title on the plot.

2. A half-hour

All the data is subdivided into half-hours, each half-hour being defined by a header card at the front and a blank card at the back of the data. The header card has the following format.

Columns	Format	Variable	Information
1-2	I2	IYEAR	the year in which the run was made
3-5	I3	IDATE	the day in the year
6-9	I4	ITIME	the time for the half-hour
10-12	I3	IBEAR	bearing of aerial for half-hour
13	I1	IREAD	film reader identification
14-15	I2	CAL	not zero if calibration follows

The date is given using a 365 day calendar, and the time is given using a twenty-four clock.

3. Range calibration

If a range calibration is to be read in, CAL will give the number of pairs of values to read in. In all cases, the range calibration comes from a separate program to be discussed later.

4. Individual meteors

The information obtained from each meteor has been discussed in chapter 5. The format used is as follows.

Columns	Format	Variable	Information
1-3	I3	N(K)	number of meteor in half-hour
4	A1	TYPE(K)	d if underdense, p if overdense
6-7	F2.0	DUR(K)	duration multiplied by 100
8	A1	CLT(K)	X if TYPE(K) uncertain
9	I1	IAMP(K)	amplitude on display
10-13	F4.1	RANGE(K)	range on display
14-17	F4.1	HEIGHT(K)	height as read from film
18	A1	CLHT(K)	X if height is uncertain
19	I1	IHT(K)	type of height (redundant)
21	A1	PIP(K)	X if half hour is subdivided
23	I1	IDOP(K)	type of Doppler
24	I1	IPER(K)	type of persistent (redundant)
25	A1	CV(K)	X if direction uncertain
26-27	F2.0	FDE	duration to first fade
28-31	F4.3	ERROR	error in measurement of Doppler
32-35	F4.3	DOPPLER	time for 360° phase change between received and transmitted signal. This gives the wind velocity.
36-39	F4.3	WS	used if large shear observed

Of these, three require some additional discussion, though they were not used in the present work.

i) PIP(K). When the meteor rate was particularly high in half an hour, time markers were inserted. These are noted by an X in column 21. This was done to investigate the effects of short time variations in the wind profiles. Müller (1966), presented results suggesting the presence of short period oscillations using this technique. However, no similar results have been observed in the present data to date.

ii) WS. If a wind shear is present and observed for at least two Doppler cycles, then the time for the second cycle is recorded in WS. It is hoped that this can be used to investigate wind shears, though it will be a very coarse measurement. These results have yet to be considered. At present, the system advocated by Müller (1968) is too difficult to carry out with the limited manpower available to read film, and a simpler method is desirable.

iii) FDE. If the amplitude shows a definite increase in amplitude after an initial decrease, the time to the change-over is recorded here. This is associated with a wind shear, which is recorded, if possible, in WS.

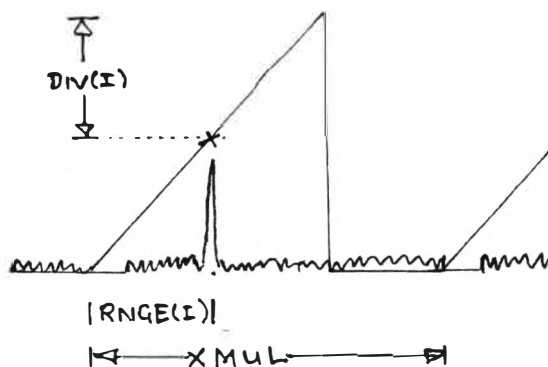
A.3 The Subprograms

No special comments are required here in addition to those already reproduced with the subprograms. In order of usage, the main program calls REDIN, which in turn calls CALIB, FACTC and RANGHC. After control returns to the main program, INDEX is called. In addition to these, LINEHR is included. This was used to produce diagram 6-9.

A.4 The Range Calibration

A separate program was written to calibrate the observed radial range in kilometers. The input to this program consists of two arrays,

DIV(I), which is measured in the same units (centimetres) as the film-readers use, and RNGE(I) which is measured in centimetres from the start of the ramp. Knowing XMUL



(= 6.6 msecs) corresponds to a radial range of 1000 km, it is possible to convert RNGE(I) to kilometres. The output, on punched cards, is DIV(I) in the same units as the input, and RNGE(I) which is now in kilometres. This is used as the range calibration in CALIB, range values measured in the units of DIV(I) are converted to kilometres by comparison with values of RNGE(I) using a simple first order interpolation.

The range calibration program follows subroutine LINEHR.

A.5 Harmonic Analysis

While not presented in any detail here, some comments on the harmonic analysis program are in order. The Fourier transform of the 24 hour data length was carried out using a discrete Fourier transform from the IBM Scientific subroutine package - subroutine FORIT. As mentioned in chapter 7, some uncertainty exists in the determination of the phase using this method. At first it appeared this was a random error, but closer inspection revealed it was very close to a change in phase by 90° . The output of FORIT contains a series of sines and cosines, pairs of which define each frequency present in the analysis. If one member of the pair is nearly

zero, then a small change in amplitude could produce a positive or a negative value. If the time series is particularly noisy, this apparently occurs, producing a 90° change in phase when the signs are used to pick the quadrant of the phase. By varying the starting point of the time series, this error was removed allowing the correct phase to be measured. By treating each height interval as an independent sample, and using the variation in phase with height as a measure of whether this error is present is probably adequate, but would not be recommended for future use. The presence of this error should be considered by other experimenters carrying out harmonic analyses by this method.

Like the main program, the harmonic analysis program can be considerably modified, and is reproduced here for completeness. The error in the phase is one feature that could be modified, for instance.

NOTE: The change in the phase discussed above is not related to the loss of zero velocities, as might be inferred from section 7.6(8).

```

C001      INTEGER CAL
C002      DIMENSION BRNG(4,3)
C003      DIMENSION RUN(32,6,2),TRCT(32,2)
C004      DIMENSION VERT(101,3)
C005      LOGICAL*1 FED(35),FET(39)

C006      C
C007      COMMON/MY/NI,IQX,ILLI,S(25)
C008      COMMON/CALI/DIV(30),RNGE(30),ICAL
C009      COMMON/DATE/IYEAR,ICATE,ITIME,IBEAR ,IREAD
C010      COMMON /NEED/ N(300),TYPE(300),HEIGHT(300),RANGE(300),V(300,3),DIR
C011      ITN(300),PIP(300)
C012      C
C013      COMMON DLR(300),IAMP(300),IHT(300),VR(300),IDCF(300),IPER(300),
C014      1CV(300),CLT(300),CLHT(300),ARF(300)
C015      C
C016      LOGICAL*4 ITYM(4)
C017      DIMENSION Y(300)
C018      C
C019      DATA NF,NP,NERGR,ILN,IMN/C,1,1,C,1/
C020      DATA D,P/'C','P'/
C021      DATA X/'X'/
C022      DATA IX/'X'/
C023      C
C024      LOGICAL*1 M1(26)/'VELOCITY TO THE EAST (M/S)'/
C025      LOGICAL*1 M2(27)/'VELOCITY TO THE NORTH (M/S)'/
C026      C
C027      LOGICAL*1 M(1)
C028      C
C029      DIMENSION AVS(300,5,2),PACE(300,2)
C030      DIMENSION PLACE(300),VEL(300)
C031      C
C032      IQX=0
C033      ILLI=0
C034      C
C035      THE HEADER CARD FOR THE RUN IS READ IN. THIS GIVES THE LENGTH OF THE
C036      PLCT IN 1/1000THS OF AN INCH AND THE TITLE FOR THE PLCT.
C037      C
C038      READ(5,753) AL,(HED(I),I=1,35),(FET(I),I=1,39)
C039      753 FORMAT(F6.0,35A1,39A1)
C040      IWRITE=0
C041      IRCT=0
C042      DO 33 I=1,32
C043      DO 33 J=1,6

```

MAIN PROGRAM

```

C030      DO 33 K=1,2
C031      33 RUN(I,J,K)=0.0
C032      DO 34 I=1,300
C033      DO 34 K=1,2
C034      PACE(I,K)=0.0
C035      DO 34 J=1,5
C036      34 AVS(I,J,K)=0.0
C
C037      REWIND 1
C
C      THE PLCT BCX IS SET UP.
C
C038      IAL=AL/50.0
C039      IBL=AL+600.
C040      IK=0
C041      ILA=AL
C042      AL=-13.0
C
C043      CALL AINIT(IBL)
C044      CALL ACRIG(300,260)
C045      CALL ALAB(-260,-240,FED,35,3,4)
C046      CALL ALAB(-230,-240,FET,39,2,4)
C047      CALL ALAB(-150,-135,M1,26,1,4)
C048      CALL ASCA(-50,-250,0,50,-100,20,11,1,2)
C049      CALL AGRID(0,-250,IAL,10,50,50,1,1)
C050      CALL AGRID(0,-250,1,2,ILA,250,2,1)
C
C051      CALL AORIG(300,810)
C052      CALL ALAB(-150,-135,M2,26,1,4)
C053      CALL ASCA(-50,-250,0,50,-100,20,11,1,2)
C054      CALL AGRID(0,-250,IAL,10,50,50,1,1)
C055      CALL AGRID(0,-250,1,2,ILA,250,2,1)
C
C      THE HEADER FOR A SINGLE HALF HOUR IS READ IN. ALLOWANCE IS MADE FOR
C      GAPS IN THE DATA AT THIS STAGE AND THE END OF THE RUN IS DETECTED.
C
C056      NI=0
C057      2 READ(5,3) IYEAR,ICATE,ITIME,IBEAR,IREAD,CAL
C058      3 FORMAT(I2,I3,I4,I3,I1,I2)
C059      AL=AL+25.
C060      IK=IK+1
C061      PACE(IK,1)=AL
C062      PACE(IK,2)=AL
C063      IF(IYEAR)2,13,5
C
C      * BEARING IS CORRECTED TO A GEOGRAPHIC BEARING.
C
C064      5 IBEAR=IBEAR-55

```

* C

C065

IF(IBEAR.LT.C) IBEAR=IBEAR+360

C
C
C
CTHE VARIATION IN THE BEARING IS MEASURED. THIS WAS IMPORTANT IN SCME
OF THE EARLY RUNS.

C066

IBAR=IBEAR

C067

IF(IBEAR.LE.315.AND.IBEAR.GT.45) GC TC 50

C068

IF(IBEAR.GT.45) IBEAR=IBEAR-360

C069

BRING(1,1)=BRING(1,1)+IBEAR

C070

BRING(1,2)=BRING(1,2)+1.C

C071

BRING(1,3)=BRING(1,3)+IBEAR*IBEAR

C072

IQL=1

C073

GC TC 59

C

C074

50 IF(IBEAR.GE.135) GC TC 51

C075

IBEAR=IBEAR-90

C076

BRING(2,1)=BRING(2,1)+IBEAR

C077

BRING(2,2)=BRING(2,2)+1.C

C078

BRING(2,3)=BRING(2,3)+IBEAR*IBEAR

C079

IQL=2

C080

GC TC 59

C

C081

51 IF(IBEAR.GE.225) GC TC 53

C082

IBEAR=IBEAR-180

C083

BRING(3,1)=BRING(3,1)+IBEAR

C084

BRING(3,2)=BRING(3,2)+1.C

C085

BRING(3,3)=BRING(3,3)+IBEAR*IBEAR

C086

IQL=1

C087

GC TC 59

C

C088

53 IQL=2

C089

IBEAR=IBEAR-270

C090

BRING(4,1)=BRING(4,1)+IBEAR

C091

BRING(4,2)=BRING(4,2)+1.C

C092

BRING(4,3)=BRING(4,3)+IBEAR*IBEAR

C093

59 CCNTINUE

C

C094

IBEAR=IBAR

C

* IF CAL IS NOT EQUAL TO ZERO, A CALIBRATION IS READ IN.

* C

C

C095

IF(CAL.EQ.C) GC TC 4

C

C096

ICAL=CAL

C097

READ(5,52) (CIV(I),RNCE(I),I=1,CAL)

C098

52 FORMAT(10(F4.1,F4.C))

C099

4 CCNTINUE

C

```

C *   K IS INITIALIZED
C   K=1
C   THE DATA FOR A SINGLE HALF HOUR IS READ IN.
C   CALL REDIN(K,NP,NERCR)
C   THE AVERAGE FOR ONE KILOMETER INTERVALS IS CALCULATED FOR ALL THE DATA IN
C   THE RUN. THIS IS CARRIED OUT FOR ZONAL (IP=2), AND MERIDIONAL (IP=1),
C   COMPONENTS.
C1C2   IB=IGL
C1C3   DO 28 I=1,32
C1C4   DO 28 J=1,2
C1C5   28 TRCT(I,J)=0.0
C1C6   DO 36 I=1,K
C1C7   IF(TYPE(I).EQ.P) GC TC 36
C1C8   II=INDEX(HEIGHT(I),80.,1.,30)
C1C9   WC=V(I,2)
C110   RUN(II,1,IB)=RUN(II,1,IB)+WC
C111   RUN(II,2,IB)=RUN(II,2,IB)+WC*WC
C112   RUN(II,3,IB)=RUN(II,3,IB)+1.0
C113   TRCT(II,1)=TRCT(II,1)+WC
C114   TRCT(II,2)=TRCT(II,2)+1.0
C115   36 CCNTINUE
C   THE MEAN, R.M.S. VELOCITY, AND THE NUMBER OF RECORDS USED IN EACH
C   HALF HOUR ARE CALCULATED FOR ALL DECAY METEORS, ALL PERSISTENT METEORS,
C   AND ALL DECAY METEORS IN 5 KM INTERVALS.
C116   AINC=25.0/K
C117   PQ=85.0
C118   PLQ=87.5
C   DC 91 I=1,15
C119   DIRTN(I)=0.0
C120   VR(I)=0.0
C121   ARH(I)=0.0
C122   CV(I)=0.0
C123   91 CLT(I)=0.0
C   DC 92 I=1,K
C125   IF(TYPE(I).EQ.P) GC TC 92
C126   II=2*INDEX(HEIGHT(I),PQ,5.,12)+1
C127   JJ=2*INDEX(HEIGHT(I),PLQ,5.,12)+2
C128   DIRTN(II)=DIRTN(II)+V(I,2)*V(I,2)
C129

```

* C

```

C130      DIRTN(JJ)=DIRTN(JJ)+V(I,2)*V(I,2)
C         C
C131      CV(II)=CV(II)+V(I,2)
C132      CV(JJ)=CV(JJ)+V(I,2)
C         C
C133      ARH(II)=ARH(II)+V(I,1)
C134      ARH(JJ)=ARH(JJ)+V(I,1)
C         C
C135      CLT(II)=CLT(II)+V(I,3)
C136      CLT(JJ)=CLT(JJ)+V(I,3)
C         C
C137      VR(JJ)=VR(JJ)+1.C
C138      VR(II)=VR(II)+1.C
C         C
C139      DIRTN(1)=DIRTN(1)+V(I,2)*V(I,2)
C140      CV(1)=CV(1)+V(I,2)
C141      ARH(1)=ARH(1)+V(I,1)
C142      CLT(1)=CLT(1)+V(I,3)
C143      VR(1)=VR(1)+1.C
C144      GC TC 92
C         C
C145      93 CV(2)=CV(2)+V(I,2)
C146      II=32
C147      WC=V(I,2)
C148      TRCT(II,1)=TRCT(II,1)+WC
C149      TRCT(II,2)=TRCT(II,2)+1.C
C150      RUN(II,1,IB)=RUN(II,1,IB)+WC
C151      RUN(II,2,IB)=RUN(II,2,IB)+WC*WC
C152      RUN(II,3,IB)=RUN(II,3,IB)+1.C
C153      DIRTN(2)=DIRTN(2)+V(I,2)*V(I,2)
C154      ARH(2)=ARH(2)+V(I,1)
C155      CLT(2)=CLT(2)+V(I,3)
C156      VR(2)=VR(2)+1.C
C157      92 CONTINUE
C         C
C158      DC 94 I=1,15
C159      IF(VR(I).EQ.C.C) GC TC 94
C160      DIRTN(I)=SQRT(DIRTN(I)/VR(I))
C161      CV(I)=CV(I)/VR(I)
C162      ARH(I)=ARH(I)/VR(I)
C163      CLT(I)=CLT(I)/VR(I)
C164      94 N(I)=CV(I)
C165      DC 20 II=1,32
C166      IF(TRCT(II,2).EQ.C.C) GO TC 2C
C167      WALK=TROT(II,1)/TRCT(II,2)
C168      RUN(II,4,IB)=WALK+RUN(II,4,IB)
C169      RUN(II,5,IB)=WALK*WALK+RUN(II,5,IB)
C170      RUN(II,6,IB)=RUN(II,6,IB)+1.C
C171      2C CCNTINUE

```

```

C
C      THE AVERAGES ARE PRINTED OUT ON THE LINE PRINTER AND ALSO ON DISK.
C
C172      IF(IB.EQ.2) GO TO 95
C173      GO TO 98
C
C174      95 CONTINUE
C175      98 CONTINUE
C176      IWrote=IWrote+1
C177      WRITE(1) (CV(I),VR(I),CLT(I),ARF(I),CIRTN(I),I=1,15),IBEAR,IYEAR,I
        1,ICATE,ITIME,IB
C
C      THE INDIVIDUAL VELOCITIES ARE PLOTTED ON THE PLOT, AND THE AVERAGES
C      FOR THE HALF HOUR ARE CALCULATED AND STORED.
C
C178      ASM=0.0
C179      ASE=0.0
C180      ASX=0.0
C181      IU=0
C182      DO 125 I=1,K
C183      IF(TYPE(I).EQ.P.CR.CLT(I).EQ.X) GO TO 125
C184      IF(V(I,2).EQ.0.0) GO TO 125
C185      IU=IU+1
C186      VEL(IU)=V(I,2)
C187      IF(VEL(IU).GT.100.0) VEL(IU)=99.99
C188      IF(VEL(IU).LT.-100.0) VEL(IU)=-99.99
C189      ASM=V(I,1)+ASM
C190      ASE=V(I,2)+ASE
C191      ASX=ASX+V(I,3)
C192      PLACE(IU)=AINC*I+AL
C193      125 CONTINUE
C
C194      AN=IU
C195      IF(AN.EQ.0.0) GO TO 220
C196      AVS(IK,1,IQL)=ASM/AN
C197      AVS(IK,2,IQL)=ASE/AN
C198      AVS(IK,3,IQL)=ASX/AN
C199      IF(VR(1).LT.2.0) GO TO 220
C200      STERR=(DIRTN(1)**2-CV(1)**2)*(VR(1)-1.0)/VR(1)
C201      STERR=SQRT(STERR/VR(1))
C
C202      AVS(IK,4,IQL)=CV(1)-STERR
C203      AVS(IK,5,IQL)=CV(1)+STERR
C
C204      220 CONTINUE
C205      IF(IQL.EQ.1) GO TO 60
C
C206      CALL ACRIG(325,260)

```

```

C2C7      GO TO 61
C2C8      6C CALL ACRIG(325,81C)
C
C
C2C9      61 CALL ALINE(PLACE,VEL,IU,C.,C.,100.,4C.,2)
C
C
C
C
C210      THE NEXT HALF HOUR IS READ IN.
C
C
C
C
C210      GC TO 2
C
C
C
C
C211      WHEN ALL THE DATA HAS BEEN READ IN CONTROL COMES TO THIS POINT,
C212      AND THE AVERAGES ARE PLCTED ON THE PLCT.
C213      C
C
C211      13 CCNTINUE
C212      IK=IK-1
C213      CALL ACRIG(325,81C)
C
C
C214      DC 770 L=1,2
C215      DO 771 J=1,5
C216      KK=0
C
C
C217      DC 80 K=1,IK
C218      IF(AVS(K,J,L).EQ.C.C) GC TO 8C
C219      KK=KK+1
C220      PLACE(KK)=PACE(K,L)
C221      VEL(KK)=AVS(K,J,L)
C222      IF(VEL(KK).GT.100.C) VEL(KK)=101.C
C223      IF(VEL(KK).LT.-100.C) VEL(KK)=-101.C
C224      8C CCNTINUE
C
C
C225      IF(J.NE.2) GC TO 1C
C226      CALL ALINE(PLACE,VEL,KK,C.,0.,100.,4C.,1)
C227      GC TO 771
C228      1C IF(J.GT.3) GC TO 72
C229      CALL ALINED(PLACE,VEL,KK,0.0,0.0,100.C,4C.C,25,25)
C
C
C230      GC TO 771
C231      72 CCNTINUE
C232      CALL ALINED(PLACE,VEL,KK,0.0,0.0,100.C,4C.C,1C,1C)
C
C
C233      771 CONTINUE
C234      CALL ACRIG(325,26C)
C
C
C235      77C CCNTINUE
C236      CALL AEND
C

```



```

C237      WRITE(7,69) IWRCTE, (HED(I), I=1,35), (HET(I), I=1,35)
C238      69 FORMAT(14,35A1,39A1)

C
C
C      THE DISK IS REWOUND AND THE HALF HOUR AVERAGES ARE READ OFF IT AND
C      PUNCHED OUT ON CARDS FOR LATER USE.

C239      REWIND 1

C
C      DO 67 J=1, IWRCTE
C240      READ(1) (CV(I), VR(I), CLT(I), ARH(I), DIRTN(I), I=1,15), IBEAR, IYEAR,
C241      1 IDATE, ITIME, IP
C242      WRITE(7,66) IYEAR, IB, IDATE, IBEAR, ITIME
C243      66 FORMAT(1X, I2, I3, I4, I3/I4)
C244      WRITE(7,426) (CV(I), VR(I), CLT(I), ARH(I), DIRTN(I), I=1,15)
C245      426 FORMAT(15F5.0)
C246      67 CONTINUE

C
C
C      THE COMPLETE AVERAGES FOR THE 1KM INTERVALS ARE CALCULATED AND PUNCHED ON
C      CARDS AND PRINTED OUT.

C247      DO 23 IB=1,2
C248      LL=0
C249      DO 23 L=1,2
C250      DO 30 I=1,32
C251      DIRTN(I)=0.0
C252      DO 30 J=1,3
C253      30 V(I,J)=0.0
C254      DO 21 I=1,32
C255      WALK=RUN(I,3+LL,IB)
C256      IF(WALK.LT.2.) GC TC 21
C257      ASE=RUN(I,LL+1,IB)/WALK
C258      ASM=RUN(I,LL+2,IB)/WALK
C259      RUN(I,LL+2,IB)=SQRT((ASM-ASE*ASE)*WALK/(WALK-1.0))
C260      RUN(I,LL+1,IB)=ASE
C261      ASM=RUN(I,LL+2,IB)
C262      DIRTN(I)=ASM/SQRT(WALK)
C263      V(I,1)=ASE-DIRTN(I)
C264      V(I,2)=ASE
C265      V(I,3)=ASE+DIRTN(I)
C266      21 CONTINUE
C267      WRITE(6,24) (HED(I), I=1,35), (HET(I), I=1,35), IB, (RUN(I,3+LL,IB), RUN(I
1 I,2+LL,IB), DIRTN(I), (V(I,J), J=1,3), I=1,32)
C268      24 FORMAT('8','1',74A1,10X,'BEARING',I5,'('C',6F20.2))
C269      WRITE(7,823) (IB, ((RUN(I,J+LL,IB), J=1,3), I=1,32))
C270      823 FORMAT(11,(16F5.0))
C271      23 LL=3

C
C
C      THE DISPERSION IN THE BEARINGS FOR THE COMPLETE RUN ARE PRINTED OUT.

```

```
C272      DO 81 I=1,4
C273      BOM=BRING(I,2)
C274      IF(BCM.LT.2) GC TC 81
C275      BRING(I,1)=BRING(I,1)/BCM
C276      BRING(I,3)=SQRT((BRING(I,3)/BCM-BRING(I,1)**2)*BCM/(BCM-1.C))
C277      81 CONTINUE
C278      WRITE(6,82)((BRING(I,J),I=1,4),J=1,3)
C279      82 FORMAT('8'/'1DISPERSION IN BEARINGS',/('C',4F20.3))
C280      END
```

CCC1

```

C ***** SUBROUTINE RECIN(K,NERRCR,NP) ***** C
C * C
C * PURPOSE. C
C * TO READ THE RAW FILM DATA IN AND PREPARE IT FOR LATER WIND FIELD C
C * STUDIES. C
C * C
C * PARAMETERS. C
C * A. COMMON/FLAT/ CARRIES ERROR INFORMATION FROM FUNCTION FACTC C
C * JA- ERROR ARRAY FROM FACTC. SEE FUNCTION FACTC FOR FURTHER C
C * INFORMATION ON ERRORS. C
C * IJI- THE NUMBER OF ERROR CODES TO READ OUT C
C * C
C * B. COMMON/LEVEL/ ERROR INFORMATION FROM FUNCTION RANGE-C. C
C * JJA - ERROR ARRAY FROM RANGE-C C
C * IJJI- NUMBER OF ERRORS IN ARRAY C
C * C. COMMON/GCCC/ C
C * K- NUMBER OF VALUES READ IN AND FOUND TO BE USABLE. C
C * SMA- +1. FOR DIRECTION AWAY,(A OR G) AND -1. FOR TOWARDS.(T OR F) C
C * C
C * D COMMON/NEED/ C
C * N- NUMBER OF METEOR C
C * TYPE- TYPE OF METEOR- C IF DECAY, P IF PERSISTENT C
C * HEIGHT-DECAY HEIGHT OF METEOR, OBTAINED BY FITTING EXPONENTIAL C
C * CURVE SLOPES BY EYE. C
C * UNITS=KILCMETERS C
C * RANGE-RADIAL, OR LINE OF SIGHT, DISTANCE TO METEOR TRAIL. C
C * UNITS=KILCMETERS, AFTER CALIBRATION. C
C * V(I,N)-ARRAY OF VELOCITY VALUES CALCULATE FOR A CURVED EARTH IN C
C * FACTC ASSUMING ALL MOTION IS HORIZONTAL.THE VALUES ARE. C
C * N=1 MAXIMUM POSSIBLE VELOCITY FOR ERRORS PRESENT C
C * N=2 VELOCITY IF ALL ERRORS ARE ZERO C
C * N=3 MINIMUM POSSIBLE VELOCITY FOR ERRORS PRESENT C
C * UNITS= METERS PER SECOND C
C * DIRTN-DIRECTION OF VELOCITY- T= TOWARDS A= AWAY C
C * IF LESS CERTAIN- F= TOWARDS G= AWAY C
C * PIP- IF A TIME INTERVAL IS RECORDED, PIP=X. C
C * E. COMMON/DATE/ C
C * IYEAR- YEAR THE OBSERVATIONS WERE MADE IN C
C * IDATE- NUMBER OF DAY (OUT OF 365/366) IN THE YEAR C
C * ITIME- TIME OF DAY USING A 24HOUR CLOCK C
C * IBEAR- CORRECTED GEOGRAPHIC BEARING FROM STATION C
C * IREAD- FILM READER IDENTIFICATION NUMBER. C
C * F. COMMON/BLANK C
C * DUR- DURATION OF DECAY METEORS, TAKEN AS THE TIME WHICH BRIGHT-UP C
C * IS PRESENT. (THIS RELATED TO RECORDED PRESENT FOR USE, NOT THE C
C * DECAY TIME TO SOME FRACTION OF THE INITIAL AMPLITUDE) C
C * IAMP- THE METEOR AMPLITUDE,AS IT APPEARS ON THE FILM, NOT AN C

```

```

C *      INDICATION OF TOTAL POWER RETURN.
C *      UNITS=1 TO 5 CENTIMETERS.
C *      IHT- TYPE OF DECAY FITTED- 1=LOVELY, 2=NCT SC GOOD, 3=CONVEX,
C *      4=BOBS UP- POSSIBLY A FIRST FACE.
C *      VR- LINE OF SIGHT VELOCITY, AS READ FROM FILM.
C *      IDOP- THE FRACTION OF A WHOLE WAVELENGTH USED TO DETERMINE THE
C *      DOPPLER. 1=A WHOLE WAVELENGTH
C *      2=HALF A WAVELENGTH TAKEN BETWEEN MAXIMUM AND
C *      MINIMUM VALUES.
C *      3=HALF A WAVELENGTH TAKEN BETWEEN ADJACENT ZERGES.
C *      4=BETWEEN A QUARTER AND HALF A WAVELENGTH.
C *      5=BETWEEN AN EIGHTH AND QUARTER OF A WAVELENGTH
C *      6=LESS THAN AN EIGHTH OF A WAVELENGTH
C *      IPER- TYPE OF PERSISTENT- SUBJECTIVE, AND PROBABLY OF NEGLIGIBLE
C *      VALUE. A SEMI-STATEMENT ABOUT THE TYPE OF DOPPLER PRESENT.
C *      BLANK=SINUSOIDAL DOPPLER- LIKE A DECAY
C *      6=COULD ONLY GUESS AT A DIRECTION
C *      7=VERY MESSY, BUT GOT A REASONABLE DIRECTION AND
C *      GUESSED AT A REPRESENTATIVE DOPPLER.
C *      CV- IF THE DOPPLER IS UNCERTAIN AN X IS PUT IN CV.
C *      CLT- IF THE TYPE IS NOT CLEAR, VALUE OF CV IS X. (GENERAL PRACTICE,
C *      IF IN DOUBT, IS TO CALL TYPE C AND PUT CV=X )
C *      CLHT- IF THE HEIGHT ASSIGNED IS PARTICULARLY UNCERTAIN, CLHT=X.
C *      ARH- HORIZONTAL RANGE ON A CURVED EARTH, AS CALCULATED IN RANGE-C.
C *      UNITS=KILOMETERS
C *      G. OTHER VARIABLES
C *      KKK- USED TO TRANSFER NUMBER OF RECORDS USED TO MAIN-PROGRAM.
C *      ERROR- THE READING ERROR IN THE DOPPLER WAVELENGTH.
C *      DOPPLER-CNE WAVELENGTH, AS READ FROM FILM
C *
C *      H. DUMMY VARIABLES
C *      VRMIN-MINIMUM LINE OF SIGHT VELOCITY USING READING ERROR.
C *      VRMAX-MAXIMUM LINE OF SIGHT VELOCITY USING READING ERROR.
C *      IJII- USED TO PREVENT THREE ERROR CODES FOR EACH METEOR, IN FACTC.
C *      (IT IS ASSUMED THAT IF AN ERROR OCCURS ONCE, IT WILL OCCUR
C *      THREE TIMES)
C *
C *      SUBROUTINES OR FUNCTIONS USED.
C *      CALIB, FACTC, RANGE-C
C *
C *      REMARKS.
C *
C *      1. TO OBTAIN VALUES CALCULATED AND READ IN, SUBROUTINE METEOR
C *      MUST BE CALLED IN THE MAIN PROGRAM.
C *
C *      2. ERROR MESSAGES PRODUCED ARE.
C *      NO DIRECTION GIVEN FOR METEOR (N). IF NO DIRECTION GIVEN
C *      FLAT EARTH FOR FOLLOWING METEORS- FROM FACTC

```

```

C  * 3. THE END OF A DATA SET IS DETECTED IF N(K) EQUALS ZERO * C
C  * 5 DATERR/DATAER ARE CN-LINE AND ALLOW FOR FORMAT ERRORS. * C
C  * ***** * C
C  ***** * C
C  COMMON/DATE/IYEAR, IDATE, ITIME, IBEAR, IREAD * C
C  COMMON /FLAT/JA(3CC), IJI * C
C  COMMON /LEVEL/ JJA(3CC), IJJI * C
C  COMMON/GCCD/Y(3CC), KL, SMA(3CC) * C
C  COMMON /NEED/ N(3CC), TYPE(3CC), HEIGHT(3CC), RANGE(3CC), V(3CC,3), CIP * C
C  1TN(3CC), PIP(3CC) * C
C  COMMON CLR(3CC), IAMP(3CC), IHT(3CC), VR(3CC), IDCF(3CC), IPER(3CC), * C
C  1CV(3CC), CLT(3CC), CLHT(3CC), ARF(3CC) * C
C  DATA X,A,G,T,F,P/'X','A','G','T','F','P' / * C
C  IJI=1 * C
C  IJJI=1 * C
C  * RAW DATA READ IN. * C
C  CALL DATERR(1591) * C
C  GC TC 4 * C
C  1591 WRITE(6,1592) N(K-1),N(K),IDATE,ITIME * C
C  1592 FORMAT('CERRCR IN CARD AFTER',I5,3X,' I.E. IN CARD',I5,1CX,'CCCLWRD C * C
C  1ED ON DAY',I5,3X,'AT TIME',I6) * C
C  4 READ(5,5) N(K),TYPE(K),CLR(K),CLT(K),IAMP(K),RANGE(K),HEIGHT(K),CLHT(K),IHT(K), * C
C  1HT(K),IHT(K), PIP(K),IDCF(K),IPER(K),CV(K),CIRTN(K),ERRCP,CCPLER * C
C  5 FORMAT(I3,A1,1X,F2.1,A1,I1,F4.1,F4.1,A1,I1,1X,A1,1X,I1,I1,A1,2X,A1, * C
C  1,F4.3,F4.3) * C
C  * A BLANK CARD IS PLACED AT THE END OF A SET OF VALUES TO BE READ IN. * C
C  * IF THIS IS DETECTED, THE CNTRL TRANSFERS TO THE END OF THE * C
C  * PROGRAM. * C
C  IF(N(K).EQ.0) GC TC 6 * C
C  * IF THERE IS NO DOPPLER INFORMATION, WE CAN DECIDE NOTHING. * C

```

```

C018      C      IF(DCPLER.EQ.C.) GC TC 4
          C
          C
          C *      DIRECTION IS ALSO DETECTED AND SMA(K) SET TO 81. IF AWAY, OTHERWISE * C
          C *      IT IS LEFT AT -1. * C
          C
C019      3      SMA(K)=-1.
CC20      IF(DIRTN(K).NE.A.AND.DIRTN(K).NE.G) GC TC 7
C021      SMA(K)=1.
C022      GC TC 45
C023      7      CCNTINUE

          C
          C *      IF NO DIRECTION IS GIVEN, AN ERROR MESSAGE IS WRITTEN ON THE * C
          C *      LINE PRINTER. * C
          C
C024      IF(DIRTN(K).EQ.T.CR.DIRTN(K).EQ.F.CR.NERRCR.EQ.1) GC TC 45
CC25      WRITE(6,2) N(K)
C026      2      FORMAT('CNC DIRECTION GIVEN FOR METEOR ',I5)
C027      GC TC 4
C028      45     CCNTINUE

          C
          C      ADJUST THE VELOCITY SO THAT NORTH AND EAST ARE POSITIVE.
          C
C029      IF(IBEAR.LT.375.AND.IBEAR.GE.135) SMA(K)=-1.C*SMA(K)

          C
          C
          C      ALLOWANCE FOR A DIFFERENT FORMAT USED BY ONE FILM READER.
          C
C030      IF(IREAD.NE.9) GC TC 562
C031      HEIGHT(K)=HEIGHT(K)*10.C
C032      DCPLER=DCPLER*C.1
C033      IF(IDCP(K).EQ.2.CR.IDCP(K).EQ.3) DCPLER=DCPLER*2.C
C034      ERROR=ERRCR*C.1
C035      562     CCNTINUE
C036      KL=K
C037      CLR(K)=CLR(K)*C.1
C038      RANGE(K)=CALIB(RANGE(K))

          C *      VELOCITIES ARE NOW CALCULATED, AND ALLOWANCE FOR MULTIPLE ERRORS FROM * C
          C *      ONE RECORD IS ALLOWED FOR. * C
          C
C039      VR(K)=SMA(K)*5.509/DCPLER
CC40      V(K,2)=FACTC(HEIGHT(K),RANGE(K),VR(K),N(K),C.,C.,TYPE(K))
C041      ARH(K)=RANGHC(RANGE(K),HEIGHT(K),N(K),TYPE(K))

          C
CC42      IF(NP.NE.1) GC TC 10

          C
C043      VRMIN=5.509/(DCPLER+ERRCR)*SMA(K)
C044      V(K,3)=FACTC(HEIGHT(K),RANGE(K),VRMIN,N(K),-3.,-1C.,TYPE(K))

```

```

C
C045      VRMAX=SMA(K)*5.5C9/(CCPLER-ERRCR)
C046      V(K,1)=FACTC(HEIGHT(K),RANGE(K),VRMAX,N(K),3.,1C.,TYPE(K))
C
C      ERRORS ARE CORRECTED FOR DIRECTION.
C
C047      IF(SMA(K).GT.C.C) GO TO 1C
C048      HCLD=V(K,1)
C049      V(K,1)=V(K,3)
C050      V(K,3)=HCLD
C
C051      1C IF (IC.EQ.1) SMA(K)=0.
C052      1C 0
C053      10 K=K+1
C
C054      GO TO 4
C
C055      6 K=K-1
C056      IF(NERRCR.EQ.1) GO TO 9
C
C *      WHEN ALL DATA IS READ IN, THE FACTC ERROR MESSAGES ARE PRINTED OUT * C
C
C057      WRITE(6,8)(JA(I),I=1,IJI)
C058      8 FORMAT('CMETECRS, OTHER THAN PERSISTENTS, FOR WHICH FLAT EARTH VALUES WERE
      10 VALUES WERE REQUIRED.'/('O',13I1C))
C059      WRITE(6,11)(JJA(I),I=1,IJJI)
C060      11 FORMAT('CMETECRS, OTHER THAN PERSISTENTS, FOR WHICH HORIZONTAL RANGE F
      12 INGE FAILED ON A FLAT EARTH.'/('O',13I1C))
C
C061      9 CONTINUE
C062      CALL DATAER
C063      END

```

CCC1

FUNCTION CALIB(RANGE)

```

*****
*
* PURPOSE.
* TO CONVERT THE RANGE READ OFF FILMS INTO KILOMETERS.
*
* USAGE.  RANGE(K)=CALIB(RANGE(K))
*
* PARAMETERS.
* DIV- CALIBRATED VALUES OF RANGE AS READ FROM FILM
* RANGE- CORRESPONDING RANGES. (IN KILOMETERS)
* RANGE- VALUE OF RANGE AS READ FROM THE FILM. (THIS IS IN THE SAME
*        UNITS AS DIV.)
* CORRECT- ALLOWANCE FOR DELAY IN THE RECEIVER.
*
* REMARKS.
*
* 1. A SIMPLE, FIRST-ORDER INTERPOLATION IS CARRIED OUT TO OBTAIN
*    THE RANGE, (IN KILOMETERS) ALLOWANCE BEING MADE FOR THE
*    ORIENTATION OF THE MONOSTABLE FLY-BACK.
*
* 2. IF THE RANGE READ FROM FILM EXCEEDS THE CALIBRATION VALUE,
*    IT WILL BE ASSIGNED THE MAXIMUM CALIBRATED RANGE.
*
* 3. VALUES OF RANGE AND DIV ARE TRANSFERRED THROUGH LABELLED
*    COMMON 'CALI'.
*
* 4 NO CORRECTION IS MADE FOR DRIFT OF OSCILSCOPE TRACES.
*****

```

C C C 2
C C C 3

```
DATA CCRECT/6.C/  
CCMCN/CALI/DIV(3C),RNGE(3C),ICAL
```

[illegible]

COC4

IF(RANGE.GT.1CC.) GC TC 6

CCC5

```
1 IF(DIV(1).LT.1.5) GC TO 21
```

```

C
C * ALLOWANCE FOR MONOSTABLE FLY-BACK ORIENTATION. * (
C

```

CCC6

CC SC I=1,ICAL

C C C 7

IF(DIV(I).LT.RANGE) GC TC 32

C0C8

50 CONTINUE

C
C
C

CALIBRATION DUE TO TRACE DRIFT.

CALIBRATION DUE TO TRACE DRIFT.

CCC 9

```
IF(RANGE.LT.DIV(ICAL)) RANGE=RNGE(ICAL)
```



```
CO10      GC TC 6
C
CO11      31 DO 33 I=1,ICAL
CO12      IF(DIV(I).GT.RANGE)GC TC 32
CO13      33 CCNTINUE
C
C      CALIBRATION DUE TO TRACE DRIFT.
C
CO14      IF(RANGE.GT.DIV(ICAL)) RANGE=RNGE(ICAL)
CO15      GC TC 6
C
CO16      32 CCNTINUE
C
C * INTERPOLATION IS CARRIED OUT.
C
CO17      RANGE=RNGE(I-1)+(RANGE-DIV(I-1))*(RNGE(I)-RNGE(I-1))/(DIV(I)-DIV(
1I-1))
C
CO18      6 CALIB=RANGE-CCRECT
C
CO19      RETURN
C
CO20      END
```

* C

0001

```

C ***** SUBROUTINE METEGR ***** C
C * C
C * PURPOSE. C
C * TC PRINT-CUT ALL RECORDS USED IN CALCULATIONS IN ORDER OF ASCENDING C
C * ALTITUDE. C
C * PARAMETERS. C
C * COMMON/GCCC/ SEE SUBROUTINE RECI FOR VARIABLE DETAILS. C
C * COMMON/DATE/ SEE SUBROUTINE RECI FOR VARIABLE DETAILS. C
C * COMMON/NEEC/ SEE RECI C
C * BLANK COMMON SEE SUBROUTINE RECI FOR VARIABLE DETAILS. C
C * OTHER VARIABLES C
C * IDUM- USED IN PRINT-CUT C
C * IWRIT-PAGE COUNTER. WHEN 30 LINES ARE WRITTEN, A NEW PAGE IS C
C * STARTED. C
C * SUBROUTINES AND FUNCTIONS CALLED. C
C * INDEX C
C * REMARKS. C
C * 1. AN ARRAY, IDUM, IS SET UP AND THE VALUE IT CARRIES IS THE C
C * POSITION OF A RECORD IN THE PRINT-CUT. C
C * 2. IN THE PRINT-CUT, PERSISTENTS WILL COME FIRST, THEN ALL C
C * RECORDS WITH HEIGHTS IN ASCENDING ORDER, AND LAST WILL COME C
C * ALL RECORDS WITH HEIGHTS LESS THAN 80KM OR GREATER THAN 110KM C
C ***** C
C
C002 COMMON/GCCC/Y(300),K
C003 COMMON/DATE/IYEAR, IDATE, ITIME, IBEAR
C004 COMMON /NEEC/ N(300), TYPE(300), HEIGHT(300), RANGE(300), V(300,3), DIR
C005 1TN(300), PIP(300)
C006 COMMON CLR(300), IAMP(300), IHT(300), VR(300), ICCF(300), IPER(300),
C007 1CV(300), CLT(300), CLHT(300), ARH(300)
C
C006 DIMENSION IDUM(300)
C
C007 DATA P/'P'/
C008 IWRITE=0
C
C * CALCULATES THE VALUE OF IDUM. IF PERSISTENT, THIS IS SET TO C. * C
C
C009 DO 1 I=1,K
C010 J=INDEX(HEIGHT(I),80.,1.,31)
C011 IF(TYPE(I).EQ.P) J=0
C012 1 IDUM(I)=J
C
C * PICKS CUT VALUES IN ORDER THAT THEY ARE TO BE PRINTED CUT. * C
C
C013 JJ=0

```

```

C014      DC 2 II=1,33
C015      JJ=II-1
C016      DC 4 I=1,K
C017      IF(IDCM(I).EQ.JJ) GC TO 5
C018      4 CCNTINUE
C019      GC TO 6
C020      5 CCNTINUE

C
C * HEADS UP A NEW PAGE IF IWRIT=3C * C
C
C021      IF(MCD(IWRITE,30).EQ.0) WRITE (6,8) IYEAR,ICATE,ITIME,IBEAR
C022      8 FCRMAT('8'/'ICATE YEAR 19',I2,' DAY ',I3,' TIME ',I4,' BEARING ',
1I3,' DEGREES'/'CNC. TYPE SECS AMP',Sx,' HEIGHT TYPE RANGES= F
1CRI. RADIAL VELCCITY= MAX. MEAN MIN. RADIAL T/A T/C T/F
1P Y CCP FT TP')

C
C * PRINTS CLT ALL INFORMATION FOR A SINGLE METECR * C
C
C023      WRITE(6,3) N(I),TYPE(I),CUR(I),IAMP(I),HEIGHT(I),IFT(I), ARF(I),RAN
1ANGE(I),V(I,1),V(I,2),V(I,3),VR(I),CIRTN(I),ICCP(I),IPER(I),Y(I),
1CV(I),CLHT(I),CLT(I)
C024      3 FORMAT('C',I3,3X,A1,2X,F6.2,I3,F15.1,3X,I3,F16.1,F7.1,1CX,3F7.1,F5.1,4X
1.1,4X,A1,2X,2I4,F3.0,3(3X,A1))

C
C025      IWRITE=IWRITE+1
C026      GC TO 4
C027      6 CCNTINUE
C028      2 CCNTINUE

C
C029      END

```

CCC1

```

C ***** FUNCTION FACTC(HL,RL,VR,N,EH,EL,T) ***** C
C * C
C * PURPOSE. C
C * TO FIND THE HORIZONTAL VELOCITY ON A CURVED EARTH GIVEN THE RADIAL C
C * VELOCITY, RADIAL RANGE AND HEIGHT C
C * USAGE. V(I,N)=FACTC(HEIGHT(K),RANGE(K),VR,N,ER,EL) C
C * PARAMETERS. C
C * A. COMMON/FLAT/ CARRIES ERROR VALUES TO SUBROUTINE RECD C
C *   JA- ERROR ARRAY C
C * B. OTHER VARIABLES C
C *   I- NUMBER OF VALUES IN THE ARRAY C
C *   RR- MAXIMUM RANGE, ALLOWING FOR RANGE ERROR C
C *   R- MINIMUM RANGE (SAME) C
C *   HL- HEIGHT C
C *   RL- RANGE C
C *   VR- RADIAL VELOCITY C
C *   N- NUMBER OF METEOR, FOR ERROR IDENTIFICATION. C
C *   EH- HEIGHT ERROR, USUALLY +3.,-3., OR C. C
C *   EL- RANGE ERROR, USUALLY +1C.,-1C. OR C. C
C *   FH- MAXIMUM HEIGHT C
C *   H- MINIMUM HEIGHT C
C * REMARKS. C
C * 1. IF THE CURVED EARTH FAILS, A FLAT EARTH IS USED AND IF THIS C
C *   FAILS A FLAT EARTH APPROXIMATION, USING A HEIGHT OF 95KM AND C
C *   A RADIAL RANGE OF 220KM. C
C * 2. ERROR MESSAGES. C
C *   A. A THREE DIGIT NUMBER IF CURVED EARTH FAILED. C
C *   B. 90XXX, WHERE XXX IS VALUE FROM A., IF FLAT EARTH FAILS. C
C ***** C
C
C   COMMON/FLAT/ JA(300),I
C   DATA P/'P'/
C   RR=RL+EL
C   R=RL-EL
C   FH=HL+EH
C
C * IF EITHER THE HEIGHT OR RANGE IS LESS THAN 50KM. THE VALUE IS INVALID * C
C
C   IF(HL.LT.50.) GO TO 1
C   IF(RL.LT.50.) GO TO 3
C
C   H=HL-EH
C
C   RA=(2.*R*(H+6371.))**2
C   RB=(R*R+FH*(FH+12742.))**2
C
C * IF RA IS LESS THAN RB A NEGATIVE SQUARE-ROOT WILL RESULT, AND IF THEY * C

```

CCC2
 CCC3
 CCC4
 CCC5
 CCC6

CCC7
 CCC8
 CCC9
 C010
 C011

```

C * ARE EQUAL A ZERO DIVIDE WILL OCCUR. FOR EITHER CASE, THE CURVED EARTH * C
C * HAS FAILED AND A FLAT EARTH IS USED. * C
C
C012 IF(RA.LE.RB) GC TC 1
C013 RH=2.*RR*(FH+6371.)
C
C014 RA=RA-RB
C015 RA=SQRT(RA)
C
C * VALUE FOR HORIZONTAL CURVED EARTH VELOCITY. * C
C
C016 FACTC=VR*RH/RA
C017 RETURN
C
C
C ACCOUNTS FOR ZERO HEIGHTS ON PERSISTENTS AND SOME DECAYS.
C
C018 1 IF(HL.EQ.O.) FH=96.+EH
C
C * IF THE RANGE IS STILL LESS THAN OR EQUAL TO THE MAXIMUM HEIGHT THE * C
C * FLAT EARTH FAILS AND AN APPROXIMATION IS USED. * C
C
C019 IF(R.LE.HH) GC TC 3
C
C * NUMBER OF RECCRD IS PLACED IN ERROR ARRAY. * C
C
C020 IF(T.EQ.P.CR.EH.NE.O.) GC TC 6
C021 I=I+1
C022 JA(I)=N
C023 6 RA=R*R-FH*FH
C024 RA=SQRT(RA)
C
C * VALUE FOR HORIZONTAL FLAT EARTH VELOCITY. * C
C
C025 FACTC=VR*RR/RA
C026 RETURN
C
C
C * 9CCCC IS ADDED TO PREVIOUS ERROR RECCRD IN ERROR ARRAY. * C
C
C027 3 IF(T.EQ.P.CR.EH.NE.O.) GC TC 9
C028 I=I+1
C029 JA(I)=N+9CCCC
C
C * VALUE FOR APPROXIMATE, HORIZONTAL FLAT EARTH VELOCITY. * C
C
C030 9 FACTC=1.523*VR
END

```

CCC1

FUNCTION RANGHC(R,H,N,T)

```

C *****
C *
C * PURPOSE.
C * TO CALCULATE THE HORIZONTAL RANGE ON A CURVED EARTH.
C * USAGE. ARH(I)=RANGHC(RANGE(K),HEIGHT(K))
C * PARAMETERS.
C * R- RANGE, IN KILOMETERS.
C * H- HEIGHT, IN KILOMETERS.
C * RE- RADIUS OF THE EARTH.
C * N- NUMBER OF RECORDS
C * REMARKS.
C * 1. IF HORIZONTAL RANGE FAILS AN ERROR CODE IS PRINTED OUT
C *****

```

CCC2

COMMON/LEVEL/IE(300),I

CCC3

DATA RE ,P/6371., 'P' /

C

CCC4

RH=RE+H

CCC5

A=(RE*RE+RH*RH-R*R)/(2.*RE*RH)

C

* IF A IS GREATER THAN 1. THE INVERSE COSINE WILL FAIL. * C

C

CCC6

IF(A.GT.1.) GO TO 1

C

CCC7

RANGHC=RH*ARCCS(A)

C

CCC8

RETURN

C

CCC9

1 IF(R.LE.H) GO TO 2

C010

IF(T.EQ.P) GO TO 6

C011

I=I+1

C012

IE(I)=N

C013

6 RH=R*R-H*H

C014

RANGH=SQRT(RH)

C015

RETURN

C016

2 IF(T.EQ.P) GO TO 10

C017

I=I+1

C018

IE(I)=N+90000

C019

10 RANGHC=197.9

C

C020

END

CCC1

```

C *****
C * FUNCTION INDEX(A,YC,YI,M)
C * PURPOSE.
C * TO CALCULATE THE POSITION, IN A MATRIX, OF A VALUE, A, IF THE ZERO
C * VALUE IS YC AND THE MAXIMUM POSITION ALLOWABLE IS M.
C * USAGE. I=INDEX(A,YC,YI,M)
C * PARAMETERS.
C * YC- ZERO VALUE. THE VALUE OF A AT M=1.
C * YI- THE INCREMENT IN A FOR ADJACENT VALUES OF M.(M=3 TO M=4, SAY)
C * A- THE VARIABLE TO BE FITTED.
C * M- THE MAXIMUM ALLOWABLE VALUE WHICH A CAN GIVE FOR INDEX.
C * REMARKS.
C * 1 THE VALUE OF INDEX COMES FROM THE SOLUTION OF THE EQUATION.
C *    $A = YC + N * YI$ , WHERE N IS THE NUMBER OF TIMES YC IS INCREMENTED.
C * WE CAN SOLVE THIS FOR N, AND THE VALUE OF INDEX FOLLOWS, BECAUSE
C * WE REQUIRE INDEX TO BE 1 FOR A=YC (N=0) AND WE WISH INDEX TO REFER
C * TO THE CENTER OF THE INCREMENT. INDEX THUS GIVES THE POSITION FOR
C * ALL VALUES BETWEEN A AND A+YI IN THE OUTPUT MATRIX IN QUESTION.
C * 2 IF THE VALUE OF A IS SUCH THAT INDEX GIVES A POSITION LESS THAN 1,
C * OR A POSITION GREATER THAN SOME VALUE, M, THE VALUE OF INDEX IS
C * PUT TO M+1.
C * 3 IT FOLLOWS FROM 2, THAT INDEX IS USED WITH, AT LEAST, AN M+1
C * DIMENSIONAL ARRAY.
C * 4 INDEX ONLY GIVES A POSITION IN AN ARRAY, IN USING IT ONE MUST
C * ENSURE THAT OTHER VALUES ARE NOT OVERWRITTEN.
C *****
C
C   INDEX=(A-YC)/YI+1.5
C
C   IF (INDEX.LT.1.OR.INDEX.GT.M) INDEX=M+1
C
C   END

```

CCC2

CCC3

CCC4

CCC1

```

C *****
C * SUPROUTINE LINEPR(Y,X,Q,V,K)
C *
C * PURPOSE.
C * TO TAKE VALUES OF HEIGHT, HORIZONTAL RANGE AND VELOCITY AND TO
C * PRINTOUT A PLOT OF THE SPACIAL VARIATION IN VELOCITY, FOR ALL
C * METEORS.
C *****
C * PARAMETERS
C * THOSE IN LABELLED COMMON 'DATE' INDICATING TIME AND PLACE
C * ADDITIONAL VARIABLES USED
C * X- THE HORIZONTAL PARAMETER- HORIZONTAL RANGE
C * Y- THE VERTICAL PARAMETER- HEIGHT
C * Q- THE TYPE OF RECORD- DECAY OR PERSISTENT
C * V- VELOCITY (M/S)
C * IV- MATRIX OF VELOCITIES TO BE PRINTED OUT
C * VV- MATRIX CONTAINING 'X' IF TWO VALUES OCCUR AT THE SAME POINT
C * SUBPROGRAMS CALLED.
C * ZEROBL-CN LINE-SUPPRESSES PRINTING OF ZEROS
C * ZEROCH-CN LINE-RESTORES PRINTING OF ZEROS
C * INDEX-FUNCTION PROGRAM- SUPPLIED BY USE-ASSIGNS MATRIX POSITION
C *****

```

CCC2

COMMON/DATE/IYEAR, IDATE, ITIME, IBEAR

CCC3

DIMENSION W(32), IV(31,25), VV(31,25), X(1), Y(1), Q(1), V(31,25)

CCC4

DATA P, XS/'P', 'X' /

CCC5

QQ=110.

CCC6

DO 10 J=1,32

CCC7

W(J)=QQ

CCC8

10 QQ=QQ-1.

```

C * INITIALIZE PRINT-OUT MATRICES TO ZERO
C *

```

CCC9

DO 8 I=1,31

CCC10

DO 8 J=1,25

CCC11

IV(I,J)=0

CCC12

8 VV(I,J)=C.

CCC13

DO 1 I=1,K

```

C * DEFINE Y COORDINATE IN PLOT, AND SET THIS TO ZERO FOR PERSISTENTS
C *

```

CCC14

AA=Y(I)

CCC15

IF(Q(I).EQ.P)AA=C.


```

C016      IY=INDEX(AA,11C.,-1.,30)
C
C017      BB=X(I)
C018      IX=INDEX(BB,C.,25.,24)
C
C *      CHECK FOR VALUES ALREADY RECORDED AT DEDUCED (X,Y) POSITION, AND SET * C
C *      VV(X,Y) TO X IF ANY VALUE EXISTS BEFORE WRITING OVER PRESENT VALUE * C
C
C019      IF(IV(IY,IX).NE.C) VV(IY,IX)=XS
C
C *      ALLOWANCE IS MADE HERE FOR FLOATING TO FIXED-POINT CONVERSION, IN * C
C *      WHICH THE LAST DECIMAL PLACE WOULD BE LOST. * C
C
C020      IF(V(I,N).LT.C.) GO TO 2
C021      IVEL=V(I,N)+C.5
C022      GO TO 3
C
C023      2 IVEL=V(I,N)-C.5
C024      3 IV(IY,IX)=IVEL
C025      1 CONTINUE
C
C *      HEADER IS PRINTED OUT, FOLLOWED BY THE MATRICES OF VALUES. * C
C
C026      WRITE(6,909) IYEAR,IDATE,ITIME,IBEAR
C027      909 FCRMAT('8'/'1HCRIZCNAL RANGE /HEIGHT PLCT.'/'CYEAR 15',I2,' DAY',I6,7
1AY',I6,7X,'TIME',I9,7X,'BEARING' I6,' DEGREES'/'HEIGHT')
C
C
C028      CALL ZERCHL
C
C029      WRITE(6,6) (W(IY),(IV(IY,IX),VV(IY,IX),IX=1,25),IY=1,31)
C030      6 FCRMAT(('C',F5.1,25(I4,A1)) )
C
C031      CALL ZERCCF
C
C032      WRITE(6,908)
C033      908 FCRMAT('C',8X,'C',12X,'1CCKM',7X,'.',7X,'2CCKM',7X,'.',7X,'3CCKM',
1,7X,'.',7X,'4CCKM',7X,'.',7X,'5CCKM',7X,'.',7X,'6CCKM')
C
C034      END

```

```

C *****
C *
C * THIS PROGRAM READS IN RAW RANGE CALIBRATION DATA AND PUNCHES OUT
C * RANGE CALIBRATION DATA TO BE USED IN WIND PROGRAMS.
C * PARAMETERS.
C * CAL- THE NUMBER OF SETS OF VALUES TO BE READ IN.
C * DIV- ARRAY OF VALUES WITH UNITS THAT NORMAL DATA WILL HAVE.
C * RNGE- INPUT- VALUES OF RANGE IN SAME UNITS AS XMUL
C * XMUL- VALUE FOR 1000KM.
C * RNGE- OUTPUT-VALUES OF RANGE IN KILOMETERS.
C * REMARKS.
C * 1. VALUES OF RNGE IN KILOMETERS CORRESPOND TO VALUES OF
C * RANGE AS THEY WOULD BE READ FROM FILM. IT IS THUS SIMPLE
C * TO RELATE FILM RANGES TO ACTUAL RANGES.
C * 2. THE UNITS OF DIV ABOVE MUST BE THE SAME AS THOSE FOR WHICH
C * THE FILM IS READ.
C * 3. THIS IS SEPARATED FROM THE MAIN PROGRAM, AS WE ONLY WANT TO
C * CHANGE ARBITRARY UNITS TO KM. ONCE.
C *****
C
C DIMENSION DIV(30),RNGE(30)
C INTEGER CAL
C
C * XMUL IS READ IN AND THE VALUE OF 1 UNIT IN KMS. IS FOUND.
C
C 3 READ(5,51) XMUL,XL,CAL
C 51 FCRMAT(F6.3,F1.0,I2)
C
C IF(XMUL.EQ.0.) GO TO 2
C 1 XMUL=1000./XMUL
C IF(XL.EQ.0.) GO TO 11
C
C READ(5,30) (DIV(I),RNGE(I),I=1,CAL)
C 30 FCRMAT(12(F3.1,F3.2))
C GO TO 1000
C
C 11 READ(5,31) (DIV(I),RNGE(I),I=1,CAL)
C 31 FCRMAT(12(2(F3.2)))
C 1000 CONTINUE
C * RNGE IS CONVERTED TO KILOMETERS.
C
C DO 52 I=1,CAL
C 52 RNGE(I)=XMUL*RNGE(I)
C
C WRITE(6,12) (DIV(I),RNGE(I),I=1,CAL)
C 12 FCRMAT(1('O',6(F5.2,3X,F5.0,8X)))
C * RESULTS ARE PRINTED AND PUNCHED.
C

```

CCC1
CCC2

CCC3
CCC4

COC5
COC6
COC7

COC8
CCC9
COC10

COC11
COC12
COC13

COC14
COC15

COC16
COC17

FCRTRAN IV MCDL 44 PS VERSION 3, LEVEL 3 DATE 73025

PAGE CCC2

```
CO18          DC 14 IKJ=1,4
CO19          WRITE(7,13) (DIV(I),RNGE(I),I=1,CAL  )
CO20          13 FORMAT(10(F4.1,F4.C))
C
CO21          14 CCNTINUE
C
CO22          GC TC 3
CO23          2 CCNTINUE
C
CO24          END
```

CCC1

SUBROUTINE CNE(A,M)

```

*****

```

TAKING A TIME-SERIES, A, THIS SUBROUTINE WILL CARRY OUT A HARMONIC ANALYSIS FOR MULTIPLES OF 24 HOURS. AN ERROR TERM IS ESTIMATED BY ASSUMING ALL COMPONENTS LESS THAN THE 6 HOUR COMPONENT ARE RANDOM NOISE CONTRIBUTIONS. THIS TERM IS THEN USED TO ASSESS THE NOISE CONTRIBUTION TO THE HARMONICS, ANY SIGNIFICANCE IN THE RESULTANT TERMS IS LEFT TO THE USER TO ASSESS, THOUGH TO MAKE THE TASK EASIER, RATIOS OF THE SINE, COSINE AND COMBINED COEFFICIENT TO THE ERROR TERM ARE GIVEN, AS WELL AS THE MAGNITUDE OF THE ERROR. THE ZERO, 24, 12, 8 AND 6 HARMONICS ARE PRINTED OUT IN A TABLE INDICATING PHASE AND AMPLITUDE. THE PHASE INDICATES THE TIME, IN HOURS, TO THE FIRST MAXIMUM AFTER THE BEGINNING OF THE TIME SERIES IF THIS IS TO BE SPECIFIED FROM SOME OTHER VALUE, ZEROES MAY BE ADDED TO THE START OF A TO COMPENSATE. THE AMPLITUDE IS IN THE SAME UNITS AS A.

ANY HEADING UP OF PAGES MUST BE DONE IN THE CALLING PROGRAM

A MINIMUM AND MAXIMUM ANGLE, BETWEEN C AND 90 DEGREES IS CALCULATED, SO FOR SOME PRINT-OUT CASES, THE MAXIMUM AND MINIMUM PHASES COULD INTERCHANGE. THIS DOES NOT REDUCE THEIR USEFULNESS AS LIMITS.

IF THE ERROR TERM IS MUCH LARGER THAN ONE OF THE COEFFICIENTS THEN THE PHASE WILL BE CHANGED BY SOME MULTIPLE OF 90 DEGREES.

VARIABLES=

A - TIME SERIES TO BE ANALYSED

M - SIZE OF SERIES

B - ALL THE 25 HARMONIC TERMS CALCULATED. IF WANTED, THESE MAY BE PRINTED OUT IN THE CALLING PROGRAM.

D - TERMS TO BE PRINTED OUT

ALL OTHER VARIABLES ARE DUMMIES FOR WORKING PURPOSES.

X - ERROR TERM

```

*****

```

COMMON/UKU/ALUK

DIMENSION BB(25),FF(25)

DIMENSION E(5,3)

COMMON/DATA/Y(100)

DIMENSION A(1),C(4,11)

DIMENSION ACSN(14),ASN(14),B(30),CC(30)

DATA PI/3.14159265/

COMMON/PASS/IPASS,AU(30)

```

CCC2
CCC3
CCC4
CCC5
CCC6
CCC7
CCC8
CCC9

```

C INITIALIZATION

C

C010
C011
C012
C013
C014

DC 20 I=1,M
2C IF(Y(I).EQ.1.C) A(I)=0.C
DC 43 I=1,30
AU(I)=0.C
43 B(I)=0.0

C

C

C

C

ALL VALUES WITH THE SAME 24HOUR CLOCK TIME ARE ADDED TOGETHER
THE MEAN FOR EACH TIME IS FOUND

C

C

C015
C016
C017

AUKU=0.0
9 DC 123 I=1,M
II=I-1

C

C

C

WHILE AVOIDING J=C, WE MUST ALSO AVOID J=2 FOR THE FIRST VALUE.

C018
C019
C020
C021
C022
C023
C024
C025
C026
C027
C028
C029
C030
C031
C032

J=MOD(II,24)+1
AU(J)=AU(J)+A(I)
123 IF(A(I).NE.0.) B(J)=B(J)+1.C
DC 567 J=1,25
BB(J)=B(J)
IF(B(J).EQ.0.C) GC TC 567
AU(J)=AU(J)/B(J)
FF(J)=0.C
IF(B(J).GT.1C.) FF(J)=AU(J)
AUKU=AUKU+1.C
567 IF(IPASS.EQ.3) CC(J)=AU(J)
AUKU=AUKU/24.C
WRITE(6,70) AUKU
70 FORMAT('+',8CX,'FRACTION OF TIME SERIES PRESENT',F8.2)
IF(AUKU.LT.0.5) RETURN

C

C

THE CYCLE IS COMPLETED AND THE DISCRETE FOURIER TRANSFORM IS FOUND

C

C033
C034
C035
C036
C037
C038
C039
C040
C041
C042

AU(25)=AU(1)
FF(25)=AU(25)
IF(IPASS.NE.2) GC TC 11
DC 13 I=1,25
IF(AU(I).NE.0.) GC TC 13
AU(I)=CC(I)
13 CCNTINUE
11 CCNTINUE
DC 15 IS=1,6
CALL FORIT(AL,12,12,ACSN,ASN,IER)

C

C

C

THE ERROR TERM IS FOUND

C

C043
C044

DX=0.C
DC 5 I=6,13

```

C045      C=ACSN(I)*ACSN(I)+ASN(I)*ASN(I)
C046      C=SQRT(C)
C047      DX=DX+C
C048      5 B(I)=C
C049      X=DX/8.0

```

```

C
C      THE ZERO, CF STEADY, COMPONENT IS WRITTEN CLT
C

```

```

C050      DX=ACSN(1)+X
C051      DNE=ACSN(1)
C052      DM=ACSN(1)-X
C053      B(1)=DNE

```

```

C
C      WRITE(6,10) DM,DNE,DX
1C  FORMAT(' ',34x,'C',58x,3F7.3)
C056      DC 16 IKJU=2,5
C057      I=IKJU-1
C058      BB(I)=+1.C
C059      FF(I)=+1.C
C060      IF(ACSN(I).LT.C.) BB(I)=-1.C
C061      16 IF(ASN(I).LT.C.) FF(I)=-1.C
C062      WRITE(6,17) (BB(I),FF(I),I=1,4)
C063      17 FORMAT('C',4(2F5.C,1CX))
C064      DC 257 I=1,2C
C065      257 BB(I+4)=AU(I)
C066      DC 21 I=21,24
C067      21 FF(I-20)=AU(I)
C068      DC 22 I=1,4
C069      22 AU(I)=FF(I)
C070      DC 23 I=5,24
C071      23 AU(I)=BB(I)
C072      AU(25)=AU(1)
C073      DC 2 II=2,5
C074      I=II-1

```

```

C
C      ALL ABSCLUTE VALLES AND SIGNS ARE SEPARATED
C

```

```

C075      SSCO=+1.
C076      SSSI=+1.
C077      CC=ABS(ACSN(II))
C078      SI=ABS(ASN(II))
C079      IF(ACSN(II).LT.C.) SSCO=-1.
C080      IF(ASN(II).LT.C.) SSSI=-1.
C081      SCC=SSCO
C082      SSI=SSSI

```

```

C
C      MAXIMUM POSSIBLE AMPLITUDES
C

```

```

C083      CCX=CC+X
C084      SIX=SI+X

```

C
C
C

MINIMUM POSSIBLE AMPLITUDES

C085
C086CCM=ABS(CC-X)
SIM=ABS(SI-X)C
C
C

THE PHASE IS NOW CALCULATED.

C087
C088
C089IF(SCC.LT.C.C.AND.SSI.GT.C.C) GC TC 1
IF(SCC.LT.C.C.AND.SSI.LT.C.C) GC TC 6
IF(SCC.GT.C.C.AND.SSI.LT.C.C) GC TC 8C090
C091
C092Q=+1.0
QQ=0.0
GC TC 4C093
C094
C0951 Q=-1.0
QQ=PI
GC TC 4C096
C097
C0986 Q=+1.0
QQ=+2
GC TC 4C099
C100
C1018 Q=-1.0
QQ=2.0*PI
4 CONTINUEC102
C103
C104SCC=SI/CC
DNE=Q*ATAN(SCC)+QQ
SCC=SIM/CCXC105
C106
C107DM=Q*ATAN(SCC)+QQ
SCC=SIX/CCM
DX=Q*ATAN(SCC)+QQ

C108

FACT=12.0/(I*PI)

C
C
C

NOW ORDER VALUES FOR PRINTING CLT

C109
C110
C111D(I,1)=DM*FACT
D(I,2)=DNE*FACT
D(I,3)=DX*FACTC112
C113
C114DO 14 IJ=1,3
14 E(I,IJ)=D(I,IJ)*I*15.0C115
C116D(I,4)=CC/X
D(I,5)=SI/X
D(I,6)=DNE/XC
C
C

THE AMPLITUDES ARE CALCULATED.

C117
C118
C1193 DNE=CC*CC+SI*SI
DM=CCM*CCM+SIM*SIM
DX=CCX*CCX+SIX*SIXC120
C121D(I,6)=DNE/X
D(I,7)=SQRT(DM)

C

```

C122      D(I,8)=SQRT(DNE)
C123      B(I)=D(I,8)
C124      D(I,9)=SQRT(DX)
C125      D(I,10)=X
C126      E(I,2)=D(I,2)*I*15.0+75.0*(IG-1)*I
C127      2 D(I,11)=24.0/I
C128      WRITE(6,7)((E(I,J),J=1,3),C(I,11),(C(I,J),J=1,10),I=1,4)
C129      7 FCRMAT('C',3F6.0,12X,F6.1,4X,3F7.1,4X,2F7.1,3X,F7.1,4X,3F7.1,5X,F7.1)
C130      1.1)
C130      WRITE(6,12)(AU(I),I=1,25),(B(I),I=1,13),(ACSN(I),I=1,13),(ASN(I),I=1
C131      1=1,13),(BB(J),J=1,25)
C131      12 FCRMAT('CINPUT ',13F 9.2,/' DATA ',12F 9.2/' CERRORS ',13F9.1/' CCC
C132      1CCSINES',13F9.1/' SINES ',13F9.1,/' C',25F4.0/)
C133      15 CONTINUE
C133      END

```


- Baggaley W.J. (1970) Mon.Not. Roy. ast. Soc. 147, 231
- Baggaley W.J. (1972) Mon. Not. Roy. ast. Soc. 159, 203
- Barnes A.A. (1968) AFCRL-68-0228, Proceedings of the
Workshop on Methods of Obtaining Winds and Densities from
Radar Meteor Trail Returns.
- Barnes A.A. (1972) AFCRL-72-0185, Results of the AFCRL Meteor
Trail Set.
- Barnes A.A. (1972) AFCRL-72-0190, Radio Meteor Trail Task.
- Batten E.S. (1961) J. Met. 18, 283
- Blackman R.B. and J.W. Tukey (1959). The Measurement of Power
Spectra, Pub. Dover.
- Blake L.V. (1966) Antennas, Pub. Wiley.
- Blamont J.E. (1961) Ann. Geophys. 17, 434
- Blamont J.E. (1967) Ann. Geophys. 23, 173
- Blamont J.E. and J. Barat (1967) Ann. Geophys. 23, 2
- Bollerman B. (1970) NASA CR-1529, A Study of 30km to 200km
Meteorological Rocket Sounding Systems.
- Booker J.R. and F.P. Bretherton (1967) J. Fluid Mech. 27, 513.
- Brooks C.E.P. and N. Carruthers (1953). Handbook of Statistical
Methods in Meteorology. Pub. Her Majesty's Stationery Office.
- Butler S.T. and K. A. Small (1963) Proc. Roy. Soc. (London)
A183, 453.
- Chapman S. and J. Bartels (1940) Geomagnetism Sec. 16.17, Pub.
Oxford Press.
- Charney J.G. and P.G. Drazin (1961) J. Geophys. Res. 66, 83
- Cook G.E. (1969) Ann. Geophys. 25, 451.
- Deegan N.F. et al., (1970) AFCRL-70-0168 (I) Study of Meteor Wind
Measurements.
- Dalgarno A. (1961) Ann. Geophys. 17, 16.
- Dickinson R.E. (1968) J. Atmos. Sci. 25, 984

- Donn W.L. and D. Rind (1972) J. Atmos. Sci. 29, 156
- Elford W.G. (1959) Planet. Space Sci. 1, 94.
- Elford W.G. (1968), in Barnes (1968) p. 11.
- Felgate D.G. (1970) J. Atmosph. Terr. Phys. 32, 241
- Fishenden R.M. and E.R. Wiblin (1949) Proc. IEE (London) Pt III, 96, 5.
- Fraser G.J. (1968) J. Atmosph. Terr. Phys. 30, 707.
- Fraser G.J. and A. Kochanski (1970) Ann. Geophys. 26, 675.
- Garcia R.V. and T.F. Malone (1966) Problems of Atmospheric Circulation, Pub. Macmillan and Co. Ltd.
- Golley M.G. and D.E. Rossiter⁽¹⁹⁷¹⁾, J. Atmosph. Terr. Phys. 33, 701.
- Granger C.W.J. and M. Hatanaka (1964) Spectral Analysis of Economic Time Series, Pub. Princeton University Press.
- Greenblum C. (1956) Q.S.T. August 1956.
- Greenhow J.S. (1954) Phil. Mag. 45, 364.
- Greenhow J.S. and J.E. Hall (1961) Planet. Space Sci. 5, 109
- Greenhow J.S. and E.L. Neufeld (1955). J. Atmosph. Terr. Phys. 6, 133.
- Greenhow J.S. and E.L. Neufeld (1956) Proc. Phys. Soc. B 69, 1068.
- Greenhow J.S. and E.L. Neufeld (1959) Proc. Phys. Soc. 74, Pt 1, 1.
- Greenhow J.S. and E.L. Neufeld (1961) Quart. J. Roy. Met. Soc. 87, 472.
- Groves G.V. (1959) J. Atmosph. Terr. Phys. 16, 344.
- Groves G.V. (1968) AF-61(052)-781, Determination of air density, temperature and winds at high altitude.
- Groves G.V. (1969) J. Brit. Interplan. Soc. 22, 285.
- Haurwitz B. (1964) W.M.O. Rept. No. 146 T.P. 69.

- Hays W.L. and R.L. Winkler (1970) Statistics: Probability, Interference and Decision. Pub. Holt, Rinehart and Winston.
- Herlofson N. (1948) Rept. Prog. in Phys. 11, 444
- Hines C.O. (1960) Can. J. Phys. 38, 1441.
- Hines C.O. (1963) Quart. J. Roy. Met. Soc. 89, 1.
- Hines C.O. (1965) J. Geophys. Res. 70, 177.
- Hines C.O. (1968) J. Atmosph. Terr. Phys. 30, 837.
- Hines C.O. (1970) Rept. I.U.C.S.T.P. Workshop 10.
- Hines C.O. (1972) Phil. Trans. Roy. Soc. London A271, 457.
- Hines C.O. and C.A. Reddy (1967). J. Geophys. Res. 72, 1015.
- Hooke J.L. (1970) Planet. Space Sci. 18, 1623.
- Huxley L.G.H. (1957) Annals of the I.G.Y. vol III, Pub. Pergamon Press.
- Jenkins G.M. (1961) Technometrics 3, 133.
- Jones J. (1969). Planet. Space Sci. 17, 1519.
- Jones J. (1970) Planet. Space Sci. 18, 1836.
- Jones J. (1972) Planet. Space Sci. 20, 301.
- Jones J. and T.R. Kaiser (1966) Mon. Not. Roy. ast. Soc. 133, 411.
- Jones J. and B.A. Read (1972) Can. J. Phys. 50, 1277
- Jones L.M. (1967) Falling sphere methods for upper-air density, temperature and wind. COSPAR Technique Manual Series.
- Jones W.L. and D.D. Houghton (1972) J. Atmos. Sci. 29, 844.
- Kaiser T.R. and R.L. Closs (1952) Phil. Mag. 43, 1
- Kaiser T.R. (1953) Adv. in Phys. (Phil. Mag. Supplement) 2, 495.
- Kaiser T.R. (1954) Mon. Not. Roy. ast. Soc. 114, 52.
- Kaiser T.R. (1961) Mon. Not. Roy. ast. Soc. 123, 265.
- Kaiser T.R. (1962) Space Sci. Rev. 1, 554.
- Kaiser T.R., W.M. Pickering and C.D. Watkins, (1969) Planet. Space Sci. 17, 519.

- Kato S. (1966) J. Geophys. Res. 71, 3201.
- Keay C.S.L. (1956) M.Sc. Thesis, University of Canterbury.
- Kellog W.W. (1961) J. Met. 18, 373.
- Kent G.S. (1970) Rev. Geophys. 8, 229.
- Kent G.S. and R.W.H. Wright (1968) J. Atmosph. Terr. Phys. 30, 657.
- Kochanski A. (1972) Mon. Weath. Rev. 100, 222.
- Lawson J.L. and G.E. Uhlenbeck (1950) Threshold Signals,
Pub. McGraw-Hill Book Co.
- Layzer D. and J.F. Bedinger (1969) Plan. Space Sci. 17, 1891.
- Liller W. and F.L. Whipple (1954) Rocket Exploration of the
Upper Atmosphere. Pl12. (Special supplement to J. Atmosph.
Terr. Phys. Vol. 1) Pub. Pergamon Press.
- Lindzen R.S. (1966) Mon. Weath. Rev. 94, 295.
- Lindzen R.S. (1967) Quart. J. Roy. Met. Soc. 93, 18.
- Lindzen R.S. (1968) Met. Monog. 9 (31), 37.
- Lindzen R.S. (1968A) Can. J. Phys. 46, 1835.
- Lindzen R.S. (1968B) Proc. Roy. Soc. A303, 219.
- Lindzen R.S. (1969) J. Atmosph. Terr. Phys. 31, 449.
- Lindzen R.S. (1970) Geophys. Fluid Dynamics 1, 333
- Lindzen R.S. and D. Blake (1971) Geophys. Fluid Dynamics 2, 31.
- Lindzen R.S. and S. Chapman (1969) Space Sci.Rev. 10, 3.
- Longuet-Higgins M.S. (1969) Phil. Trans. Roy. Soc. A269, 511.
- Low C.H., K.H. Lloyd, R.G. Roper and D. Rees (1969) Tech. Note,
HSA 158 (Weapons Research Establishment, Salisbury),
Determination of the structure of the atmosphere between
90-120 km.
- Lysenko I.A., B.L. Kashcheyev, K.A. Karimov, M.K. Nazarenko,
A.D. Orlyanskiy, Ye. I. Fialko and R.P. Chebotarev (1969).
Izvestiia, Atmospheric and Oceanic Physics 5, 508.

- Manning L.A. (1959) J. Geophys. Res. 64, 1415.
- Manning L.A., O.G. Villard and A.M. Peterson (1950) Proc. Inst. Rad. Eng. 38, 877,
- Marshall J.C. (1969) J. Appl. Met. 8, 641.
- McIntosh B.A. (1969) Can. J. Phys. 47, 1337.
- McKinley D.W.R. (1961) Meteor Science and Engineering. Pub. McGraw-Hill.
- Morris J.E. and B.T. Miers (1970), in Webb (1970), P531.
- Müller H.G. (1966) Planet.Space Sci 14, 1253.
- Müller H.G. (1968) Planet.Space Sci. 16, 61.
- Müller H.G. (1970) Quart. J. Roy. Met. Soc. 96, 195.
- Müller H.G. (1972) Phil. Trans. Roy. Soc. (London) A271, 457.
- Murgatroyd R.J. (1957) Quart. J. Roy. Met. Soc. 83, 417.
- Murgatroyd R.J. (1965) Proc. Roy. Soc. (London) A288, 575.
- Murgatroyd R.J. (1970) Rept. Prog. in Phys. 33, 817.
- Murray E.L. (1959) Planet. Space Sci. 1, 125.
- Newell R.E. (1966), in Garcia (1966).
- Newell R.E. (1968) Met. Monog. 9 (31), 98.
- Nowak R. (1964) AFCRL-64-1016, Some techniques for recording doppler shifts.
- Nowak R. (1966) AFCRL-67-0108, Height determination of radar echoes from meteor trails.
- Nowak R. (1967) AFCRL-67-0347, An integrated meteor radar system.
- Nowak R., E.M. North and M.G. Frankel (1970) AFCRL-70-0365 , The Stanford radar Mark II.
- Pittway M.L.V. and C.O. Hines (1963) Can. J. Phys. 41, 1935.
- Pittway M.L.V. and C.O. Hines (1965) Can. J. Phys. 43, 2222
- Pokrovskiy G.B. and G.M. Teptin (1970) Izvestiia, Atmospheric and Oceanic Physics 6, 69.

- Poole L.M.G. and T.R. Kaiser (1967) Planet. Space Sci. 15, 1131.
- Poulter M.J. (1971) Meteor region wind shears. Hons III project, University of Canterbury.
- Pupyshev Y.A. and G.M. Teptin (1971) Geomag. and Aeronomy 11, 421.
- Quesada A.F. (1971) AFCRL-71-0233, Application of matrix methods to triangulation of chemical releases.
- Ratcliffe J.A. (1956) Rept. Prog. Phys. 19, 188.
- Rayner J. (1971) An introduction to spectral analysis. Pub. Pion Ltd. London.
- Revah I. (1969) Ann. Geophys. 25, 1
- Revah I. (1970) J. Atmosph. Terr. Phys. 32, 1313.
- Rice D.W. and P.A. Forsyth (1963) Can. J. Phys. 41, 679.
- Rice D.W. and P.A. Forsyth (1964) Can. J. Phys. 42, 2035.
- Roper R.G. (1966) J. Geophys. Res. 71, 5785.
- Rossiter D.E. (1971) Aust. J. Phys. 24, 103.
- Siebert M. (1961) Adv. in Geophys. 7, 105.
- Smith L.B. (1969) SC-RR-68-523. (Sandia Labs.),
Observations of atmospheric density, temperature and winds over Kauai.
- Smith L.B. (1971) SC-RR-71-0008, Vapour trail experiments over Kauai, Hawaii and Tonopah, Nevada.
- Smith, W.S., J.S. Theon, P.C. Swartz, and L.B. Katchen (1967) NASA TR R-263. Temperature, pressure and wind measurements in the upper stratosphere and mesosphere, 1965.
- Southworth R.B. (1970), in Deegan, et al (1970).
- Starr V.P. (1968) Physics of Negative Viscosity. Pub. McGraw-Hill.
- Taffe W.J. (1969) AFCRL-69-0350, The variation of the upper atmospheric scale height and its effects on atmospheric tidal wavelengths.

- Teptin G.M. and V.M. Starostin (1971) J. Atmosph. Terr. Phys. 33, 807.
- Topping J. (1965) Errors of Observations. (Inst. of Physics and Physical Society Monograph).
- Tukey J.W. (1961) Technometrics 3, 191.
- Verniani F. (1968) Paper presented at Convention of the Italian Geophysical Association, Rome 7 March 1968.
- Walkinshaw W. (1946) J. Inst. Elect. Engrs. 93, IIIA, 598.
- Watkins, C.D., R. Eames and T.F. Nicholson (1971) J. Atmosph. Terr. Phys. 33, 1907.
- Webb W.L. (1970) Stratospheric Circulation Pub. Academic Press.
- Weekes K. and Wilkes M.V. (1947) Proc. Roy. Soc. (London) A192, 80.
- Weiss A.A. (1955) Aust. J. Phys. 8, 279.
- Wilkes M.V. (1949) Oscillations of the Earth's Atmosphere. Pub. Cambridge University Press.
- Witt G. (1962) Tellus 14, 1.
- Wright J.W. (1968) J. Atmosph. Terr. Phys. 30, 919.
- Yanowitch M. (1967) J. Fluid Mech. 29, 209.
- Zadorina F.K., G.B. Pokrovskii, V.V. Sidorov, G.M. Teptin, and A.M. Fakhrutdinova, (1967) Izvestiia, Atmospheric and Oceanic Physics 3, 3.